2024

Bridging the Gap:

Innovations and Translations in Pharmacology

15 - 17 May 2024

Mandarin Hotel Bangkok

PROCEEDINGS

The 45th International Meeting of the Pharmacological and Therapeutic Society of Thailand

THE PHARMACOLOGICAL AND THERAPEUTIC SOCIETY OF THAILAND

มหาวิทยาลัยมหิดล
Mahidol University

This publication includes abstracts of the invited speakers and poster abstracts and papers presented at the 45th International Meeting of the Pharmacological and Therapeutic Society of Thailand under the theme "Bridging the Gap: Innovations and Translations in Pharmacology". The conference was held at Mandarin Hotel, Bangkok from May 15-17, 2024, organized by Department of Pharmacology, Faculty of Medicine Siriraj Hospital, Mahidol University, Bangkok, Thailand.

Disclaimer

Matters of copyright of all images and text associated with the abstracts and papers within the Proceedings of the 45th International Meeting of the Pharmacological and Therapeutic Society of Thailand (PTST) are the responsibility of the authors. The PTST does not accept responsibility for any liabilities arising from the publication of any of the submissions.

Copyright

National Library of Thailand Cataloging in Publication Data

Proceedings of the 45th International Meeting of the Pharmacological and Therapeutic Society of Thailand. -- Bangkok : The Pharmacological and Therapeutic Society of Thailand, 2024.
140 p.

1. Pharmacy. I. Title.

615.1

ISBN 978-616-94260-1-1

Table of Contents

Symposium III: Translating Applied Traditional Medicine in the Post-Genomic Era

Plenary Session II

Plenary Session III

Plenary Session IV

Plenary Session V

Poster Abstracts

Poster Papers

Welcome Message from the Chair of Organizing Committee

Dear Colleagues,

It's a pleasure to welcome you to the 45th Meeting of the Pharmacological and Therapeutic Society of Thailand, themed **"Bridging the Gap: Innovation and Translations in Pharmacology,"** taking place from May 15-17, 2024, in Bangkok.

Our society is dedicated to enhancing scientific partnerships and advancing pharmacology excellence, both in Thailand and internationally. This year's international conference continues our tradition of excellence and serves as a crucial forum for translating pharmacological innovations.

Our agenda spans diverse topics, including Ethnopharmacological Approaches to Drug Development, Translations in Precision Oncology and Applied Traditional Medicine, as well as cutting-edge areas like Pharmacological Advances for the Elderly and Innovations in Targeted Antibody Therapies and Mitochondrial Research. This event is not just about lectures and presentations; it's an opportunity for valuable networking and collaboration. We hope you will find the event both educational and inspiring, creating and renewing connections within the pharmacology community.

We would like to express our heartfelt thanks to our dedicated assistants, staff, and the organizing committee, whose efforts have been instrumental in organizing this conference. Additionally, we appreciate the support of the Pharmacological and Therapeutic Society of Thailand. Your participation is greatly valued, and it is what truly enriches our annual conference. We invite you to fully engage with the sessions, network with colleagues, and hopefully, enjoy your time at the conference.

Wishing you a productive and enjoyable experience at the conference.

Professor Uraiwan Panich, M.D., Ph.D.
Chair of the Organizing Committee

Welcome Message

Kesara Na-Bangchang

President, Pharmacological and Therapeutic Society of Thailand

With immense pleasure and excitement, we announce the upcoming 45th Pharmacological and Therapeutic Society of Thailand Annual Meeting, scheduled from 15 to 17 May 2024 at the Mandarin Hotel, Bangkok, Thailand. This special annual meeting of the society is organized at the international level under the scientific theme "Bridging the Gap: Innovations and Translations in Pharmacology". This theme encapsulates the essence of our collective efforts to translate groundbreaking discoveries into tangible solutions that improve healthcare outcomes and enhance the quality of life for individuals worldwide. Pharmacology, as a discipline, thrives on innovation. It is fueled by the relentless pursuit of novel therapeutic targets, the development of cutting-edge drug delivery systems, and the exploration of innovative treatment modalities. However, the journey from laboratory bench to bedside is often fraught with challenges, necessitating a concerted effort to bridge the gap between innovation and translation.

It is imperative to seamlessly transition from concept to clinical application. This involves not only harnessing the potential of emerging technologies and scientific breakthroughs but also navigating the complex regulatory landscape and addressing the practical considerations of healthcare delivery. One of the key challenges in bridging this gap is the need for interdisciplinary collaboration. Pharmacology, by its very nature, is a multidisciplinary field that draws upon insights from various disciplines such as chemistry, biology, medicine, and engineering. Effective collaboration across these domains is essential for driving innovation and accelerating the translation of research findings into clinical practice.

Moreover, bridging the gap requires a concerted effort to address the unmet needs of patients. It involves identifying therapeutic targets that hold the greatest promise for addressing prevalent diseases and improving patient outcomes. Additionally, it entails developing patient-centric approaches to drug discovery and development, ensuring that treatments are not only efficacious but also accessible and affordable to those in need.

Furthermore, the advent of personalized medicine has ushered in a new era of pharmacological innovation. By leveraging advances in genomics, proteomics, and other omics technologies, we now have the unprecedented ability to tailor treatments to the individual characteristics of patients. This paradigm shift holds immense potential for optimizing therapeutic outcomes and minimizing adverse effects.

Our conference aims to provide a platform for diverse perspectives on the pivotal role of pharmacology in driving forward research and development for combating crucial diseases. We are privileged to have with us esteemed speakers who are leaders and pioneers in their respective fields. Their insights and expertise will undoubtedly enrich our understanding and inspire us to push the boundaries of what is possible.

Throughout the meeting, delegates will be privileged to explore new developments and breakthroughs in pharmacology, alongside insights from various disciplines. The discussions and recommendations stemming from this gathering are poised to shape the future trajectory of drug research, ultimately contributing to improving global health and wellness. Most importantly, it is our great pleasure to announce the "Professor Ouay Ketusingh Honorary Award" and "Young Investigator Award" to commemorate his significant contributions to pharmacology in Thailand. Additionally, we have the Chaired Poster Presentation Competition, designed to recognize and celebrate excellence in our field.

Beyond the scientific agenda, this congress offers a unique opportunity to connect with leading experts from diverse professional backgrounds, fostering collaboration and friendship. It is a chance to exchange novel scientific findings, initiate research partnerships, and forge lasting connections that transcend geographical boundaries.

On behalf of the president of the Pharmacological and Therapeutic Society of Thailand, I would like to extend a warm invitation to all participants to immerse themselves in the rich tapestry of Thai culture and hospitality and to explore the unforgettable scenic sites that Thailand has to offer.

We eagerly anticipate your active participation in what promises to be a transformative and enriching experience. Together, let us chart new frontiers in pharmacology and pave the way for a healthier and brighter future for all.

Thank you, and we look forward to welcoming you to the conference.

Warm regards,

Professor Kesara Na-Bangchang
President, the Pharmacological and Therapeutic Society of Thailand (PTST)

Day 1 (Wed 15 May 2024)	
Time	**Sessions**
08.00 - 08.30	**Registration**
08.30 - 09.00	**Welcome Ceremony** Professor Dr. Apichart Assawamongkolkul Dean of Faculty of Medicine Siriraj Hospital, Mahidol University; and Professor Kesara Na-Bangchang President of the Pharmacological and Therapeutic Society of Thailand *Moderated by Assistant Professor Suvimol Niyomnaitham*
09.00 - 10.00	**[Eng] Chiravat Sadavongvivad Memorial Lecture** **"Challenges and Opportunities for Postgraduate Education"** Professor Prasit Watanapa, M.D., PhD. Faculty of Medicine Siriraj Hospital, Mahidol University *Moderated by Assistant Professor Suvimol Niyomnaitham*
10.00 - 10.30	**Morning refreshments**
10.30 - 11.30	**[Eng] Symposium I: Translations in Precision Oncology** **"CAN-Scan: A Phenotype-Driven Precision Oncology Platform or Target and Biomarker Discovery"** Ramanuj Dasgupta, Ph.D. Laboratory of Precision Oncology and Cancer Evolution, Genome Institute of Singapore *Moderated by Assistant Professor Somponnat Sampattavanich* **"Translation of Mouse Models for Human Diseases to the Research Services and Pharma Collaborations"** Professor Seiji Okada, M.D., Ph.D. Joint Research Center for Human Retrovirus Infection and Graduate School of Medical Sciences, Kumamoto University, Japan *Moderated by Associate Professor Siwanon Jirawatnotai*
11.30 - 12.00	**[Eng] Ouay Ketusingh Honorary Award Ceremony and Award Lecture** Professor Uraiwan Panich, M.D., Ph.D. Faculty of Medicine Siriraj Hospital, Mahidol University *Moderated by Assistant Professor Suvimol Niyomnaitham*
12.00 - 13.15	**Luncheon Symposium I**
13.15 - 14.15	**[Eng] Plenary Session I** **"Enabling the Cancer-Immunity Cycle for Liver Cancer Immunotherapy"** Assistant Professor Zhou Jingying, Ph.D. School of Biomedical Sciences, The Chinese University of Hong Kong *Moderated by Associate Professor Adisak Wongkajornsilp*
14.15 - 15.00	**Afternoon refreshments**
15.00 - 16.30	**[Thai] Symposium II: Pharmacological Frontiers for Elderly Populations** **"Medications and Supplements for Muscle Mass"** Lecturer Chalobol Chalermsri, Ph.D., M.D. Department of Preventive Medicine, Faculty of Medicine Siriraj Hospital, Mahidol University *Moderated by Assistant Professor Weerawadee Chandranipapongse* **"Novel Medications for Dementia"** Lecturer Panas Jesadaporn, M.D. Department of Internal Medicine, Faculty of Medicine, Chiang Mai University *Moderated by Assistant Professor Weerawadee Chandranipapongse* **"Novel Medications for Osteoporosis"** Associate Professor Varalak Srinonprasert, M.Med. (Clinical Epidemiology) Department of Internal Medicine, Faculty of Medicine Siriraj Hospital, Mahidol University *Moderated by Assistant Professor Weerawadee Chandranipapongse*
16.30 - 17.30	**Poster Session**
17.30 - 18.15	**Annual Member Meeting (1st Call)** The Pharmacological and Therapeutic Society of Thailand
18.30 - 20.30	**Social dinner and Honoring Ceremony**

Day 2 (Thu 16 May 2024)	
Time	**Sessions**
08.30 - 09.00	**Registration**
09.00 - 10.00	**[Eng] Keynote Session** **"Bridging the gap: the Ethnopharmacological Approach to Drug Development"** Professor Michael Heinrich, Ph.D. (Dr.rer.nat.habil.) Faculty of Life Sciences, University College London, United Kingdom *Moderated by* Lecturer *Weerawon Thangboonjit*
10.00 - 10.30	**Morning refreshments**
10.30 - 12.00	**[Eng] Symposium III: Translating Applied Traditional Medicine in the Post-Genomic Era** **"Herbal Medicine Research: The Challenge in Precision Medicine"** Associate Professor Pravit Akarasereenont, M.D., Ph.D. Department of Pharmacology, Chairman of Center of Applied Thai Traditional Medicine, Faculty of Medicine Siriraj Hospital, Mahidol University *Moderated by* Lecturer *Weerawon Thangboonjit*
	"Preclinical Research in Herbal Medicine" Associate Professor Chatchai Chaotham, Ph.D. Department of Biochemistry and Microbiology, Faculty of Pharmaceutical Sciences, Chulalongkorn University *Moderated by Professor Uraiwan Panich/ Professor Pithi Chanvorachote*
	"Challenges and Opportunities for Clinical Trial of Herbal Products" Professor Kwanchanok Yimtae, M.D. Clinical Research Center, Faculty of Medicine Ramathibodi Hospital, Mahidol University *Moderated by Assistant Professor Suvimol Niyomnaitham*
12.00 - 13.15	**Luncheon Symposium II**
13.15 - 14.00	**[Eng] Plenary session II** **"Case Study on Nan Sandbox Project – the Attempts to End the Deforestation by Pushing YaYa into Commercialization"** Puthita Kachintorn, M.Sc. (Entrepreneurship and Innovation) Pharma-Agro Business team lead, K-Agro Innovate Institute, Kasikornthai Foundation *Moderated by Assistant Professor Somponnat Sampattavanich*
14.00 - 14.30	**[Eng] Plenary Session III** **"Organoid Modelling Human Diseases"** Professor Elizabeth Vincan, Ph.D. Victorian Infectious Diseases Reference Laboratory, Department of Infectious Diseases, The University of Melbourne, Australia *Moderated by Assistant Professor Somponnat Sampattavanich*
14.30 - 14.45	**Afternoon refreshments**
14.45 - 15.15	**[Eng] Plenary Session IV** **"Using Model-Informed Drug Discovery and Development (MID3) to Accelerate Development of Targeted Antibody Therapies"** Bjorn Millard, Ph.D. Co-founder and Head of Computational Biology, Residual Dynamics, LLC., USA *Moderated by Assistant Professor Somponnat Sampattavanich*
15.15 - 15.45	**[Eng] Plenary Session V** **"The Role of Mitochondrial Sulfide Delivery Molecules in Metabolic Reprogramming: from Research Bench to Clinical Translation"** Professor Matt Whiteman, Ph.D. University of Exeter Medical School, United Kingdom *Moderated by Lecturer Weerawon Thangboonjit*
15.45 - 16.00	**Poster Award Announcement and Closing Ceremony** *Moderated by Associate Professor Siwanon Jirawatnotai*

Day 3 (Fri 17 May 2024) Field trip @ Siriraj Hospital (09.00-12.00)		
Station	**Site Visit**	**Venue**
I	**Srisavarindhira Building**	
	Siriraj Initiative in Systems Pharmacology (SISP)	11th floor
	Laboratory of Clinical Pharmacology Unit	12th floor
II	**Siriraj Medical Research (SiMR) Building**	
	Siriraj Institute of Clinical Research (SiCRES)	10th Floor
III	**Piyamaharajkarun Building (SIPH)**	
	"Sappaya Sathana" for health promotion (Center of Applied Thai Traditional Medicine)	7th floor
	Siriraj Bimuksthan Museum	His Majesty the King Bhumibol 72nd Birthday Anniversary Park

Challenges and Opportunities for Postgraduate Education

Prasit Watanapa

Faculty of Medicine Siriraj Hospital, Mahidol University, Thailand

E-mail: prasit.wat@mahidol.ac.th

Abstract

Higher education has been impacted by "The 7 Cyclones of Changes*" since the start of the 21st century. Postgraduate education can serve as a trouble preventer, problem solver, or damage controller. These changes present an opportunity for postgraduate education, particularly in life sciences, to act as a white knight in resolving challenges. Utilizing digital technology to enhance tele-education can mitigate inequities in education, potentially reducing global healthcare disparities. By enabling postgraduate students from various universities and countries to join simultaneous lectures, a common classroom, and platform for in-dept discussions are created, fostering future collaboration. Utilizing such technologies should reduce the overall cost of postgraduate education while maintaining learning quality. Despite these advancements, the opposite trend is observed. In an era marked by technological advancements and evolving job markets, traditional degrees' relevance is challenged. The rise of skills-based hiring prompts a re-evaluation of the value of academic qualifications. For postgraduate education, knowledge alone is insufficient, the program should incorporate essential hard, soft, 21st-century, and meta-skills.

**The 7 cyclones of changes include globalization, digitalization, disintermediation, global warming and climate changes, disruptive technologies, geopolitic conflicts, and socio-demographic changes*

CAN-Scan: A Phenotype-Driven Precision Oncology Platform or Target and Biomarker Discovery

Ramanuj Dasgupta

Laboratory of Precision Oncology and Cancer Evolution, Genome Institute of Singapore

E-mail: dasguptar@gis.a-star.edu.sg

Abstract

Application of machine learning (ML) approaches on pharmacogenomic datasets holds immense promise in the identification of response biomarkers, which remains a critical unmet need for indications lacking clear biomarker-guided strategies for patient stratification. Here, we introduce CAN-Scan, a response-driven precision-oncology platform that leverages on a freeze-viable biobank of high-throughput screen (HTS)-amenable patient-derived primary cell lines (PDCs), their multi-omic profiling, and response to ~80 FDA-approved drugs evaluated at clinically rele8vant dosage (C_{max}). Integration of phenotypic and molecular profiles of PDCs revealed novel prognostic gene expression signatures for resistance against of 5-fluorourcil (5FU)-based drugs in colorectal cancer (CRC), along with the unexpected discovery of a focal copy number gain on chromosome 7 that harbour some of the genes critical for defining the resistant state. Importantly, we validate the CAN-Scan derived response signatures in two independent patient cohorts by demonstrating that the platform can accurately predict clinical response and outcome.

Keywords: Precision oncology, machine learning, multi-omics, patient-derived models, pharmacogenomics

Translation of Mouse Models for Human Diseases to the Research Services and Pharma Collaborations

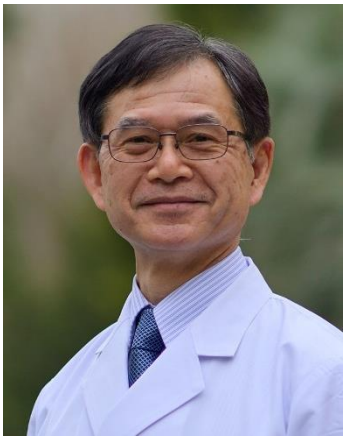

Seiji Okada

Division of Hematopoiesis, Joint Research Center for Human Retrovirus Infection, Graduate School of Medical Sciences, Institute of Industrial Nanomaterials, Kumamoto University, Japan

E-mail: okadas@kumamoto-u.ac.jp

Abstract

In the field of drug development, basic research has been conducted in academia, while the applied research phase has been conducted by companies. In recent years, Bio ventures have been making significant contributions to the creation of new drugs and there is also growing momentum to promote drug discovery in academia. However, since the process of drug development takes a long term of more than 10 years and costs more than 6 million US dollars, pharmaceutical companies and academia collaboration is needed for the success of drug development. The initial phase of drug development begins with understanding the pathogenesis and pathophysiology of the target disease. After identifying the target molecules, drug candidates are screened from the library (chemical and natural product libraries) or designed by computer simulation, and are optimized. The drug candidates which passed the pre-clinical animal model will proceed to the clinical trials. However, it is known that over 90% of the candidates fail at clinical studies. In particular, more than 95% of anti-cancer drug development fails at clinical due to inadequate efficacy (approx. 60%) and safety reasons (approx. 25%). It is explained that animal models display limited translational value in predicting human outcomes as animal models cannot fully replicate physiology, genetic, molecular, inflammatory, pharmacokinetics, and cellular responses to humans.

We generated novel highly immunodeficient mice (NOD NOD/SCID/Jak3(Janus kinase 3)null (NOJ) and BALB/c Rag-2 null /Jak3 null (BRJ) mice to make suitable evaluation mice system, and we established humanized mice, AIDS model mice, and human cancer model mice based on these highly immunodeficient mice, and apply these mice for the evaluation of anti-cancer drugs in collaboration with pharmaceutical companies and Bio ventures. The establishment and application of appropriate animal models are essential for drug development through industry-academia collaboration.

Keywords: Immunodeficient mice, PDX (patient-derived xenograft), *in vivo* drug evaluation system, industry-academia collaboration, human cancer, avatar mice

Enabling the Cancer-Immunity Cycle for Liver Cancer Immunotherapy

Zhou Jingying

School of Biomedical Sciences, The Chinese University of Hong Kong, Hongkong

E-mail: zhoujy@cuhk.edu.hk

Abstract

The clinical advancement of cancer immunotherapy highlights the significance of cellular immune responses, especially T cell responses in cancer elimination. An effective anti-cancer T cell that can recognize and kill cancer cells is generated by the Cancer-Immunity Cycle. The basic concept of cancer immunotherapy is to enable or restore the Cancer-Immunity Cycle, with the aim of amplifying and propagating anti-cancer T cell response for cancer eradication. During this plenary session, I will share with you our recent findings on the development of combinatory cancer immunotherapy strategies that target the key stages of the Cancer-Immunity Cycle. Specifically, I will focus on liver cancer, which exhibits a relatively low response rate to immune-checkpoint blockade (ICB) using current combination approaches (up to 27%). I will discuss our recent findings on how to enhance the therapeutic effectiveness of ICB in liver cancer by understanding the molecular mechanisms for the T cell tumor infiltration and myeloid cell-driven immunosuppression in TME. Furthermore, I will discuss our recent advancements in supplementing the Cancer-Immunity Cycle in metastatic liver cancers, with a particular focus on the unique immune microenvironment of the liver. Our ultimate goal is to develop mechanism-driven immunotherapy approaches for cancer cure.

Keywords: Immune-checkpoint blockade therapy, cancer-immunity cycle, chemotaxis, immunosuppressive myeloid cells, liver immune microenvironment

Medications and Supplements for Muscle Mass

Chalobol Chalermsri

Division of Geriatric Medicine, Department of Preventive and Social Medicine, Faculty of Medicine Siriraj Hospital, Mahidol University, Thailand

Email: Chalobolsi@gmail.com

Abstract

Low muscle mass is used as a part of diagnosis sarcopenia which is associated with several adverse outcomes. Age-related, hormonal change, inflammation, inadequate protein intake, and physical inactivity are the main risk factors for low muscle mass. Due to the strong relationship between muscle mass and protein intake, protein intake at least 1.0 g/kg/day and 1.2 g/kg/day is recommended for healthy older people and older people with sarcopenia, respectively. In case adequate dietary protein is not possible, a protein supplement, oral nutritional supplement containing leucine or beta-hydroxy-beta-methylbutyrate (HMB), or specific amino acids such as leucine may be considered. High-quality protein supplement such as whey protein is associated with improvements in muscle mass and overall performance. Leucine is an essential amino acid that is proven it can increase muscle protein synthesis in older people whereas HMB which is a metabolite of leucine can attenuate the muscle protein breakdown. Additionally, vitamin D plays a role in maintaining muscle health. Besides muscle strength improvement, vitamin D has been proven to have positive effects on muscle protein synthesis and increase muscle mass. Vitamin D deficiency is associated with an increased risk of sarcopenia. In case of vitamin D insufficiency, vitamin D supplementation (800-1000 IU/day) may have the benefit of improving muscle health. Besides supplements, many medications have been used as potential treatments for sarcopenia such as dehydro-epiandrosterone (DHEA) or testosterone, however, there is limited use due to its adverse effects. Currently, there are several medications are being developed and tested in different phases of clinical trials such as selective androgen receptor modulators (SARMs), myostatin inhibitors, growth hormone supplementation, or ghrelin analogs, however, no FDA-approved medications for the treatment of sarcopenia. In conclusion, multimodal interventions including increased physical activity and nutritional intervention are approved for prevention and treatment of sarcopenia.

Keywords: Sarcopenia, nutritional supplement, leucine, beta-hydroxy-beta-methylbutyrate, vitamin D

Novel Medications for Dementia

Panas Jesadaporn

Department of Internal Medicine, Faculty of Medicine, Chiang Mai University, Thailand

Email: panas.j@cmu.ac.th

Abstract

Alzheimer's disease (AD) is a major cause of dementia, starting with an irreversible decline in episodic memory and then in overall cognitive ability. The hallmark pathological features are amyloid plaques deposition in the cerebral cortex and hippocampus, loss of functioning neurons and synapses, and acetylcholine deficiency. Typical treatments of AD are cholinesterase inhibitors and an NMDA receptor antagonist. They implicated cholinergic deficiency and synaptic dysfunction hypotheses. The AD drug development is advancing agents directed at a variety of target processes listed in the Common Alzheimer's Disease Research Ontology. Treatments intended to change the biology of AD are classified as disease modifying therapies (DMTs). Amyloid beta and tau proteins are the canonical pharmacologic targets for DMTs. Three anti-amyloid monoclonal antibodies (MABs)—aducanumab, lecanemab, and donanemab—have been approved for early AD treatment. They have been developed based on the amyloid hypothesis, and that the clearance of brain plaques will halt the amyloid cascade that promotes neurodegeneration and the resulting cognitive and functional decline. Their benefit was assessed in phase III randomized placebo-controlled trials, including thousands of healthy individuals with mild cognitive impairment (MCI) or mild dementia due to AD who had a positive brain amyloid pathology. MABs treatment significantly slowed cognitive and functional decline, and amyloid plaque removal compared with the placebo group. As of the index date of January 1, 2023, there were 187 clinical trials phase 1-3 assessing 141 novel treatments for AD. Novel agents addressing non-amyloid, non-tau (non-canonical) targets in AD comprise 70% of agents currently in clinical trials. Inflammation and synaptic plasticity/neuroprotection are the categories with the largest number of novel candidate therapies. Currently active phase III inflammation drugs clinical trials are masitinib, NE3107, and semaglutide. Whereas AGB101, blarcamesine, fosgonimeton, simufilam, tertomotide target synaptic plasticity/neuroprotection.

Keywords: Alzheimer's disease, disease modifying therapies, anti-amyloid monoclonal antibodies, non-canonical target for AD

Novel Medications for Osteoporosis

Varalak Srinonprasert

Department of Internal Medicine, Faculty of Medicine Siriraj Hospital, Mahidol University, Thailand

Email: varalaksi@gmail.com

Abstract

Osteoporosis is a skeletal disorder classified by the reduced in bone density leading to compromised bone strength and an increased fracture risk. Current fundamental classes of medications used in the treatment of osteoporosis, apart from calcium and vitamin D, are antiresorptive agents and anabolic agents. Nevertheless, current medication regimes could not reach the maximum level of fracture prevention. Therefore, innovative strategies have been sought to fill the gap. One of the novel approaches is the stepwise prescribing of existing medications, particularly in patients with high fracture risk or sustained a new fracture despite having active treatment. With potential side effects for long-term use of current medications and gaps in treatment outcomes, novel agents are still warranted. Up until now, limited agents for osteoporosis treatment have successfully tested at clinical trial level. Testosterone has recently been discovered to increase fracture risk in men with hypogonadism. Immuno-modulatory nanomedicine for osteoporosis treatment remains in the very early stage of discovery.

With the advancement in medical treatments leading to higher life expectancy world-wide, the aging population and the prevalence of osteoporosis will be steadily increasing. Providing the limited number of promising novel agents, the fundamental concepts for prevention with non-pharmacological approaches would remain to be crucial.

Keywords: Osteoporosis, fracture, antiresorptive, anabolic, immunomodulatory nanomedicine

Keynote Session

Bridging the gap: the Ethnopharmacological Approach to Drug Development

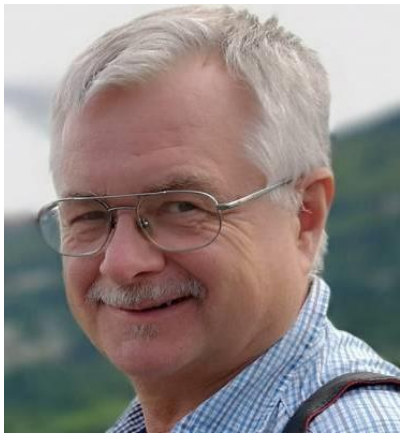

Michael Heinrich

UCL School of Pharmacy, Pharmacognosy and Phytotherapy, United Kingdom
Yushan Fellow, China Medical University, Taichung, Taiwan

E-mail: m.heinrich@ucl.ac.uk

Abstract

It has been pointed out very often now, that the drug discovery pipeline has 'run dry'. In other words, we have fewer new medicines, than we used to develop and there remain many unmet needs. Precision medicine offers some tremendous opportunities but is limited to some very specific and often rare diseases. Natural product research has continued to make important contributions to drug development, but also faces some important challenges. Chemical and biocultural diversity remains an inspiration especially in a country like Thailand. With the important advantage of natural products, being chemically complex and often well suited as leads due to their role in plants and fungi or based on local and traditional experiences, 'Access and Benefit Sharing' (ABS) has come centre stage in the context of research and development on biodiversity and its multiple uses.

Within the context of pharmacology, a wider debate has been going on regarding the reproducibility and validity of pharmacological research, a topic which also needs to be addressed within medicinal plant research/ethnopharmacology (Heinrich et al 2022). The use of extracts in research poses particular challenges, since, obviously. The activities will vary based on the composition resulting in potentially misleading conclusions. All too often an extract, which is investigated, remains a 'black box' putting patients and the reputation of scientists at risk.

We also face the challenges of (re-)supply of material, a topic which is closely linked not only to environmental and climate research, but also offers opportunities for agricultural and silvicultural regional development.

One often overlooked aspect is disease prevention. Natural product-based preparations are ideal to contribute to a healthier life and are one element for reducing the burden of diseases in the globally aging populations.

In this presentation, I will discuss examples of how we can improve our strategies based on the specific challenges we face with regards optimising our research with the aims to develop new medicines and functional products. Future drug discovery research will continue to be driven by industry (Schumacher et al 2023). There is a need for an integrated approach combining clinical, pharmacological and analytical research and here there are numerous important contributions academic research can and will make.

Heinrich M, Jalil B, Abdel-Tawab M, Echeverria J, Kulić Ž, McGaw LJ, Pezzuto JM, Potterat O, Wang J-B. Best Practice in the chemical characterisation of extracts used in pharmacological & toxicological research—The ConPhyMP—Guidelines. Front. Pharmacol. 2022;13:953205. doi: 10.3389/fphar.2022.953205.

Schuhmacher A, Hinder M, Dodel A, Gassmann O, Hartl D. Investigating the origins of recent pharmaceutical innovation. Nat Rev Drug Discov. 2023 Oct;22(10):781-782. doi: 10.1038/d41573-023-00102-z.

Herbal Medicine Research: The Challenge in Precision Medicine

Pravit Akarasereenont

Pharmacology Department, Center of Applied Thai Traditional Medicine, Siriraj Metabolomics and Phenomics Center, WHO Collaborating Center for Traditional Medicine (SEARO), Faculty of Medicine Siriraj Hospital, Mahidol University, Thailand

Email: pravit.auk@mahidol.ac.th

Abstract

Herbal medicine research is currently focused on several key directions such as **1. Efficacy and Safety:** Studying the effectiveness and safety of various herbal remedies for different health conditions. This involves clinical trials and observational studies to assess their therapeutic potential and potential side effects. **2. Mechanisms of Action:** Investigating the underlying mechanisms of how herbs work in the body. This includes understanding the bioactive compounds present in herbs and their interactions with biological systems. **3. Standardization and Quality Control:** Developing methods for standardizing herbal products to ensure consistency in quality and potency. This involves advancements of measuring compound technology such as metabolomics study and establishing guidelines for cultivation, harvesting, extraction, and formulation processes. **4. Combination Therapies:** Exploring the synergistic effects of combining different herbs or integrating herbal medicine with conventional treatments to improve efficacy and reduce side effects. **5. Personalized Medicine:** Researching individualized approaches to herbal medicine based on multi-omics factors, lifestyle, and other personal characteristics to optimize treatment outcomes. **6. Ethnobotanical Studies:** Documenting traditional knowledge about medicinal plants from various cultures and indigenous communities, and validating their efficacy through scientific research. **7. Biotechnology and Novel Formulations:** Utilizing biotechnological approaches to enhance the production of bioactive compounds from herbs and developing novel formulations for improved delivery and bioavailability. **8. Preventive and Lifestyle Medicine:** Exploring the role of herbal medicine in preventive healthcare and promoting overall wellness, including the management of chronic diseases and lifestyle-related conditions **9. Selfcare:** Guiding the use of herbal medicine for self remedy based on evidence inform practice (EIP) and selfcare concept consisting of self awareness, self testing and self management. These research directions aim to advance our understanding of herbal medicine and its potential contribution to healthcare while ensuring evidence-based practice (EBP), EIP and patient safety. Challenging, herbal medicine research has evolved significantly, particularly in the context of precision medicine. Traditionally, herbal remedies were often administered based on historical usage rather than individual genetic or metabolic differences. However, with advancements in technology of multi-omics study and understanding of molecular biology, research in herbal medicine now integrates principles of precision medicine. This approach involves identifying the specific bioactive compounds within herbs, understanding their mechanisms of action, and tailoring treatments to individuals based on genetic variations, metabolomic profiles, and other multi-omics factors. This shift towards precision herbal medicine aims to enhance efficacy, minimize adverse effects, and optimize treatment outcomes for individuals.

Keywords: Herbal medicine, precision medicine, metabolomics

Preclinical Research in Herbal Medicine

Chatchai Chaotham

Department Biochemistry and Microbiology, Faculty of Pharmaceutical Sciences, Chulalongkorn University, Thailand

E-mail: chatchai.c@chula.ac.th, cchoatham@gmail.com

Abstract

Besides infections, non-communicable diseases like cancer and obesity have gained more attention as emerging threats to human health in recent years. Rising economic growth and increasing urbanization are among the possible factors that provoke the incidence of such diseases. Herbal medicine – the most ancient approach to healing pains, injuries, and illnesses, has become an alternative tool in pharmacotherapy for centuries. However, this cure from nature is still underexplored for its implementation to treat non-communicable diseases. Only a few natural products (e.g., curcumin from turmeric rhizomes) have been acceptable for integrative cancer therapy, but none have been valid for preventing and curing obesity. One of the critical limitations of herbal medicine is the decline of natural products' pharmacological efficacy when conducting *ex vivo* or *in vivo* trials compared to *in vitro* assessments. Our team at Chulalongkorn University has been working on various projects focused on overcoming this limitation by 1) improving our insights into the biology and pathology of non-communicable diseases using omics tools and meta-analysis and 2) advancing our analytical platforms to assess precise bioactivity and pharmaceutical potential of natural products. We recently used metabolomics to unveil that some metabolites and their associated metabolic pathways are linked with metabolomic reprogramming in lung cancer cells to evade anoikis. Another ongoing project is to fill knowledge gaps on how different lung cancer cells evolve their molecular mechanisms to underlie anoikis resistance using flow cytometry and transcriptomics. In parallel, we are developing an *ex vivo* assay to culture hair follicles for investigating the roles of natural products in melanin production of mouse melanocytes. We are also a part of an international laboratory collaboration to reduce the use of experimental animals by developing 3-dimensional organoids using patients' biopsies for a more representative *ex vivo* studied model in cancer research and anticancer drug discovery.

Keywords: Herbal medicine, natural products, non-communicable disease, omics, 3-dimensional organoid

Challenges and Opportunities for Clinical Trial of Herbal Products

Kwanchanok Yimtae

Ramathibodi Clinical Research Center, Innovation and Cooperation Division
Faculty of Medicine Ramathibodi Hospital, Mahidol University, Thailand

E-mail: kwayim@gmail.com

Abstract

Herbal products have a long history of use as traditional medicines. Even though the toxicity is seldom addressed and makes the public less concerned about safety, the efficacy is insidious and require a plenty of time to demonstrate the result. The efficacy mostly comes from synergistic use of multiple herbs as a regimen rather than an individual herb. The indications for use are usually based on symptoms or non-specific disorders. This led to the decline in popularity in the western medicine era. Recently, herbal products come to public interest due to the raised concern of global warming and increasing demand of eco-friendly health environment. However, herbal medicines have less scientific validation than that of modern medicine, and technological standardization to assure the quality is needed. The proof of efficacy and safety shown in clinical trials of modern medicine is also required. Therefore, this session will discuss on the challenges and opportunities of clinical trials in herbal products.

Keywords: Herbal products, herbal medicine, clinical trial

Case Study on Nan Sandbox Project – the Attempts to End the Deforestation by Pushing YaYa into Commercialization

Puthita Kachintorn

Pharma-Agro Business team lead, K-Agro Innovate Institute, Kasikornthai Foundation

E-mail: puthita.k@kasikornbank.com

Abstract

The Nan Sandbox Project stands as a pioneering endeavor aimed at curbing deforestation in Thailand by promoting the commercialization of plant-based medicine. This case study delves into the milestones achieved and obstacles encountered by the project team as they navigate the complex landscape of Thailand's socio-economic and environmental contexts. The project's inception was marked by a vision to address the root causes of deforestation in the Nan region, particularly driven by the expansion of stock-fed corn cultivation. Leveraging the rich biodiversity of the Nan pristine headwater forest, the team sought to harness the medicinal properties of indigenous plants and facilitate their commercialization as a sustainable alternative livelihood for local communities. Throughout the journey, the project team encountered multifaceted challenges, including regulatory hurdles, technical complexities, and socio-economic barriers. Regulatory compliance posed a significant obstacle, requiring extensive navigation of Thailand's regulatory framework for herbal medicines and agricultural practices. Technical challenges included optimizing cultivation techniques, standardizing extraction processes, and ensuring product quality and efficacy. Moreover, the socio-economic landscape presented its own set of challenges, including limited access to resources, insufficient infrastructure, and entrenched farming practices. Addressing these challenges required a holistic approach, encompassing community engagement, capacity building, and stakeholder collaboration. The project team worked closely with local communities, providing training, resources, and support to transition towards sustainable plant-based medicine production. Ultimately, the Nan Sandbox Project serves as a testament to the potential of plant-based medicine as a sustainable solution to deforestation. While obstacles abound, the project's successes underscore the importance of perseverance, collaboration, and innovation in addressing complex socio-environmental challenges in Thailand's context.

Keywords: Plant-based medicine, Nan Sandbox, deforestation, sustainability, socio-environmental

Organoid Modelling Human Diseases

Elizabeth Vincan

Victorian Infectious Diseases Reference Laboratory, Department of Infectious Diseases, The University of Melbourne, Australia

E-mail: e.vincan@unimelb.edu.au

Abstract

The global urgency to uncover medical countermeasures to combat the COVID-19 pandemic caused by the severe acute respiratory syndrome-coronavirus 2 (SARS-CoV-2) revealed an unmet need for robust tissue culture models that faithfully recapitulate key features of human tissues and disease. Infection of the nose is considered the dominant initial site for SARS-CoV-2 infection and models that replicate this entry portal offer the greatest potential for examining and demonstrating the effectiveness of countermeasures designed to prevent or manage this highly communicable disease. To this end, we established an air-liquid-interface (ALI) differentiated human nasal epithelium (HNE) culture model of SARS-CoV-2 infection. We demonstrated robust, reproducible SARS-CoV-2 infection of ALI-HNE established from different donors. Viral entry and release occurred from the apical surface, and infection was primarily observed in ciliated cells. Furthermore, the ALI-HNE model revealed stark differences in cytopathology associated with highly transmissible variants like Delta, and proved to be a discerning neutralisation and anti-viral assay. Human organoid models of viral infection are now adopted globally.

Keywords: Organoids, infectious disease, COVID-19, SARS-CoV-2, pre-clinical models

Plenary Session IV

Using Model-Informed Drug Discovery and Development (MID3) to Accelerate Development of Targeted Antibody Therapies

Bjorn Millard

Co-founder and Head of Computational Biology, Residual Dynamics, LLC., USA

E-mail: bmillard@residualdynamics.com

Abstract

Despite recent advances in diagnosis, prevention, and disease management, cancer remains to be one of leading causes of death worldwide. Our growing understanding of the complexity of the disease has led to increased development of molecularly targeted agents (MTAs); however, designing the right drug at the right dose for the right target remains a challenge in a field where the current development paradigm is based on cytotoxic chemotherapy agents (CTAs). This can lead to poorly designed molecules and dosing strategies that are inadequately characterized before initiating registration trials. Model-informed drug discovery and development (MID3) is an evolving field that uses computational models to inform drug design and dosing strategies based on multi-scale preclinical and clinical data. This talk is focused on a MID3 case study that outlines the process and utility of using fit-for-purpose, semi-mechanistic PK/PD modeling to inform the design and dosing regimen of a theoretical CD47 bispecific antibody (bsAb) targeted to a generic tumor-associated antigen (CD47xTAA bsAb). Model projections demonstrate how lowering the binding affinity to CD47 may improve PK exposure in the tumor compartment by reducing systemic CD47 target-mediated drug disposition (TMDD) while maintaining engagement to CD47 in the tumor via avid binding interactions with the TAA. This modeling exercise demonstrates how MID3 models can be used in the early stages of drug development to improve efficacy, tolerability, PK, and dosing by leveraging the targeting advantage of avid bispecific antibodies.

Keywords: Modeling and simulation (M&S), model-informed drug discovery and development (MID3), quantitative systems pharmacology (QSP), translational modeling, semi-mechanistic PK/PD

The Role of Mitochondrial Sulfide Delivery Molecules in Metabolic Reprogramming: from Research Bench to Clinical Translation

Matt Whiteman

University of Exeter Medical School, Exeter, UK
MitoRxTherapeutics, Oxford, UK

E-mail: m.whiteman@exeter.ac.uk

Abstract

The gas hydrogen sulfide (H_2S) has been fundamental in human evolution and cellular bioenergetics. Primitive life (bacteria; prokaryotes) first emerged on the earth in the primordial H_2S-rich environment ~3.6 billion years ago and used atmospheric H_2S to generate metabolic energy (e.g. ATP). These primitive bacteria were subsequently assimilated by later eukaryotic cells and today, human cells (eukaryotic) have retained this ability to use H_2S as the only inorganic electron source for ATP generation. Human cells have at least three separate enzyme systems to supply mitochondria with H_2S in times of cellular stress for energy metabolism; two of these enzyme systems are located in the cytoplasm but cellular stress (e.g. oxidative stress) causes them to translocate to mitochondria. The third enzyme system is predominantly mitochondrial and pharmacological inhibition or genetic silencing/ removal of any of the three enzymes, renders cells and animals more prone to oxidative and inflammatory injury, and reduces animal life span i.e. cellular H_2S is an 'emergency fuel' for mitochondria, and for cell survival. In many disease states typical of 'accelerated ageing', the ability of cells to synthesise H_2S is gradually lost, or synthesised H_2S is depleted (e.g. by detrimental oxidant species; oxidative stress), and we very recently showed that this loss of H_2S over life span is evolutionary conserved (i.e. in yeast, worms, flies, rodents and humans), whereas longer lived animals have increased tissue H_2S generation and added resilience. The decline in H_2S through life results in, or at the very least contributes to, the gradual failure of cellular bioenergetics (ATP generation) and several (reversible) hallmarks of 'ageing' such as oxidative stress, DNA damage, mitochondrial and tissue/organ dysfunction; particularly highly energy-dependent tissue such as brain, heart, skeletal muscle etc. As with mitochondrial function, the loss of cellular H_2S may represent a novel and common pathway by which ageing, and particularly diseases associated with accelerated ageing (i.e. most human diseases) occur, targeting mitochondria with H_2S could overcome, limit or prevent age (and disease) associated tissue injury. We have developed a novel series of patented compounds (mtH_2SD) which selectively target mitochondria by various mechanisms and generate minute fluxes of H_2S, as well as compounds to target specific tissues. These compounds have excellent "drug-like" characteristics and are highly potent at inducing cellular bioenergetics (< 100 nM; some < 1 nM). By using disparate animal models of human disease with established mitochondrial and bioenergetic dysfunction, we have also shown mtH_2SD to be highly efficacious and potent (i.e. active between 0.07-1 mg/kg) at reversing the pathological phenotype when used by a variety of administration established drug routes. Collectively, these studies strongly suggest that awakening and targeting this evolutionary

conserved metabolic pathway with minute quantities of H_2S generated slowly via mtH_2SD, could at least delay some of the detrimental effects of ageing and diseases associated with accelerated ageing, and crucially improve health span and quality of life into old age, and beyond. This talk will summarise our latest findings with mtH_2SD in several models of human disease and the progress we've made in the commercial space in developing compounds for clinical use.

Keywords: Mitochondria, ATP, ageing, skeletal muscle, neuromuscular, neurodegenerative, primary mitochondrial disease

Elevated Stem Cell Factors are Associated with Palbociclib Resistance in Cholangiocarcinoma Cells

Chanettee Jamyuang[2], Jantappapa Chanthercrob[1], Amphun Chaiboonchoe[1], Orawan Suppramote[3], Somponnat Sampattavanich[1,2], Siwanon Jirawatnotai[1,2*]

[1] *Siriraj Center of Research Excellence for Precision Medicine and Systems Pharmacology, Faculty of Medicine Siriraj Hospital, Mahidol University, Bangkok, Thailand*
[2] *Department of Pharmacology, Faculty of Medicine Siriraj Hospital, Mahidol University, Bangkok, Thailand*
[3] *Princess Srisavangavadhana College of Medicine, Chulabhorn Royal Academy, Bangkok, Thailand*

*E-mail: siwanon.jir@mahidol.ac.th

Abstract

Cholangiocarcinoma presents a formidable challenge within clinical settings owing to its tendency for rapid drug resistance, thereby amplifying treatment difficulties and ultimately contributing to heightened patient mortality. The elucidation of specific biomarkers associated with drug resistance in cholangiocarcinoma is indispensable for formulating precise therapeutic strategies. This study focuses on a comprehensive exploration of the role played by stemness proteins, particularly their heightened expression within the milieu of drug-resistant cholangiocarcinoma cells. The research employed the CDK4/6-resistant cholangiocarcinoma model, i.e., wildtype KKU055 cells and the Palbociclib-resistant clones. Reverse Phase Protein Array (RPPA) was used to examine protein expressions within pathways related to drug resistance. Remarkably, an elevated expression of stemness proteins, including CD44, was identified in drug-resistant cells, particularly in the presence of Palbociclib. This change was less clear in the wildtype cells indicating that phenotype might be specific to the drug resistant clones. Additionally, an independent validation by flow cytometry confirmed the specific upregulation of CD44, in the drug-resistant cell clones. This result corroborated those obtained through RPPA. The derived implications from these results suggest that stem cells may indeed wield a pivotal influence in instigating drug resistance in cholangiocarcinoma. Subsequent investigations are warranted to delve deeper into the nature of these protein alterations.

Keywords: Cholangiocarcinoma, CDK4/6 drug resistance, reverse phase protein array (RPPA), stem cell

A02

Enhancing CDK 4/6 Inhibitor Efficacy in Cholangiocarcinoma through Combination with HDAC Inhibitor

Tongchai Payungwong, Sunisa Prasopporn, Siwanon Jirawatnotai*

Siriraj Center of Research Excellence in Systems Pharmacology, Department of Pharmacology, Faculty of Medicine Siriraj Hospital, Mahidol University, Bangkok, Thailand

*E-mail: siwanon.jir@mahidol.ac.th

Abstract

Cholangiocarcinoma (CCA) poses a significant clinical challenge due to its aggressive nature and limited treatment options. Despite advancements in systemic therapies, disease progression remains nearly inevitable in CCA patients. This raises the need for better therapy strategies. While CDK 4/6 inhibitors (CDK4/6i) have demonstrated efficacy in CCA cell lines, clinical trials utilizing CDK4/6i monotherapy have yielded limited clinical activity. In this study, we investigated the potential of enhancing CDK4/6 inhibitor efficacy through drug combination strategies. Initial screening of drug libraries, in combination with CDK4/6i palbociclib, was conducted on 4 CCA cell lines (RBE, YSCCC, KKUD-068, and HuH-28). Subsequently, selected drugs from drug libraries were evaluated for their ability to enhance palbociclib sensitivity across 18 CCA cell lines using dose-response and combination index analyses at the IC_{50}. Additionally, colony formation assays were employed to assess the efficacy of single and combination drugs in preventing the emergence of resistance. Our findings revealed that HDAC inhibitors (HDACi) exhibited notable hypersensitivity in the tested CCA cell lines when combined with CDK4/6i. This combination was confirmed by combination index analyses which showed a synergistic effect (combination index < 0.8) across 18 CCA cell lines. Furthermore, the combination of HDACi and CDK4/6i demonstrated efficacy in preventing the emergence of resistance compared to a single drug either HDACi or CDK4/6i, highlighting its potential clinical utility in overcoming treatment resistance in CCA. Moreover, pre-treatment with HDACi for 3 days before adding CDK4/6i significantly enhanced the efficacy of CDK4/6i compared to a combination of the HDACi and the CDK4/6i. These results show the potential of HDACi to enhance CDK 4/6i efficacy in CCA cell lines, thereby offering a promising therapeutic strategy for CCA patients. The mechanisms of the synergistic effect between HDACi and CDK4/6i will warrant further investigation. This will offer potential therapeutic targets for enhancing treatment efficacy in CCA.

Keywords: Cholangiocarcinoma (CCA), drug combination, CDK 4/6 inhibitors (CDK4/6i), HDAC inhibitors (HDACi)

A03

Exploring the Single-Cell Dynamics of FOXM1 Under Cell Cycle Perturbations

Tooba Jawwad[1], Maliwan Kamkaew[1,2], Kriengkrai Phongkitkarun[1,3], Porncheera Chusorn[4], Somponnat Sampattavanich[1*]

[1] *Siriraj Center of Research Excellence for Systems Pharmacology, Department of Pharmacology, Faculty of Medicine Siriraj Hospital, Mahidol University, Bangkok, Thailand*
[2] *Department of Molecular Biology and Microbiology, Tufts University School of Medicine, Boston, MA, USA*
[3] *Department of Biomedical Engineering, Faculty of Engineering, Mahidol University, Salaya Campus, Nakhon Pathom, Thailand*
[4] *Faculty of Liberal Arts and Science, Roi Et Rajabhat University, Roi Et, Thailand*

*E-mail: Somponnat.sam@mahidol.edu

Abstract

The cell cycle is critical in maintaining normal cellular functions and preventing abnormal cell growth. The transcription factor FOXM1 has emerged as a crucial regulator of cell cycle progression and has been implicated in various physiological and pathological processes. Notably, FOXM1 overexpression has been observed in numerous cancer types, including liver, prostate, breast, lung, and colon cancer. Despite prior findings, our understanding of how FOXM1 dynamic behaves under different cell cycle perturbagens and its link to cell-fate decision heterogeneity remains limited. In this study, we employed high-content imaging to investigate the dynamic responses of FOXM1 in individual cells subjected to various cell cycle perturbagens. Our findings revealed that, despite both Abemaciclib and Palbociclib being CDK4/6 inhibitors, their distinct FOXM1 trajectories resulted in their clustering into different groups. Furthermore, cell cycle analysis confirmed that Palbociclib induces a more pronounced G1 arrest than Abemaciclib. Our results presented intriguing evidence that at higher concentrations, ranging from 10 μM to 2.5 μM, PLK1 inhibitors manifested a G1 arrest phenotype. Conversely, at lower concentrations, they transitioned to a G2/M arrest phenotype. Analysis at single-cell resolution identified six distinct cellular phenotypes, predicted through FOXM1 dynamical responses across various drug types and doses. Remarkably, exclusive heterogeneity was observed in PLK1 inhibitors. Collectively, our study contributed towards the groundwork for predictive modeling which could be utilized in the initial stages of drug development to assess the potential efficacy and cellular effects of candidate compounds, aiding in the selection of promising drug candidates.

Keywords: Fork head box protein M1 (FOXM1), cell cycle, single cell tracking, living cell-based biosensor

A04

The Impact of CYP3A5 Polymorphism on Sildenafil Concentrations and Cardiovascular Biomarkers in Pulmonary Hypertension

Pranisa Wongwien[1*], Burabha Pussadhamma[2], Thikhumporn Areesimpitak[1], Nontaya Nakkam[1], Sirimas Kanjanawart[1], Wichittra Tassaneeyakul[1], Suda Vannaprasaht[1]

[1] *Department of Pharmacology, Faculty of Medicine, Khon Kaen University, Khon Kaen, Thailand*
[2] *Cardiology Unit, Department of Medicine, Faculty of Medicine, Khon Kaen University, Khon Kaen, Thailand*

*E-mail: pranisa.w@kkumail.com

Abstract

Introduction: The outcomes of sildenafil treatment in pulmonary hypertension (PH) varied due to many factors, such as inter-individual pharmacokinetic differences and drug interaction. CYP3A5 is the major metabolic enzyme responsible for sildenafil metabolism. *CYP3A5* mutant alleles showed a decrease in enzyme function. Moreover, the prevalence of *CYP3A5* polymorphism was different between Asians and Caucasians. Therefore, this may affect the efficacy of sildenafil treatment in different ethnicities. The established role of *CYP3A5* genotypes in influencing sildenafil blood levels and their specific impact on sildenafil in PH patients remains limited in Thais. N terminal pro-B natriuretic peptide (NT-proBNP) is the one biomarker released from cardiomyocyte overstretching; therefore, the lower NT-proBNP levels refer a better treatment efficiency. ***Objective*:** This study evaluated the correlation between *CYP3A5* variants, sildenafil concentration, and cardiovascular biomarkers in Thai PH patients. ***Method*:** Forty-four patients were enrolled in this study. After patients fasted overnight, blood samplings were performed 1 h before and after taking the usual morning dosage of sildenafil in each patient for sildenafil trough and peak levels and *CYP3A5* genotypes. Sildenafil levels were determined using HPLC, and *CYP3A5* genotyping was performed using Taqman® SNP assay. ***Result*:** The sildenafil trough concentrations were statistically significant higher in *CYP3A5*1/*3* and *CYP3A5*3/*3* variants compared to *CYP3A5*1/*1* (wild type) (93.28±97.25 vs. 41.84±20.41 ng/mL; *P*=0.022). The sildenafil trough concentration per daily dose of *CYP3A5*1/*3* and *CYP3A5*3/*3* was higher than *CYP3A5*1/*1* genotypes (0.817±0.868 vs. 0.540±0.366 ng/mL.mg; *P*=0.329). The mean NT-proBNP levels were high in *CYP3A5*1/*3* and *CYP3A5*3/*3* when compared to wild type (1225.13±169.98 vs. 559.67±509.32 ng/L, *P*=0.104). ***Conclusion*:** *CYP3A5* mutant allele affected sildenafil trough concentration in PH patients. Because of higher severity, NT-proBNP levels in the mutant allele are higher than in the wild type. Further study in a larger population to investigate the significant impact of the *CYP3A5* polymorphism on sildenafil concentrations may be beneficial.

Keywords: Sildenafil, pulmonary hypertension, CYP3A5 genotypes, HPLC

A05

Identification of Biomarkers for Fibroblast Activation and Myofibroblast Differentiation following angiotensin II and Endothelin-1 Stimulation

Ratchanee Duangrat[1], Narawat Nuamnaichati[2], Sarawuth Phosri[3], Warisara Parichatikanond[4], Supachoke Mangmool[5*]

[1] *Department of Pharmacology, Faculty of Science, Mahidol University, Bangkok, Thailand*
[2] *Department of Pharmacology, Faculty of Medicine, Srinakharinwirot University, Bangkok, Thailand*
[3] *Department of Pharmacology and Pharmaceutical Care, Faculty of Pharmaceutical Sciences, Huachiew Chalermprakiet University, Samut Prakan, Thailand*
[4] *Department of Pharmacology, Faculty of Pharmacy, Mahidol University, Bangkok, Thailand*
[5] *Department of Pharmaceutical Care, Faculty of Pharmacy, Chiang Mai University, Chiang Mai, Thailand*

*E-mail: supachoke.man@cmu.ac.th

Abstract

Following cardiac injury, many profibrotic mediators such as angiotensin II (Ang II) and endothelin-1 (ET-1) accelerate cardiac fibroblast activation and myofibroblast differentiation, resulting in cardiac fibrosis. The progression of fibrosis within the heart leads to cardiac dysfunctions, distortion of cardiac structure, and ultimately heart failure. Thus, the early detection of activation and transdifferentiation of cardiac fibroblast might represent an attractive therapeutic approach for prevention and treatment of cardiac fibrosis. In this study, we identify fibrotic markers involving fibroblast activation and myofibroblast differentiation in adult and fetal human cardiac fibroblasts (HCFs). Treatment with Ang II significantly upregulated the mRNA levels of CTGF, VEGF, TGF-β1, fibronectin, and periostin, resulting in up to a 2-fold increase. In addition, ET-1 treatment also induced up to 2-fold increases in the mRNA levels of CTGF, VEGF, TGF-β1, α-SMA, COL1A1, COL1A2, fibronectin, and periostin in HCFs. These identified fibrotic mRNAs may serve as potential biomarkers for the early detection of cardiac fibrosis in patients with heart failure.

Keywords: Angiotensin II, biomarker, cardiac fibrosis, endothelin-1, human cardiac fibroblast

A06

Candidate HLA Alleles for Prediction of Severe Cutaneous Adverse Reactions Induced by Non-Steroidal Anti-Inflammatory Drugs in Thai Population

Jenita Kosanlawit[1], Sirimas Kanjanawart[1], Warayuwadee Amornpinyo[2], Parinya Konyoung[3], Wichittra Tassaneeyakul[1], Nontaya Nakkam[1*]

[1] *Department of Pharmacology, Faculty of Medicine, Khon Kaen University, Khon Kaen, Thailand*
[2] *Division of Dermatology, Department of Internal Medicine, Khon Kaen Hospital, Khon Kaen, Thailand*
[3] *Pharmacy Unit, Udon Thani Hospital, Udon Thani, Thailand*

*E-mail: nontna@kku.ac.th

Abstract

Non-steroidal anti-inflammatory drugs (NSAIDs) are commonly prescribed for the treatment of pain and inflammation, however, these drugs have been reported as one of the most common causative drugs of severe cutaneous adverse reactions (SCARs) including Stevens–Johnson syndrome (SJS), toxic epidermal necrolysis (TEN) and drug reactions with eosinophilia and systemic symptoms (DRESS). Although the genetic polymorphisms of human leukocyte antigen (*HLA*) genes have been proposed as genetic factors of the development of drug-induced SCARs, the information on genetic markers for SCARs induced by NSAIDs is still limited. Therefore, this study aimed to determine the associations between *HLA* class I and II polymorphisms and NSAIDs-induced SCARs in Thai population. Sixteen patients with NSAIDs-induced SCARs, consisting of 15 SJS/TEN and 1 DRESS patients were enrolled in this study. All NSAIDs-induced SCARs cases are Northeastern Thais. A control group was obtained from 183 unrelated healthy native Northeastern Thais who had no history of drug allergy. The *HLA* class I and II alleles were genotyped using the polymerase chain reaction-sequence-specific oligonucleotide probes (PCR-SSOP) method. The strength of associations was estimated by calculating the odds ratios (ORs) and 95% confidence intervals (CIs). The results showed that six *HLA* alleles including *HLA-A*68:01*, *HLA-B*56:01*, *HLA-DQA1*01:01*, *HLA-DQA1*01:02*, *HLA-DQA1*03:01* and *HLA-DQB1*03:02* were significantly associated with NSAIDs-induced SCARs. The odds ratios of NSAIDs-induced SCARs in the patients who carried one of these alleles ranged from 5.22- to 12.93-fold. The highest risk of SCARs was observed in patients with *HLA-B*56:01* allele, which was 12.93-fold significantly higher compared with those who did not carry this allele (95% CI = 1.69-98.83, *P*-value = 0.0330), followed by the *HLA-DQA1*01:01* allele and the *HLA-A*68:01* allele. These findings demonstrated the candidate *HLA* alleles that could be valid pharmacogenetic markers for the prediction of SCARs induced by NSAIDs, however, these associations deserve further exploration in larger sample sizes and other ethnicities.

Keywords: Non-steroidal anti-inflammatory drugs (NSAIDs), severe cutaneous adverse reactions (SCARs), human leukocyte antigen (HLA), pharmacogenetic

A07

Preliminary Investigation into the Anticancer Potential of Phytochemical Isothiocyanates against Cholangiocarcinoma

Nanthawut Buachaban[1], Laddawan Senggunprai[1,2], Auemduan Prawan[1,2], Sarinya Kongpetch[1,2], Piman Pocasap[1*]

[1] *Department of Pharmacology, Faculty of Medicine, Khon Kaen University, Khon Kaen, Thailand*
[2] *Cholangiocarcinoma Research Institute, Khon Kaen University, Khon Kaen, Thailand*

*E-mail: pimapo@kku.ac.th

Abstract

Cholangiocarcinoma (CCA) is an aggressive malignancy due to a difficult diagnosis, limited treatment options, and chemotherapy resistance. New therapeutic strategies are necessary to improve CCA patients' survival and quality of life. Isothiocyanates (ITCs) are phytochemical compounds in cruciferous vegetables like broccoli, cabbage, and Brussels sprouts. These compounds gained interest owing to their potential health benefits. ITCs display potent anticancer, antioxidant, and anti-inflammatory properties, inhibiting tumor progression and metastasis. Unfortunately, limited information is available regarding the role of ITC in the CCA's anticancer effect. The present study investigated the potential impact of three ITCs (sulforaphane, sulforaphane, and iberin) on the growth of the CCA cell line (KKU-452). Cell viability and cell cycle analysis were evaluated by sulforhodamine-B assay (SRB) and propidium iodide (PI) staining, respectively. The results showed that ITCs decreased cell viability in KKU-452 cells in a dose- and time-dependent manner. IC_{50} of sulforaphane, sulforaphene, and iberin were 18.23±2.06, 17.01±4.77, and 23.63±5.02 mM, respectively, after 24 h treatment, and 11.45±0.8, 10.84±0.95 and 13.60±1.11 mM, respectively, after 48 h treatment. In addition, ITCs induced cell cycle arrest at G1 and G2/M phases at 12 h and 24 h. Additional experiments are necessary to illustrate the potential of ITCs against CCA and to understand the underlying mechanisms.

Keywords: Cholangiocarcinoma (CCA), KKU-452, isothiocyanates, sulforaphane, sulforaphene, iberin

The Potential of Ethanolic Extract from *Calotropis gigantea* (L.) Dryand. Stem Bark in Combating Pathogenic Microorganisms

Chanakarn Chailom[1,2], Khemmachat Pansooksan[1,2], Naphat Kaewpaeng[1,2], Dumrongsak Pekthong[2,3,4], Piyarat Srisawang[2,5,6], Nareeluk Nakaew [7,8*], Supawadee Parhira[2,4,9*]

[1] *Department of Pharmaceutical Chemistry and Pharmacognosy, Faculty of Pharmaceutical Sciences, Naresuan University, Phitsanulok, Thailand*
[2] *Center of Excellence for Innovation in Chemistry, Naresuan University, Phitsanulok, Thailand*
[3] *Department of Pharmacy Practice, Faculty of Pharmaceutical Sciences, Naresuan University, Phitsanulok, Thailand*
[4] *Center of Excellence for Environmental Health and Toxicology, Faculty of Pharmaceutical Sciences, Naresuan University, Phitsanulok, Thailand*
[5] *Department of Physiology, Faculty of Medical Science, Naresuan University, Phitsanulok, Thailand*
[6] *Center of Excellence in Medical Biotechnology, Faculty of Medical Science, Naresuan University, Phitsanulok, Thailand*
[7] *Department of Microbiology and Parasitology, Faculty of Medical Science, Naresuan University, Phitsanulok, Thailand*
[8] *Center of Excellence in Fungal Research, Faculty of Medical Science, Naresuan University, Phitsanulok, Thailand*
[9] *Department of Pharmaceutical Technology, Faculty of Pharmaceutical Sciences, Naresuan University, Phitsanulok, Thailand*

*E-mail: nareelukn@nu.ac.th, supawadeep@nu.ac.th

Abstract

Crown flower commonly known as "*Rak*" in Thai (*Calotropis gigantea* (L.) Dryand., Apocynaceae Family) is a medicinal plant traditionally used in various medicinal applications, including for bacterial infections. Some parts, i.e., flowers and leaves, of Apocynaceae plants possess antimicrobial properties, but there is not enough information available for the stem bark of *C. gigantea*. Therefore, this research aimed to screen the antimicrobial activity of the *C. gigantea* stem bark extract to examine its potential for further investigation as an antimicrobial agent. The dry powder of *C. gigantea* stem bark was extracted with 95% ethanol using ultrasonic assistance, followed by evaporation to obtain the *C. gigantea* stem bark ethanolic crude extract (CGE). The antimicrobial activities of CGE (10 mg/mL) against 12 strains of selected pathogenic microorganisms, including two strains of gram-positive bacteria and four strains of gram-negative bacteria, four strains of fungi, and two multidrug-resistant strains (one gram-positive and one gram-negative), were evaluated using the agar disc diffusion method (30 µL/disc). The inhibition zones of CGE were observed against seven strains: two gram-positive bacteria *Staphylococcus aureus* ATCC6538 and *S. aureus* TISTR 1466; two gram-negative bacteria *Pseudomonas aeruginosa* TISTR 1467 and *Acinetobacter baumannii* ATCC 19606; one fungi *Candida krusei* TISTR 5351; and two drug-resistant strains, *S. aureus* NU 139 and *A. baumannii* AB98. CGE exhibited broad-spectrum activity against the tested microorganisms. In summary, the findings of this research demonstrated the potential of the ethanolic extract from *C. gigantea* stem bark as a valuable source for discovering antimicrobial agents, especially against multidrug-resistant strains. However, the cytotoxicity against a normal human cell line to demonstrate its safety may be required.

Keywords: *Calotropis gigantea*, stem bark, antimicrobial activity, drug-resistant bacteria

A09

Unveiling Heterogeneity in Tumor-Stroma Interactions in Multiple Myeloma Using an *In-Vitro* Co-Culture Model

Kodcharat Cheevapruk [1,3], Siwanon Jirawatnothai[1,2], Seiji Okada[3,4], Somponnat Sampattavanich[1,2*]

[1] *Department of Pharmacology, Faculty of Medicine Siriraj Hospital, Mahidol University, Bangkok, Thailand*
[2] *Siriraj Center of Research Excellence (SiCORE) for Systems Pharmacology, Department of Pharmacology, Faculty of Medicine Siriraj Hospital, Mahidol University, Bangkok, Thailand*
[3] *Graduate School of Medical Sciences, Kumamoto University, Kumamoto, Japan*
[4] *Division of Hematopoiesis, Joint Research Center for Human Retrovirus Infection, Kumamoto University, Kumamoto, Japan*

*E-mail: somponnat.sam@mahidol.edu

Abstract

Multiple myeloma (MM) is a heterogeneous cancer of plasma cells and is still largely incurable despite the availability of diverse drug options. Interactions between malignant plasma cells and bone marrow stromal cells (BMSCs) within the tumor microenvironment contribute to cancer progression and drug resistance. This study aimed to establish an *in-vitro* co-culture model of MM and BMSCs (HS-5) using a high content imaging platform for drug sensitivity testing and to investigate how stromal-MM cell interactions affect sensitivity to standard MM treatment across different genetic subtypes. In this study, we co-cultured GFP-tagged MM cell lines with HS-5 cell line to profile stroma-induced drug sensitivity shifts for major MM regimens. Our drug response profiling identified subgroup of MM cell lines exhibiting drug resistance after co-culturing, with reverse-phase protein array revealing high upregulation of proteins in the PI3K-AKT pathway. These results suggest that targeting the PI3K-AKT pathway could be a potential therapeutic target to overcome the stroma-induced drug resistance. Overall, our study provides a comprehensive resource for examining stroma-induced drug sensitivity shifts and identifying effective combinatorial regimens for MM treatment.

Keywords: Bone marrow stromal cells, drug resistance, multiple myeloma, tumor micro-environment

Anti-Inflammatory Effects of Oxyresveratrol and Resveratrol against Lead (Pb) Exposure to Human Astrocytes

Putin Nudaeng[1], Pichsinee Woonfak[2], Promsuk Jutabha[2], Pornpun Vivithanaporn[2*]

[1] *Faculty of Medicine Ramathibodi Hospital, Mahidol University, Bangkok, Thailand*
[2] *Chakri Naruebodindra Medical Institute, Faculty of Medicine Ramathibodi Hospital, Mahidol university, Samut Prakan, Thailand.*

*E-mail: pornpun.viv@mahidol.edu

Abstract

Astrocytes serve as a deposition site for lead (Pb) that enters the central nervous system. The excessive accumulation of lead in the nervous system potentiates the risk of many neurological defects, especially in young children. Lead induces the activation of astrocytes and the release of inflammatory factors and interleukins in the brain. Resveratrol and its hydroxylated derivative, oxyresveratrol, decrease the expression of proinflammatory cytokines in astrocytes. The present study hypothesized that resveratrol and oxyresveratrol can reduce Pb-induced interleukin-6 expression in human astrocytoma cells, U-87 MG. Cell viability and IL-6 production were measured at 24 h by MTT and ELISA, respectively. Pb up to 500 µM showed no cytotoxicity. Co-treatment of Pb with resveratrol and oxyresveratrol at 50 µM did not decrease cell viability. Pb at 50 and 500 µM increased IL-6 secretion of U-87 cells by 6.1 and 23.9 folds, respectively. Resveratrol and oxyresveratrol reduced Pb-induced IL-6 secretion by approximately 40%. Our results show that both resveratrol and oxyresveratrol could reduce Pb-induced inflammation in astrocytes. Thus, both compounds could potentially be developed for treating Pb-related inflammation in the central nervous system.

Keywords: Oxyresveratrol, resveratrol, lead (Pb), interleukin-6, astrocytes

CYP3A5 Polymorphism Affected Quetiapine Concentration in Psychiatric Patients

Sootthikarn Mungkhunthod[1*], Apichaya Puangpetch[3], Pongsatorn Paholpak[2], Nontaya Nakkam[1], Chonlaphat Sukasem[3,4], Wichittra Tassaneeyakul[1], Suda Vannaprasaht[1]

[1] *Department of Pharmacology, Faculty of Medicine, Khon Kaen University, Khon Kaen, Thailand*
[2] *Department of Psychiatry, Faculty of Medicine, Khon Kaen University, Khon Kaen, Thailand*
[3] *Division of Pharmacogenomics and Personalized Medicine, Departments of Pathology, Faculty of Medicine Ramathibodi Hospital, Mahidol University, Bangkok, Thailand*
[4] *Pharmacogenomics and Precision Medicine, Bumrungrad Genomic Medicine Institute (BGMI), Bumrungrad International Hospital, Bangkok, Thailand*

*E-mail: sootthikarn_m@kkumail.com

Abstract

Background: Quetiapine (QTP) is an atypical antipsychotic drug. CYP3A4/5 is the main enzyme that metabolizes QTP to N-desalkylquetiapine, an active metabolite. CYP3A5*3 was a common non-functional variant and caused the decrease of function in CYP3A5 activity. CYP3A5 mutant allele may affect the plasma concentration of QTP and treatment outcomes. Moreover, the prevalence of polymorphism of CYP3A5 was different between Asians and Caucasians. **Purpose:** This study investigated the effect of CYP3A5 polymorphism on quetiapine concentration in Thai psychiatric patients. **Method:** Fifty-three patients receiving QTP at the psychiatric outpatient department of Srinagarind Hospital, Faculty of Medicine, Khon Kaen University, Thailand, were enrolled in this study. The plasma concentration of QTP at steady state was measured using the LC-MS/MS method. Patients were genotyped of *CYP3A5*3* using a real-time PCR technique with a specific TaqMan® probe and primer. **Results:** Thirty-seven (69.81%) patients were female. The prevalence of *CYP3A5*1/*1*, *CYP3A5*1/*3*, and *CYP3A5*3/*3* were 11.32%, 41.51%, and 47.17%, respectively. The patients who carried *CYP3A5*3/*3* had 4.3-fold higher mean plasma concentrations of the QTP than *CYP3A5* 1/*3* and *CYP3A5*1/*1* but no statistical significance difference (84.89±81.94, 49.77±102.32 and 19.87±11.68, respectively, *P*=0.181). The concentration per dose (C/D) ratio of QTP was 2.3-fold higher in *CYP3A5*3/*3* than in wild-type and *CYP3A5*1/*3* patients (0.64±0.45 vs. 0.28±0.40, *P*=0.05). **Conclusions:** The C/D ratio of QTP for the patients carrying *CYP3A5*3/*3* was higher than for wild-type and heterozygous patients. Therefore, homozygous mutant patients may have an increased risk of adverse effects compared to other groups. The investigation of *CYP3A5* genotypes may help adjust the dosage of QTP to reduce adverse effects and improve treatment outcomes for psychiatric patients.

Keywords: Quetiapine, CYP3A5 polymorphisms, psychiatric patients, pharmacogenetic, plasma level

Comparison of Effector Functions between γδ T cells and NK Cells against cholangiocarcinoma Cells

Inthu-on Kulma[1,2], Kesara Na-Bangchang[2], Masashi Iwasaki[3], Hiromi Tomono[4], Craig T. Morita[5], Haruki Okamura[6], Hiroshi Mukae[4], Yoshimasa Tanaka[1,3*]

[1] *Center for Medical Innovation, Nagasaki University, Nagasaki, Japan*
[2] *Graduate Program in Bioclinical Sciences, Chulabhorn International College of Medicine, Thammasat University (Rangsit Campus), Pathumthani, Thailand*
[3] *Center for Innovation in Immunoregulative Technology and Therapeutics, Graduate School of Medicine, Kyoto University, Kyoto, Japan*
[4] *Department of Respiratory Medicine, Graduate School of Biomedical Sciences, Nagasaki University, Nagasaki, Japan*
[5] *Division of Immunology, Department of Internal Medicine, University of Iowa, Veterans Health Care System, Iowa City, IA, USA*
[6] *Laboratory of Tumor Immunology and Cell Therapy, Hyogo College of Medicine, Nishinomiya, Japan*

*E-mail: ystanaka@nagasaki-u.ac.jp

Abstract

Cholangiocarcinoma (CCA) is a rare disease characterized by malignant cells derived from the epithelial cells of the biliary duct system. One identified risk factor is infection with *Opisthorchis viverrini*, a parasitic worm found in fresh waters in Southeast Asia. Despite extensive treatments, the prognosis for CCA remains poor, emphasizing the critical need for the development of novel treatments. Considerable attention has been directed towards innate immune effector cells, which can recognize tumor cells independently of the major histocompatibility complex, laying the foundation for developing off-the-shelf drugs. In this study, we cultured innate immune cells obtained from the peripheral blood of healthy adults. We conducted a comparative analysis of the effector functions of γδ T cells and NK cells against the eight CCA cell lines, i.e., HuCCT1, TFK-1, SkChA1, RBE, MzChA1, MzChA2, TGBC1TKB, and TGBC2TKB. This analysis was performed using standard short- and long-term cytotoxicity assays (incubation period of 1 and 72 h, respectively) and ELISA for IFN-γ level. γδ T cells demonstrated cytotoxicity and IFN-γ production in response to CCA cell lines in a TCR-dependent manner, particularly in the presence of a bisphosphonate prodrug. In contrast, direct killing or antibody-independent and antibody-dependent cellular cytotoxicity were relatively slow and weak. Conversely, NK cells displayed potent, direct cytotoxicity against CCA cells. In summary, both γδ T cells and NK cells show promise as innate immune effector cells for adoptive transfer therapy in the context of CCA.

Keywords: Bisphosphonate, cancer immunotherapy, cholangiocarcinoma, γδ T cell, interleukin-18, natural killer cell

Anti-HER2 Treatment in CCA Cell Lines Provides Variable Anti-Cancer Effects on HER2 Pathway Activity

Satinee Aroonpruksakul, Siwanon Jirawatnotai*

Department of Pharmacology, Faculty of Medicine Siriraj Hospital, Faculty of Medicine Siriraj Hospital, Mahidol University, Bangkok, Thailand

*E-mail: siwanon.jir@mahidol.ac.th

Abstract

HER2 plays crucial roles in carcinogenesis and HER2 aberrations were frequently found in various types of cancer such as breast cancer, stomach cancer, and non-small cell lung cancer (NSCLC). HER2 amplification was found in approximately 10-15% of cholangiocarcinoma (CCA) cases, however, the effect of anti-HER2 in CCA is still controversial. In this study, we examined the effect of lapatinib on cell proliferation together with the background of HER2 protein basal level and the status of HER2 downstream signaling in 14 CCA cell lines. Concentration-dependent antiproliferative effects of lapatinib were found in 4 CCA cell lines at the GR50 less than 1 μM, however, the sensitivity of lapatinib was not directly correlated to HER2 protein level or HER2 phosphorylation. We further tested the effects of lapatinib on the growth signaling pathways throughout various time points up to 24 h and found that Akt and ERK activation were decreased in a time-dependent manner. Furthermore, by overexpressed HER2 in CCA cells, we found an increase in ERK activation especially in lapatinib-sensitive cell lines while the GR50 of lapatinib in these cells were increased compared with the empty vector cells which supported the roles of HER2 signaling on CCA survival and anti-HER2 sensitivity. Taken together, the results from this study suggest that anti-HER2 treatment is effective in subsets of CCA cell lines through the alteration of HER2 downstream signaling.

Keywords: HER2, cholangiocarcinoma, CCA, HER2 downstream signaling, ERK

The Role of UVB in Keratinocyte Migration Through Mediating Inflammatory Response and Oxidative Stress: The *In Vitro* Wound-Healing Potential of Nicotinamide

Kannika Nola, Uraiwan Panich*

Departments of Pharmacology, Faculty of Medicine Siriraj Hospital, Mahidol University, Bangkok, Thailand

*E-mail: uraiwan.pan@mahidol.ac.th

Abstract

Ultraviolet radiation (UVR) is a significant environmental stressor that affects the skin, primarily targeting keratinocytes as the main receptors of UVB light. The primary cellular targets for UVB-induced inflammation and compromised wound healing are the epidermal keratinocytes. Despite considerable research, the precise impacts of UVB radiation on skin wound healing and the migration of keratinocytes are still not well understood. In this study, our aim was to investigate whether UVB impairs keratinocyte migration by mediating cellular differentiation and inflammation. We also explored the potential wound migration effects of mitochondrial-targeted compounds including nicotinamide, on human keratinocyte cell line (HaCaT) exposed to UVB irradiation using as cell migration assay. Our findings revealed that UVB doses of 15 and 30 mJ/cm^2 did not induce toxicity in HaCaT cells but significantly increased intracellular ROS levels, as determined by PI and DCFDA flow cytometry assays, respectively. Additionally, UVB exposure delayed HaCaT cell migration, correlating with the induction of keratinocyte differentiation genes, such as keratin 1 (KRT1), keratin 10 (KRT10), and involucrin (IVL). Furthermore, UVB radiation stimulated the expression of inflammatory genes, including interleukin-6 (IL-6) and tumor necrosis factor-alpha (TNF-α), in HaCaT cells, as detected by real-time quantitative PCR (qPCR). Moreover, our findings demonstrated that nicotinamide promoted cell migration in UVB-irradiated HaCaT cells. We conclude that UVB exposure impaired the migration of HaCaT cells through the activation of ROS formation and induction of keratinocyte differentiation genes (KRT1, KRT10, and IVL), as well as increased expressions of IL-6 and TNF-α mRNA. Nicotinamide demonstrates promise in improving the migration of UVB-irradiated HaCaT cells, and its effects on wound healing in the context of UVB-induced photooxidative stress warrant further study. These findings may pave the way for the development of novel wound healing agents, addressing the challenges posed by chronic wounds and advancing therapeutic approaches.

Keywords: Keratinocyte migration, ultraviolet B, nicotinamide, inflammation

PM2.5 Affects Migration of HaCaT Keratinocytes via Modulating Nrf2 Activity and Stimulating Matrix Metalloproteinases

Punyapa Laprattanawiboon, Uraiwan Panich*

Departments of Pharmacology, Faculty of Medicine Siriraj Hospital, Mahidol University, Bangkok, Thailand

*E-mail: uraiwan.pan@mahidol.ac.th

Abstract

Fine particulate matter (PM2.5) significantly impacts multiple body tissues, notably the skin, by disrupting the wound healing process via various biological mechanisms including oxidative stress and inflammatory response. Understanding the specific impacts of PM2.5 pollution is vital for the development of preventive and therapeutic interventions that aim to lessen its negative effects on the healing of wounds. The objective for this study is to assess the role of PM2.5 in modulating migration of HaCaT keratinocytes via stimulation of oxidative stress and matrix metalloproteinase (MMP)-1, MMP-9 and nuclear factor E2-related factor 2 (Nrf2). PM2.5 was purchased as Standard Reference Material (SRM) which prepared in FBS-free media before each experiment. Our results demonstrated that the exposure of HaCaT keratinocytes to PM2.5 induced ROS formation as measured through DCFDA flow cytometry assay. It was found to decrease cell migration in association with lower Nrf2 expression as well as higher MMP-1 and MMP-9 expression through immunofluorescence. RT-PCR results also suggested higher mRNA expressions of cellular differentiation genes, including keratin 1 (KRT1), keratin 10 (KRT10), and involucrin (IVL). With Nrf2 as the main regulator in cellular homeostasis and its contribution to wound healing, our findings revealed that PM2.5 decreased migration of HaCaT keratinocytes in association with modulation of cellular differentiation genes (KRT1, KRT10, IVL), and inflammatory proteins including MMP-1 and MMP-9. Our study concluded that PM2.5 impaired HaCaT keratinocyte migration via stimulation of inflammatory responses, oxidative stress and downregulation of Nrf2 activity. Further studies are warranted to identify candidate proteins involved in PM2.5-regulated wound healing *in vitro* and *in vivo*.

Keywords: Human keratinocytes, reactive oxygen species, nrf2, particulate matter ≤2.5 μm (PM2.5), aryl hydrocarbon, cell migration

Systems Biology-Based Drug Screening to Overcome Drug Resistance for Asian Cholangiocarcinoma

Supawan Jamnongsong[1], Piyathida Tawornparcha,[1,2], Siwanon Jirawatnotai[1], Somponnat Sampattavanich[1*]

[1] *Siriraj Center of Research Excellence for Systems Pharmacology, Department of Pharmacology, Faculty of Medicine Siriraj Hospital, Mahidol University, Bangkok, Thailand*
[2] *Science Division, Mahidol University International College, Nakhon Pathom, Thailand, Thailand*

*E-mail: somponnat.sam@mahidol.edu

Abstract

Our research group has recently identified repurposable drugs for treatment of Asian-derived cholangiocarcinoma (CCA) based on comprehensive drug response and pan-omic profiling. We also developed the CCA45 gene-expression signature, which is highly accurate in predicting prognosis for Asian CCA patients. To gain further insight into therapeutic candidates and potential resistance mechanisms, we established CCA1 subgroup cell lines that were resistant to their subgroup-specific drug candidates, namely MEK and SRC inhibitors. Reverse-phase protein arrays (RPPA) revealed distinct pathway activation between MEKi-resistant (MEKi-R) and SRC-resistant (SRCi-R) CCA1 subgroup cell lines. MEKi-R cells showed upregulation of SRC and Ras-MAPK pathways, whereas SRCi-R cells exhibited upregulation of PI3K-mTOR and cell cycle pathways. Interestingly, CDK4/6 inhibitors could effectively kill MEKi-R cells, while SRCi-R cells developed cross-resistance to MEK inhibitors and only weak sensitivity to CDK4/6 inhibitors. Our findings contribute to the development of alternative regimens in drug-resistant Asian CCA.

Keywords: Cholangiocarcinoma, systems biology, drug resistance, drug screening

The Selective HDAC8 Proteolysis Targeting Chimera Induces S-phase Arrest and Apoptosis in Glioblastoma

Jiranan Chotitumnavee[1], Chareerat Pruksaniyom[1], Rapeewan Settacomkul[2], Ratchanon Sukprasert[2], Sirada Srihirun[1], Yukihiro Itoh[3], Takayoshi Suzuki[3], Pornpun Vivithanaporn[2*]

[1] *Department of Pharmacology, Faculty of Dentistry, Mahidol University, Bangkok, Thailand*
[2] *Chakri Naruebodindra Medical Institute, Faculty of Medicine Ramathibodi Hospital, Mahidol University, Samut Prakan, Thailand*
[3] *SANKEN, Osaka University, Mihogaoka, Ibaraki-shi, Osaka, Japan*

*E-mail: pornpun.viv@mahidol.edu

Abstract

Histone deacetylase (HDAC) proteins are crucial enzymes for cell proliferation and survival. The selective HDAC8 Proteolysis Targeting Chimera (HDAC8 PROTAC) is a heterobifunctional molecule equipped with an HDAC8 ligand and an E3 ligase ligand which induces the ubiquitin-proteasome system for the degradation of HDAC8 protein. While HDAC8 inhibitors showed the anti-proliferation effect in glioblastoma cell lines and prolonged CT2A-bearing mice survival, the novel strategy applying the HDAC8 PROTAC has not yet been explored for its effects. In this study, we aimed to investigate the effect of the pioneer selective HDAC8 PROTAC on a glioblastoma cell line, U-87 MG cells. We first investigated the cell cytotoxicity effect using 2,5-diphenyl-2H-tetrazolium bromide (MTT) assay, the result showed the HDAC8 PROTAC caused cell cytotoxicity effect in a dose-dependent manner with the half-maximal inhibitory concentration (IC_{50}) of 4.87 μM. The anti-proliferative effect was examined using Cell Proliferation Staining Deep Red Cytopainter. In addition, real-time fluorescence shift was captured via Incucyte®. The results suggested that the HDAC8 PROTAC inhibited cell proliferation in dose- and time-dependent manners. Using cell cycle analysis by propidium iodide DNA labelling technique, HDAC8 PROTAC induced S-phase cell cycle arrest by increasing the accumulation of cells in the S-phase. Lastly, we examined whether the HDAC8 PROTAC could induce glioblastoma cell apoptosis by using the Annexin V-PE apoptosis assay, the results showed that HDAC8 PROTAC induced cell apoptosis in a dose-dependent manner with the half maximal effective concentration (EC_{50}) of 4.68 μM. The inhibition of cell proliferation and induction of apoptosis of HDAC8 PROTAC is greater than those of the conventional HDAC8 inhibitor. Collectively, our study, encompassing cell cytotoxicity, antiproliferation, apoptotic cell death, and cell cycle arrest, highlights the potential of the HDAC8 PROTAC as an effective strategy against glioblastoma cell proliferation.

Keywords: Proteolysis targeting chimera, glioblastoma, histone deacetylase 8, histone deacetylase, HDAC8 Protac

Understanding the Mutation Landscapes: Pre-Treatment vs. Recurrent Squamous Cell Carcinoma of the Oral Cavity and Possible Mechanism of Resistance to Standard Treatment

Tongchai Payungwong[1], Krittaya Angkulkrerkkrai[2], Amphun Chaiboonchoe[1], Wirote Lausoontornsiri[3], Siwanon Jirawatnotai[1], Somjin Chindavijak[2*]

[1] *Siriraj Center of Research Excellence in Systems Pharmacology, Department of Pharmacology, Faculty of Medicine Siriraj Hospital, Mahidol University, Bangkok, Thailand*
[2] *Center of Excellence of Otolaryngology Head and Neck Surgery, Rajavithi Hospital, Bangkok, Thailand*
[3] *Medical Oncology, Samitivej Hospital, Bangkok, Thailand*

*E-mail: jksomjin@hotmail.com

Abstract

Oral squamous cell carcinoma (OSCC) poses a significant challenge due to its high recurrence rate. Understanding the genetic mutation landscape of OSCC may elucidate mechanisms of resistance to standard treatment. This study delves into the genetic mutations associated with pathobiology and treatment response by comparing the mutation landscapes of matched pre-treatment and recurrent OSCC tumors. In this study, 33 Formalin-fixed paraffin-embedded (FFPE) samples of recurrent tumors, primary tumors, and pre-recurrence primary tumors were sequenced from Rajavithi Hospital's collection using Oncomine Ion Torrent-based next-generation sequencing targeting a 517 cancer-associated gene panel. Our analysis revealed KMT2D, a histone methyltransferase, as the most frequently mutated gene (54.55%), suggesting a potential role of epigenetic dysregulation in OSCC tumorigenesis. Functional protein association network analysis highlighted the enrichment of genes regulating the cancer cell cycle (MRE11A, CDKN2A, and CYLD) in recurrent tumors, confirmed in primary-recurring matched pairs, suggesting their role in tumor recurrence. Moreover, recurrent tumors exhibited a distinct subset of genes, possibly sub-clonal mutations driving recurrence, absent in primary tumors responsive to standard treatment. Conversely, non-recurrent tumors showed enrichment of DNA repair genes (ATR, BRCA1, BRCA2, RAD50, MUTYH), suggesting their involvement in treatment response variability. Our pilot study identifies key pathways of oral cancer carcinogenesis and specific gene sets indicative of treatment responses and prognoses, shedding light on potential therapeutic targets and personalized treatment strategies for OSCC patients.

Keywords: Recurrent oral squamous cell carcinoma, mutation landscape, cancer cell cycle, DNA repair, epigenetics

Genetic Alterations of Suppressor Genes TP53 and CDKN2A in Intrahepatic Cholangiocarcinoma in Thailand

Rehab Osman Idris[1], Kesara Na-Bangchang[1,2], Wanna Chaijaroenkul[1*]

[1] *Chulabhorn International College of Medicine, Thammasat University, Rangsit Center, Klong Luang, Pathum Thani, Thailand*
[2] *Center of Excellence in Pharmacology and Molecular Biology of Malaria and Cholangiocarcinoma, Chulabhorn International College of Medicine, Thammasat University, Rangsit Center, Klong Luang, Pathum Thani, Thailand*

*E-mail: wn_ap39@yahoo.com

Abstract

Intrahepatic cholangiocarcinoma (iCCA) is the second most common malignancy of primary liver cancer, accounting for about 10-20% of all cholangiocarcinoma. It arises from the bile duct epithelium and can be classified based on its location within the biliary tree. The incidence of iCCA has been increasing globally, with particularly high rates observed in Southeast Asia, especially Thailand. *Opisthorchis viverrini* (OV) infection is endemic in some parts of the northeastern region of Thailand and is associated with a higher risk of developing CCA. Early stages of iCCA are a challenge to be diagnosed, which contributes to a poor prognosis. The study aims to investigate genetic alterations in the TP53(rs1042522) and CDKN2A(rs 3731249) tumor suppressor genes among the study groups. This research is conducted by extracting genomic DNA from blood samples obtained from 156 healthy volunteers, 115 patients with iCCA, and 60 patients with OV-infection patients. The genotyping of TP53 and CDKN2A variants was performed using PCR-RFLP. The genotype frequencies of TP53: GG, GC, and CC in the iCCA group were 26.1%, 53.9%, and 20%, respectively. In OV-infection patients, the TP53 genotype was 21.7%, 46.7%, and 31.7% of GG, GC, and CC, respectively. And the TP53 genotype in the healthy group was 31.4% for GG, 41.7% for GC, and 26.9% for CC. In contrast to TP53, the variation of gene CDKN2A was less than 1%. Only 1% of heterozygous TC was found in the iCCA group. In conclusion, we found that TP53 (rs1042522) is the most frequently altered gene among the three groups.

Keywords: Intrahepatic cholangiocarcinoma, TP53, CDKN2A, RFLP-PCR

A20

Nrf2 Plays a Role in Temozolomide Resistance in Glioblastoma under Hypoxia

Tasanee Onkoksoong[1], Pinpat Tripatara[1], Sunisa Prasopporn[2], Sith Sathornsumetee[3], Siwanon Jirawatnotai[1,2], Uraiwan Panich[1,2*]

[1] *Department of Pharmacology, Faculty of Medicine Siriraj Hospital, Mahidol University, Bangkok, Thailand*
[2] *Siriraj Center of Research Excellence (SiCORE) for Systems Pharmacology, Department of Pharmacology, Faculty of Medicine Siriraj Hospital, Mahidol University, Bangkok, Thailand*
[3] *Department of Medicine, Faculty of Medicine Siriraj Hospital, Mahidol University, Bangkok, Thailand*

*E-mail: uraiwan.pan@mahidol.edu

Abstract

Hypoxia is suggested to contribute to chemoresistance of malignant solid tumors including glioblastoma (GBM). Activation of nuclear factor erythroid 2-related factor 2 (Nrf2) is proposed to be involved in the mechanisms underlying hypoxia-induced chemotherapeutic resistance. In this study, we aimed to investigate an involvement of Nrf2 in hypoxia-mediated temozolomide (TMZ) resistance in GBM and whether a well-known Nrf2 inhibitor, brusatol, increased TMZ sensitivity under hypoxia. U87MG cell lines were treated with TMZ and brusatol under normoxia and hypoxia then, analyzed cell viability, determined the half maximal inhibitory concentration (IC_{50}) and performed combination index (CI) analysis to assess the effects of combined TMZ and brusatol treatment. The results showed that treatment with TMZ markedly suppressed U87MG cell proliferation under both normoxic and hypoxic conditions. However, hypoxia was observed to attenuate TMZ sensitivity in U87MG cells as the IC_{50} of TMZ under hypoxia was significantly higher than that under normoxia. Furthermore, the cells under hypoxia showed the substantial induction of HIF-1α protein and Nrf2 nuclear translocation. Hypoxia led to a transient increase in cellular reactive oxygen species (ROS) formation at the early time-point and its decline was observed at later time-points in U87MG cells. Our results suggested that brusatol combined with TMZ effectively suppress U87MG cell proliferation more than TMZ alone. The combination showed synergistic effects on cell cytotoxicity under both hypoxic and normoxic conditions, although cells were more resistant to the co-treatment under hypoxia. Hypoxia might cause TMZ resistance in GBM cells via HIF-1α and Nrf2 upregulation. Brusatol could enhance TMZ sensitivity in U87MG, suggesting that combination of the Nrf2 inhibitor with TMZ may represent promising therapeutic approach for GBM treatment.

Keywords: Glioblastoma, brusatol, hypoxia, nuclear factor erythroid 2-related factor 2, temozolomide, chemoresistance, reactive oxygen species

A21

Conditional Antimicrobial Peptide Therapeutics

Chayanon Ngambenjawong[1,2,3], Leslie W. Chan[1,4], Sangeeta N. Bhatia[1,2,5,6,7,8*]

[1] *Koch Institute for Integrative Cancer Research, Massachusetts Institute of Technology, Cambridge, MA, USA*
[2] *Institute for Medical Engineering and Science, Massachusetts Institute of Technology, Cambridge, MA, USA*
[3] *Present address: School of Biomolecular Science and Engineering, Vidyasirimedhi Institute of Science and Technology, Rayong, Thailand*
[4] *Present address: Wallace H. Coulter Department of Biomedical Engineering, Georgia Institute of Technology and Emory School of Medicine, Atlanta, GA, USA*
[5] *Howard Hughes Medical Institute, Cambridge, MA, USA*
[6] *Department of Electrical Engineering and Computer Science, Massachusetts Institute of Technology, Cambridge, MA, USA*
[7] *Department of Medicine, Brigham and Women's Hospital and Harvard Medical School, Boston, MA, USA*
[8] *Broad Institute of Massachusetts Institute of Technology and Harvard, Cambridge, MA, USA*

*E-mail: sbhatia@mit.edu

Abstract

Antimicrobial resistance represents a global threat that calls for development of new antibiotics and alternatives. Antimicrobial peptides (AMPs) represent a promising alternative to antibiotics with diverse mechanisms of action including bacterial membrane lysis, biofilm disruption, and immunomodulation. However, systemic application of AMPs is hampered by short circulation time and toxicity, limiting their application to topical formulation. Here, we aimed to develop a conditional therapeutic for formulation of AMPs to address the above-mentioned issues. Specifically, we formulated an albumin-binding domain (ABD)-AMP conjugate as a long-circulating conditional AMP therapeutic with a masked activity that can be conditionally activated by proteases specific to the site of bacterial infection. In a mouse model of *Pseudomonas aeruginosa* lung infection, we demonstrated that our ABD-AMP conjugate delivered more active AMP to the infected lungs compared to the free AMP treatment. In addition, the ABD-AMP conjugate minimally released active AMP in other off-target organs (liver, spleen, and kidney) leading to improved safety profile of the conjugate over the free AMP. Our report on ABD-AMP conjugate and its optimization pipeline provides a framework for development of conditional therapeutics to treat infection as well as other diseases.

Keywords: Nanomedicine, conditional therapeutic, antimicrobial peptide, protease, albumin

A22

Establishment of Novel Cholangiocarcinoma Cell Lines with ARID1A Deficiency and Preclinical Validation of Synthetic Lethality Therapies

Sunisa Prasopporn[1,2], Gunya Sittithumcharee[2], Jantappapa Chanthercrob[2], Somchai Limsrichamrern[3], Arada Hirunkitti[2], Pimkanya More-Krong[2], Sakda Sathirareuangchai[4], Amphun Chaiboonchoe[2], Somponnat Sampattavanich[1,2], Seiji Okada[5], Siwanon Jirawatnotai[1,2*]

[1] *Department of Pharmacology, Faculty of Medicine Siriraj Hospital, Mahidol University, Bangkok, Thailand*
[2] *Siriraj Center of Research Excellence for Precision Medicine and Systems Pharmacology, Faculty of Medicine Siriraj Hospital, Mahidol University, Bangkok, Thailand*
[3] *Hepato-Pancreato-Biliary and Transplantation Surgery Unit, Department of Surgery, Faculty of Medicine, Siriraj Hospital, Mahidol University, Bangkok, Thailand*
[4] *Department of Forensic Medicine, Faculty of Medicine, Siriraj Hospital, Mahidol University, Bangkok, Thailand*
[5] *Division of Hematopoiesis, Joint Research Center for Human Retrovirus Infection, Kumamoto University, Kumamoto, Japan*

*E-mail: iwanon.jir@mahidol.ac.th

Abstract

Cholangiocarcinoma (CCA) is a highly lethal malignancy of the bile duct. The high mortality rate is primarily due to the unresponsive nature of the cancer to the standard chemotherapies and the lack of targetable oncogenes. Loss of a tumor suppressor protein ARID1 A, is a recurrent event in several types of cancer, including cholangiocarcinoma. Synthetic lethality caused by ARID1A loss of function is among the most studied strategies for treating cancer with ARID1A mutation. To establish authentic ARID1A-deficient CCA cell lines which can be used as models for drug testing and studying for roles of ARID1A in CCA. We established and characterized two CCA cell lines from the moderately differentiated CCA of intrahepatic origin. We characterized the cell lines, i.e. tumor markers, karyotype, growth rate and doubling time, exome and transcriptome analyses, and *in vivo* tumorigenesis, and performed drug testing on these cell lines. Two novel cell lines named SiSP-K01 and SiSP-K05carry heterozygous loss of ARID1A loci and a complete loss of ARID1A protein expression. SiSP-K01and SiSP-K05had doubling times in culture of 37.17±2.37 and 44.55±1.83 h, respectively. They expressed putative markers of cholangio-carcinoma, such as EMA, CA19-9, CEA, CK7, and CK19, consistent with the tissues of origin. Gene expression profiles confirmed the resemblance of the cell lines to cancer cells from the gastrointestinal origin. Both cell lines showed high uptake rates of tumorigenicity in immunocompromised animals. We showed that these CCA cell lines were hypersensitive to PI3K/AKT and PARP inhibitors. We have established two authentic ARID1A loss-of-function cholangiocarcinoma cell lines that are suitable for the study of ARID1A-negative cancer and as models for CCA drug development.

Keywords: Cholangiocarcinoma, ARIDA, synthetic lethality, PI3K inhibitor, AKT inhibitor, PAPR inhibitor

A23

In Vivo Evaluation of *Andrographis paniculata* and *Boesenbergia rotunda* Extract Activity against SARS-CoV-2 Delta Variant in Syrian Golden Hamsters: Potential Herbal Alternative for COVID-19 Treatment

Supasek Kongsomros[1], Tussapon Boonyarattanasoonthorn[2], Teetat Kongratanapasert[2,3], Piyanate Sunyakumthorn[4], Rawiwan Im-Erbsin[4], Luis A. Lugo-Roman[4], Jiraporn Paha[1], Suwimon Manopwisedjaroen[1], Pakakrong Kwankhao[5], Kittitach Supannapan[5], Nittaya Ngamkhae[5], Nitipol Srimongkolpithak[6], Pornpun Vivithanaporn[2], Suradej Hongeng[7], Arunee Thitithanyanont[1], Phisit Khemawoot[2*]

[1] *Department of Microbiology, Faculty of Science, Mahidol University, Bangkok, Thailand*
[2] *Chakri Naruebodindra Medical Institute, Faculty of Medicine Ramathibodi Hospital, Mahidol University, Samutprakarn, Thailand*
[3] *Program in Translational Medicine, Faculty of Medicine Ramathibodi Hospital, Mahidol University, Bangkok, Thailand*
[4] *Department of Veterinary Medicine, United States Army Medical Directorate, Armed Forces Research Institute of Medical Sciences (USAMD-AFRIMS), Bangkok, Thailand*
[5] *Chao Phraya Abhaibhubejhr Hospital Foundation, Prachinburi, Thailand*
[6] *National Center for Genetic Engineering and Biotechnology (BIOTEC), National Science and Technology Development Agency (NSTDA), Pathum Thani, Thailand*
[7] *Department of Pediatrics, Faculty of Medicine Ramathibodi Hospital, Mahidol University, Bangkok, Thailand*

*E-mail: phisit.khe@mahidol.ac.th

Abstract

The COVID-19 pandemic has hastened the development of effective medication, particularly for the highly pathogenic variants of the SARS-CoV-2 virus. This research aimed to evaluate the efficacy of *Andrographis paniculata* and *Boesenbergia rotunda* extract in SARS-CoV-2-infected hamsters. A total of 36 Eight-week-old male hamsters were randomly divided into three groups. At day 0, all hamsters in each group were intranasally infected with 50 µL of 5×10^4 PFU of SARS-CoV-2. At 12 h post-infection, either a 2 mL/kg/day of vehicle control (DMSO) or 1,000 mg/kg/day of the treatment (*B. rotunda* or *A. paniculata* extract with a loading dose of 1,000 mg/kg on the first day) were orally administered for 7 consecutive days. Samples were collected and processed to determine the viral loads, the concentrations of panduratin a and andrographolide, histopathology of hamster lungs, and inflammatory cytokines levels at day 1, 3, and 7 post-infection. The oral administration of *A. paniculata* extract significantly reduced both the lethality and severity of the infection compared with the vehicle control and *B. rotunda* extract. However, neither extract showed direct antiviral activity by decreasing viral load in the lungs. *A. paniculata* extract significantly decreased interleukin-6 (IL-6) protein levels in the lung tissues, which was consistent with the reduction of histological lesions in the lungs of infected hamsters. In addition, both extracts significantly reduced IL-6 and interferon-gamma-induced protein 10 mRNA expression in peripheral blood mononuclear cells of infected hamsters. The potential of *A. paniculata* extract as a medication for SARS-CoV-2 arises from its ability to alleviate inflammation and lung pathology.

Keywords: *Andrographis paniculata*, *Boesenbergia rotunda*, Syrian golden hamster, SARS-CoV-2, COVID-19

Preliminary Investigation the Potential of Injectable Hydrogels Containing Collagen Hydrolysate for an Articular Cartilage Repair in a Rat Osteochondral Defect Model

Jiraporn Sriwong[1], Kitipong Pasanaphong[2], Nirada Srianake[1], Scarlett Desclaux[1], Nuttapol Tanadchangsaeng[2], Nuttapol Risangud[3], Sutee Wangtueai[4], Tulyapruek Tawonsawatruk[5], Ruedee Hemstapat[1*]

[1] *Departments of Pharmacology, Faculty of Science, Mahidol University, Bangkok, Thailand*
[2] *College of Biomedical Engineering, Rangsit University, Lak-Hok, Pathumthani, Thailand*
[3] *The Petroleum and Petrochemical College, Chulalongkorn University, Pathumwan, Bangkok, Thailand*
[4] *College of Maritime Studies and Management, Chiang Mai University, Tha Chin, Muang, Samut Sakhon, Thailand*
[5] *Department of Orthopaedics, Faculty of Medicine Ramathibodi Hospital, Mahidol University, Thung Phaya Thai, Ratchathewi, Bangkok, Thailand*

*E-mail: ruedee.hem@mahidol.ac.th

Abstract

An osteochondral defect occurs when a portion of the cartilage in a joint is damaged, often due to factors like excessive weight and age-related wear and tear. Various treatments exist to restore the osteochondral defect including microfracture and transplant procedures. However, these techniques often have limitations and may not provide the desired long-term efficacy, the quest for improved techniques continues. Collagen hydrolysate, known for its anti-inflammatory properties has emerged as a promising candidate for treating osteo-arthritis (OA). Additionally, pluronic-F127 and click chemistry based injectable biodegradable hydrogel have been investigated as scaffolds for cell cultures, in which it helps facilitating the adhesion of stem cells derived from bone marrow to repair bone gaps. Therefore, this study aimed to investigate the potential of using a combination of pluronic-F127 and click chemistry based injectable hydrogel and collagen hydrolysate derived from tuna tendon as a scaffold for osteochondral repair in a rat osteochondral defect model. Macroscopic observation of the femoral condyle surface along with micro-computed tomography (CT) were performed to assess lesion repair in three groups of rats treated with either phosphate-buffered saline (PBS), hydrogel without collagen hydrolysate and hydrogel containing collagen hydrolysate. It was observed that the articular surface area of the damaged femoral condyle demonstrated a trend towards restoration when treated with a hydrogel containing collagen hydrolysate compared to hydrogel without collagen hydrolysate and PBS, which yielded comparable results. Similar trend was also observed from 3D micro-CT imaging. These findings suggest that the injectable hydrogel containing collagen hydrolysate may be effective in promoting cartilage regeneration and may also help with bone repair. However, further histological examination is needed to confirm these findings.

Keywords: Hydrogel, collagen hydrolysate, osteochondral defect rat model

F01

Dapagliflozin Improves Vascular Reactivity via Decreasing Vascular Superoxide Production and Enhancing Antioxidant Enzyme Activity in Metabolic Syndrome Rats

Nattawut Chaisuk, Kampeebhorn Boonloh, Patchareewan Pannangpetch, Panot Tangsucharit*

Department of Pharmacology, Faculty of Medicine, Khon Kaen University, Khon Kaen, Thailand

*E-mail: npantan@kku.ac.th

Abstract

High-Fat High-fructose Diet (HFFD) can cause metabolic syndrome (MS) including insulin resistance, hyperglycemia, dyslipidemia, and hypertension. We aimed to investigate a vasoprotective effect and a possible mechanism of action of DAPA in HFFD-induced MS rats. Male Wistar rats were fed a normal diet or HFFD for 10 weeks, and the MS animals were then treated with DAPA (1 and 5 mg/kg/day), metformin 200 mg/kg/day or distilled water (MS control group) for further 6 weeks. At the end of treatment, fasting blood glucose (FBG), oral glucose tolerance (OGT), serum insulin, lipid profile, oxidative stress markers, nitric oxide (NO) production and hemodynamic parameters were measured. The vascular responses to vasodilators (acetylcholine and sodium nitroprusside) and vasoconstrictor (phenylephrine) were assessed. The MS controls showed significantly increased FBG, impaired OGT, increased insulin resistance, dyslipidemia, together with increased systolic blood pressure (SBP), diastolic blood pressure (DBP) and mean arterial pressure (MAP) as compared to normal controls. A significant decrease in endothelial dependent-vasodilatation and increase in adrenergic vasoconstriction were also found. All the oxidative markers were significantly disordered. DAPA or metformin administration significantly corrected all of those disturbed parameters of glucose and lipid metabolism. Interestingly, DAPA significantly lower the high blood pressure: SBP, DBP and MAP. Remarkably, DAPA significantly improved the decrease in BP in response to endothelial dependent vasodilator acetylcholine, and DAPA possessed antioxidant activity: decreasing of oxidants (vascular superoxide production), and increasing of antioxidant enzyme activity (CAT and SOD). The serum NO level was also significantly increased. Since, it has been known that free radicals could damage vascular endothelial cells resulting in decreasing of NO production which finally lessening of endothelial dependent vasodilatation. Thus, it is plausible that DAPA could decrease the blood pressure via improving endothelial dependent vasodilatation by decreasing vascular superoxide production and enhancing antioxidant enzyme activity.

Keywords: Dapagliflozin, SGLT2 inhibitor, metabolic syndrome, high-fat high-fructose diet, blood pressure, vascular reactivity

Introduction

MS also known as metabolic disorder or insulin resistance syndrome, is a chronic condition characterized by abdominal obesity, dyslipidemia, hyperglycemia, and high blood pressure. Cardiovascular disease, type 2 diabetes mellitus (T2DM), and non-alcoholic fatty

liver disease are all linked to MS. High fat-high carbohydrate and also high-fat high-fructose diet (HFFD) have been reported to induce MS and type 2 DM. Insulin resistance and chronic hyperglycemia have a significant role in causing of vascular complications or vascular dysfunction in diabetes patients which involve several mechanisms: increased formations of advanced glycation end products, oxidative stress, and inflammatory cytokines.[1]

DAPA is a sodium-glucose cotransporter-2 inhibitor (SGLT2i) used to treat type 2 diabetes. By blocking SGLT2 in the proximal convoluted tubule, DAPA lowers glucose reabsorption in the kidneys and facilitates its excretion in the urine resulting in decreasing glucose levels independently of insulin action.[2] Recently, there have been several reports of cardioprotective effect of DAPA in heart failure patients both with or without diabetes.[3,4] However, still there are a few reports on whether the benefit of SGLT2 inhibitor on vascular dysfunction in metabolic syndrome condition.

In the present study, we aimed to investigate the effect of DAPA on the hemo-dynamic status and vascular responses to vasoactive agents with emphasize on a mechanism of action in HFFD-induced metabolic syndrome rats. The importance and novelty of this study is to provide a more specific mechanisms underlying the effects of SGLT2 inhibitors in improving vascular dysfunction in metabolic syndrome.

Methods

Experimental Animals

Male Wistar rats (160-180 g) were obtained from the Northeast Laboratory Animal Center, Khon Kaen University, Khon Kean, Thailand. The animals were housed under a standard environment at the Northeast Laboratory Animal Center, Khon Kaen University, and all animal procedures were approved by the Animal Ethics Committee of Khon Kaen University, Khon Kean, Thailand (IACUC-KKU-13/2565).

The rats were divided into 2 major groups. Group 1 was fed a normal diet and regular drinking water throughout the experiment (n=10, normal diet control group) and the second group was fed a HFFD and 10% fructose in drinking water for a period of 10 weeks. After that, the HFFD rats were assigned to 4 groups (n=6-10 each) as follows; receiving distilled water (MS control group), DAPA (1 or 5 mg/kg/day), and metformin 200 mg/kg/day (positive control group) once daily by oral gavage for a further 6 weeks with continued HFFD feeding.

The normal rat diet (3.04 kcal/g) was obtained from CP Mice Feed, Samut Prakan Province, Thailand. The HFFD (5.16 kcal/g) was composed of 40% normal rat diet, 40% fat (lard) and 20% fructose (5). DAPA and metformin were dissolved in distilled water.

At the end of 16th week, an oral glucose-tolerance test was performed, and blood samples were collected from the lateral tail vein to measure glucose, serum lipid, and insulin levels. Then, the animals were anesthetized using intraperitoneal injection of xylazine 5 mg/kg and zoletil 25 mg/kg for measuring of hemodynamic and vascular reactivity parameters. At the end of hemodynamic measuring, blood was collected from the abdominal aorta to determine oxidative stress markers and NO, and common carotid artery was isolated to examine superoxide production.

Oral glucose tolerance test (OGTT)

OGTT was performed as described earlier.[6] Briefly, the rats were fasted for 10-12 h, and then the blood glucose was examined at 0, 30, 60, 90 and 120 min after oral glucose loading (2 g/kg) using an Accu-Chek Performa glucose meter (Roche Diagnostics, Mannheim, Germany). An area under the curve (AUC) of blood glucose from 0 to 120 min was calculated using a trapezoidal rule.

Hemodynamic parameters measurement

Blood pressure in anesthetized animals was directly measured via the femoral artery which was continuously monitoring of SBP, DBP, MAP and HR using a PowerLabTM System coupled with LabChart 8.1 analysis software (AD Instruments, Co. Bella Vista, NSW, Australia).

Vascular reactivity measurement

Vasoactive substances: acetylcholine (ACh, 3, 10, 30 nmol/kg), sodium nitroprusside (SNP, 1, 3, 10 nmol/kg), and phenylephrine (PE, 0.01, 0.03, 0.1 μM) were injected via the femoral vein, and the changes in blood pressure were recorded. Each vasoactive agent was injected in a stepwise concentration at 10 min interval.

Biochemical analysis

Fasting serum insulin concentrations were measured by an enzyme-linked immuno-sorbent assay (ELISA) kits (EMD Millipore, Billerica, MA, USA). Homeostasis model assessment of insulin resistance (HOMA-IR), an index of insulin resistance, was calculated using the following formula: Fasting glucose (mmol/L) x fasting insulin (μIU/mL)/22.5.[6]

Lipid profiles, serum triglycerides[7], low-density lipoprotein cholesterol (LDL-C) and high-density lipoprotein cholesterol (HDL-C) were measured using an enzymatic colorimetric method (Wako, Osaka, Japan).

Vascular super oxide ($O_2^{\bullet -}$) production was measured using lucigenin-enhanced chemiluminescence method as described previously.[8] In brief, the carotid arteries were quickly isolated and the vascular segments were placed in Krebs-KCl buffer, and allowed to equilibrate at 37° C for 30 min. Lucigenin was added, and placed in luminometer (Turner Biosystems, 23 CA, USA). The proton counts were integrated every 30 s for 5 min and averaged. Super oxide ($O_2^{\bullet -}$) production in vascular segment was expressed as relative light unit counts per min per mg of vascular segment dry weight.

Amount of serum malondialdehyde (MDA) was measured as thiobarbituric acid reactive substances (TBARS). 1,1,3,3-Tetraethoxypropane (TEP) was used as the standard pink chromogen detected by spectrophotometry. The MDA concentrations were expressed as μM.[9]

Serum catalase activity was determined using a colorimetric assay based on the reaction of undecomposed hydrogen peroxide with ammonium molybdate to produce a yellowish color. CAT activity was expressed as U/mL.[10]

Serum superoxide dismutase (SOD) activity was determined based on the inhibition of nitroblue tetrazolium. The SOD activity is presented in percent of inhibition of the reduction of nitroblue tetrazolium.[11]

Serum nitrate/nitrite (NOx) concentrations is representative of NO, and was measured using an enzymatic conversion followed by a Griess reagent reaction as previous described.[12] The absorbance of reaction was examined using an ELISA plate reader at wavelength of 540 nm (Tecan GmbH., Grodig, Australia). The standard curve was established using $NaNO_2$ reacting with a Griess substance, and the amount of NOx was expressed as μM.

Statistical analysis

All results are shown as the means ± standard deviation (SD). Data were analyzed using a one-way analysis of variance (ANOVA) followed by Student-Newman-Keuls post-hoc test for multiple comparisons analysis (SigmaStat Software, CA, USA). The acceptable value of significance was set at $p < 0.05$.

Results

Effect of DAPA on parameters of glucose and lipid metabolism in MS rats

At the end of experiment, in MS control group, FBG was significantly high, OGT was significantly impaired (increased AUC of blood glucose), and insulin resistance (high levels of serum insulin and HOMA-IR scores) was significantly increased relative to the values of normal controls (**Table 1**). For lipid profiles of MS controls, serum LDL and TG were significantly high, and HDL was significantly low as compared to normal controls (**Table 1**). As expected in MS rats, DAPA or metformin treatment improved all the changes of these parameters of glucose and lipid metabolism as compared to MS controls (**Table 1**). The results demonstrated that DAPA (1 and 5 mg/kg) and metformin (200 mg/kg) treatments improved glucose and lipid metabolism in HFFD-induced MS animals. In addition, DAPA and metformin decreased the atherogenic index.

Effect of DAPA on hemodynamic parameters in MS rats

The MS control group had the significant increases in SBP, DBP and MAP compared to the normal controls ($p < 0.05$). DAPA or metformin significantly reduced SBP, DBP and MAP of MS animals as compared to MS controls ($p < 0.05$) (**Figure 1**). The results indicated that DAPA or metformin treatment could decrease the high blood pressure in HFFD-induced MS rats.

Effect of DAPA on vascular reactivity in MS rats

To investigate the vascular response to vasoconstrictor agent, PE at various doses were injected via femoral vein and the changes in blood pressure were recorded. The vaso-constrictive response to PE was significantly enhanced in the MS controls as compared to normal controls (**Figure 2A**, $p < 0.05$). Interestingly, DAPA or metformin could significantly diminish the vasoconstrictive response to PE as compared to MS control rats (**Figure 2A**, $p < 0.05$). This result showed that DAPA may ameliorate the adrenergic induced vaso-constriction in MS rats.

Table 1. Effect of DAPA administration on metabolic parameters.

Parameters	Groups				
	Normal control	MS control	MS+DAPA (1 mg/kg)	MS+DAPA (5 mg/kg)	MS+MET (200 mg/kg)
FBG (mg/dL)	97.70 ± 9.45	115.00 ± 8.96*	101.56 ± 8.08#	90.88 ± 8.04#	103.90 ± 5.70#
AUC of blood glucose (min.mg/dL)	14886 ± 1287	19566 ± 4578*	16591 ± 2064	15155 ± 1388#	15879 ± 587#
Serum insulin (ng/mL)	4.15 ± 1.18	10.97 ± 2.84*	5.02 ± 1.12#	4.14 ± 0.88#	4.14 ±1.60#
HOMA-IR	20.01 ± 6.07	70.31 ± 21.26*	25.37 ± 5.17#	19.09 ± 4.49#	22.91 ± 8.25#
Serum TG (mg/dL)	55.37 ± 10.94	114.37 ± 9.53*	95.16 ± 8.83#	73.18 ± 7.98#,†	69.62 ± 9.63#
Serum LDL-C (mg/dL)	26.50 ± 5.15	73.10 ± 12.96*	52.40 ± 10.30#	37.65 ± 4.97#,†	38.50 ± 7.26#
Serum HDL-C (mg/dL)	54.85 ± 7.39	26.21 ± 4.78*	33.33 ± 5.05#	44.46 ± 4.75#,†	48.07 ± 3.89#
Atherogenic index (TG/HDL)	1.02 ± 0.22	4.46 ± 0.66*	2.94 ± 0.65#	1.66 ± 0.24#	1.46 ± 0.24#

Results are expressed as means ± SD (n=6-10). *$p < 0.05$ versus normal control group, #$p < 0.05$ versus MS control group, †$p < 0.05$ versus MS+DAPA1 group; MS, Metabolic syndrome; DAPA, Dapagliflozin; MET, Metformin; AUC, Area under the curve; HOMA-IR, Homeostasis model assessment of the insulin resistance index

Vasorelaxation (decreased BP) in response to an endothelial-dependent vasodilator ACh was significantly blunted in MS controls relative to the normal controls (**Figure 2B**). This indicated that the endothelial-dependent vasodilatation was impaired in MS rats. Treatment with DAPA or metformin could significantly improve the vasodilatation in response to ACh as compared to MS controls (**Figure 2B**, $p < 0.05$). However, vasorelaxation in response to SNP were similar in all groups (**Figure 2C**) indicating that this model of HFFD-induced MS, the function of vascular smooth muscle cells still be intact.

Effect of DAPA on oxidative stress in MS rats

Effect of DAPA on vascular superoxide production The results showed that super-oxide production of carotid arteries was significantly increased in MS control rats (**Figure 3A**, $p < 0.05$). DAPA or metformin significantly decreased vascular superoxide production compared to MS controls (**Figure 3A**, $p < 0.05$).

Effect of DAPA on serum MDA The level of serum MDA was significantly increased in MS control rats compared to the normal controls ($p < 0.05$). DAPA or metformin significantly reduced the level of serum MDA as compared to MS controls (**Figure 3B**, $p < 0.05$).

Effect of DAPA on antioxidant enzymes activity The level of serum CAT and SOD were significantly decreased in MS controls relative to the normal controls (**Figure 3C** and **3D**, $p < 0.05$). Interestingly, DAPA or metformin could significantly increase the level of CAT and SOD as compared to MS controls ($p < 0.05$).

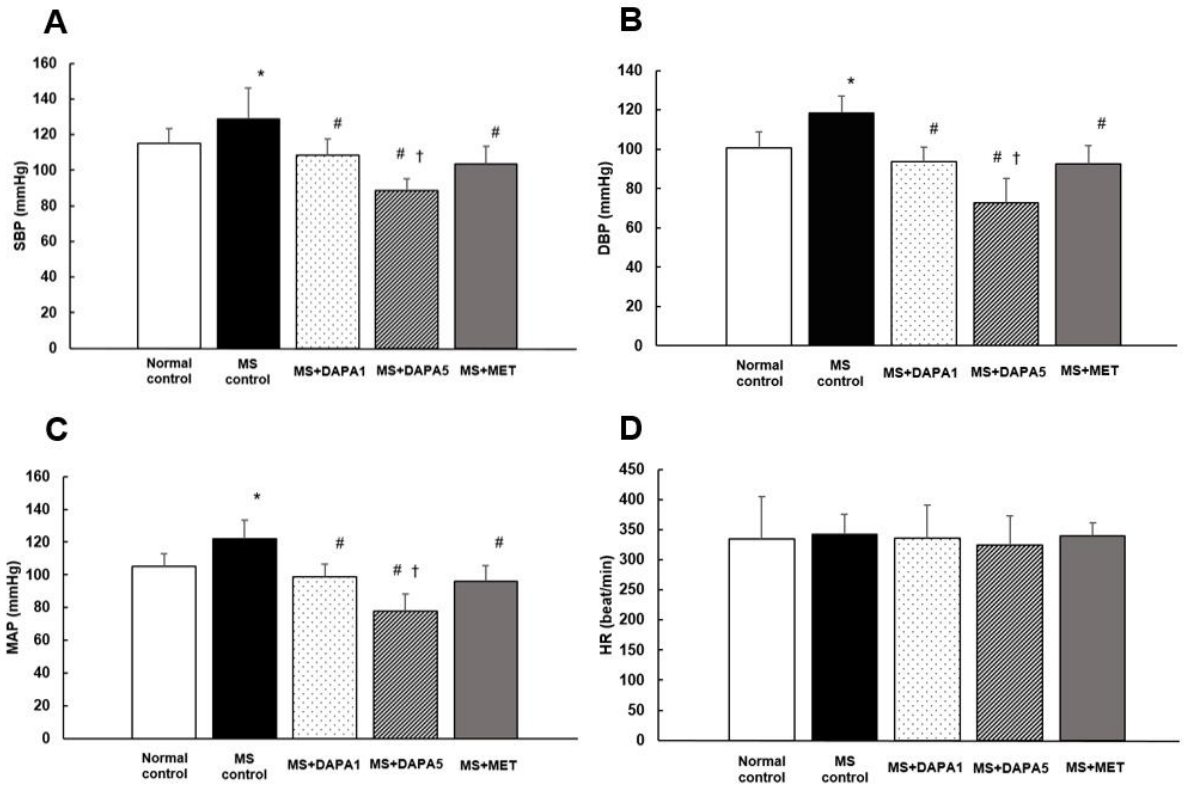

Figure 1. Effect of DAPA on (A) systolic blood pressure (SBP), (B) diastolic blood pressure (DBP), (C) mean arterial blood pressure (MAP) and (D) heart rate (HR). Results are expressed as means ± SD (n=6-10). $^{*}p < 0.05$ versus normal control group, $^{\#}p < 0.05$ versus MS control group, $^{\dagger}p < 0.05$ versus MS + DAPA1; MS, Metabolic syndrome; DAPA1 and DAPA5, Dapagliflozin 1 and 5 mg/kg/day; MET, Metformin 200 mg/kg/day.

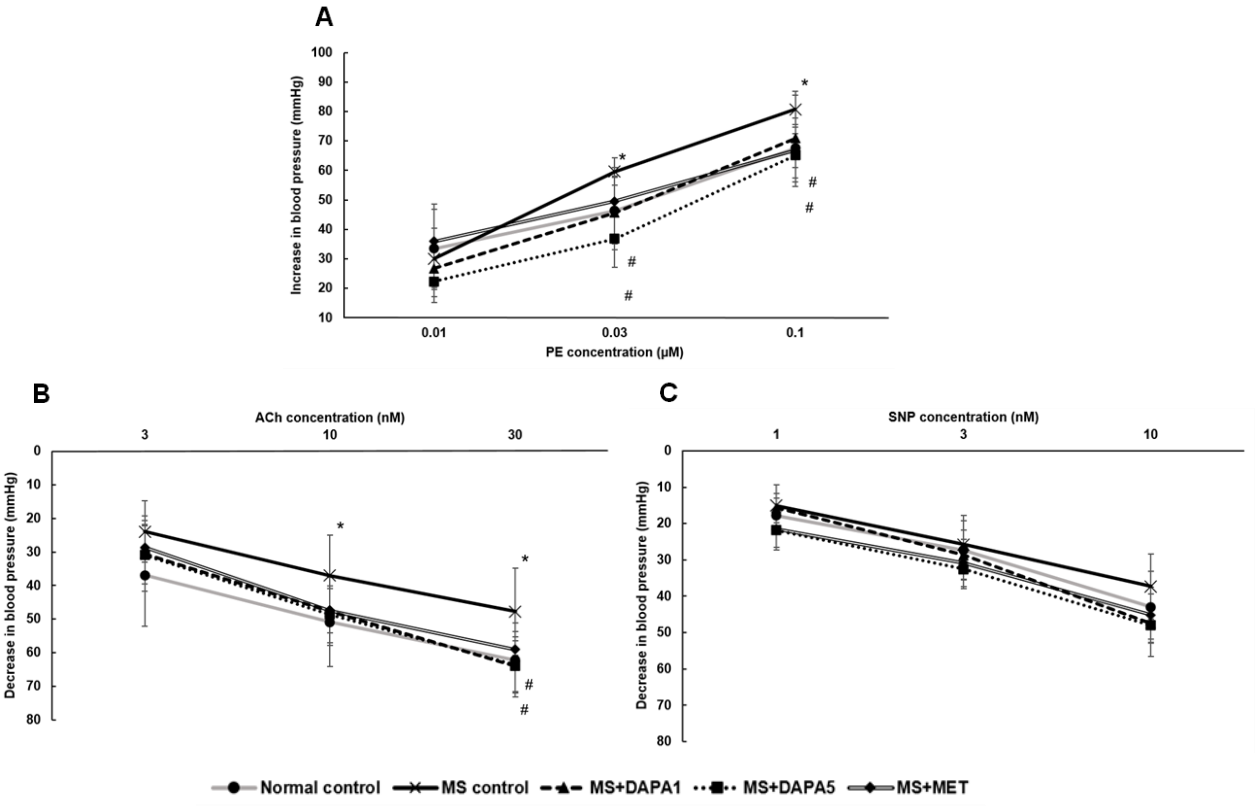

Figure 2. The changes of blood pressure in response to vasoconstrictor (A) phenylephrine (PE) and vasodilators (B) acetylcholine (ACh) and (C) sodium nitroprusside (SNP)**.** Results are expressed as mean ± SD (n=6-10). *p < 0.05 vs. normal control group, $^{\#}p$ < 0.05 vs. MS control group; MS, Metabolic syndrome; DAPA1 and DAPA5, Dapagliflozin 1 and 5 mg/kg/day; MET, Metformin 200 mg/kg/day.

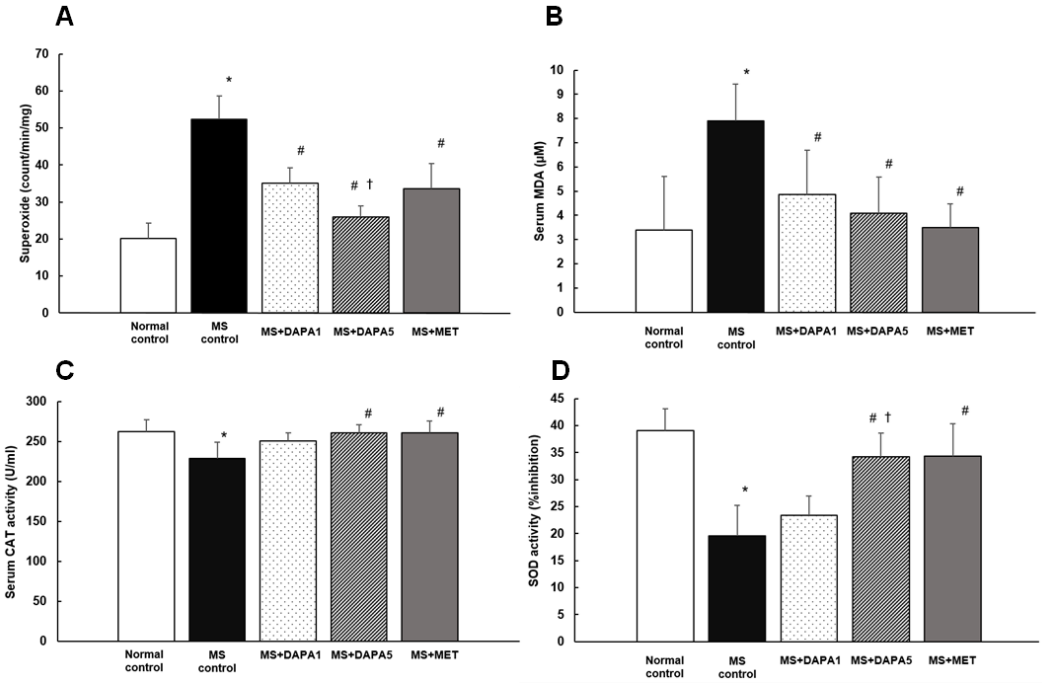

Figure 3. Effect of DAPA on (A) carotid artery superoxide production, (B) serum malondialdehyde and anti-oxidant enzyme activity (C) catalase and (D) superoxide dismutase. Results are expressed as mean ± SD (n=6-10). *p < 0.05 vs. normal control group, $^{\#}p$ < 0.05 vs. MS control group, $^{\dagger}p$ < 0.05 vs. MS+DAPA1; MS, Metabolic syndrome; DAPA1 and DAPA5, Dapagliflozin 1 and 5 mg/kg/day; MET, Metformin 200 mg/kg/day; MDA, Malondialdehyde; CAT, Catalase; SOD, Superoxide dismutase.

Effect of DAPA on serum nitrate/nitrite (NOx) level in MS rats

The level of serum NOx, metabolites of NO, was significantly decreased in MS controls as compared to normal controls (**Figure 4**, $p < 0.05$). The MS rats treated with DAPA or metformin, the level of NOx was significantly increased compared to MS controls (**Figure 4**, $p < 0.05$). This may imply that DAPA could improve the ACh vasodilatation via enhancing vascular endothelial cell function in the MS animals.

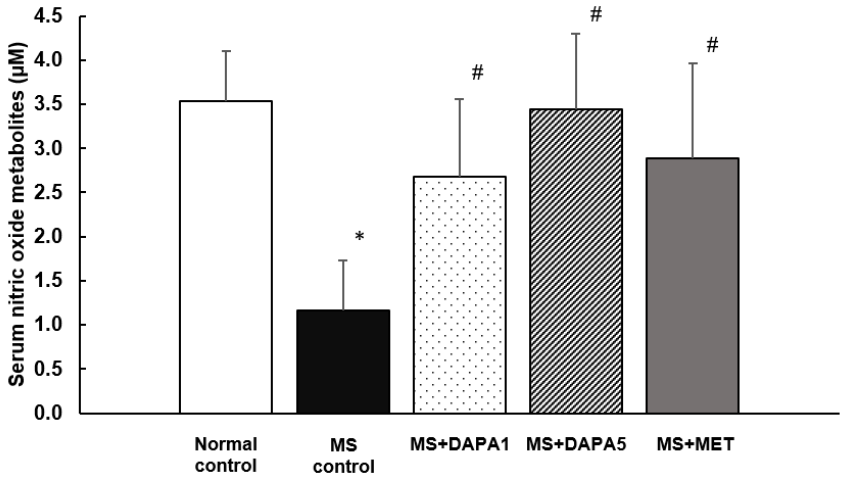

Figure 4. Effect of DAPA on serum nitrate/nitrite (NOx) level. Results are expressed as mean ± SD (n=6-10), $^{*}p<0.05$ vs. normal controls, $^{\#}p < 0.05$ vs. MS controls; MS, Metabolic syndrome; DAPA1 and DAPA5, Dapagliflozin 1 and 5 mg/kg/day; MET, Metformin 200 mg/kg/day.

Discussion

Our results demonstrated that DAPA at doses of 1 and 5 mg/kg could decrease the high blood pressure and improve vascular reactivity including ACh induced endothelial-dependent vasodilatation and PE induced-adrenergic vasoconstriction in metabolic syndrome rats. Concurrently, DAPA could decrease oxidative stress: decreased vascular superoxide production, decreased serum MDA, and increased CAT and SOD activity.

It is well established that HFFD could induce insulin resistance leading to metabolic syndrome which referred to impaired glucose tolerance, hyperglycemia, dyslipidemia (6) and hypertension in rats.[13] DAPA is a glucose lowering agent for type 2 diabetic patient with the mechanism of inhibition of SGLT-2 in renal tubules. As expected, the present study showed that DAPA could decrease FBG and insulin resistance, and improve glucose tolerance and dyslipidemia. An improving in dyslipidemia situation of DAPA might result in the decreasing of atherogenic index effect.[14]

Insulin resistance not only induces metabolic abnormalities but also predisposes to hypertension, vascular stiffness, and associated cardiovascular disease. Rodents fed HFFD for 2-4 months were observed to develop insulin resistance, hypertension, and eventually cardio-vascular remodeling.[15] The mechanisms of provoking hypertension in insulin resistance situation or diabetes include inappropriate activation of the renin-angiotensin-aldosterone system, sympathetic nervous system, mitochondria dysfunction, excessive oxidative stress, systemic inflammation and dysregulation of renal SGLT2.[16] The present study found that rats feeding HFFD (the MS rats) had a significant high SBP, DBP and MAP, interestingly, the high blood pressure of MS rats could be reduced by DAPA administration for the last 6 weeks. Therefore, we furthered to explore the possible mechanisms of DAPA in reducing this pathology.

By examining the effect of DAPA on vascular responsiveness, NO production and oxidative stress situation. We found that DAPA improved the endothelial-dependent vasodilatation as indicated by improving vasodilatation in response to ACh, and especially DAPA caused an increase in nitric oxide production which is an endothelial-derived mediator of ACh. Corresponding to a recent study using isolated aortic ring showed that DAPA increased endothelium-dependent vasorelaxation in diabetic mice.[17] In addition, DAPA could decrease the increased adrenergic vasoconstriction response to PE in the MS rats, this might be because DAPA decreases the peripheral vascular sympathetic response in MS rats. There are some reports for relationship between SGLT2 inhibition and reduction of sympathetic activity[18], as well this might be a mechanism for decreasing of blood pressure in addition to an established diuretic effect of DAPA. Furthermore, a decreasing in peripheral sympathetic activity may also contribute to ameliorating effect of DAPA on adrenergic vasoconstriction.

Insulin resistance and hyperglycemia also induce activation of redox-sensitive protein kinase C and polyol-hexosamine pathways, mitochondrial dysfunction which further contributing to free radical production, and the consequent vascular endothelial cells damage with reduced bioavailability of the vasodilator nitric oxide or impaired endothelial dependent vasodilatation.[1] Our experimental model, insulin resistance and high blood glucose induced oxidative stress is evidenced by increased vascular superoxide production, increased lipid peroxidation product, and decreased antioxidant enzyme activities. Interestingly, DAPA administration could correct all these indicators of oxidative stress. Based on the glucose lowering effect of DAPA, this action may lead to the decrease of hyperglycemia-induced oxidative stress. It has been proposed that the antioxidant effects of SGLT2 inhibitors in T2DM may be mediated by multiple mechanisms including downregulating pro-oxidant enzymes, reducing AGE-RAGE interactions, improving mitochondrial function and reducing proinflammatory cytokines.[19] Here, we report that DAPA may show antioxidant activity by reducing vascular superoxide production and enhancing antioxidant enzyme activity.

Thus, we propose that DAPA could decrease the high blood pressure and improve vascular reactivity by (a) reduction of vascular superoxide production which resulting in protection of vascular endothelial cells and eventually vasodilatation, and (b) possibly by peripheral sympathetic modulating activity.

Presently, there have been both clinical and experimental evidences showing that metformin can reduce the incidence of cardiovascular events in DM patients. This therapeutic effect may link to the cellular energy regulator, AMPK which resulting in improving of endothelial dysfunction and oxidative stress.[20]

Conclusion

HFFD caused metabolic syndrome including insulin resistance, hyperglycemia, dyslipidemia and hypertension in rats. DAPA could decrease the high blood pressure and improve vascular reactivity plausibly by decreasing vascular superoxide production and enhancing antioxidant enzyme activity which resulting in protection of vascular endothelial cells finally an endothelial-dependent vasodilatation. A peripheral sympathetic modulating activity may be one of the mechanisms of DAPA which is our ongoing study.

Acknowledgement

This research was financially supported by a postgraduate scholarship and an invitation research grant from the Faculty of Medicine, Khon Kaen University, Thailand.

References

1. Petrie JR, Guzik TJ, Touyz RM. Diabetes, hypertension, and cardiovascular disease: clinical insights and vascular mechanisms. Can J Cardiol. 2018 May;34(5):575-584.
2. Dhillon S. Dapagliflozin: A review in type 2 diabetes. Drugs. 2019 Jul;79(10):1135-46.
3. Ali AE, Mazroua MS, ElSaban M, Najam N, Kothari AS, Mansoor T, et al. Effect of dapagliflozin in patients with heart failure: a systematic review and meta-analysis. Global heart. 2023 Aug 22;18(1):45.
4. Xie Y, Wei Y, Li D, Pu J, Ding H, Zhang X. Mechanisms of SGLT2 inhibitors in heart failure and their clinical value. J Cardiovasc Pharmacol. 2023 Jan 1;81(1):4-14.
5. Apiboon P, Senggunprai L, Prajaney P, Kongyingyoes B, Pannangpetch P. Effect of aril extract of *Momordica cochinchinensis* Spreng. on glucose and fat metabolism in high fat and high fructose diet induced insulin resistant rats. Thai J Pharmacol. 2017;39(1):38-47.
6. Singdam P, Naowaboot J, Senggunprai L, Boonloh K, Pannangpetch P. *Pluchea indica* leaf extract alleviates dyslipidemia and hepatic steatosis by modifying the expression of lipid metabolism-related genes in rats fed a high fat-high fructose diet. Prev Nutr Food Sci. 2022 Dec 31;27(4):384-398.
7. Montgomery MK, Turner N. Mitochondrial dysfunction and insulin resistance: an update. Endocr Connect. 2015 Mar;4(1):R1-R15.
8. Luangaram S, Kukongviriyapan U, Pakdeechote P, Kukongviriyapan V, Pannangpetch P. Protective effects of quercetin against phenylhydrazine-induced vascular dysfunction and oxidative stress in rats. Food Chem Toxicol. 2007 Mar;45(3):448-55.
9. Nakmareong S, Kukongviriyapan U, Pakdeechote P, Donpunha W, Kukongviriyapan V, Kongyingyoes B, et al. Antioxidant and vascular protective effects of curcumin and tetrahydrocurcumin in rats with L-NAME-induced hypertension. Naunyn Schmiedebergs Arch Pharmacol. 2011 May;383(5):519-29.
10. Adam SH, Giribabu N, Kassim NM, Kumar KE, Brahmayya M, Arya A, et al. Protective effect of aqueous seed extract of Vitis Vinifera against oxidative stress, inflammation and apoptosis in the pancreas of adult male rats with diabetes mellitus. Biomed Pharmacother. 2016 Jul;81:439-52.
11. Xu W, Luo Q, Wen X-y, Xiao M, Mei Q. Antioxidant and anti-diabetic effects of caffeic acid in a rat model of diabetes. Trop J Pharm Res. 2020;19:1227-32.
12. Poasakate A, Maneesai P, Rattanakanokchai S, Bunbupha S, Tong-Un T, Pakdeechote P. Genistein prevents nitric oxide deficiency-induced cardiac dysfunction and remodeling in rats. Antioxidants (Basel). 2021 Feb 4;10(2):237.
13. Bunbupha S, Prasarttong P, Poasakate A, Maneesai P, Pakdeechote P. Imperatorin alleviates metabolic and vascular alterations in high-fat/high-fructose diet-fed rats by modulating adiponectin receptor 1, eNOS, and $p47^{phox}$ expression. Eur J Pharmacol. 2021 May 15;899:174010.
14. Pahud de Mortanges A, Salvador D, Jr., Laimer M, Muka T, Wilhelm M, Bano A. The Role of SGLT2 inhibitors in atherosclerosis: a narrative mini-review. Front Pharmacol. 2021 Nov 5;12:751214.
15. Geetha R, Yogalakshmi B, Sreeja S, Bhavani K, Anuradha CV. Troxerutin suppresses lipid abnormalities in the heart of high-fat-high-fructose diet-fed mice. Mol Cell Biochem. 2014 Feb;387(1-2):123-34
16. Jia G, Sowers JR. Hypertension in diabetes: an update of basic mechanisms and clinical disease. Hypertension. 2021 Nov;78(5):1197-1205.
17. Zhou Y, Tai S, Zhang N, Fu L, Wang Y. Dapagliflozin prevents oxidative stress-induced endothelial dysfunction via sirtuin 1 activation. Biomed Pharmacother. 2023 Sep;165:115213.
18. Dimova R, Tankova T. Does SGLT2 inhibition affect sympathetic nerve activity in type 2 diabetes? Horm Metab Res. 2021 Feb;53(2):75-84.
19. Tsai KF, Chen YL, Chiou TT, Chu TH, Li LC, Ng HY, et al. Emergence of SGLT2 inhibitors as powerful antioxidants in human diseases. Antioxidants (Basel). 2021 Jul 22;10(8):1166.
20. Bu Y, Peng M, Tang X, Xu X, Wu Y, Chen AF, et al. Protective effects of metformin in various cardiovascular diseases: clinical evidence and AMPK-dependent mechanisms. J Cell Mol Med. 2022 Oct; 26(19):4886-4903.

F02

Protective Effect of Naringenin against Lysosomal Toxicity in Human Colon Carcinoma Caco-2 Cells

Kaitsuda Saiprom[1], Cherdsak Boonyong[2], Suree Jainmogkol[1*]

[1] *Department of Pharmacology and Physiology, Faculty of Pharmaceutical Sciences, Chulalongkorn University, Bangkok, Thailand*
[2] *Pharmacology and Toxicology Unit, Department of Medical Science, Faculty of Sciences, Rangsit University, Pathum Thani, Thailand*

*E-mail: suree.j@pharm.chula.ac.th

Abstract

An increase in lysosomal membrane permeabilization (LMP) can impair lysosome integrity, leading to a release of cathepsin B, and subsequently contribute to cell death. This study aimed to investigate the effect of naringenin, a natural bioactive flavonoid, on lysosome toxicity and cell death in human colon carcinoma Caco-2 cells following exposure to a lysosome toxicant ammonium chloride. Additionally, involvement of autophagy was also determined. Cells were pretreated with naringenin (100 μM) for 24 h before adding ammonium chloride (40 mM) for another 72 h. At the end of treatment period, the cells were evaluated for viability by an MTT assay, LMP by an acridine orange uptake assay, expression of target proteins (namely cathepsin B, mTOR, LC3 II/I) by western blot analysis. Our results showed that at a concentration of 100 μM, naringenin did not exhibit toxicity to caco-2 cells. When combined with ammonium chloride, it increased cell viability and red fluorescence intensity of acridine orange compared to ammonium chloride alone. This, coupled with reduced cathepsin B expression, suggested its effectiveness in preventing LMP and lysosomal toxicity. Furthermore, the presence of naringenin significantly inhibited mTOR, accompanied by an increase of LC3 II/I compared to ammonium chloride alone, implying an induction of autophagy and increased autophagosome formation. In summary, the protective effect of naringenin against lysosome toxicity was associated with its ability to inhibit LMP and induce autophagy.

Keywords: Naringenin, lysosome toxicity, autophagy, lysosomal membrane permeabilization

Introduction

Lysosome, an acidic organelle, plays a crucial role in eliminating damaged cellular components. It collaborates with mitochondria, golgi apparatus, and peroxisome to regulate cellular metabolism and homeostasis.[1] The key molecular mechanism connecting lysosome to cell death and survival is lysosomal membrane permeabilization (LMP) and the autophagy pathway.[1-2] Increased LMP leads to lysosomal damage, release of cathepsins into cytosol, subsequent induction of mitochondria dysfunction, and activation of apoptosis.[3] Additionally, LMP can disrupt the fusion process between lysosome and autophagosomes, leading to a suppression of autophagy. Autophagy is widely recognized as a cellular process triggered in response to cellular stress, initiated through the inhibition of mTOR expression.[4] Hence, inhibiting LMP may modulate the autophagy process, thereby preventing cell death.

Naringenin is a natural bioactive flavonoid found abundantly in citrus fruits, bergamot, and tomatoes.[5] This flavonoid exhibits diverse pharmacological activities, including antioxidant properties, immune system modulation, and anticarcinogenic effects.[5] Its cytotoxic activity has been linked to the activation of endoplasmic reticulum (ER) stress-induced apoptosis, LMP, increased autophagosomes and autophagy-induced cell death.[6-7] However, under specific condition, naringenin demonstrated protective effects against cell stress, suppressing ER stress, enhancing cell survival through the induction of autophagy.[8-10]

This study aimed to investigate the effect of naringenin at the non-cytotoxic concentration on lysosome toxicity and autophagy process in Caco-2 cells following exposure to the lysosome toxicant ammonium chloride. The results of this study would improve our understanding of how naringenin responds to lysosomal toxicants, providing insights into its potential applications.

Methods

Cell culture and treatment

Human colon cancer adenocarcinoma Caco-2 cells (ATCC, USA) were grown in DMEM medium supplemented with 10% fetal bovine serum (Gibco, USA), 1%penicillin-streptomycin solution, 1%nonessential amino acid, 2.5 mM L-glutamine at 37 °C in a 5%CO_2 incubator. The cells were seeded at the density of 6.25 x 10^4 cells/cm^2 overnight. Then, the cells were treated with naringenin at non-toxic concentration (100 µM) for 24 h, followed by ammonium chloride (NH_4Cl, 40 mM) for another 72 h. At this concentration (40 mM), NH_4Cl was reported not to induce significant changes in the osmolarity and pH of incubation medium.[11-13] In this study, the unchanged color of phenol red in DMEM after treatment with NH_4Cl suggested a medium pH of approximately 7.4.

Cytotoxicity

After treatment, an MTT assay was used to determine cell viability. Briefly, the cells were washed with warm PBS (three times), then incubated with 0.5 mg/ml of MTT solution for 4 h. At the end of incubation period, MTT solution was replaced with 100% DMSO to dissolve purple formazan crystal. The absorbance was read at 570 nm.

Lysosomal membrane permeabilization (LMP)

LMP was determined through measuring the accumulation of acridine orange in lysosome.[3] In this experiment, cells were seeded at the density 4.0 x 10^4 cells/cm^2 onto 60 mm glass dish for 24 h. Then, the cells were subjected to 72-h treatment with ammonium chloride, with or without naringenin, as mentioned above. After treatment, the cells were washed and further incubated with the complete media containing 1 µg/mL acridine orange for 15 min. Following three washes with PBS, imaging medium (phenol-red-free DMEM, 10% FBS, 2mM glutamine, 25 mM HEPES (pH 7.4) was introduced, and the cells were visualized under 20x magnification using fluorescence microscopy with a blue light filter.

Protein expression

Expression of target proteins (i.e., Cathepsin B, mTOR, LC3 II/I) was determined and quantified by western blot analysis. At the end of treatment period, the cells were harvested, lysed in the ice-cold lysis buffer containing 1%PMSF, 1%SDS, 1%Triton-x and protease inhibitor cocktails. Cell lysate was centrifuged at 15000 x *g* at 4°C for 15 min, and the supernatant was collected for protein quantification and western blot analysis. Total amount of proteins in each sample was quantified using BCA protein assay kit, according to manufacturer's instruction. Equal amount of proteins (60 µg) was loaded onto 7-15% SDS-

PAGE gels for protein separation, followed by electrical transferred to an Immobilon-PVDF membrane. Then, the membrane was treated with 5% skim milk in TBS-T for 1 h, followed by primary antibodies i.e., cathepsin B (1:1000), mTOR (1:1000), MAPLC3 α/β (1:1000), and β-actin (1:2000) at 4°C overnight. After washing with TBS-T, the membranes were incubated with HRP-conjugated secondary antibody (1:2000) at room temperature for 1 h. Protein bands were revealed using the SuperSignal® West Pico Chemiluminescent substrate kit, detected on X-ray film, and densitometrically quantified through the Image J program (NIH, USA). In this study, β-actin was served as the internal standard for assessing protein loading.

Statistical analysis

The presented data reflect the mean ± standard error of mean (SEM) from three independent experiments. Group comparisons were analyzed using Student's t-test, with statistical significance set at $P < 0.05$.

Results

Ammonium chloride (NH_4Cl) is a known lysosomal inhibitor that can induce apoptotic cell death.[14] According to our MTT assay, the viability of Caco-2 cells significantly decreased to 64% following exposure to NH_4Cl 40 mM for 72 h (**Figure 1**). Naringenin alone at 100 μM demonstrated no cytotoxicity. Addition of naringenin effectively increased the viability of NH_4Cl-treated cells from 64% to 74%. Our results suggested that naringenin was able to prevent cytotoxic effect induced by NH_4Cl.

In order to evaluate the effect of naringenin on lysosome toxicity, lysosomal membrane permeabilization (LMP) was assessed through the acridine orange uptake assay. Acridine orange, a weak base dye, displays red fluorescence within normal acidic lysosomes. Hence, a reduction in red fluorescence suggested a loss of lysosomal membrane integrity. (i.e., increased LMP) or elevation in lysosomal pH. As shown in **Figure 2**, exposure to NH_4Cl led to a significant decrease in red fluorescence compared to the control group, indicating its induction of lysosome toxicity and LMP in Caco-2 cells under our experimental condition. Naringenin alone had no effect on lysosome integrity. Furthermore, in combination with NH_4Cl, its markedly elevated red fluorescence by approximately 2-fold compared to NH_4Cl alone. These findings suggested that naringenin elicited the potential to preserve lysosomal integrity by preventing an increase in LMP.

In addition to LMP, we assessed the expression level of cathepsin B, a lysosomal enzyme released into the cytosol after lysosome damage, triggering apoptosis activation. As shown in **Figure 3a** and **3b**, exposure to NH_4Cl alone led to a significantly elevated cathepsin B levels compared to control, suggesting lysosome damage and increased LMP.

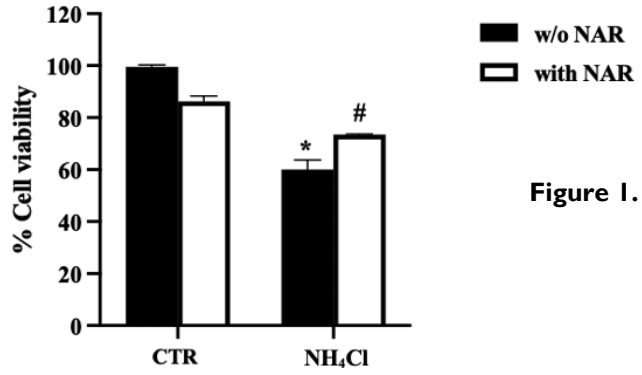

Figure 1. Cell viability after 72-h treatment with ammonium chloride (NH_4Cl) in the presence and absence of naringenin (NAR) in Caco-2 cells, as measured by an MTT assay. $^{*}P < 0.05$ vs. control; $^{\#}P < 0.05$ vs. NH_4Cl alone (NH_4Cl) (n=3).

Moreover, the similar levels of cathepsin B in both the naringenin alone and control groups suggested that naringenin did not induce lysosomal damage under our experiment condition. Interestingly, when combined with NH_4Cl, naringenin demonstrated the ability to suppress the increase in cathepsin B level in the NH_4Cl-treated cells.

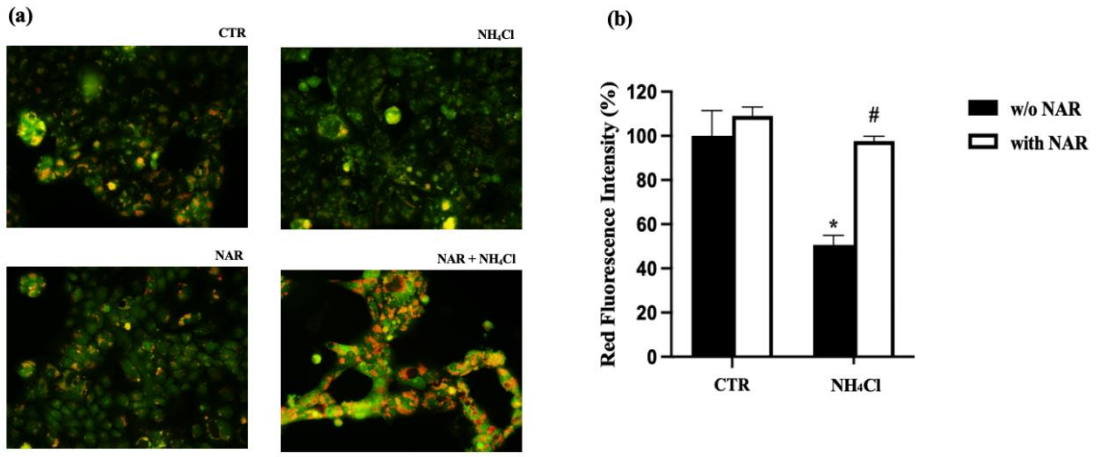

Figure 2. Lysosomal membrane permeabilization (LMP) after 72-h treatment with ammonium chloride (NH_4Cl) in the presence or absence of naringenin (NAR) in Caco-2 cells at 72 h, as measured by acridine orange uptake assay. (a) Cells were visualized under fluorescence microscope (20x magnification; scale bar = 500 μM). (b) Red fluorescence intensity was quantified by Image J program and calculated as the percentage of control. $^{*}P < 0.05$ vs. control; $^{\#}P < 0.05$ vs. NH_4Cl alone (n=3).

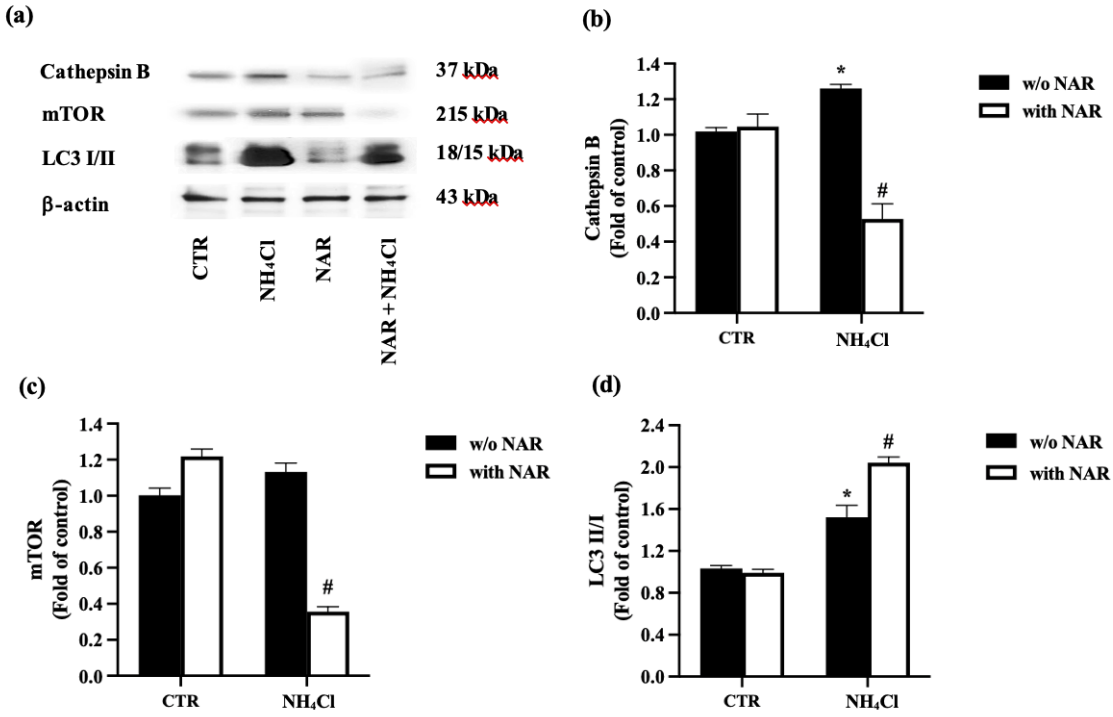

Figure 3. (a) Immunoblots and (b) their densitometrical analysis of cathepsin B, mTOR, and LC3 II/I proteins in Caco-2 cells after 72-h treatment with ammonium chloride (NH_4Cl) in the presence and absence of naringenin (NAR). Each bar represents the mean ± SEM (n=3). $^{*}P$ <0.05 vs. control; $^{\#}P$ < 0.05 vs. NH_4Cl alone (n=3).

The effects of NH_4Cl and naringenin on the autophagy process were also investigated in this study by assessing two autophagy markers, namely mTOR, and LC3 II/I. As shown in **Figure 3b**, **3c** and **3d**, neither NH_4Cl nor naringenin, when administered alone, significantly affected the expression of mTOR in Caco-2 cells compared to the control. Nevertheless, they both markedly increased the expression of LC3 II/I in the treated cells, suggesting a notable enhancement in autophagosome formation. Interestingly, when naringenin was combined with NH_4Cl, it significantly reduced mTOR level by 3.17-fold while further increasing the expression of LC3 II/I by 1.34-fold compared to the group treated with NH_4Cl alone. These findings suggested that naringenin could promote autophagy and autophagosome formation in response to a lysosomal toxicant NH_4Cl.

Discussion

In this study, we demonstrated that naringenin, at its non-cytotoxic concentration, effectively prevented lysosomal toxicity and induced autophagy in Caco-2 cells exposed to NH_4Cl. Ammonium chloride has been recognized for mediating lysosomal toxicity by elevating lysosomal pH, inducing LMP, and inhibiting autolysosome formation.[15-16] In our experiments, NH_4Cl decreased the viability of Caco-2 cells, correlating with mitochondria dysfunction and compromised lysosomal membrane integrity. This was evident through reduced mitochondrial dehydrogenase activity, increased LMP, and elevated expression levels of the cathepsin B. It is known that the release of lysosomal enzyme cathepsin B into the cytosol enhances cytotoxicity and contributes to apoptotic cell death.[3,17] Although our results revealed that NH_4Cl did not inhibit mTOR expression, it significantly increased the expression of LC3 II/I, a marker of autophagosome formation. Therefore, it is likely that ammonium chloride induced autophagy process in Caco-2 cells under our experimental condition.

This study clearly demonstrated the protective effect of naringenin against NH_4Cl exposure in human colon carcinoma Caco-2 cells. Naringenin has been reported both cyto-toxicity and anti-cytotoxicity, depending on its concentrations, experiment models and conditions.[6-10] In this study, at its non-cytotoxic concentration, naringenin did not elicit any observable effect on mitochondria and lysosome integrity, although it might have intrinsic capability to increase cell stress, LMP, and autophagy.[8,9] When combined with ammonium chloride, naringenin effectively preserved mitochondria and lysosome integrity, thereby preventing cell death. Our study further indicates that its ability to maintain lysosome integrity arises from the inhibition of LMP and suppression of cathepsin B level. In addition, this flavonoid explicitly enhances both the autophagy process and autophagosome formation, as evidenced by mTOR inhibition and a further increase LC3 II/I. However, additional investigation is warranted to assess the lysosome-preserving impact of naringenin against other lysosome toxicants like indomethacin and diclofenac, across diverse experimental settings. Moreover, further investigation into whether naringenin can reverse or alleviate lysosome toxicity after the damage occurs is worthwhile.

Conclusion

Naringenin could prevent lysosome toxicity by inhibiting lysosomal membrane permeabilization and inducing autophagy in human colon carcinoma Caco-2 cells.

Acknowledgement

Faculty of Pharmaceutical Sciences, Chulalongkorn University.

References

1. Kavčič N, Pegan K, Turk B. Lysosome in programed cell death pathways: from initiators to amplifiers. Biol Chem. 2017 Mar;398(3):289-301.
2. Mahapatra KK, Mishra SR, Behera BP, Patil S, Gewirth DA, Bhutia SK. The lysosome as an imperative regulator of autophagy and cell death. Cell Mol Life Sci. 2021 Dec;78(23):7435-7449.
3. Wang F, Gómez-sintes R, Boya P. Lysosomal membrane permeabilization and cell death. Traffic. 2018 Dec; 19(12):918-931.
4. Lu G, Wang Y, Shi Y, Zhang Z, Huang C, He W, Wang C, Shen HM. Autophagy in health and disease: From molecular mechanisms to therapeutic target. MedComm (2020). 2022 Jul 10;3(3):e150.
5. Salehi B, Fokou PVT, Sharrifi-Rad M, Zucca P, Pezzani R, Martins N, et al. The therapeutic potential of naringenin: A review of clinical trials. Pharmaceuticals (Basel). 2019 Jan 10;12(1):11.
6. Lee CW, Huang CC, Chi MC, Lee KH, Peng KT, Fang ML, Chiang YC, Liu JF. Naringenin induces ROS-mediated ER stress, autophagy, and apoptosis in human osteosarcoma cell lines. Molecules. 2022 Jan 7; 27(2):373.
7. Raha S, Kim SM, Lee HJ, Yumnum S, Saralamma VV, Ha SE, Lee WS, Kim GS. Naringin induces lysosomal membrane permeabilization and autophagy cell death in AGS gastric cancer cells. Am J Chin Med, 2020; 48(3): 679-702.
8. Ahmedy OA, Salem HH, Sayed NH, Ibrahim SM. Naringenin affords protection against lipopolysaccharide/ D-galactosamine-induced acute liver failure: Role of autophagy. Arch Biochem Biophys. 2022 Mar 15:717: 109121.
9. Ahsan AU, Sharman VL, Wani A, Chopra M. Naringenin upregulates AMPK-Mediated autophagy to rescue neuronal cells from β-Amyloid (1-42) Evoked Neurotoxicity. Mol Neurobiol. 2020 Aug;57(8):3589-3602.
10. Boonyong C, Vardhanabhuti N, Jainmongkol S. Natural polyohenols prevent indomethacin-induced and diclofenac induced Caco-2 cell death by reducing endoplasmic recticulum stress regardless of their direct reactive oxygen species scavenging capacity. J Pharm Pharmacol. 2020 Apr;72(4):583-591.
11. Klungkist J and Haaker H. Inhibition of nitrogenase activity by ammonium chloride in *Azobactor vinelandii*. J Bacteriol. 1984 Jan;157(1):148-51.
12. Cardelli JA, Richardson J, Miears D. Role of acidic intracellular compartments in the biosynthesis of Dictyostelium lysosomal enzymes. J Biol Chem. 1989 Feb 25;264(6):3454-63.
13. Ling H, Ardjomand P, Samvakas S, Simm A, Busch GL, Lang F, Sebekova K, Heidland A. Mesangial cell hypertrophy induced by NH_4Cl: role of depressed activities of cathepsins due to elevated lysosomal pH. Kidney Int. 1998 Jun;53(6):1706-12.
14. Hu P, Li H, Sun W, Wang H, Yu X, et al.. Cholesteral-associated lysosomal disorder triggers cell death of hematological malignancy: Dynamic analysis on cytotoxic effect of LW-218. Acta Pharm Sin B. 2021 Oct;11(10):3178-3192.
15. McLaren MD, Mathavarajah S, Kim WD, Yap SQ, Huber RJ. Aberrant autophagy impact growth and multicellular development in a dictyoselium knockout model of CLN5 Disease. Front Cell Dev Biol. 2021 Jul 5:9:657406.
16. Jacquin E, Leclerc-Mercier S, Judon C, Blanchard E, Fraitag S, et al., Pharmacological modulators of autophagy activate a parallel noncanonical pathway driving unconventional LC3 lipidation. Autophagy. 2017 May 4;13(5):854-867.
17. Yamashita G, Takano N, Kazama H, Tsukahara K, Miyazawa K. p53 regulates lysosomal membrane permeabilization as well as cytoprotective autophagy in response to DNA-damaging drugs. Cell Death Discov. 2022 Dec 29;8(1):502.

F03

Antimigratory Effect of Ovalitenin A in Human Bile Duct Cancer Cells

Putu Ririn Andreani[1], Laddawan Senggunprai[1,2], Sarinya Kongpetch[1,2], Piman Pocasap[1], Chanakan Pornchoo[1], Chavi Yenjai[3], Arthan, Supakorn[4], Auemduan Prawan[1,2*]

[1] *Department of Pharmacology, Faculty of Medicine, Khon Kaen University, Khon Kaen, Thailand*
[2] *Cholangiocarcinoma Research Institute, Khon Kaen University, Khon Kaen, Thailand*
[3] *Department of Chemistry, Faculty of Science, Khon Kaen University, Khon Kaen, Thailand*
[4] *Program of Chemistry, Faculty of Science and Technology, Sakon Nakhon Rajabhat University, Sakon Nakhon, Thailand*

*E-mail: peuamd@kku.ac.th

Abstract

Ovalitenin A, a chalcone compound derived from the roots of *Millettia brandisiana* Kurz, has exhibited remarkable cytotoxicity against various cancer types. However, its potential as anti-tumor agent in cholangiocarcinoma (CCA), an aggressive malignancy originating in the bile duct epithelia, remains inadequately explored. Therefore, the current study aims to elucidate the anti-metastatic potential of ovalitenin A and the underlying molecular mechanisms of its actions in CCA cells. The cell viability and migration ability of CCA cells following ovalitenin A treatment were assessed using sulforhodamine B (SRB) and wound healing assays, respectively. Protein expression levels of the NF-κB signalling pathway and its downstream proteins were determined via western blot analysis. Our findings demonstrated that ovalitenin A exerted a dose-dependent inhibitory effect on the proliferation of CCA cells. Furthermore, treatment with ovalitenin A led to a reduction in the migratory potential of CCA cells. Notably, treatment with ovalitenin A resulted in a marked elevation in the expression of the basal form of IκBα and NF-κB proteins. Subsequently, the level of VEGF, a NF-κB-targeted protein that plays pivotal roles in driving cancer metastasis, displayed a significant decrease following exposure to ovalitenin A. In conclusion, our study has yielded compelling evidence supporting the remarkable anti-metastatic potential of ovalitenin A in CCA cells. Ovalitenin A's pronounced effects on anti-migration are intricately linked to the suppression of the NF-κB signalling pathway.

Keywords: *Millettia brandisiana*; NF-κB; ovalitenin A; bile duct cancer; metastasis

Introduction

Cholangiocarcinoma (CCA) is a cancer that affects the cells in the epithelia biliary tree. It is the second most common type of liver cancer, responsible for 13% of cancer-related deaths globally.[1] The mortality rate of CCA is greater in men than in women, particularly in Asian countries compared to those in Western regions. Furthermore, Asian individuals are found to have the highest rate of mortality.[2]

Early-stage CCA can be effectively treated with surgery, resulting in a median overall survival of 51.1 months. Despite the high median overall survival of curative resection, CCA patients often report unsatisfactory outcomes because of the high rate of post-operative recurrence.[2] On the other hand, patients with severe or metastatic cancer and unresected

tumors typically receive gemcitabine and cisplatin as the initial chemotherapy treatment, leading to a median survival of 11.7 months, which is shorter than that achieved by surgery.[2,3] In fact, metastasis appears to play a significant role in the poor response to cancer therapy as the disease progresses. Therefore, there is an urgent need for developing novel treatments, including investigating natural compounds that may inhibit CCA metastasis.

Metastasis is the process by which cancer cells form secondary tumors in distant locations from the original site.[4] The metastatic cascade involves cancer cells infiltrating the basement membrane and subsequently disseminating into the stromal environment.[5] Afterwards, cancer cells migrate into adjacent tissue and intravasate into a nearby blood vessel, resulting in metastasis.[6] Excessive activation of Nuclear Factor Kappa B (NF-κB) has been associated with promoting metastasis in research studies.[7] The most recent research indicates that NF-κB activation is a result of the formation of an inflammatory micro-environment during the development of cancer. It serves as a crucial link between inflammation and cancer.[8] NF-κB transcription factors can be activated by either canonical and non-canonical signaling. The canonical NF-κB pathway requires inhibitor of κB kinase (IKK), while the non-canonical pathway relies solely on NF-κB-inducing kinase (NIK). Remarkably, the canonical NF-κB pathway has been revealed to modulate vascular endothelial growth factor (VEGF) gene expression.[9] VEGF plays a role in metastasis by promoting the growth of new blood vessels to provide growing tumors with oxygen and nutrition.[10] Additionally, there is a report indicating that VEGF can rapidly enhance vascular permeability, leading to plasma protein leakage and the development of an extravascular matrix, which enhances the conditions for subsequent endothelial cell proliferation.[11]

Growing evidence emphasizes the role of NF-κB in the development of CCA and suggests that targeting NF-κB may be beneficial for treating CCA. This was verified by the overexpression of NF-κB in cancer tissues from patients with CCA. Research has shown that dehydroxymethylepoxyquinomicin (DHMEQ), a new NF-κB inhibitor, effectively hinders the growth of CCA cells and tumor growth in a xenograft heterotopic model of CCA.[12] Subsequent studies also revealed that VEGF expression was higher in CCA compared to normal tissues in CCA patients.[13] This was confirmed by the finding of VEGF expression in KKU-452, KKU-023, and KKU-100.[14] Additionally, a study indicated that isomorellin, a caged xanthones, could inhibit the migration and invasion of CCA cells by increasing NF-κB inhibitor alpha (IκB-α) levels.[15] According to another study, treatment of cucurbitacin B, a dietary triterpenoid, inhibited KKU-213 cells' migration and invasion mediated by Src activator in a dose-dependent manner. Upon further investigation, it was shown that cucurbitacin B reduced the expression of VEGF, one of the proteins related to metastasis.[16] These pieces of evidence suggest the crucial role of NF-κB signaling pathway and its downstream mediator, VEGF, in the CCA metastasis cascade.

Ovalitenin A, a chalcone isolated from the roots of *Millettia brandisiana* Kurz, has demonstrated significant cytotoxic properties.[17] Ovalitenin A has shown notable toxicity against several types of cancer, including human prostate cancer (DU145), cervical cancer (HeLa), chronic myelogenous leukemia (K562), hepatoma (HepG2), leukemia (HL6), and cholangiocarcinoma (KKU-M156).[17,18] An investigation into ovalitenin A's apoptotic mechanism revealed its ability to decrease Bcl-2 protein, increase Bax protein, and decrease COX-2 protein expression in HeLa cells.[18] Given COX-2's role in tumour progression and metastasis promotion, this finding suggests that ovalitenin A might not only suppress tumor growth, but also inhibit metastasis.[19] However, its potential as an anti-metastasis agent remains largely unexplored. Therefore, this study aims to investigate the anti-metastasis potential of ovalitenin A in CCA and elucidate its underlying mechanism. The findings from this research provide valuable evidence supporting the therapeutic potential of ovalitenin A in combating metastasis.

Methods

Chemicals and reagents

Ham's F12 medium, fetal bovine serum (FBS), and Dulbecco's modified Eagle's medium (DMEM) were purchased from Gibco BRL Life Technologies (NY, USA). Trichloroacetic acid and sulforhodamine B (SRB) were obtained from Sigma-Aldrich (St. Louis, USA). Antibodies against β-actin (sc-47778), NF-κB (sc-109), VEGF (sc-7269), and goat anti-rabbit IgG-HRP (sc-2357) were obtained from Santa Cruz Biotechnology (Texas, USA). IκBα (#4814) and anti-mouse IgG (#7076) were purchased from Cell Signaling (MA, USA).

Ovalitenin A preparation

Ovalitenin A used in this study was provided by Prof. Chavi Yenjai, Faculty of Science, Khon Kaen University. It was extracted from *M. brandisiana* Kurz roots and purified by preparative thin-layer chromatography (TLC). The chemical structure of isolated ovalitenin A was then identified using spectroscopic methods, including 1D-NMR, 2D-NMR, MS, IR, and CD data.[17]

Cell lines and cell cultures

The human CCA cell line KKU-452 was developed at the Cholangiocarcinoma Research Institute, Khon Kaen University.[14] The cells were cultured in Ham's F12 complete medium containing 4-(2-hydroxyethyl)-1-piperazineethanesulfonic acid (HEPES; pH 7.3), sodium bicarbonate ($NaHCO_3$), penicillin (100 µg/mL), gentamicin (80 µg/mL), and 10% FBS. CCA cells were cultured under an atmosphere of 5% CO_2 in air at 37°C and subcultured using 0.25% trypsin-EDTA when the cells reached 70–80% confluence.

SRB cell viability assay

The CCA cells, with a density 7,500 cells/100 µL/well, were plated in a 96-well-plate and incubated under 5% CO_2 overnight.[20] The following day, the cells were treated with ovalitenin A at concentrations of 0, 0.63, 1.25, 2.5, 5, and 20 µg/mL. After 24 h incubation, the cells were fixed with ice-cold 10% trichloroacetic acid and stained with 0.4% SRB. The absorbance was then measured at 540 nm using a microplate reader (Sunrise™ Elisa Plate Reader; Tecan Group, Ltd.). Cell viability was expressed as a percentage of the treated group relative to the untreated group. The half-maximal inhibitory concentration (IC_{50}) was calculated by using GraphPad Prism 8.

Wound healing assay

The CCA cells, with a density 300,000 cells/mL/well, were plated in a 24-well-plate and incubated under 5% CO_2 overnight. The following day, the cells were scraped off using sterile pipette tips and then washed with PBS to remove undetached cells.[21] Subsequently, the cells were treated with ovalitenin A at concentrations of 0, 0.31, 0.63, and 1.25 µg/mL, and the images of wound gap were captured at 0-24 h post-treatment. Cell migration, as measured by closure of the wound gap, was analyzed using Image Pro Plus software.

Western blot assay

The cells, with density 250,000 cells/mL/well, were plated in a 6-well-plate and incubated under 5% CO_2 overnight. They were then treated with ovalitenin A at concentrations of 0, 0.31, 0.63 and 1.25 µg/mL for 24 h. The following day, the cells were lysed with RIPA cell lysis buffer containing 1X Halt™ Protease Inhibitor Cocktail (Thermo Fisher Scientific Inc.). After centrifugation, the supernatants were collected. The protein level was determined using Bradford protein assay (Bio-Rad Laboratories Inc.). A total of 25 µg of protein was loaded

onto 10% SDS-PAGE and separated using SE 260 mini-vertical gel electrophoresis. Upon completion of electrophoresis, the proteins in the gel were transferred onto PVDF membranes using Owl™ HEP-1 Semidry Electroblotter.[20] Subsequently, the membranes were incubated with polyclonal IgG antibodies against IκBα (1:1000), NF-κB (1:1000), and VEGF (1:1000), followed by incubation with the corresponding secondary antibodies. Finally, the protein bands were imaged using the Chemi DOC™ MP imaging system. The intensity of the protein bands was analyzed using Gel-Pro Analyzer 4 software and expressed as a ratio to the housekeeping reference protein, β-actin.

Statistical analysis

All results were presented as the mean ± SD, whereas statistical comparison between control and treatment group was performed by one-way ANOVA followed by Tukey's post hoc test. The results were statistical significance at $p < 0.05$.

Results

The effect of ovalitenin A on the cell viability of KKU-452 cells was assessed using the SRB assay. The cells were treated with various concentrations of ovalitenin A. The findings demonstrated that the compound reduced the cell viability of CCA cells in a concentration-dependent manner, with the IC 50 at 24 h being 2.01 μg/mL (**Figure 1**).

Furthermore, ovalitenin A demonstrated a significant inhibitory effect on the migration of KKU-452 cells, as observed in the wound healing assay. The percentage of wound closure area at concentrations of 0.31, 0.63, and 1.25 ug/mL were 58.74%, 44.03%, and 28.37%, respectively (**Figure 2**). The findings demonstrated that the compound significantly reduced the cell migration of CCA cells compared to the untreated control.

The protein expression of NF-κB, a key transcription factor involved in metastasis[22], was analyzed using western blot analysis. It was shown that concentrations of 0.63 and 1.25 μg/mL of ovalitenin A exhibited a notable increase of NF-κB following 24 h of treatment (**Figure 3A-B**). Similarly, there was a significant increase in IκBα, a family of inhibitory proteins that bind to NF-κB, at concentrations of 0.63 and 1.25 μg/mL (**Figure 3C-D**).

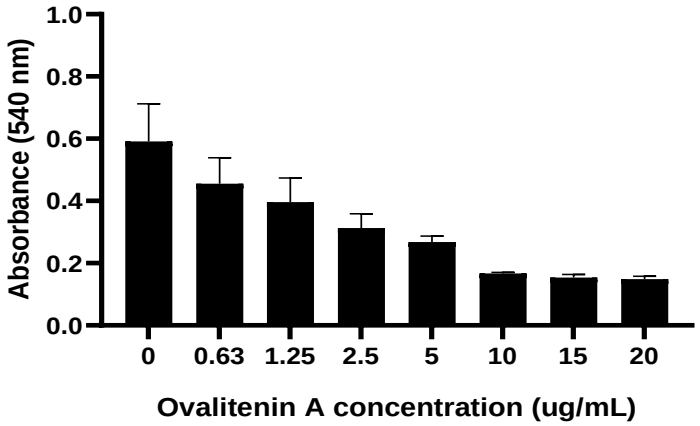

Figure 1. Ovalitenin A reduced the cell viability in CCA cells. KKU-452 cells were treated with 0, 0.63, 1.25, 2.50, 5, 10, 15, 20 μg/mL ovalitenin A for 24 h to measure the capability of cell viability. The data present as mean ± SD from three independent experiments.

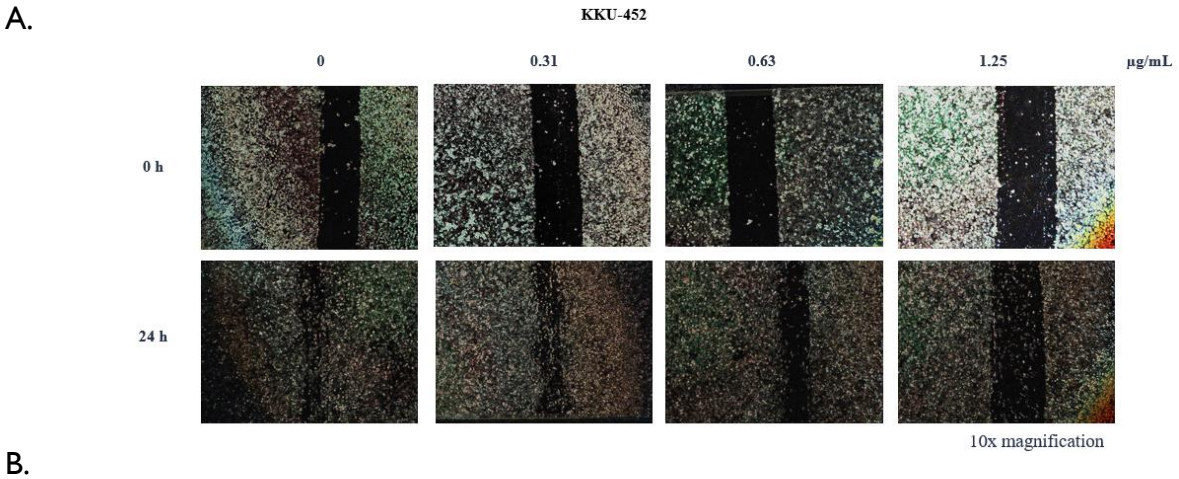

Figure 2.
Ovalitenin A suppressed the migration of CCA cells. A wound healing assay was performed following a 24 h treatment with concentrations of 0, 0.31, 0.63, and 1.25 µg/mL ovalitenin A. Cell migration was measured as the closing distance of the wound gap. Representative images of cell migration (magnification, x10) (A) and percentage of migrated cells (B) are shown. The data present as mean ± SD from three independent experiments. $^{*}p < 0.05$ compared to the untreated control group.

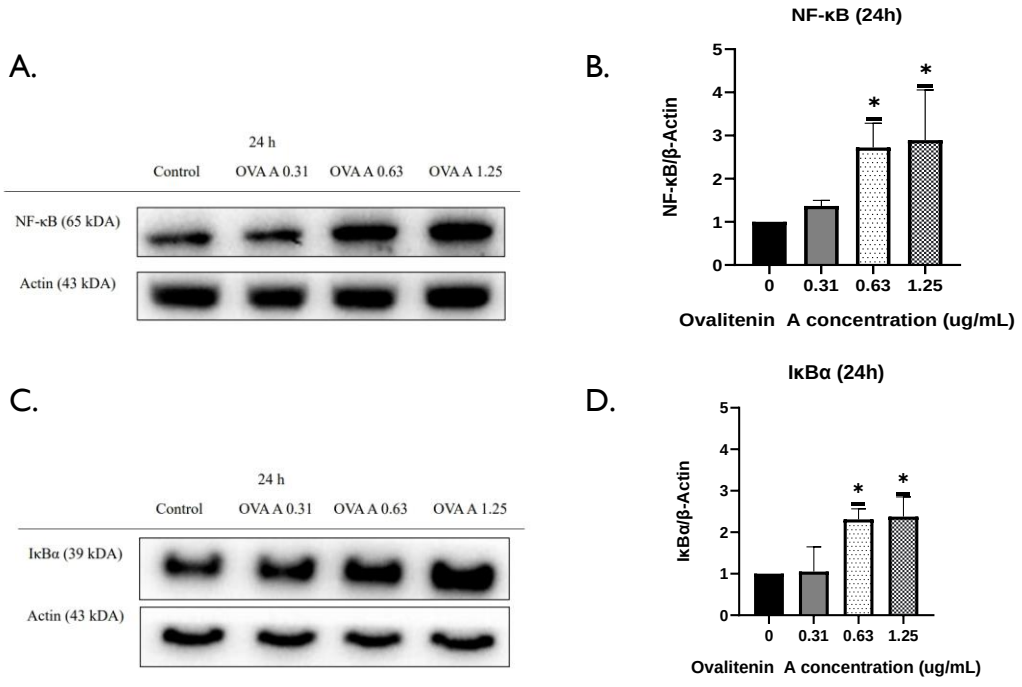

Figure 3. Ovalitenin A increased the expression of NF-κB and IκBα in CCA cells. KKU-452 cells were treated with 0, 0.31, 0.63 and 1.25 ug/mL of ovalitenin A for 24 h. The expression of NF-κB and IκBα were determined by western blot analysis. Representative images and expression levels of NF-κB (A, B) and IκBα (C, D) are shown. The graph depicts the relative expression of specific protein normalized to β-actin expression. The data are presented as mean ± SD from three independent experiments. $^{*}p < 0.05$ compared to the untreated control group.

Subsequently, the protein level of VEGF, a NF-κB-targeted protein which plays pivotal roles in driving cancer metastasis[8], was determined. It displayed a significant decline after 24 h treatment with 0.63 and 1.25 μg/mL of ovalitenin A (**Figure 4**).

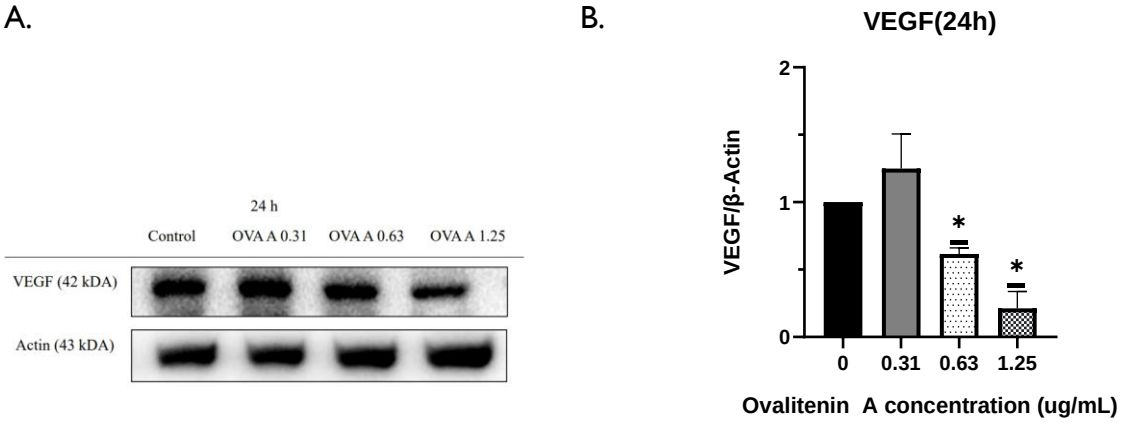

Figure 4. Ovalitenin A reduced the expression of VEGF in CCA cells. KKU-452 cells were treated with 0, 0.31, 0.63 and 1.25 ug/mL of ovalitenin A for 24 h. The expression of VEGF was determined by western blot analysis. Representative images (A) and the expression level (B) are shown. The graph depicts the relative expression of specific protein normalized to β-actin expression. The data are presented as mean ± SD from three independent experiments. $^{*}p < 0.05$ compared to the untreated control group.

Discussion

The findings of the present study revealed the inhibitory effects of ovalitenin A on the proliferation and migration of CCA cells. Ovalitenin A exhibited antiproliferative effects in KKU-452, with an IC_{50} of 2.01 μg/mL after 24 h of treatment. Moreover, the wound healing closure comparison between the untreated group and the group treated with ovalitenin A also demonstrated inhibited cell migration, suggesting the anti-metastatic potential of ovalitenin A.

Prior research demonstrated the cytotoxicity of ovalitenin A from the dried root tuber of *M. pulchra*. Assessment using the MTT assay revealed its inhibitory effect on the growth of HeLa, Hep G2, HL-60, K562, and DUI 145. HeLa cell exhibited the highest sensitivity to ovalitenin A among the five cancer cells tested, with an IC_{50} value of about 10 μg/mL.[18] Recently, ovalitenin A from the roots of *M. brandisiana* Kurz had been reported for its strong cytotoxic activity against Hep G2 and KKU-M156 with IC_{50} values of 1.74 and 1.95 μg/mL respectively.[17] The IC_{50} value observed in KKU-M156 resembled that seen in KKU-452 (IC_{50} value of 2.01 μg/mL), indicating that ovalitenin A displayed sensitivity towards CCA cells. In accordance with this, ovalitenin A was found to induce apoptosis through the mitochondrial pathway, by reducing COX-2, increasing PARP-1 expression, and altering the Bcl-2-Bax ratio[18]. Evidence indicated that COX-2 may contribute to multiple stages of cancer development by promoting the growth of mutated cells, enhancing tumor growth, affecting cell death processes, impacting the effectiveness of cancer treatments, and ultimately being involved in metastasis.[19] It is worth noting that COX-2 was linked to NF-κB as a key regulator of proinflammatory gene expression.[23] Moreover, ovalitenin A also showed anti-inflammatory properties by significantly decreasing nitrite levels in lipopolysaccharide-stimulated RAW264.7

macrophage cells.[24] Hence, ovalitenin A may have the ability to modify the NF-κB signaling pathway.

A wound healing assay was conducted to assess the antimigratory capability of ovalitenin A at concentrations of 0.31, 0.63, and 1.25 µg/mL, which exhibited slight inhibition of cell proliferation. The study demonstrated that ovalitenin A at these concentrations significantly inhibited the migration of KKU-452 in a concentration-dependent manner compared to the untreated control group. The concentration of 1.25 µg/mL prevented approximately 70% of migration. These outcomes revealed a superior efficacy in inhibiting cell migration compared to rice bran hydrolysates, which achieved a comparable 70% inhibition at concentration of 1200 µg/mL.[15,25]

Ovalitenin A's antimigratory effect is likely linked to alterations in the NF-kB signalling pathway. Inactive NF-κB dimers are usually found in the cytoplasm, where they are bound to protein inhibitors called IκBs.[26] Within the canonical pathway, the activation of IKK-dependent cascade leads to the phosphorylation of IκBs, allowing the NF-κB complex to enter the nucleus.[27] Protein analyses using western blotting showed that ovalitenin A induced a significant increase in the expression of the basal form of both NF-κB and IκBα, leading to suppression of NF-κB signaling. VEGF expression in KKU-452 cells was also investigated in the current study. VEGF has been associated with tumor metastasis, and NF-κB has been identified as one of its promoters.[8] The study demonstrated a reduction in VEGF expression following an upregulation in NF-κB and IκBα levels. This outcome aligns with isomorellin's impact on suppressing KKU-100 cell viability, invasion, and migration, which was correlated with the inhibition of the translocation of NF-κB to the nucleus in a dose-dependent manner by upregulating IκBα.[15] Furthermore, in human umbilical vein endothelial cells (HUVECs), the anti-malarial drug dihydroartemisinin (DHA) shown an ability to decrease both cell proliferation and migration by elevating IκBα protein levels and inhibiting the nuclear translocation of NF-κB p65. Subsequent research revealed that DHA could decrease the mRNA and protein levels of VEGFR2 in endothelial cells, indicating that NF-κB signalling might be responsible for the effects of DHA on VEGFR2 expression.[28] Additionally, in a recent observation, it was demonstrated that treating colon cancer cells (HT-29 and Caco-2) with crocin, a dietary carotenoid, could suppress colon carcinoma cell angiogenesis and metastasis by reducing TNF-α production and preventing NF-kB activation, which in turn decreased the expression of VEGF. This research implies that crocin may prevent colon cancer metastasis by interfering with the TNF-α/NF-kB/VEGF pathways.[29]

The proposed underlying mechanisms of the antiproliferative and antimigratory effects of ovalitenin A in CCA cells are summarized in **Figure 5**. It is essential to acknowledge that this study solely focused on examining IκBα and NF-κB proteins after ovalitenin A treatment. Although these proteins play crucial roles in the metastasis process, future investigations should broaden the scope to include IKKα, IKKβ, phosphorylated IKKα/β, phosphorylated IκBα, phosphorylated NF-κB, and explore the involvement of NF-κB-targeting metastasis-related proteins, particularly MMP-9 and ICAM-1. Such a comprehensive approach would offer deeper insights into ovalitenin A's impact on CCA cells and its potential therapeutic applications.

Conclusion

The current research demonstrates that ovalitenin A's significant impact on inhibiting migration in CCA is closely associated with the inhibition of NF-κB signaling pathway and downregulation of VEGF.

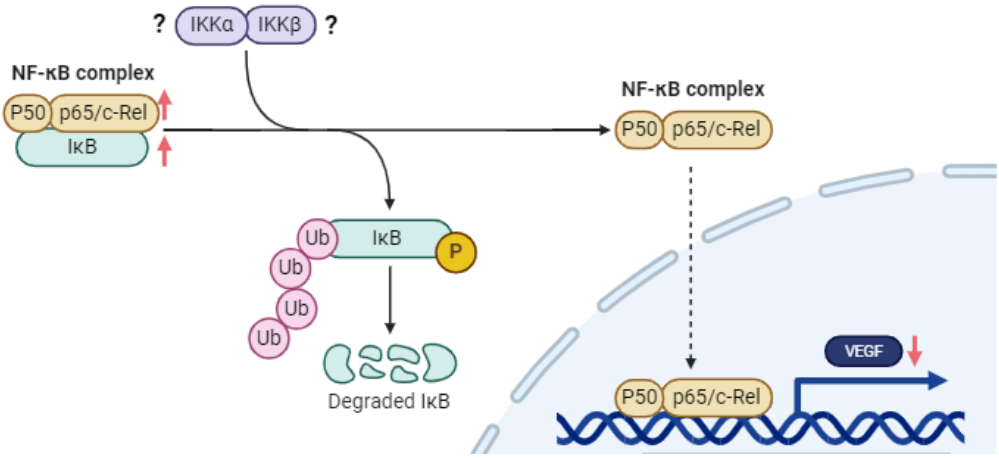

Figure 5. The proposed underlying mechanisms of antiproliferative and antimigratory effects of ovalitenin A in CCA cells. (Created with BioRender.com)

Acknowledgments

This research was supported by NSRF under the Basic Research Fund of Khon Kaen University through Cholangiocarcinoma Research Institute (CARI-BRF65-8). Putu Ririn Andreani was supported by a KKU Scholarship for ASEAN & GMS Countries Personnel.

References

1. Kirstein MM, Vogel A. Epidemiology and risk factors of cholangiocarcinoma. Visc Med. 2016 Dec;32(6): 395-400.
2. Banales JM, Marin JJG, Lamarca A, Rodrigues PM, Khan SA, Roberts LR, et al. Cholangiocarcinoma 2020: the next horizon in mechanisms and management. Nat Rev Gastroenterol Hepatol. 2020 Sep;17(9):557-88.
3. Brindley PJ, Bachini M, Ilyas SI, Khan SA, Loukas A, Sirica AE, et al. Cholangiocarcinoma. Nat Rev Dis Prim. 2021 Sep 9;7(1):66.
4. Fares J, Fares MY, Khachfe HH, Salhab HA, Fares Y. Molecular principles of metastasis: a hallmark of cancer revisited. Signal Transduct Target Ther. 2020 Mar 12;5(1):28.
5. Hapach LA, Mosier JA, Wang W, Reinhart-King CA. Engineered models to parse apart the metastatic cascade. NPJ Precis Oncol. 2019 Aug 21;3:20.
6. Jonckheere S, Adams J, De Groote D, Campbell K, Berx G, Goossens S. Epithelial-mesenchymal transition (EMT) as a therapeutic target. Cells Tissues Organs. 2022;211(2):157-82.
7. Xi Y, Shen S, Verma IM. NF-κB, an active player in human cancers. Cancer Immunol Res. 2014 Sep;2(9): 823-30.
8. Yan M, Xu Q, Zhang P, Zhou X jian, Zhang Z yuan, Chen W tao. Correlation of NF-κB signal pathway with tumor metastasis of human head and neck squamous cell carcinoma. BMC Cancer. 2010 Aug 17; 10:437.
9. Noort AR, van Zoest KPM, Weijers EM, Koolwijk P, Maracle CX, Novack D V., et al. NF-κB-inducing kinase is a key regulator of inflammation-induced and tumour-associated angiogenesis. J Pathol. 2014 Nov; 234(3):375-85.
10. LaValley DJ, Zanotelli MR, Bordeleau F, Wang W, Schwager SC, Reinhart-King CA. Matrix stiffness enhances VEGFR-2 internalization, signaling, and proliferation in endothelial cells. Converg Sci Phys Oncol. 2017; 3:044001.
11. Carmeliet P. VEGF as a key mediator of angiogenesis in cancer. Oncology. 2005;69 Suppl 3:4-10.
12. Seubwai W, Wongkham C, Puapairoj A, Khuntikeo N, Pugkhem A, Hahnvajanawong C, et al. Aberrant expression of NF-κB in liver fluke associated cholangiocarcinoma: Implications for targeted therapy. PLoS One. 2014 Aug 19;9(8): e106056.
13. Pan S, Hu Y, Hu M, Xu Y, Chen M, Du C, et al. S100A8 facilitates cholangiocarcinoma metastasis via upregulation of VEGF through TLR4/NF-κB pathway activation. Int J Oncol. 2020 Jan;56(1):101-12.

14. Saensa-ard S, Leuangwattanawanit S, Senggunprai L, Namwat N, Kongpetch S, Chamgramol Y, et al. Establishment of cholangiocarcinoma cell lines from patients in the endemic area of liver fluke infection in Thailand. Tumor Biol. 2017 Nov;39(11):1010428317725925.
15. Hahnvajanawong C, Sahakulboonyarak T, Boonmars T, Reutrakul V, Kerdsin A, Boueroy P. Inhibitory effect of isomorellin on cholangiocarcinoma cells via suppression of NF-κB translocation, the phosphorylated p38 MAPK pathway and MMP-2 and uPA expression. Exp Ther Med. 2021 Feb;21(2):151.
16. Kaewmeesri P, Kukongviriyapan V, Prawan A, Kongpetch S, Senggunprai L. Cucurbitacin B diminishes metastatic behavior of cholangiocarcinoma cells by suppressing focal adhesion kinase. Asian Pac J Cancer Prev. 2021 Jan 1;22(1):219-225.
17. Arthan S, Pornchoo C, Prawan A, Tontapha S, Amornkitbamrung V, Yenjai C. Brandisianones F and G from *Millettia brandisiana* Kurz and their cytotoxicity. Nat Prod Res. 2022 Mar;36(5):1236-44.
18. Liu D yu, Guo Y, Si J yong, Sun G bo, Zhang B, Cao L. Inhibition of ovalitenin A on proliferation of HeLa cells via apoptosis, G2/M cell cycle arrest, and down-regulation of COX-2. Chinese Herb Med. 2016 July; 8(3):259-66.
19. Diederich M, Sobolewski C, Cerella C, Dicato M, Ghibelli L. The role of cyclooxygenase-2 in cell proliferation and cell death in human malignancies. Int J Cell Biol. 2010:2010:215158.
20. Butsri S, Kukongviriyapan V, Senggunprai L, Kongpetch S, Prawan A. 13-*cis*-retinoic acid inhibits the self-renewal, migration, invasion and adhesion of cholangiocarcinoma cells. Int J Mol Med. 2023 Mar;51(3):20.
21. Jaidee R, Kongpetch S, Senggunprai L, Prawan A, Kukongviriyapan U, Kukongviriyapan V. Phenformin inhibits proliferation, invasion, and angiogenesis of cholangiocarcinoma cells via AMPK-mTOR and HIF-1A pathways. Naunyn Schmiedebergs Arch Pharmacol. 2020 Sep;393(9):1681-90.
22. Xu D, Ma Y, Zhao B, Li S, Zhang Y, Pan S, et al. Thymoquinone induces G2/M arrest, inactivates PI3K/Akt and nuclear factor-κB pathways in human cholangiocarcinomas both *in vitro* and *in vivo*. Oncol Rep. 2014 May;31(5):2063-70.
23. Tak PP, Firestein GS. NF-κB: A key role in inflammatory diseases. J Clin Invest. 2001 Jan;107(1):7–11.
24. Huo X, Zhang L, Gao L, Guo Y, Zhang L, Li L, et al. Antiinflammatory and analgesic activities of ethanol extract and isolated compounds from *Millettia pulchra*. Biol Pharm Bull. 2015;38(9):1328-36.
25. Phusrisom S, Senggunprai L, Prawan A, Kongpetch S, Kukongviriyapan U, Thawornchinsombut S, et al. Anti-tumor activity of rice bran hydrolysates on migration, invasion and angiogenesis. Asian Pac J Trop Biomed. 2021 July;11(7):317-26.
26. Zhang H, Sun SC. NF-κB in inflammation and renal diseases. Cell Biosci. 2015 Jan 5;5(1):1.
27. Zhang Q, Lenardo MJ, Baltimore D. 30 Years of NF-κB: A blossoming of relevance to human pathobiology. Cell. 2017 Jan 12;168(1-2):37-57.
28. Dong F, Zhou X, Li C, Yan S, Deng X, Cao Z, et al. Dihydroartemisinin targets VEGFR2 via the NF-κB pathway in endothelial cells to inhibit angiogenesis. Cancer Biol Ther. 2014;15(11):1479-88.
29. Bakshi HA, Quinn GA, Nasef MM, Mishra V, Aljabali AAA, El-Tanani M, et al. Crocin inhibits angiogenesis and metastasis in colon cancer via TNF-α/NF-kB/VEGF pathways. Cells. 2022 Apr 29;11(9):1502.

F04

Analyzing Anchorage-Independent Tumorigenesis of the Live Cholangiocarcinoma Stem Cell Biosensor Using High-Throughput Imaging and Computational Pipelines

Krittiyabhorn Kongtanawanich[1*], Supawan Jamnongsong[1,2], Somponnat Sampattavanich[1,2], Methichit Wattanapanitch[3], Siwanon Jirawatnotai[1,2]

[1] *Department of Pharmacology, Faculty of Medicine Siriraj Hospital, Mahidol University, Bangkok, Thailand*
[2] *Center of Research Excellence for Precision Medicine and Systems Pharmacology, Faculty of Medicine Siriraj Hospital, Mahidol University, Bangkok, Thailand*
[3] *Siriraj Center for Regenerative Medicine, Research Department, Faculty of Medicine Siriraj Hospital, Mahidol University, Bangkok, Thailand*

*E-mail: krittiyabhorn.kon@student.mahidol.edu

Abstract

Cancer stem cell (CSC) biosensors became an emerging tool for plasticity-capturing in various cancer types. Tumorigenesis is one of the CSC properties that stands for the gold standard for verifying CSC phenotype. Three-dimensional (3D) multi-spheroid, an outstanding *in vitro* tumorigenesis model, showed some limitations and technical biases. However, accurate tumorigenic assay with full usage of CSC live biosensor advantages is still lacking. Here, a high-accuracy *in vitro* tumorigenic assay of cholangiocarcinoma stem cells (CCA CSC) live biosensor in a 3D multi-spheroid culturing context is developed using high-throughput imaging and a computational pipeline. A SOX2/OCT4 functional-based live biosensor expressing dsCopGFP as fluorescence reporter (SORE6-mCMV-dsCopGFP) was constructed in CCA cell lines. Our analysis demonstrated that the high purity of SORE6^{POS} cells grew greater in both the number and area of spheroids. As a benefit of live spheroid expressing CSC biosensor, spontaneous differentiation was revealed in an anchorage-independent environment. This analysis in which the spheroid was analyzed by area displayed a positive correlation with spheroid diameter, a traditional spheroid measurement. Accordingly, this is applied to distinct spheroid shapes. Altogether, the *in vitro* tumorigenic analyzed pipeline together with CSC live biosensor was effective and accurate in verifying CSC phenotype. Moreover, this analysis would apply to other 3D tumorigenic tests such as organoids.

Keywords: Cancer stem cells, reporter, biosensor, tumorsphere, spheroid, organoid, high-throughput

Introduction

Anchorage-independent model is the closest *in vitro* model as clinical representation.[1] In studies of cell lines, spheroid models such as multicellular spheroid, and multi-spheroid were used for various purposes.[2] While Intratumor heterogeneity is well known making cancer a challenging disease that is difficult to remission, and easy to recurrence.[3] Thus, single-cell techniques such as reporter cells enable real-time observation in many research fields, especially in cancer stem cell (CSC) studies.[4] CSC is a group of cells that engages the ability of both cancer and normal stem cells which show extraordinary behaviors including metastasis, treatment resistance, evading apoptosis, cancer recurrence, etc.[5-7]

CSC live biosensor become one of the outstanding techniques to identify CSC in many types of cancer.[4] In the CSC study, the spheroid model has been notably used for CSC properties verification and drug testing by which 3D multi-spheroid has remarkably applied for both objectives.[2,8,9] Altogether, the 3D multi-spheroid model created from the CSC biosensor cells becomes a reasonable model for powerful CSC study and allows us to investigate deeper CSC biology in the context of an anchorage-independent manner. *In vivo* tumorigenic assay is used as the gold standard of CSC verification.[10] However, animal experimentation is expensive and moral, so non-ethical preliminary steps especially *in vitro* tumorigenesis need to be first explored. The 3D multi-spheroid has been notably used for this purpose, but it is labor-intensive. Moreover, sampling and selection bias might be encompassed toward the expected hypothesis. Moreover, the determined cut-off of the spheroid by using the sphere diameter is inapplicable in some cases due to the non-spherical shape of the spheroid even within the same cancer type.

Here, we developed high-throughput procedures and analysis methods using a CSC-biosensor-based CCA cell line model to investigate *in vitro* tumorigenesis. *SOX2* together with *OCT4* impairs clinical outcomes in CCA patients (unpublished data), thus the SORE6 biosensor[11] which detects SOX2 and OCT4 protein as dual transcription factors on NANOG promoter was used for *in vitro* tumorigenicity exploration. The 3D multi-spheroids from the $SORE6^{POS}$ population and $SORE6^{NEG}$ population were determined by area and then counted by imaging and a simple R-based programming pipeline. We also solved considerable problems such as cell aggregation prevention, and adaptable analysis for irregular spheroid shape.

Methods

Cell culture

In this study, TFK-1 and KKU-068 (obtained from the Japanese Collection of Research Bioresources (JCRB) cell bank, Osaka, Japan) CCA cell lines were included in this study. The complete medium was prepared by basal medium supplemented with 10% fetal bovine serum (FBS) and 1% penicillin/streptomycin. Roswell Park Memorial Institute 1640 Medium (RPMI 1640) and Dulbecco's modified Eagle's medium (DMEM) were used as basal medium for TFK-1 and KKU068, respectively. All cell lines were maintained at 37 °C in a humidified atmosphere containing 5% CO_2.

Generation of CSC-biosensor-based CCA cell line model

The CSC-biosensor-based CCA cell line models were generated using a lentiviral-based live biosensor. To detect dual activity of SOX2 and OCT4 protein, the six tandem repeats of SOX2/OCT4 response element (SORE6) coupled with minimal cytomegalovirus (mCMV) promoter are used to drive the short half-life of green fluorescence protein (SORE6-dsCopGFP) expression as a fluorescence reporter. Thus, the identical biosensor without SORE6 sequence (mCMV-dssCopGFP) was used as gating control and background control for fluorescence-activated cell sorting (FACS) and fluorescence imaging, respectively. The lentiviral plasmids of CSC biosensor[11] was a kind gift from Dr. Lalage M. Wakefield, NCI, USA. To generate lentiviral biosensor, either SORE6-mCMV-dsCopGFP or mCMV-dsCopGFP lentiviral plasmid was co-transfected with second-generation packing plasmids (psPAX2 and pMD2.G) into HEK293T cells to produce viral supernatant. To transduce the viral biosensor into the cells, the viral supernatant was collected, filtered, and mixed with 5 μg/mL polybrene and fresh culture medium in 1:1 ratio. Then, the mixture was exposed to each CCA cell line for 24 h. To confirm the availability of live biosensor, both SORE6-mCMV-dsCopGFP and mCMV-dsCopGFP were constructed together with puromycin resistance gene, thus puromycin was treated onto the sub-confluent transduced CCA cell lines for 5 days.

Fluorescence-activated Cell Sorting (FACS)

The SORE6^{POS} and SORE6^{NEG} populations were distracted by dsCopGFP intensity in which mCMV-dsCopGFP was used as background control cells. The SORE6-containing biosensor cells were separately sorted by BD FACS Aria™ III Cell Sorter (BD Biosciences) according to standard protocol. The sorted cells were immediately re-run through the same FACS to confirm their purity.

In vitro tumorigenic assay

The anchorage-independent plate was prepared by mixing 1:1 ratio of complete medium and 2.8% methyl cellulose (MC) (#HSC011, R&D systems), then fill 100 µL of the mixture (1.4% MC in complete medium) onto an ultra-low attachment (ULA) flat-bottoms 96-well plate (#3474, Corning). The single-cell expansion in anchorage-independent growth was assessed by seeding the SORE6^{POS} and SORE6^{NEG} cells at 1,000, 500, and 250 cells per 100 µL of the complete medium onto a prepared anchorage-independent plate, thus the final concentration of MC was 0.7% in complete medium. For 14 days of the culturing period, 20 µL of complete medium was gently added every 5 days.

High-content confocal imaging

The spheroids were fixed and stained using the on-top technique with 4% para-formaldehyde (PFA) for 30 min and 10 µg/mL Hoechst 33342 (#H1399, Invitrogen) overnight, respectively. The stained plates were imaged using a high-content confocal imaging machine (Operetta® CLS™) (PerkinElmer) for 3 channels including bright field (emission 655-760 nm), Hoechst 33342 (excitation 355-385 nm; emission 430-500 nm), and dsCopGFP (excitation 460-490 nm; emission 500-550 nm). The images were taken in every field of each well to prevent field selection bias.

Image and data analysis

The images were processed using an in-house image analysis pipeline which was created in Columbus™ Image Data Storage and Analysis System by PerkinElmer. Briefly, the images from confocal mode were acquired in different z-axis, then all images in the z-axis were combined into one image called maximum projection image which is 2D image. All nuclei in maximum projection image were detected by Hoechst 33342. The nuclear area, length, width/length, and GFP intensity of each spheroid were measured. Afterward, the data was exported and further analyzed using in-house R code in R Studio® software. The objects with Hoechst 33342-stained area greater than 8,000 µm^2 were counted as spheroid.

Statistical Analysis

Statistical significance was determined between groups using t-test and the Wilcoxon rank-sum test as stated in figure legend. A p-value < 0.05 was considered statistically significant for most of the tests.

Results

The ability to create malignant tumors is a unique CSC behavior apart from healthy stem cell characteristics. The SOX2/OCT4 expressing cells were speculated to be CSC in CCA (unpublish data), thus SOX2/OCT4 functional-based live biosensor (SORE6 biosensor) was used for the SOX2/OCT4 detection which a short half-life of CopGFP (dsCopGFP) was as fluorescence reporter protein (SORE6-dsCopGFP). We applied high-content confocal imaging and simple R-based programming for high-throughput analysis to evaluate the *in vitro* tumorigenic assay of SORE6 biosensor in CCA cell lines (**Figure 1**).

The anchorage-independence culturing system using a ULA flat-bottom plate was optimized for creating uniform 3D multi-spheroids, thus MC as a suspending agent was used in this protocol to prevent cell aggregation (**Figure 2a**). By culturing 3D multi-spheroid created from different CCA cell lines, spherical and non-spherical shapes of 3D multi-spheroid were found as nature of each cell line. KKU-068 grew a non-spherical shape (**Figure 2b**). To straightforwardly verify tumorigenesis which also applicable for all spheroid shapes, the determination of spheroid by area was developed to substitute traditional diameter (**Figure 2c**). Simultaneously, the spheroid area positively correlated with spheroid width and length (**Figure 2d**). The 1,000 to 250 cells/well of SORE6^{POS} and SORE6^{NEG} cells were separately cultured in the 3D optimized culturing system, the SORE6^{POS} cells had higher spheroid creation ability (**Figure 3a**, **b**) and formed larger spheroid (**Figure 3b**, **c**) than SORE6^{NEG} cells suggesting that SORE6^{POS} cells possessed greater tumorigenicity.

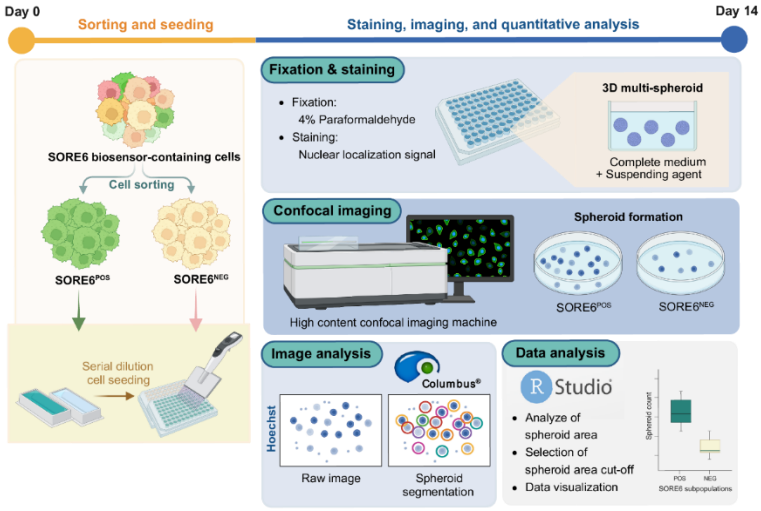

Figure 1. Schematic diagram of high-throughput imaging and a computational pipeline for CSC live-biosensor-based the *in vitro* tumorigenic assay.

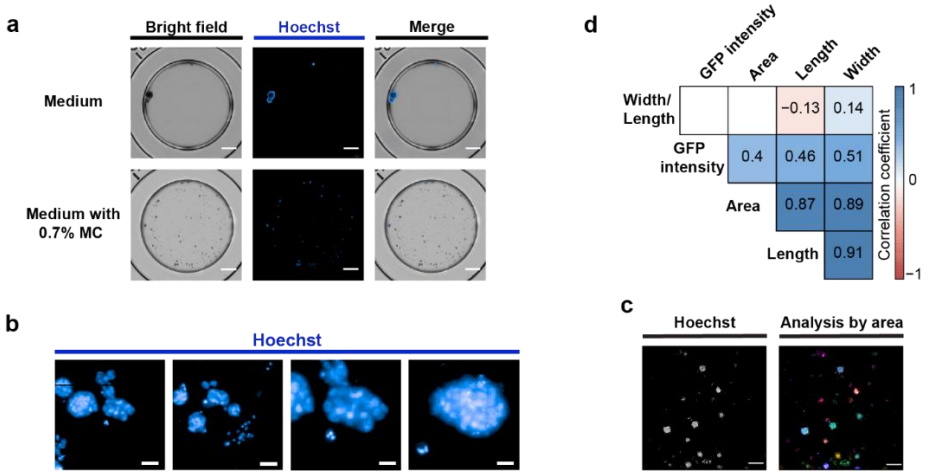

Figure 2. Applicable of spheroid area analysis for non-spherical shape. (a) SORE6 biosensor-containing TFK-1 cells at a seeding density of 1,000 cells/well cultured in an ULA flat-bottom for 14 days. (Upper) culture medium alone and (Lower) culture medium supplemented with 0.7% MC. The images were taken using 4x objective lens images, scale bar = 1 mm; (b) Appearance of KKU068 spheroid stained by Hoechst 33342. The images were taken by using 20x objective water lens, scale bar = 50 µm; (c) Spheroid segmentation and area analysis of the 3D multi-spheroid stained by Hoechst 33342 a seeding density of 1,000 cells/well. Scale bar = 300 µm. The images were taken using a 4x objective lens; (d) Correlation matrix showed correlation analysis between each analyzed factor of spheroids. Colors represent either positive (Blue) or negative correlation (Red), number in each box = Pearson's correlation coefficient (R), blank = correlation was not significant. Statistical significances were analyzed by unpair t-test, p-value ≤ 0.01.

From the aspect of CSC biology, CSC fate determination was able to be investigated in the tumor microenvironment mimicking context. Differentiation capability where non-CSC daughter cells are created from CSC was investigated. The spheroids from the sorted SORE6^{POS} population lost the GFP signal (**Figure 4**), suggesting that SORE6^{POS} spontaneously differentiated to SORE6^{NEG}.

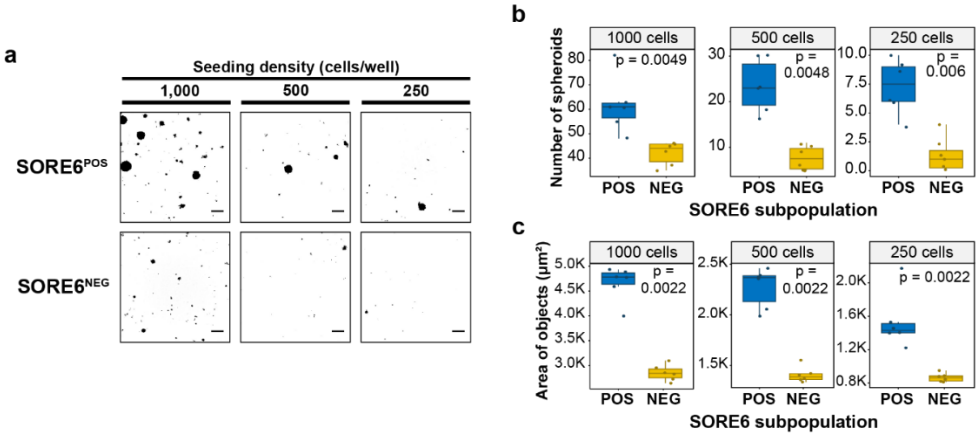

Figure 3. SORE6^{POS} cells harboring greater *in vitro* tumorigenesis. (a) Representative images of SORE6^{POS} and SORE6^{NEG} TFK1 cells at seeding densitiesfrom 1,000 to 250 cells/well which were stained by Hoechst 33342. Scale bar = 300 µm. The images were taken using a 4x objective lens. (b) Box plots showed the spheroid number of SORE6^{POS} and SORE6^{NEG} TFK1 cells. 8,000 µm^2 was used as a cut-off for spheroid determination. (c) Box plots showed the area of Hoechst 33342-positive objects of SORE6^{POS} and SORE6^{NEG} TFK1 cells. Data represents 6 replicates ± SD. Statistical significances were analyzed by unpair Wilcoxon rank-sum test.

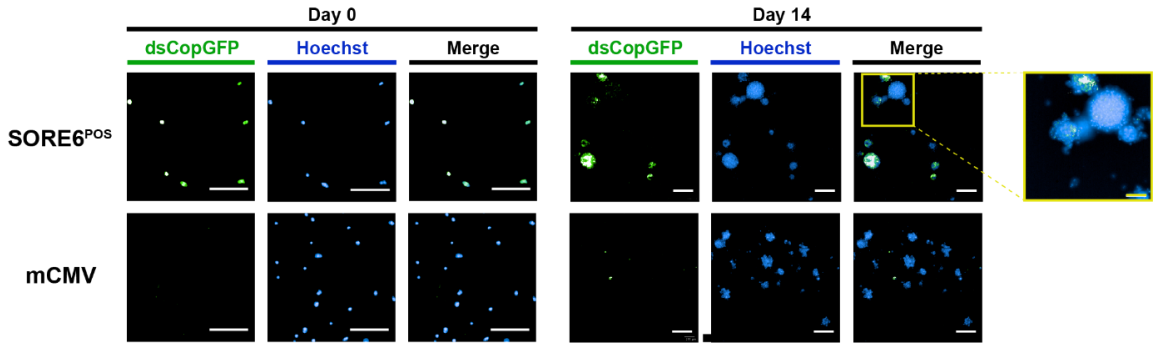

Figure 4. Spontaneous differentiation in an anchorage-independent culture system. The SORE6^{POS} cells were seeded at 1,000 cells/well and imaged on day 0, while the spheroids were investigated in 3D on day 14. White scale bar = 200 µm, yellow scale bar = 100 µm. The images were taken using a 20x air objective lens.

Discussion

In vitro tumorigenesis is performed by culturing the speculated CSC and non-CSC with a range of very low seeding densities in an anchorage-independent environment[12], the spheroid(s) are grown in the ULA plate either round or flat bottom which created a 3D multicellular spheroid and 3D multi-spheroids, respectively. According to clonal expansion[13], the 3D multi-spheroid is a more reliable model than the aggregation model. According to the advantages of live biosensors, CSC biology is permitted to investigate without the staining required. Hence, the high-throughput imaging and computational pipelines for *in vitro* tumorigenesis using SORE6 live biosensor was developed. Cell aggregation and the non-

spherical shape of the spheroids were concerned with reducing culturing and analysis bias, respectively. Nevertheless, the utilization of our spheroid area analysis was undoubtedly shown by a positive correlation with the traditional spheroid diameter. However, the spheroid area analysis was still based on the maximum projection image (2D information), while the optimal parameter which represented 3D clonal expansion liked spheroid volume was not performed due to the machine limitation. Apart from the *in vitro* tumorigenic assay, spontaneous differentiation occurred in anchorage-independent culture, this implied the preservation of equilibrium CSC content. Altogether, the fusion of the CSC live biosensor and the high-throughput imaging and computational pipelines for *in vitro* tumorigenesis generated a great procedure to capture CSC biology.

Conclusion

CSC properties including tumorigenesis and differentiation of the SOX2/OCT4 expressing cell in CCA have been verified in the context of 3D multi-spheroid using the SORE6 biosensor. Nevertheless, the accurate high-throughput imaging and computational pipelines for *in vitro* tumorigenesis was applicable for various shapes of spheroid and authorized multi-analysis in one experiment, time saving, and reproducibility.

Acknowledgment

This work was supported by Chulabhorn Foundation and the Royal Golden Jubilee Ph.D. Scholarship Program (RGJ-PHD) (Grant No. PHD/0060/2561) under Thailand Research Fund (TRF) and National Research Council of Thailand (NRCT).

References

1. Barbosa MAG, Xavier CPR, Pereira RF, Petrikaite V, Vasconcelos MH. 3D Cell culture models as recapitulators of the tumor microenvironment for the screening of anti-cancer drugs. Cancers (Basel). 2021 Dec 31;14(1):190.
2. Atat OE, Farzaneh Z, Pourhamzeh M, Taki F, Abi-Habib R, Vosough M, El-Sibai M. 3D modeling in cancer studies. Hum Cell. 2022 Jan;35(1):23-36.
3. Burrell RA, McGranahan N, Bartek J, Swanton C. The causes and consequences of genetic heterogeneity in cancer evolution. Nature. 2013 Sep 19;501(7467):338-45.
4. Mohan A, Raj RR, Mohan G, K PP, Maliekal TT. Reporters of cancer stem cells as a tool for drug discovery. Front Oncol. 2021 Apr 22;11:669250.
5. Reya T, Morrison SJ, Clarke MF, Weissman IL. Stem cells, cancer, and cancer stem cells. Nature. 2001 Nov 1;414(6859):105-11.
6. Bajaj J, Diaz E, Reya T. Stem cells in cancer initiation and progression. J Cell Biol. 2020 Jan 6;219(1):e201911053.
7. Shibue T, Weinberg RA. EMT, CSCs, and drug resistance: the mechanistic link and clinical implications. Nat Rev Clin Oncol. 2017 Oct;14(10):611-29.
8. Dogan E, Kisim A, Bati-Ayaz G, Kubicek GJ, Pesen-Okvur D, Miri AK. Cancer stem cells in tumor modeling: challenges and future directions. Adv Nanobiomed Res. 2021 Nov;1(11):2100017.
9. Lee CH, Yu CC, Wang BY, Chang WW. Tumorsphere as an effective *in vitro* platform for screening anti-cancer stem cell drugs. Oncotarget. 2016 Jan 12;7(2):1215-26.
10. Adorno-Cruz V, Kibria G, Liu X, Doherty M, Junk DJ, Guan D, et al. Cancer stem cells : targeting the roots of cancer, seeds of metastasis, and sources of therapy resistance. Cancer Res. 2015 Mar 15;75(6):924-9.
11. Tang B, Raviv A, Esposito D, Flanders KC, Daniel C, Nghiem BT, et al. A flexible reporter system for direct observation and isolation of cancer stem cells. Stem Cell Reports. 2015 Jan 13;4(1):155-69.
12. Hu Y, Smyth GK. ELDA: extreme limiting dilution analysis for comparing depleted and enriched populations in stem cell and other assays. J Immunol Methods. 2009 Aug 15;347(1-2):70-8.
13. Beck B, Blanpain C. Unravelling cancer stem cell potential. Nat Rev Cancer. 2013 Oct;13(10):727-38.

F05

Acute Toxicity Study of Herbal Remedies in Rat

Kannika Keawmorakot[1], Sukanya Dej-adisai[2], Sucharat Tungsukruthai[1], Jirapa Puntarut[1], Wandee Udomuksorn[1*]

[1] *Pharmacology Program, Division of Health and Applied Science, Faculty of Science, Prince of Songkla University, Hat Yai, Songkhla, Thailand*
[2] *Department of Pharmacognosy and Pharmaceutical Botany, Faculty of Pharmaceutical Sciences, Prince of Songkla University, Hat Yai, Songkhla, Thailand*

*E-mail: wandee.u@psu.ac.th

Abstract

The term "herbal remedies" (HR) refers to a combination of medicinal herbs that are used to support organ function, overall health, illness prevention, and long life. For maximum advantage, it is usually used continuously over an extended period of time. An *in vitro* investigation was conducted to determine which alpha glucosidase inhibitors might be most effective in HR development to prevent diabetes. Additionally, acute oral toxicity testing in laboratory animals should essentially be performed together with a preliminary safety assessment. The objective of this study was to conduct an acute oral toxicity test of HR ethanolic extract according to OECD Guideline 423. Six female Wistar rats were orally administered HR ethanolic extract at a single dose of 2,000 mg/kg BW. The signs of toxicity were closely observed (0.5, 1, 2, 3, 4, and 24 h.) on the first day and then monitored once daily for 14 days. The results revealed that neither mortality nor abnormal symptoms occurred in the tested animals. A normal growth rate, food and water consumption were observed. In addition, the hematological parameters [HB (15± 1.1 g/dL), HCT (47± 3.3 %), Total RBC (8± 0.6 x10^6/mm^3), PLT (560± 30.5 x10^3/mm^3), WBC (3± 0.9 x10^3/mm^3), and biochemical parameters [BUN (17± 1.1 mg/dL), Cr (0 .3 ± 0 .0 mg/dL), Bilirubin (0.1± 0.0 mg/dL), AST (104±14.2 U/L), ALT (15±2.0 U/L) and FBS (81±9.8 mg/dL)] were all within the normal range. There were no obvious abnormalities in the vital organs' outward appearance (liver, kidney, lung, heart, spleen, reproductive organs). According to the histological analyses, there were no anomalies in the nephron or liver lobule cell structures. Based on these findings, it can be concluded that the LD_{50} of the HR ethanolic extract is greater than 2,000 mg/kg, oral. Thus, in the short term, using HR as a dietary supplement might be safe. Further research must focus on sub-chronic toxicity.

Keywords: herbal remedies, safety, toxicity test, OECD guideline 423, dietary supplement

Introduction

Diabetes mellitus (DM) is characterized by abnormalities in glucose metabolism and hyperglycemia.[1] It is mostly caused by factors like eating a lot of starch or sugar and not exercising. Many people suffer from diabetes mellitus type II (TII-DM), which is associated with low insulin production or insulin resistance due to genetic and/or epigenetic causes.[2] Normalizing blood sugar levels is the main goal of treatment for diabetes. Modern medications like acarbose achieve this by inhibiting the alpha-glucosidase enzyme, reducing the absorption

of glucose into the bloodstream. However, patients often face discomfort due to side effects such as increased flatulence, fart, diarrhea, nausea, etc.[3] As a result, researchers are looking for herbal remedies (HR) that have a strong α-glucosidase inhibitory property from Thai medicine herbs known as traditional medicine, that have a long history of being used to maintain body balance, enhance prevention or treatment effectiveness, and reduce the risk of treatment ADRs.[4] For example, trisamo (myrobalan wood, beleric myrobalan, and arjun tree) is the remedy used for expectorants, antipyretics, and nourishment. Trisan (wildbetal leafbush, mai sakhaan, and scarlet leadwort) is known to promote body balance, lower blood sugar levels, and enhance blood circulation. Chatutiphayakhantha (jequirity, licorice, Spanish cherry, and ginger) is used for expectorants, heart tonics, nourishment, laxatives and carminatives.[5] According to an *in vitro* study, the researcher discovered that among 60 remedies in Thai traditional medicine, there is one HR remedy, composed of three main herbs: two from the Piperaceae family and one from the Zingiberaceae family. This HR exhibited the highest percentage inhibition of the α-glucosidase enzyme. It has long been utilized and well-known for its health-promoting and nourishing benefits. However, there is no scientific data on safety information, particularly for animals. Therefore, the objective of this study is to evaluate the acute toxicity of HR ethanolic extract following the OECD guidelines.

Methods

Preparation of crude extracts for HR

The HR was soaked in 80% ethanol and kept at room temperature for 3 days. The extract was then filtered through filter paper, and the excess solvent was removed with a rotary evaporator at 60°C. The crude extract was weighed and determined to have a yield of 25% w/w. It was then stored at 4°C, awaiting for further testing.

Animals

Six female Wistar rats (aged 7-8 weeks, weight 180-200 g) were obtained from Nomura Siam Internaltional. They were given unrestricted access to a standard diet and water. The rats were maintained in a temperature-controlled room (25±2°C), with a 12-h light/dark cycle and a relative humidity of 60±10%. They were acclimatized to the laboratory conditions for one week prior to the experiments. All procedures were approved by the Animal Ethical Committee of Prince of Songkla University under Ref. No. AR073/2022.

Acute toxicity test

The acute oral toxicity of HR ethanolic extract was evaluated in rats following the OECD Guideline 423.[6] HR ethanolic extract was dissolved in propylene glycol (PG). All animals were fasted overnight prior to dosing and for 3 h after treatment. For the limit test, six female rats were single dose orally administered with HR at dose of 2000 mg/kg BW. Then the signs of toxicity and behavior were closely observed at the first period 24 h (0.5, 1, 2, 3, 4, and 24 h). Animals were weighed and observed once daily for 14 days with a focus on general appearance, toxic signs, behavior patterns, eyes, skin, fur, mucous membranes, respiration, and somatomotor activity. Attention was directed to diarrhea, tremors, itching, convulsions, mortality, and coma. If some animal die, necropsy was performed to do gross observation of internal organs. After 14 days, all animals were fasted overnight and anesthetized by an intraperitoneal injection of thiopental dose 60 mg/kg, BW. Blood samples were collected via cardiac puncture and used for hematological (total RBD, HGB, HCT, MCV, MCH, MCHC, PLT, and WBC etc.) and biochemical analysis (AST, ALT, Bilirubin, BUN/Cr, and FBS). After taking the blood sample, the internal organs were examined for gross observational

abnormalities. The organs such as the liver, kidney, heart, lung, spleen, uterus, and ovary were weighed, and the relative weight of each organ was calculated. The liver and kidney were immediately fixed in 10% neutral buffered formalin for histopathological analysis by the pathologist from N Health Services at Bangkok Hospital Hatyai.

Statistical analysis

The data on body weight, relative organ weight, hematological, and biochemical parameters were presented as the mean ± standard error of the mean (SEM) for six female rats.

Results

Effect of HR ethanolic extract on body weight and the relative organ weight

Oral administration of HR ethanolic extract at a dose of 2000 mg/kg BW. After 14 days of HR treatment, all animals had a normal growth rate (**Figure 1**). The organs (heart, liver, kidney, lung, spleen, uterus, and ovary) did not differ in relative weight from body weight (**Table 1**).

Effect of HR ethanolic extract on general appearance and behavioral observations

The HR ethanolic extract did not show any toxic signs or abnormal behavior at an oral dose of 2000 mg/kg, BW in female rats. There were no abnormal parameters, including convulsions, tremors, itching, coma, and mortality (**Table 2**).

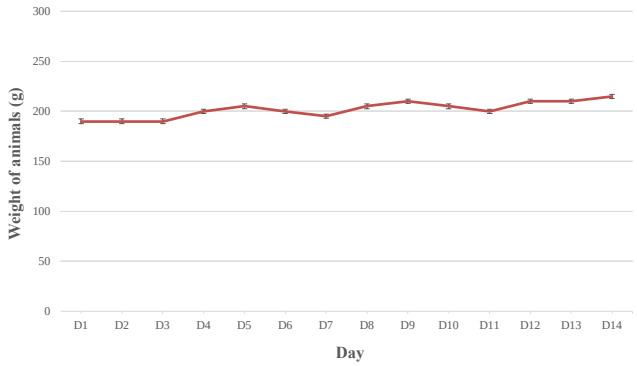

Figure 1. Effects of HR ethanolic extract (2000 mg/kg BW) on the body weight of rats over a period of 14 days (n=6) (HR=Herbal Remedies).

Table 1. Effect of the HR ethanolic extract (2000 mg/kg BW) on the relative organ weight (organ weight in grams/ 100 g of animal weight) in rats

Organs	Relative organ weight
Heart	0.3±0.0
Liver	0.9±0.0
Kidney	0.7±0.0
Lung	0.5±0.0
Spleen	0.2±0.0
Uterus	0.2±0.1
Ovary	0.1±0.0

Values are presented as the mean ± SEM (*n* = 6)
(HR =herbal remedies)

Table 2. Effect of the HR ethanolic extract (2000 mg/kg BW) on general appearance and behavioral observations in rats.

	Observations time					
Parameters	0.5 h	4 h	24 h	48 h	7 day	14 day
Eyes	N	N	N	N	N	N
Salivation	N	N	N	N	N	N
Fur & skin	N	N	N	N	N	N
Respiration	N	N	N	N	N	N
Urination (color)	N	N	N	N	N	N
Faeces consistency	N	N	N	N	N	N
Somatomotor activity	N	N	N	N	N	N
Behavior pattern	N	N	N	N	N	N
Sleep	N	N	N	N	N	N
Mucous membrane	N	N	N	N	N	N
Convulsions & tremors	N.F	N.F	N.F	N.F	N.F	N.F
Itching	N.F	N.F	N.F	N.F	N.F	N.F
Coma	N.F	N.F	N.F	N.F	N.F	N.F
Mortality	N.F	N.F	N.F	N.F	N.F	N.F

Note: N = Normal, N.F = Not found

Effect of HR ethanolic extract on hematological parameters

The study examined the effects of administering the HR ethanolic extract at a dose of 2000 mg/kg, BW on the hematology values of rats. Several markers, including HGB, RBC, HCT, MCH, MCV, MCHC, RDB, PLT, WBC, NEUT, LYMPH, MONO, EO, and BASO, were found to be within the normal range (**Table 3**).

Table 3. Effect of the HR ethanolic extract (2000 mg/kg, BW) on hematological parameters in rats.

Parameters	HR 2000 mg/kg	Normal range[7]	Unit
HGB	15±1.1	13.7-16.8	g/dL
Total RBD	8±0.6	7.07-9.03	$x10^6/mm^3$
HCT	47±3.3	39.6-52.5	%
MCV	56±0.2	48.9-57.9	fL
MCH	18±0.1	17.1-20.4	Pg
MCHC	33±0.0	32.9-37.5	g/dL
RDW	14±0.3	11.1-15.2	%
PLT	560±30.5	638-1177	$x10^3/mm^3$
WBC	3±0.9	1.13-7.5	$x10^3/mm^3$
NEUT	5±4.0	7.1-33.2	%
LYMPH	94±4.5	66.2-90	%
MONO	0±0.0	0.8-4.0	%
EO	1±0.5	0-0.8	%
BASO	0±0.0	0-0.7	%

Values are presented as mean ± SEM (n = 6) (HR =Herbal Remedies)

Effect of HR ethanolic extract on biochemical parameters

Various indicators values of liver function, including ALT, AST, and bilirubin (total and direct), were within the normal range. Furthermore, renal function markers such as creatinine and BUN levels show normal values. Fasting blood sugar (FBS) levels were normal (**Table 4**).

Table 4. Effect of the HR ethanolic extract (2000 mg/kg, BW) on biochemical parameters in rats.

Parameters	HR 2000 mg/kg	Normal range[7]	Unit
SGPT (ALT)	15±2.0	26-230	U/L
SGOT (AST)	104±14.2	65-203	U/L
Bilirubin (Total)	0.1±0.0	0.05-0.18	mg/dL
Bilirubin (Direct)	0.1±0.0	0.03-0.06	mg/dL
Creatinine	0.3±0.0	0.3-0.6	mg/dL
BUN	17±1.1	13.5-14.5	mg/dL
Fasting blood sugar (FBS)	81±9.8	89-163	mg/dL

Values are presented as mean ± SEM (n = 6) (HR =Herbal Remedies)

Effect of the HR ethanolic extract on histopathology

Gross observation of the vital organs (liver, kidneys, heart, lung, spleen, and reproductive organs) did not reveal any gross pathological lesions. Histopathological examinations of the nephrons and liver lobule cell structures in the HR treated group showed no abnormalities (**Figure 2**).

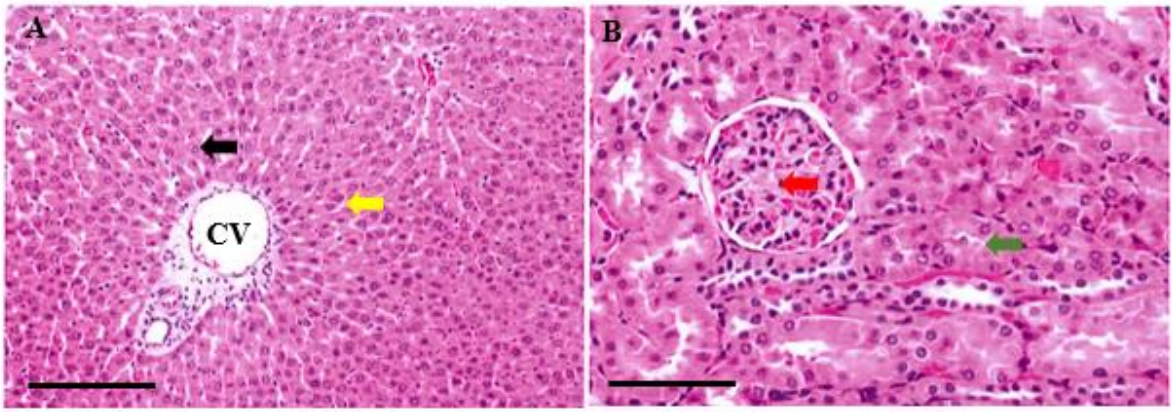

Figure 2. Histological examination of the liver (A) and kidney (B) in rats treated with HR (2000 mg/kg, BW). Black arrows represent normal hepatocytes; yellow arrows represent sinusoidal space; red arrows represent normal glomerulus; and green arrows represent normal proximal convoluted tubule. (H&E stained) (40x) (CV= central vein)

Discussion

The consumption of herbal products has increased worldwide for nutritional supplements and medicinal purposes. The beneficial therapeutic effects of the product are only observed when used in the correct doses and for the appropriate duration of treatment, and prolonged consumption of large amounts could lead to serious side effects.[8] Therefore, it is necessary to test the potential toxicity of formulated herbal products before they are introduced to the market. Therefore, the present work aimed to evaluate the acute toxicity of the HR ethanolic extract in rats. The main ingredients of this HR are three various types of herbs, primarily two from the Piperaceae family and one from the Zingiberaceae family. These remedies have been used for a long time to promote health, nourish, and treat a variety of ailments.

Our findings reported that the LD_{50} of HR ethanolic extract was greater than 2000 mg/kg, oral. In addition, this remedy showed no effect on growth, weight gain, behavior, or internal organs. The hematological and biochemical parameters in the blood were found to be within normal ranges. To support our results, a previous study found that the water extract from the dried fruits of Piperaceae species, for example, *Piper nigrum* or *Piper retrofractum*, did not produce signs of toxicity, behavioral changes, mortality, changes in gross appearance, or histopathological changes of internal organs in acute and/or subchronic toxicity studies.[9] Besides, the LD_{50} of *Zingiber officinale* (Zingiberaceae) was greater than 5000 mg/kg.[10] Taken together, we assumed that the ethanolic extract of HR was considered non-toxic for acute toxicity evaluation.

Conclusion

Based on the acute toxicity test data following OECD 423 guidelines, the HR ethanolic extract was orally administered at a dose of 2,000 mg/kg, demonstrating safety without causing acute toxic symptoms. The estimated LD_{50} for the HR ethanolic extract was greater than 2,000 mg/kg. According to the globally harmonised system for classification and labeling of chemicals (GHS), the HR ethanolic extract falls under Category 5 with a low acute toxicity hazard. However, further long-term toxicity research in experimental animals should be considered for the development of health products from the HR.

Acknowledgement

We would like to thank Fundamental Fund (FF) in 2024 (PHA6701075S) for funding this research. We appreciated the Pharmacology Program, Division of Health and Applied Science, Faculty of Science, Prince of Songkla University, for facilitating the research fund. We express our thanks to the Graduate School Scholarship and the Faculty of Science Research Fund for supporting the expenses associated with presenting our research.

References

1. Przeor M. Some common medicinal plants with antidiabetic activity, known and available in Europe (a mini-review). Pharmaceuticals (Basel). 2022 Jan 4;15(1):65.
2. Ouassou H, Zahidi T, Bouknana S, Bouhrim M, Mekhfi H, Ziyyat A, et al. Inhibition of α-glucosidase, intestinal glucose absorption, and antidiabetic properties by *Caralluma europaea*. Evid Based Complement Alternat Med. 2018 Jul 18:2018:1072403.
3. Modak M, Dixit P, Londhe J, Ghaskadbi S, Devasagayam TP. Indian herbs and herbal drugs used for the treatment of diabetes. J Clin Biochem Nutr. 2007 May;40(3):163-73.
4. Chusri S, Singthong P, Kaewmanee T. Antioxidant, anticancer, and cytotoxic effects of Thai traditional herbal preparations consumed as rejuvenators. CyTA – J Food. 2015;13(1):40-8.
5. Barber E, Houghton MJ, Williamson G. Flavonoids as human intestinal α-glucosidase inhibitors. Foods. 2021 Aug 20;10(8):1939.
6. OECD. Test no. 423: acute oral toxicity - acute toxic class method, OECD guidelines for the testing of chemicals, Section 4. Paris: OECD Publishing; 2002.
7. Patel S, Patel S, Kotadiya A, Patel S, Shrimali B, Joshi N, Patel T, Trivedi H, Patel J, Joharapurkar A, Jain M. Age-related changes in hematological and biochemical profiles of Wistar rats. Lab Anim Res. 2024 Feb 26; 40(1):7.
8. Ekor M. The growing use of herbal medicines: issues relating to adverse reactions and challenges in monitoring safety. Front Pharmacol. 2014 Jan 10:4:177.
9. Wiwattanawanichakun P, Ratwatthananon A, Poonsri W, Yooboon T, Pluempanupat W, Piyasaengthong N, Nobsathian S, Bullangpoti V. The possibility of using isolated alkaloid compounds and crude extracts of *Piper retrofractum* (Piperaceae) as larvicidal control agents for *Culex quinquefasciatus* (Diptera: Culicidae) larvae. J Med Entomol. 2018 Aug 29;55(5):1231-6.
10. Chang CJ, Tzeng TF, Liou SS, Chang YS, Liu IM. Acute and 28-day subchronic oral toxicity of an ethanol extract of *Zingiber zerumbet* (L.) Smith in Rodents. Evid Based Complement Alternat Med. 2012:2012:608284.

F06

Establishment of an Induced Human Treg Cell Culture Protocol Suitable for *In Vitro* Pharmacological Compound Evaluation

Pornpimon Ek-eudomsuk, Poomrapee Siripala, Kitipong Soontrapa*

Department of Pharmacology, Faculty of Medicine Siriraj Hospital, Mahidol University, Bangkok, Thailand

*E-mail: kitipong.soo@mahidol.ac.th

Abstract

Regulatory T (Treg) cells play a crucial role in maintaining immune homeostasis and preventing autoimmune diseases. This study aimed to develop an effective protocol for expanding induced Treg (iTreg) cells from naïve $CD4^+$ T cells *in vitro* and evaluating their phenotypes and functions. Naïve $CD4^+$ T cells were cultured in the iTreg polarizing conditions with administration of anti-CD3, anti-CD28, IL-2, and TGF-β1. The expression of *FOXP3*, a key transcription factor in Treg cell function, was significantly upregulated during iTreg cell expansion. Flow cytometry analysis showed an increase in the $CD4^+CD25^+FoxP3^+$ population, indicating the development of a Treg cell phenotype. Functional assays demonstrated the suppressive activity of iTreg cells on PBMC proliferation in a ratio-dependent manner. These findings highlight an efficient protocol for iTreg cell expansion with stable phenotype and functional characteristics, providing a basis for examining pharmacological compounds regulating Treg cells *in vitro*.

Keywords: Regulatory T cells, induced Treg cells, Treg cell phenotype, suppression of PBMC proliferation, suppressive function

Introduction

Regulatory T (Treg) cells maintain immune homeostasis and prevent autoimmune diseases by limiting the responses of proinflammatory and autoimmune T cells. The Treg cells are characterized in mice and human by high level of expression of the α-subunit of the IL-2 receptor ($CD25^+$), lack of expression of the IL-7 receptor α-subunit ($CD127^-$) and expression of the transcription factor FoxP3, which essential for Treg cell development and function. The mechanisms by which these cells maintain immune homeostasis involve four groups of action.[1-9] Firstly, secretion of inhibitory cytokines such as interleukin-10 (IL-10), TGF-β, and IL-35. Secondly, cytolysis mediated by granzymes A, B, and perforin. Thirdly, metabolic disruption, through depleting IL-2, generating adenosine nucleosides through CD39 and CD73 and transferring cyclic AMP (cAMP) into effector T cells. Lastly, modulation of dendritic cells (DC) function via regulating DCs co-stimulatory molecules.

There are two major types of natural Treg (nTreg) cells: thymus Tregs (tTreg) developed in the thymus and peripheral Treg (pTreg) cells generated in peripheral sites. Under normal conditions, the number of Treg in the body is very small accounting for 5% to 10% of $CD4^+$ T cells. To expand Treg cells, several protocols for Treg cell culture, so-called

induced Treg (iTreg) cells, had been developed. Basically, a majority of studies indicated that TCR activation of naïve $CD4^+$ T cells using anti-CD3 and anti-CD28 with inclusion of TGF-β and IL-2 for 4-14 days were proven to be not only effective, but also simple way to culture iTreg cells.

As Treg cells play crucial roles in many physiological and pathological conditions, it is of importance to develop a novel drug that can modulate Treg cell activities for treatment of various diseases. Here, based on previous reports (**Table1**)[10-14], with some modifications, we established a Treg cell culture protocol suitable for *in vitro* pharmacological compound evaluation.

Table 1. Published concentration ranges for iTreg polarizing condition.[10-14]

Induced Treg (iTreg)	
Stimulation reagents	**Concentration range(s)**
Anti-CD3	1-10 μg/mL
Anti-CD28	0.5-10 μg/mL
Blocking antibodies	
Anti-IFN-g	1-10 μg/mL
Anti-IL-4	1-10 μg/mL
Cytokines	
TGF- β1	1-15 ng/mL
IL-2	30-100 U/mL

Methods

Regulatory T cell generation

To obtain approximately $2\text{-}3\times10^6$ starting naïve CD4 cells from PBMCs, 20 mL of blood should be used. The blood samples were collected from healthy volunteers after obtaining their written informed consent. All experimental protocols were approved by the Institutional Review Board of the Faculty of Medicine, Siriraj Hospital (SIRB), Mahidol University (COA no. Si 728/2021). The peripheral blood mononuclear cells (PBMCs) were isolated from buffy coats by Ficoll-Paque density centrifugation (IsoPrep, Robbins Scientific, CA, USA). Cell viability was examined using the trypan blue exclusion assay. The immuno-magnetic negative selection of naïve $CD4^+$ T cells was performed using RoboSep™ Kit (Stemcell Technologies, #17952RF) following the manufacturer's instructions. Isolated $CD4^+$ cells were seeded in a 96-well round bottom plate that was previously coated with 10 μg/mL of anti-CD3 monoclonal antibody (Invitrogen, USA), and incubated at 4 °C overnight. The cell density was 2×10^5 cells per well in 100 μL of TexMACS media (Miltenyi Biotech, Germany) supplemented with 10% FBS (Biochrom, Germany), 100 μg/mL streptomycin, 100 U/mL penicillin (Gibco, USA), 0.2 μM 2-Mercaptoethanol (Gibco, USA) and 10 mM HEPES (Sigma-Aldrich, USA). The cells were activated using 1 μg/mL of anti-CD28 monoclonal antibody (Invitrogen, USA), 100 IU/mL recombinant human IL-2 (Miltenyi Biotech, Germany) and 15 ng/mL of TGF- β1 (Biolegend, USA) for a duration of 4-7 days, then harvested for the further experiments (**Figure 1**).

Detection of Treg cell immunophenotypes by flow cytometry

The immunophenotypes of Treg cells were analyzed using flow cytometry to determine specific cell surface and transcription factor protein marker. The iTreg cells were stained with FITC-conjugated anti-human CD4 (clone RPA-T4, BD Bioscience, USA) and PE-conjugated anti-human CD25 (clone M-A251, BD Bioscience, USA) in FACS buffer (PBS with 1% v/v FBS)

for 30 min at 25 °C and protected from light. For transcription factor protein FoxP3 staining, the Human FoxP3 Buffer Set (BD Bioscience, USA) with APC-conjugated anti-human FoxP3 (clone 259D/C7, BD Bioscience, USA) was used for fixation and permeabilization, following the manufacturer's instructions. Data analysis was performed using the CytoFLEX™ flow cytometer and FlowJo.

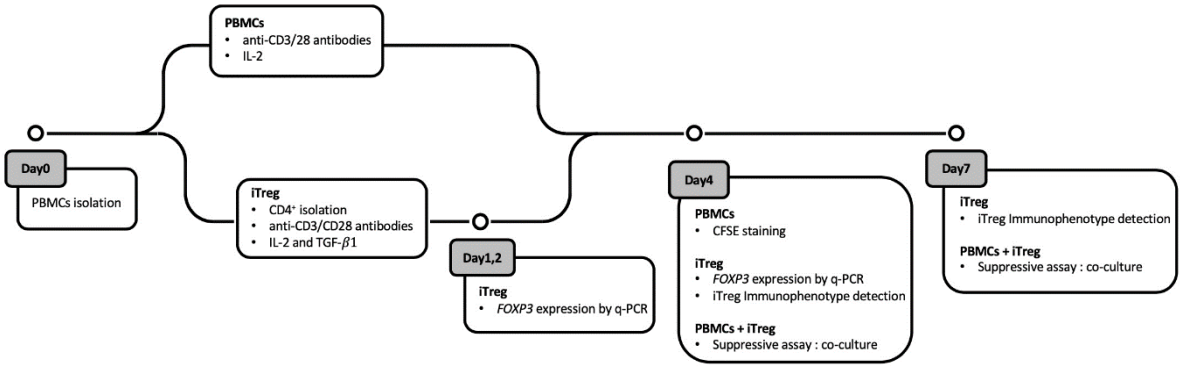

Figure 1. Schematic representation of expansion, detection of phenotype, and investigation of function of iTreg cells. iTreg cells were cultured from naïve $CD4^+$ T cells and used in the *in vitro* iTreg suppression assay by co-culturing iTreg cells with PBMCs at various ratios. Immunophenotype and suppressive function were analyzed by flow cytometry.

Suppression of PBMC proliferation evaluation by flow cytometry

The PBMCs derived from the same donor were generated at the same time as iTreg cells through activation with anti-CD3, anti-CD28, and IL-2, using the same concentration as that in the iTreg cell culture condition. The PBMCs were cultured for 4 days and used as targets in a suppressive assay. On day 4, PBMCs were stained with 1.5 μM of CFSE (Thermo-fisher, USA) according to the manufacturer's instructions. iTreg cells were washed and co-cultured with PBMCs in 96-well flat-bottom plate that were pre-coated with anti-CD3 antibody. The number of PBMCs in each well was fixed at 50,000 cells. The ratios of PBMCs to iTreg cells used were 1:0, 1:0.5, 1:1, 1:2, and 1:4. The cells in co-culture were stimulated with anti-CD28 and IL-2 for 3 days. The analysis of cell proliferation was performed using flow cytometry by examining the dilution of CFSE.

Quantitative real-time PCR analysis

The samples used for total RNA extraction were iTreg cells cultured for 24, 48 and 96 h. The Real Genomics Total RNA extraction kit (RBC Bioscience, Taiwan) was used to extract total RNA, following the manufacturer's guidelines. Subsequently, the synthesis of complementary DNA (cDNA) was performed using the iScript™ Select cDNA Synthesis Kit (Bio-Rad, CA), according to the manufacturer's instructions. The gene of interest was *FOXP3*, and the housekeeping gene used for normalization was *GAPDH*. The primer sequences employed for *FOXP3* were forward: 5'TTCATCTGTGGCATCATCCG3' reverse: 5'TCGCAT GTTGTGGAACTTGA3', while those for *GAPDH* were forward: 5'AAATTCCATGGCACCG TCAAG3', reverse: 5'TGGTTCACACCCATGACGAA3'. The annealing temperatures for the *FOXP3* and *GAPDH* primers were 54°C and 57°C, respectively. The design of these primer sequences was accomplished using the Primer-BLAST tool. The real-time PCR amplification was performed using the Applied Biosystems QuantStudio 5 instrument and SYBR Green Master Mix. The PCR cycling conditions comprised of a first step at 95°C for 3 min, followed by 40 amplification cycles at 95°C for 10 s, 54/57°C for 45 s, and 72°C for 1 s. Gene expression levels were evaluated using the $2^{-\Delta\Delta CT}$ technique.

Statistical analysis

One-way ANOVA was used to compare the number of cells, protein marker percentage, gene expression level, and PBMC proliferation suppression percentage. Results were presented as mean ± SEM. Differences were considered significant for $p < 0.05$ (*), $p < 0.01$ (**), $p < 0.001$ (***), and $p < 0.0001$ (****).

Results

The CD4^{+}CD25^{+}FoxP3^{+} population is increased in CD4^{+} cells cultured under the Treg polarizing condition

As FoxP3 plays a crucial role in differentiation and suppressive function of Treg cells, the analysis of *FOXP3* expression was performed using real-time PCR. By culturing naïve CD4^{+} T cells in Treg polarizing condition, the levels of *FOXP3* expression were increased by 1.3-fold on day2 and 2.1-fold on day4 compared to day1 (**Figure 2**).

Moreover, as shown in **Figure 3B** and **3C**, the total number of viable cells increased significantly after 4 days ($3.5x10^5 \pm 0.2x10^5$ cells) and 7 days ($4.8x10^5 \pm 0.7x10^5$ cells) of culture compared to the first day ($2.0x10^5$ cells). Furthermore, at day 4, the stimulated group exhibited an expansion of iTreg cells, with a mean of percentage of CD4^{+}CD25^{+}FoxP3^{+} at 34.17% (±0.7%) and decreased to 26.33% (±3.7%) at day 7 whereas the unstimulated group showed a lower percentage of CD4^{+}CD25^{+}FoxP3^{+} at 2.77% (±0.2%). The flow cytometry gating strategy employed was shown in **Figure 3A**.

iTreg cells demonstrate suppressive function on PBMCs in a ratio-dependent manner

The suppressive assay was performed by co-culturing CFSE-labeled PBMCs with iTreg cells at different ratios, PBMCs: iTreg at 1:0, 1:1, 1:2 and 1:4 in the presence of anti-CD3/CD28 antibodies and IL-2. After 3 days, the proliferation of PBMCs was analyzed by calculating the division index using the FlowJo Version 10.9 Proliferation Platform. The percentage of suppression significantly increased with an increase in the ratio, from 12.74% (±3.97%) of PBMCs:iTreg at 1:0.5 to 30.57% (±2.91%) at 1:2, and 34.39% (±2.91%) at 1:4 (**Figure 4A** and **4B**).

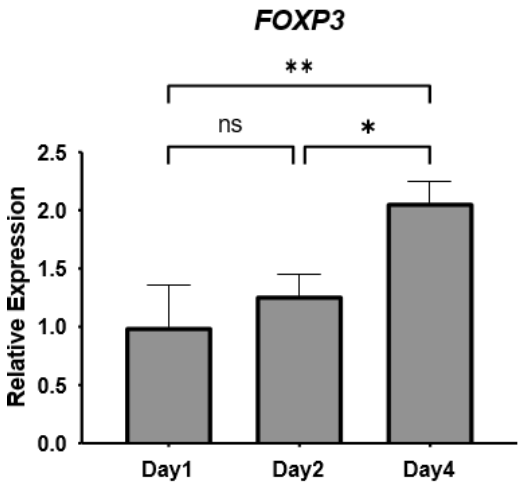

Figure 2. Relative mRNA expression of *FOXP3* during iTreg cell culture. The relative mRNA expression of *FOXP3* in iTreg cells was measured at day 1, day 2 and day 4 using *GAPDH* as the endogenous control. Relative fold changes were determined using the $2^{-\Delta\Delta CT}$ method.

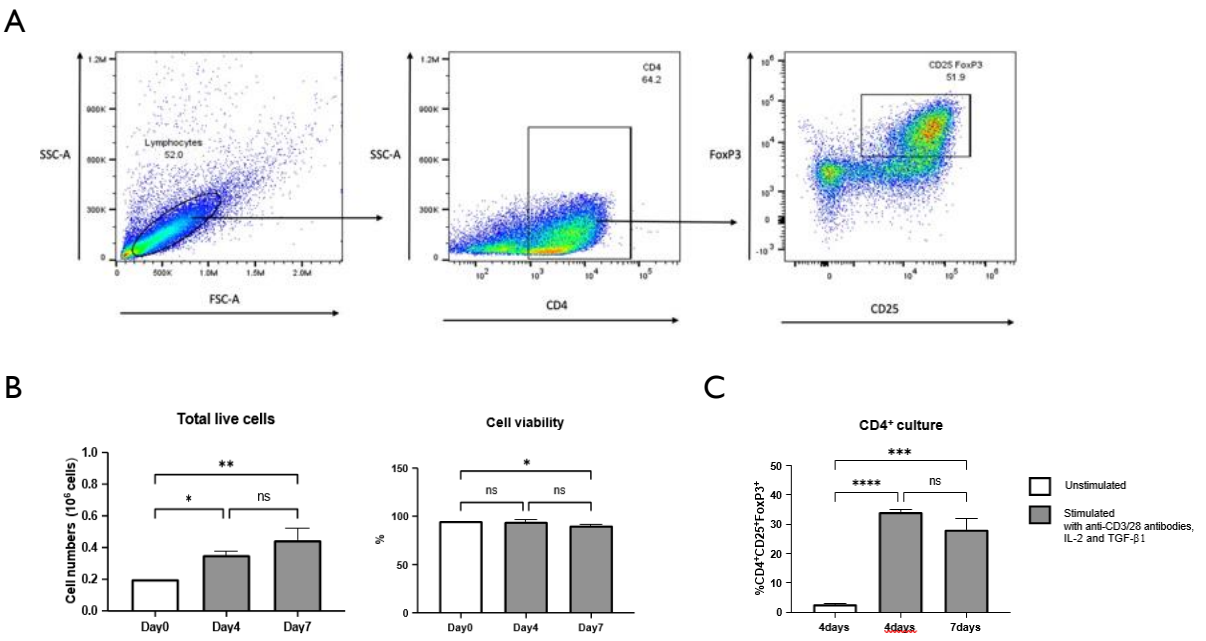

Figure 3. Quantification and immunophenotyping of specific markers of $CD4^+$ T cells following culturing in iTreg polarizing condition. A) Gating strategies for iTreg cells. B) Histogram showing the absolute number of total live cells and percentage of cell viability in iTreg cell culture. C) Histogram comparing the percentage of specific iTreg markers between unstimulated and stimulated groups.

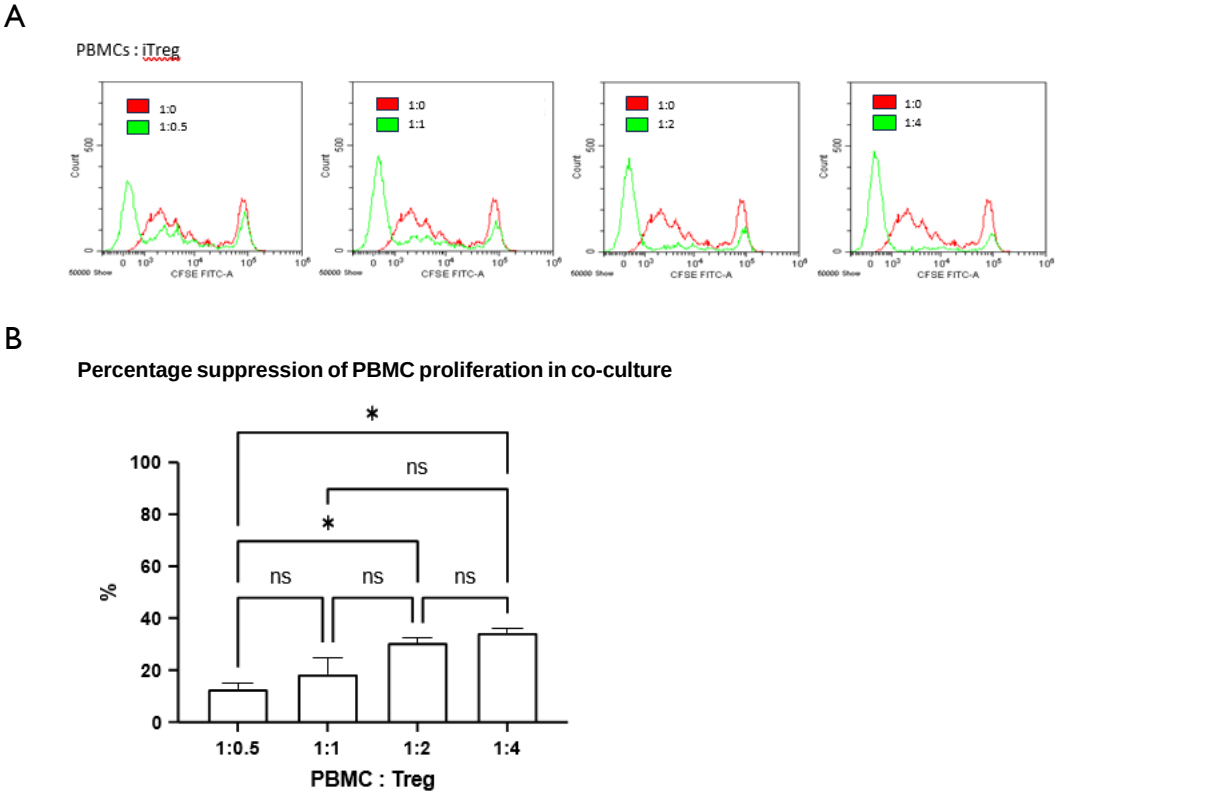

Figure 4. Suppression assay analysis using flow cytometry. A) Histogram overlay comparing the proliferation of PBMCs cultured alone to that of PBMCs co-cultured with iTreg cells at different ratios. B) Percentage inhibition of PBMC proliferation by iTreg cells at different ratios in the co-culture

Discussion

Development of a novel drug modulating Treg cells is key to treatment of many immune-associated diseases, including autoimmune disorders, allergies, and cancers. So, this study focused on the culture methodology and characterization of the phenotype and evaluation of the suppressive activity of iTreg cells appliable for *in vitro* pharmacological compound evaluation. The results showed notable phenotypes of iTreg through an augmentation of the *FOXP3* gene over a duration of 4 days. Moreover, the induction of naïve $CD4^+$ T cells into iTreg cells resulted in the expression of crucial regulatory markers, including CD25 and FoxP3, indicating their suppressive function. Furthermore, the functional assay demonstrated suppression of PBMC proliferation when co-cultured with iTreg cells, suggesting their ability to suppress immune responses.

Conclusion

This study presents a protocol for *in vitro* iTreg cell expansion with stable cell phenotypes and effective function by culturing naïve $CD4^+$ cells in the Treg cell polarizing condition, anti-CD3, anti-CD28, Il-2 and TGF-β, for 4 days together with functional examination of iTreg cells by using the Treg suppression assay based on suppressing PBMC proliferation by iTreg cells. We hope that this study can be a basis protocol for examining pharmacological compounds regulating Treg cell expansion and functions *in vitro*.

Ethics approval

The study protocol received approval from the Institutional Review Board of the Faculty of Medicine, Siriraj Hospital (SIRB), Mahidol University (COA no. Si 728/2021).

Acknowledgement

This research was supported by Siriraj Foundation.

References

1. Lucca LE, Dominguez-Villar M. Modulation of regulatory T cell function and stability by co-inhibitory receptors. Nat Rev Immunol. 2020 Nov;20(11):680-693.
2. Vignali DAA, Collison LW, Workman CJ. How regulatory T cells work. Nat Rev Immunol. 2008 Jul;8(7): 523-32.
3. Bopp T, Becker C, Klein M, Klein-Heßling S, Palmetshofer A, Serfling E, et al. Cyclic adenosine monophosphate is a key component of regulatory T cell–mediated suppression. J Exp Med. 2007 Jun 11;204(6): 1303-10.
4. Collison LW, Workman CJ, Kuo TT, Boyd K, Wang Y, Vignali KM, et al. The inhibitory cytokine IL-35 contributes to regulatory T-cell function. Nature. 2007 Nov 22;450(7169):566-9.
5. Deaglio S, Dwyer KM, Gao W, Friedman D, Usheva A, Erat A, et al. Adenosine generation catalyzed by CD39 and CD73 expressed on regulatory T cells mediates immune suppression. J Exp Med. 2007 Jun 11; 204(6):1257-65.
6. Grossman WJ, Verbsky JW, Tollefsen BL, Kemper C, Atkinson JP, Ley TJ. Differential expression of granzymes A and B in human cytotoxic lymphocyte subsets and T regulatory cells. Blood. 2004 Nov 1; 104(9):2840-8.
7. Joetham A, Takada K, Taube C, Miyahara N, Matsubara S, Koya T, et al. Naturally occurring lung $CD4^+CD25^+$ T cell regulation of airway allergic responses depends on IL-10 induction of TGF-β1. J Immunol. 2007 Feb 1;178(3):1433-42.

8. Oberle N, Eberhardt N, Falk CS, Krammer PH, Suri-Payer E. Rapid suppression of cytokine transcription in human $CD4^+CD25^-$ T cells by $CD4^+$Foxp3+ regulatory T cells: Independence of IL-2 consumption, TGF-β, and various inhibitors of TCR signaling. J Immunol. 2007 Sep 15;179(6):3578-87.
9. Shevach EM, Thornton AM. tTregs, pTregs, and iTregs: similarities and differences. Immunol Rev. 2014 May;259(1):88-102.
10. Schmidt A, Eriksson M, Shang M-M, Weyd H, Tegnér J. Comparative analysis of protocols to induce human $CD4^+Foxp3^+$ regulatory T cells by combinations of IL-2, TGF- β, retinoic acid, rapamycin and butyrate. PLOS ONE. 2016 Feb 17;11(2):e0148474.
11. Gu J, Shao Q, Zhou J, Chen Q, Lu L. Protocol for *in vitro* isolation, induction, expansion, and determination of human natural regulatory T cells and induced regulatory T cells. STAR Protocols. 2022 Dec 16;3(4):101740.
12. Read KA, Powell MD, Sreekumar BK, Oestreich KJ. *In vitro* differentiation of effector $CD4^+$ T helper cell subsets. In: Allen IC, editor. Mouse models of innate immunity: Methods and protocols. New York, NY: Springer New York; 2019. p. 75-84.
13. Sekiya T, Yoshimura A. *In vitro* Th differentiation protocol. In: Feng X-H, Xu P, Lin X, editors. TGF-β signaling: Methods and protocols. New York, NY: Springer New York; 2016. p. 183-91.
14. Wongchang T, Pluangnooch P, Hongeng S, Wongkajornsilp A, Thumkeo D, Soontrapa K. Inhibition of DYRK1B suppresses inflammation in allergic contact dermatitis model and Th1/Th17 immune response. Sci Rep. 2023 Apr 29;13(1):7058.

F07

A Preliminary Study to Investigate the Potential Pain-Relieving Effect of Sulfated Galactans in a Rat Model of Knee Osteoarthritis Pain

Nirada Srianake[1], Jiraporn Sriwong[1], Scarlett Desclaux[1], Borwornporn Tangketsarawan[1], Ratirat Sangpayap[1], Amarin Thongsuk[2], Alita Kongchanagul[3], Kanokpan Wongprasert[2], Ruedee Hemstapat[1*]

[1] *Department of Pharmacology, Faculty of Science, Mahidol University, Bangkok, Thailand*
[2] *Department of Anatomy, Faculty of Science, Mahidol University, Bangkok, Thailand*
[3] *Center for Vaccine Development, Institute of Molecular Biosciences, Mahidol University, Bangkok, Thailand*

*E-mail: ruedee.hem@mahidol.ac.th

Abstract

Osteoarthritis (OA) is a degenerative joint disease that progresses over time. The most dominant symptom of OA is joint pain, which reduces patients' mobility and their quality of life. Emerging evidence suggests that marine algae could provide therapy beneficial for OA due to their biological properties with fewer side effects. *Gracilaria fisheri* is a red alga that contains sulfated galactans (SG) as the major component. Previous *in vivo* studies have reported that SG extracted from *Gelidium crinale* exhibit anti-inflammatory and anti-nociceptive effects. Therefore, this study aimed to explore the therapeutic potential of SG in monoiodoacetate (MIA)-induced OA pain in rats. Male Wistar rats were divided into three groups: Saline + vehicle, MIA + vehicle, and MIA + a single intra-articular (i.a.) injection of SG. OA was induced by an i.a. injection of MIA (2 mg/50 µL), whereas the saline group received normal saline as a control. On day 2 post-MIA injection, MIA-injected rats were i.a. injected with SG (50 µg/50 µL), while the other two groups were i.a. injected with saline (50 µL). Pain behavioral assessments, including weight-bearing distribution tests and gait analysis, were performed twice weekly for 2 weeks. OA-related knee pain was observed in this model for both behavioral tests throughout the study period. The present findings demonstrated that a single i.a. injection of SG was ineffective in attenuating knee joint pain measured by weight-bearing distribution tests. Despite this result, it is interesting to observe a tendency of improvement in gait impairment, although lacking significance following a single i.a. injection of SG. Therefore, further studies are required to investigate the analgesic effect of multiple i.a. injections of SG in this model or in other surgically-induced rat OA models, which have been shown to mimic post-traumatic OA.

Keywords: Osteoarthritis, monoiodoacetate, sulfated galactans, weight-bearing distribution test, gait analysis

Introduction

Osteoarthritis (OA) is a degenerative joint disease that affects cartilage and surrounding tissue and commonly occurs at weight-bearing joint.[1] OA is caused by an imbalance in function between synthesis and degradation of extracellular matrix in the articular cartilage, leading to the common characteristics of OA, including articular cartilage destruction,

osteophyte formation, and synovial inflammation.[2,3] The main symptoms of OA are joint stiffness and painful condition, resulting in impaired patient quality of life.[4] Non-steroidal anti-inflammatory drugs (NSAIDs) are often used as the first-line treatment for OA-related pain symptoms. However, the use of NSAIDs is limited due to their adverse effects such as gastrointestinal ulceration, high risk of bleeding, and cardiovascular disease.[5] Although intra-articular corticosteroid injection has been widely used, it offers a short-term therapy.[6] Therefore, to overcome the limitations, several natural compounds have been investigated for their therapeutic potential for OA-related pain.

Recently, marine algae have become increasingly interested in the pharmaceutical industry due to their wide variety of biological activities. In the southern part of Thailand, several types of marine algae have been discovered. *Gracilaria fisheri* (also known as Phom-nang) has been reported to contain a high amount of sulfated galactans (SG). SG is a sulfated polysaccharide that is structurally similar to heparan sulfate proteoglycans, which is the major component of the extracellular matrix (ECM) in the articular cartilage. SG have been shown to promote ECM production, chondrocyte activity, and cell adhesion.[7-9] Interestingly, an *in vitro* study of SG extracted from *G. fisheri* reported that SG enhance collagen production as well as inhibit ECM-degrading enzyme activity.[10] Moreover, previous research showed that SG extracted from *Gelidium crinale* present an anti-inflammation and anti-nociceptive activity in a rat paw edema model.[11] However, the pain-relieving effect of SG has not been elucidated in a rat model of knee osteoarthritis pain. Thus, the present study aimed to explore the therapeutic potential of SG in chemically induced OA pain in rats.

Material and Methods

Animals and experimental groups

All animal care and experimental procedures were approved by the Institutional Animal Care and Use Committee (IACUC) of the Faculty of Science, Mahidol University (Protocol No MUSC66–061–691). Twelve, six-week-old male Wistar rats weighing 160-180 g were purchased from Nomura Siam International, Bangkok, Thailand and were housed in groups of three in an Association for Assessment and Accreditation of Laboratory Animal Care (AAALAC) accredited facility. They were allowed to acclimatize for 5-7 days before starting the experiment. Rats were allocated into 3 groups:

Group-1: Saline + vehicle (saline; n=3)
Group-2: MIA + vehicle (saline; n=3)
Group-3: MIA + 50 µg sulfated galactans (SG) (n=6)

Sulfated galactans extraction

Sulfated galactan (SG) was obtained by extracting depigmented *G. fisheri* powder as previously described.[12] The structure of SG consists of a linear chain of alternating units of 3-linked-β-D-galactopyranose (G) and 4-linked 3,6-anhydro-α-L-galactose (LA) or α-L-galactose-6-sulfate (L6S) with partial methylation (CH3) at C-2 of LA and C-6 of G, and sulfation of C-4 and C-6 of D-galactose units (G4S and G6S). HPLC analysis of SG showed 90% purity.

Induction of OA-related knee pain and treatment

Following anesthesia with isoflurane (5% for anesthesia induction, 2-3% for maintenance), knee OA pain was induced in the rats in group-2 and -3 by an intra-articular (i.a.) injection of 50 µL of either sterile saline or freshly prepared MIA solution (2 mg MIA in 0.9 % normal saline) through a 26-G needle into the right knee joint cavity of each rat. On day 2 post-MIA injection, SG (50 µg/25 µL) or saline (25 µL) was i.a. injected into the right knee joint of each rat according to the experimental groups as previously mentioned.

Pain-related behavioral assessment

OA-related pain induced by MIA was evaluated for 2 weeks post-MIA injection. The static weight bearing distribution test was conducted using an incapacitance meter (Columbus Instruments, Columbus, OH, USA), while the gait assessment test was performed using Catwalk XT (Noldus Information Technology, Wageningen, The Netherlands). The incapacitance meter determined changes in weight distribution between the ipsilateral (injured limb) and contralateral hindlimb, utilized as an index of knee joint pain. Results are expressed as the mean (±SEM) % weight-bearing distribution. Catwalk XT was used to assess the walking pattern of rats by allowing them to walk freely on the glass plate from left to right side in the dark room. Images of paw prints were recorded by a video camera underneath and computer software was used to evaluate gait parameters. Before starting the experiment period, rats underwent three days of training to walk on the glass plate. Mean stand parameters were recorded for each rat based on the mean of three quality runs. Baseline pain thresholds were obtained from both tests one day before MIA injection and on days 3, 7, 10, and 14 post-MIA injection for the weight-bearing distribution test. Gait assessment for pain evaluation was conducted on days 4, 6, 9, and 13 post-MIA injection (**Figure 1**).

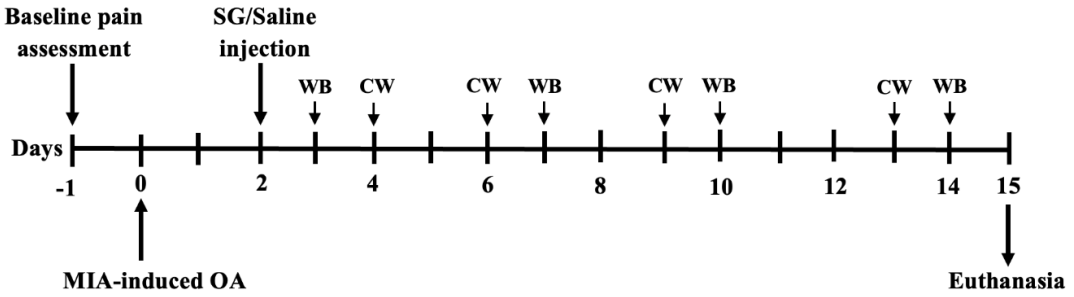

Figure 1. Schematic diagram summarizing the experimental design in this study.

Statistical analysis

Statistical analyses were performed using GraphPad Prism version 6.0.1 (GraphPad Software, La Jolla, CA, USA). All data are expressed as mean ± SEM. Statistical analyses were determined using a two-way analysis of variance (2-way ANOVA), followed by post hoc Bonferroni multiple comparison tests. Statistical significance was considered when the *P*-value < 0.05.

Results

Lack of pain-relieving effect of a single dose intra-articular injection of SG in MIA-induced knee OA pain

The ability of SG to improve weight-bearing asymmetry in MIA-induced OA rats was assessed using the weight-bearing distribution test. A significant reduction in the mean ± SEM % weight-bearing asymmetry was observed in the vehicle-treated MIA group compared with the vehicle-treated saline group, indicating the successful development of the knee joint pain. However, no significant difference in the mean ± SEM% weight-bearing asymmetry was observed in MIA treated receiving a single i.a. injection of SG compared to the MIA-treated rats receiving vehicle at any investigated timepoint (**Figure 2**).

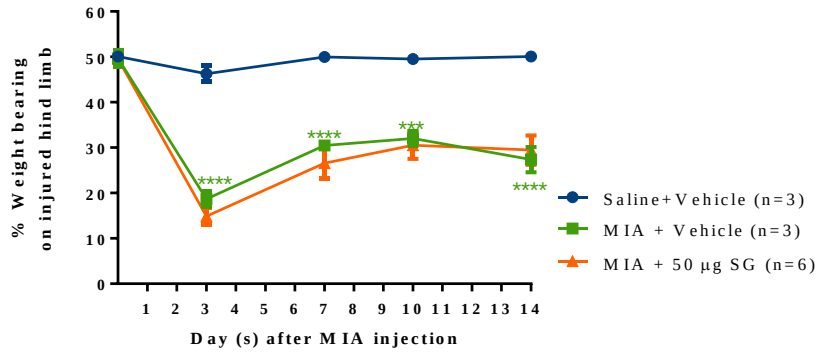

Figure 2. Time course profile of OA-related knee joint pain induced by an i.a. injection of MIA. The mean ± SEM% weight-bearing asymmetry of MIA-injected rats compared with saline-injected rats (control) was assessed. Each rat received an i.a. injection of SG (50 µg/ 25 µL) or vehicle (saline) on day 2 after MIA injection. All data are expressed as mean ± SEM. $^{***}p < 0.001$, $^{****}p < 0.0001$ vs. saline-injected group.

Partial improvement of gait impairment in MIA-induced OA model with a single dose intra-articular injection of SG

A significant increase in the difference in the mean stand between contralateral and ipsilateral hind limbs (Δ Stand) was observed in the vehicle-treated MIA group compared with the vehicle-treated saline group. Although a significant difference in the mean stand was only observed at day 6 post-MIA injection (4 days post-SG injection), there was a trend of reduction in the mean of Δ Stand in the SG-treated MIA group compared with the vehicle-treated MIA group. (**Figure 3**).

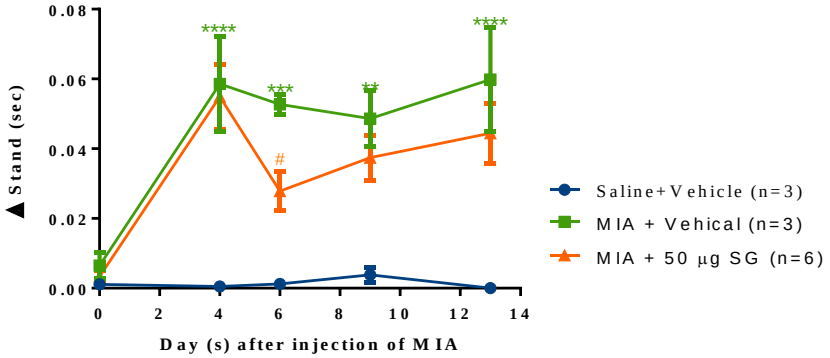

Figure 3. Time course profile of gait impairment induced by an i.a. injection of MIA. The difference in the mean stand between the contralateral and ipsilateral hind limb (Δ Stand, sec) of MIA-or saline-injected rats over 14 days was assessed. Each rat received an intra-articular SG (50 µg/ 25 µL) or vehicle (saline) on day 2 after MIA injection. Error bars represent the standard error of the mean (SEM). Δ Stand was determined on days 0, 4, 6, 9, and 13 post-MIA injection. All data are expressed as mean ± SEM. $^{**}p < 0.01$, $^{***}p < 0.001$, $^{****}p < 0.0001$ vs saline-injected group, $^{\#}p < 0.05$ vs. MIA-injected + vehicle group.

Discussion and Conclusion

The present findings demonstrate that a single i.a. injection of SG was ineffective in attenuating knee joint pain induced by MIA injection. Despite this result, it is interesting to observe a tendency of improvement in gait impairment, although lacking significance following a single i.a. injection of SG. It could be possible that a single dose of i.a. SG is not sufficient

for treating knee joint pain induced by MIA injection. The MIA-induced OA model is one of the most often used models to study the efficacy of novel analgesic agents. However, MIA at 2 mg induced a robust inflammatory response and persistent pain-like behavior, raising the question of the suitability of MIA to induce a translational model to study OA knee pain similar to that observed in humans.[13] Furthermore, since this research is a preliminary study to assess the efficacy of SG in this model, only small number of animals (n=3-6) were used. However, a larger number of animals are required to obtain statistically valid results. In addition, further studies are also required to investigate the analgesic effect of multiple i.a. injections of SG in surgically-induced OA models such as an anterior cruciate ligament transection plus medial meniscectomy, a rat model that has been shown to mimic post-traumatic OA, in which knee joint pain spontaneously develops.[14]

Acknowledgment

This research project is supported by Mahidol University (Fundamental Fund: fiscal year 2024 by the National Science Research and Innovation Fund (NSRF). This research project was also supported by the CIF and CNI Grant, Faculty of Science, Mahidol University.

References

1. Litwic A, Edwards MH, Dennison EM, Cooper C. Epidemiology and burden of osteoarthritis. Br Med Bull. 2013; 105:185-99.
2. Man GS, Mologhianu G. Osteoarthritis pathogenesis - a complex process that involves the entire joint. J Med Life. 2014 Mar 15;7(1):37-41.
3. Loeser RF, Goldring SR, Scanzello CR, Goldring MB. Osteoarthritis: A disease of the joint as an organ. Arthritis Rheum. 2012 Jun;64(6):1697-707.
4. Sarzi-Puttini P, Cimmino MA, Scarpa R, Caporali R, Parazzini F, Zaninelli A, et al. Osteoarthritis: an overview of the disease and its treatment strategies. Semin Arthritis Rheum. 2005 Aug;35(1 Suppl 1):1-10.
5. Magni A, Agostoni P, Bonezzi C, Massazza G, Menè P, Savarino V, Fornasari D. Management of osteoarthritis: Expert opinion on NSAIDs. Pain Ther. 2021 Dec;10(2):783-808.
6. Guermazi A, Hunter DJ, Kloppenburg M. Debate: Intra-articular steroid injections for osteoarthritis – harmful or helpful? Osteoarthr Imaging. 2023 Sep;3(3):100163.
7. Pomin VH, Mourão PA. Structure, biology, evolution, and medical importance of sulfated fucans and galactans. Glycobiology. 2008 Dec;18(12):1016-27.
8. Pomin VH, Mahdi F, Jin W, Zhang F, Linhardt RJ, Paris JJ. Red algal sulfated galactan binds and protects neural cells from HIV-1 gp120 and Tat. Pharmaceuticals (Basel). 2021 Jul 23;14(8):714.
9. Sarrazin S, Lamanna WC, Esko JD. Heparan sulfate proteoglycans. Cold Spring Harb Perspect Biol. 2011 Jul 1;3(7):a004952.
10. Pariwatthanakun C, Rudtanatip T, Boonsri B, Pratoomthai B, Wongprasert K. *In vitro* evaluation of wound healing potential of sulfated galactans from red alga *Gracilaria fisheri* in fibroblast cells. Songklanakarin J Sci Technol. 2021 Sep-Oct;43(5):1374-81.
11. de Sousa AA, Benevides NM, de Freitas Pires A, Fiúza FP, Queiroz MG, Morais TM, et al. A report of a galactan from marine alga *Gelidium crinale* with *in vivo* anti-inflammatory and antinociceptive effects. Fundam Clin Pharmacol. 2013 Apr;27(2):173-80.
12. Wongprasert K, Rudtanatip T, Praiboon J. Immunostimulatory activity of sulfated galactans isolated from the red seaweed *Gracilaria fisheri* and development of resistance against white spot syndrome virus (WSSV) in shrimp. Fish Shellfish Immunol. 2014 Jan;36(1):52-60.
13. Thakur M, Rahman W, Hobbs C, Dickenson AH, Bennett DL. Characterisation of a peripheral neuropathic component of the rat monoiodoacetate model of osteoarthritis. PLoS One 2012;7(3):e33730.
14. Hayami T, Pickarski M, Zhuo Y, Wesolowski GA, Rodan GA, Duong LT. Characterization of articular cartilage and subchondral bone changes in the rat anterior cruciate ligament transection and meniscectomized models of osteoarthritis. Bone. 2006 Feb;38(2):234-43.

F08

Inhibitory Effect of *Curcuma zedoaria* Extract and Curcumin on CYP3A-Mediated Erlotinib Metabolism

Akaraphon Chaiwongse[1], Chumaphorn Rodseeda[2], Paveena Yamanont[3], Porntipa Korprasertthaworn[3*]

[1] *International Undergraduate Program in Biomedical Science, Faculty of Science, Mahidol University, Bangkok, Thailand*
[2] *Department of Occupational Health and Safety, School of Public Health, University of Phayao, Phayao, Thailand*
[3] *Department of Pharmacology, Faculty of Science, Mahidol University, Bangkok, Thailand*

*E-mail: porntipa.kor@mahidol.edu

Abstract

Currently, there exists a wide range of anti-cancer treatments, spanning from standard medications like tyrosine kinase inhibitors to natural complementary medicines such as *Curcuma zedoaria* (*C. zedoaria*) and curcumin supplements. However, lacks of thorough understanding in concurrent use of drugs and herbs may result in drug toxicity due to potential drug interactions. This study seeks to investigate the inhibitory effect of *C. zedoaria* extract and curcumin on the metabolism of erlotinib through cytochrome P450 (CYP) activity *in vitro* using high-performance liquid chromatography (HPLC) analysis. The established CYP3A inhibitor, ketoconazole, served as the positive control. To determine the inhibitory impact of *C. zedoaria* extract and curcumin on erlotinib metabolism, they were co-incubated with erlotinib and human liver microsomes. Subsequently, the concentration of erlotinib was measured by HPLC. The percentage of enzyme activity was used to construct the half-maximal inhibitory concentration (IC_{50}). The results showed the potent inhibition of ketoconazole toward erlotinib metabolism with an IC_{50} value of 0.29±0.03 µM or 0.15 µg/mL, indicating the importance of CYP3A activity in the erlotinib metabolism. Even with lower potency, *C. zedoaria* extract and curcumin also showed potent inhibition toward erlotinib metabolism with IC_{50} values of 3.93±2.20 µg/mL and 6.49±2.49 µg/mL, respectively, indicating the potential drug interaction and inhibitory effects of both inhibitors on CYP3A activity. As the *C. zedoaria* extract has higher inhibitory potency compared to curcumin, this implies that other bioactive compounds within the extract also possess inhibitory effects toward CYP activity. In conclusion, our study demonstrated the potent inhibitory effect of *C. zedoaria* extract and curcumin on erlotinib metabolism via CYP3A activity. Further study regarding the *in vivo* effects and the other bioactive compounds is suggested for a better understanding of the potential interaction of *C. zedoaria* and its active compounds.

Keywords: Drug-herb interaction, CYP3A inhibitor, cytochrome P450, erlotinib metabolism, *Curcuma zedoaria*, curcumin

Introduction

Cancer represents a significant global cause of mortality. In recent years, cancer chemotherapy has emerged as a pivotal medical advancement and a standard treatment option. Due to the narrow therapeutic windows and uncertain responses associated with

previous anti-cancer drugs, targeted therapy has been introduced, emphasizing specific cancer components to limit nonspecific toxicity. Targeting the protein kinase, a crucial protein associated with cancer signaling, led to the development and approval of protein kinase inhibitors effective against tumors in the clinical trial.[1] Besides standard cancer treatment, Thai patients often turn to complementary and alternative medicine, including herbal therapy, to alleviate the side effects of anti-cancer drugs.[2,3] Additionally, healthcare products and supplements claiming anti-cancer properties have become more common. However, not all standard drugs and herbal products can be safely co-administered, as the safety of such combinations remains inadequately understood.[4] Patients with cancer may potentially utilize both standard anti-cancer drugs and herbal products, but herbal products might strongly inhibit cytochrome P450 (CYP) activity, leading to decreased drug clearance and potential drug toxicity. Clinicians face challenges in making decisions regarding the utilization of standard drugs and herbal products due to the absence of clinical interaction data.[5]

Erlotinib can reversibly inhibit tyrosine kinase activity of the epidermal growth factor receptor, a crucial for cancer cell activities such as cell proliferation and metastasis.[6] Erlotinib is used in treatments of various cancers, including head and neck, pancreatic, and ovarian cancers, and is a second-line drug against non-small lung cancer with brain metastasis.[6,7] The structure of erlotinib is shown in **Figure 1**. Major contributors to erlotinib metabolism include CYP3A4, CYP3A5, and CYP1A1.[8] Previous findings have shown the impact of ketoconazole, a potent CYP3A inhibitor, on erlotinib metabolism, increasing the area under the curve of erlotinib by 1.7 folds.[9] Despite being an available cancer treatment option, there is insufficient or limited scientific evidence regarding herbal interactions with erlotinib.

In Thailand and other Asian countries, *Curcuma zedoaria* (*C. zedoaria*), or white turmeric, is commonly used as an herb or spice with reported anti-cancer potential.[10-12] A recent study by Rodseeda et al.[13] demonstrated the potent inhibitory effect of *C. zedoaria* extract on CYP3A-mediated metabolism of some protein kinase inhibitors and testosterone. Apart from the extract itself, major bioactive compounds within *C. zedoaria* extract called curcuminoid including curcumin, demethoxycurcumin, and bisdemethoxycurcumin have been identified.[14] Curcumin, in particular, has been extensively studied and introduced as a typical supplement claimed to have anti-cancer properties. Previous studies have shown curcumin competitively inhibited recombinant CYP3A4 activities with an IC_{50} of 16.3 μM.[15]

In this study, we aim to investigate the inhibitory effect of *C. zedoaria* extract and curcumin on the erlotinib metabolism via CYP activity *in vitro* using high-performance liquid chromatography (HPLC) analysis to provide insights into the potential interactions.

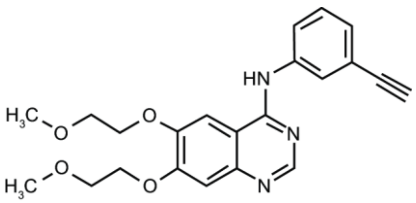

Figure 1. Erlotinib-chemical structure.
Notes: Chemical name, N-(3-ethynylphenyl)-6,7-bis (2-methoxyethoxy)- 4quinazolinamine

Methods

Materials

C. zedoaria powder was purchased from Vejpongpharmacy, a local herb distributor (Bangkok, Thailand). Erlotinib was purchased from LC Laboratories (Woburn, MA, USA). Curcumin, nicotinamide adenine dinucleotide phosphate (NADP), and ketoconazole were purchased from Sigma–Aldrich (St. Louis, MO, USA). Acetonitrile, ammonium acetate, acetic

acid, dimethyl sulfoxide (DMSO), and methanol were purchased from Merck KGaA (Darmstadt, Germany). Pooled human liver microsomes (HLMs; from 50 donors) were purchased from Gibco BRL Life Technologies (Grand Island, NY, USA). High-purity water was from MilliQ Synergy UV Ultrapure water system (Merck KGaA, Darmstadt, Germany). All other solvents and reagents were analytical grade or higher.

C. zedoaria extraction

To extract the *C. zedoaria*, 25 g of dried *C. zedoaria* was dissolved in 125 mL of methanol for 24 h on a rotary shaker at room temperature. Subsequently, the herbal solution was sonicated in an ultrasonic water bath at room temperature for 10 min. The solution was filtered twice through Whatman® no. 1 filter paper. Finally, a rotary evaporator and a speed vacuum concentrator were used to evaporate the herbal solution into dried herbal extract which was kept at -20 °C until use.

Co-incubation of erlotinib with C. zedoaria extract, curcumin, and ketoconazole

To determine the inhibitory effect of *C. zedoaria* extract, curcumin, and ketoconazole on the erlotinib metabolism, erlotinib was co-incubated with *C. zedoaria* extract, curcumin, and ketoconazole. Erlotinib and inhibitors were dissolved in DMSO. To establish the control standard for potent inhibition against erlotinib, ketoconazole, a potent CYP3A inhibitor, was used at concentrations ranging from 5 nM to 5 µM. Initially, each 100 µL reaction contained distilled water, phosphate buffer (0.1 M; pH 7.4), HLMs (0.05 mg), erlotinib (5 µM), and varying concentrations of *C. zedoaria* extract or curcumin or DMSO. The organic solvent in each incubation was not more than 2%. The reactions were then pre-incubated in a shaking water bath at 37 °C for 5 min. The generating system, containing 2 mM NADPH and 10 mM $MgCl_2$, was added to start the reaction. After 2 h of incubation, the reactions were terminated by adding ice-cold 4% acetic acid in methanol and placed on ice for 10 min. Subsequently, the reactions were centrifuged at 4 °C, 5000 x g for 10 min. The supernatant was aliquoted into HPLC vials for further analysis.

Determination of erlotinib by HPLC analysis

The previously published HPLC condition with slight adjustments was used to determine the concentration of erlotinib.[16] The HPLC system was Waters 2695 Separations Module (Waters Corporation, MA, USA). The UV detection was set to 260 nm. Analytes were separated on Ascentis® C18 analytical column [150 mm × 4.6 mm (id), 5 µm; Supelco, USA]. The mobile phase composition was 60% ammonium acetate (pH 5.7) with 10% acetonitrile and 40% acetonitrile with 1 mL/min flow rate. The retention time of erlotinib was approximately 5.6 min.

Data analysis

The experiments were performed in quadruplicate on different days. The concentrations of erlotinib were calculated by comparing the integrated peaks of the chromatograms with the calibration curves. Using HPLC analysis in the substance depletion approach, the amount of erlotinib remaining in the reaction was used to calculate the percentage of enzyme activity. To determine the half maximal inhibitory concentration (IC_{50}), a logarithmic plot of *C. zedoaria* extract and curcumin concentrations versus the percentage of remaining enzyme activity was constructed using the GraphPad Prism (version 10.1.1). The data were expressed as means ± standard deviation. Statistical analysis was conducted using a T-test. Results were considered significant when the *P*-value was < 0.05.

Results

Inhibitory effect of C. zedoaria extract, curcumin, and ketoconazole toward erlotinib metabolism

After co-incubation of *C. zedoaria* extract, curcumin, and ketoconazole with erlotinib, the samples underwent HPLC analysis. The data were then used to calculate the percentage of enzyme activity, and a logarithmic plot was constructed to determine the IC_{50} values (**Figure 2**), indicating the potency of the inhibitory effect. The experiments were conducted in quadruplicate. In terms of inhibitory potency, the order from the highest to lowest was as follows: ketoconazole (IC_{50} = 0.29±0.03 µM or 0.15 µg/mL) > *C. zedoaria* extract (IC_{50} = 3.93±2.20 µg/mL) > curcumin (IC_{50} = 6.49±2.49 µg/mL). Ketoconazole exhibited significantly greater inhibition of erlotinib metabolism compared to both the *C. zedoaria* extract and curcumin (*P*-values were 0.041 and 0.015 when compared to *C. zedoaria* extract and curcumin, respectively). However, no significant difference was observed between the inhibitory effects of the *C. zedoaria* extract and curcumin on erlotinib metabolism.

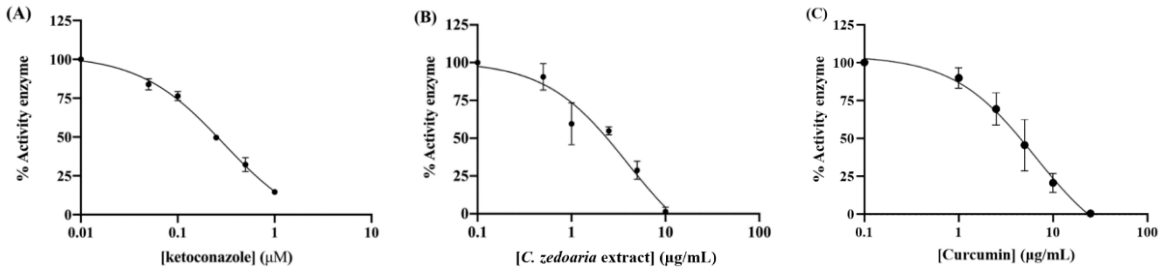

Figure 2. The logarithmic plots illustrate the percentage enzyme activity, represented as mean ± SD of quadruplicate determinations, against the concentration of three substances: ketoconazole (A), *C. zedoaria* extract (B), and curcumin (C).

Discussion

The potent inhibitory effect of ketoconazole on erlotinib metabolism reaffirms the significant role of CYP3A as the primary enzyme responsible for erlotinib metabolism, consistent with previous research.[9] Given this, we hypothesized that both *C. zedoaria* extract and curcumin might also exert substantial effects on CYP3A activity, warranting further investigation due to the pivotal role of CYP3A in drug metabolism.

The IC_{50} values of the three inhibitors against CYP-mediated erlotinib metabolism were determined, with ketoconazole serving as control due to its well-known potency as a CYP3A inhibitor. While both *C. zedoaria* extract and curcumin exhibited lower inhibitory potency compared to ketoconazole, they nevertheless displayed potent inhibition of erlotinib metabolism. Previous study has shown the inhibitory effects of curcuminoid extract and individual curcuminoid on various CYP enzymes, including CYP3A.[17] The curcuminoid extract, containing predominantly of curcumin, demethoxycurcumin, and bisdemethoxycurcumin, inhibited CYP3A activities with IC_{50} value of 25.3±1.3 µM. Interestingly, individual curcuminoids exhibited differing levels of inhibition, with IC_{50} values of 58.0±3.5, 43.5±3.8, and 41.7±3.5 µM for curcumin, demethoxycurcumin, and bisdemethoxycurcumin, respectively. This finding is consistent with the observed potency of *C. zedoaria* extract and curcumin in our study. Given that *C. zedoaria* extract contains a variety of bioactive compounds, including curcuminoids, it is reasonable to expect its inhibitory effect on CYP3A-mediated erlotinib metabolism to be more pronounced than that of pure curcumin.

Our study focused on investigating the inhibitory effects of both *C. zedoaria* extract and curcumin on CYP-mediated erlotinib metabolism. With the widespread availability of healthcare products and supplements containing herbal extracts, it is essential to consider potential interactions with standard medications, such as tyrosine kinase inhibitors like erlotinib. While our findings demonstrate the inhibitory effect of *C. zedoaria* extract on erlotinib metabolism, the specific secondary metabolites within the extract responsible for this effect remain unknown. Consequently, further research into the identification and characterization of these metabolites is warranted to better understand and mitigate potential interactions between erlotinib and supplements containing specific bioactive compounds from herbs like *C. zedoaria*.

Conclusion

In conclusion, our study provides valuable insights into the inhibitory effects of *C. zedoaria* extract and curcumin on CYP3A-mediated erlotinib metabolism. Our findings confirm that both *C. zedoaria* extract and curcumin possess inhibitory potency against erlotinib metabolism. Additionally, *in vivo* studies are warranted to validate our findings and assess the clinical relevance of these interactions in a more physiologically relevant setting.

Acknowledgments

This research was supported by the Biomedical Science Program and the IPS grant, Faculty of Science, Mahidol University.

References

1. Arora A, Scholar EM. Role of tyrosine kinase inhibitors in cancer therapy. J Pharmacol Exp Ther. 2005 Dec; 315(3):971-9.
2. Chukasemrat N, Charakorn C, Lertkhachonsuk AA. The use of complementary and alternative medicine in Thai gynecologic oncology patients: Influencing factors. Evid Based Complement Alternat Med. 2021 Nov 10;2021:1322390.
3. Puataweepong P, Sutheechet N, Ratanamongkol P. A survey of complementary and alternative medicine use in cancer patients treated with radiotherapy in Thailand. Evid Based Complement Alternat Med. 2012; 2012:670408.
4. Roe AL, Paine MF, Gurley BJ, Brouwer KR, Jordan S, Griffiths JC. Assessing natural product-drug interactions: An end-to-end safety framework. Regul Toxicol Pharmacol. 2016 Apr;76:1-6.
5. Adiwidjaja J, Boddy AV, McLachlan AJ. Physiologically-based pharmacokinetic predictions of the effect of curcumin on metabolism of imatinib and bosutinib: *In vitro* and *in vivo* disconnect. Pharm Res. 2020 Jun 11; 37(7):128.
6. Bareschino MA, Schettino C, Troiani T, Martinelli E, Morgillo F, Ciardiello F. Erlotinib in cancer treatment. Ann Oncol. 2007 Jun;18 Suppl 6:vi35-41.
7. Wu YL, Zhou C, Cheng Y, Lu S, Chen GY, Huang C, et al. Erlotinib as second-line treatment in patients with advanced non-small-cell lung cancer and asymptomatic brain metastases: a phase II study (CTONG-0803). Ann Oncol. 2013 Apr;24(4):993-9.
8. Li J, Zhao M, He P, Hidalgo M, Baker SD. Differential metabolism of gefitinib and erlotinib by human cytochrome P450 enzymes. Clin Cancer Res. 2007 Jun 15;13(12):3731-7.
9. Deeken JF, Beumer JH, Anders NM, Wanjiku T, Rusnak M, Rudek MA. Preclinical assessment of the interactions between the antiretroviral drugs, ritonavir and efavirenz, and the tyrosine kinase inhibitor erlotinib. Cancer Chemother Pharmacol. 2015 Oct;76(4):813-9.
10. Shehna S, Sreelekshmi S, Remani P, Padmaja G, Lakshmi S. Anti-cancer, anti-bacterial and anti-oxidant properties of an active fraction isolated from *Curcuma zedoaria* rhizomes. Phytomed Plus. 2022 Feb; 2(1): 100195.

11. Fitriana N, Rifa'i M, Masruri, Wicaksono ST, Widodo N. Anticancer effects of *Curcuma zedoaria* (Berg.) Roscoe ethanol extract on a human breast cancer cell line. Chem Pap. 2023;77:399-411.
12. Pal P, Prasad AK, Chakraborty M, Haldar S, Majumder P, Halder PK. Evaluation of anti-cancer potential of methanol extract of *Curcuma zedoaria*. Asian J Pharm Clin Res. 2015;8(5):271-5.
13. Rodseeda C, Yamanont P, Pinthong D, Korprasertthaworn P. Inhibitory effects of Thai herbal extracts on the cytochrome P450 3A-mediated the metabolism of gefitinib, lapatinib and sorafenib. Toxicol Rep. 2022 Oct 4;9:1846-52.
14. Paramapojn S, Gritsanapan W. Quantitative analysis of curcuminoids in *Curcuma zedoaria* rhizomes in Thailand by HPLC method. Acta Hortic. 2008;786(786):169-74.
15. Appiah-Opong R, Commandeur JN, van Vugt-Lussenburg B, Vermeulen NP. Inhibition of human recombinant cytochrome P450s by curcumin and curcumin decomposition products. Toxicology. 2007 Jun 3;235(1-2): 83-91.
16. Burns K, Nair PC, Rowland A, Mackenzie PI, Knights KM, Miners JO. The nonspecific binding of tyrosine kinase inhibitors to human liver microsomes. Drug Metab Dispos. 2015 Dec;43(12):1934-7.
17. Volak LP, Ghirmai S, Cashman JR, Court MH. Curcuminoids inhibit multiple human cytochromes P450, UDP-glucuronosyltransferase, and sulfotransferase enzymes, whereas piperine is a relatively selective CYP3A4 inhibitor. Drug Metab Dispos. 2008 Aug;36(8):1594-605.

F09

Ovalbumin (OVA)-Induced Acute and Chronic Asthma Mouse Models, the simple but Complete *In Vivo* System for Airway Inflammation and Fibrosis Study

Chaiphichit Phayangke, Panwadee Pluangnooch, Kitipong Soontrapa*

Department of Pharmacology, Faculty of Medicine Siriraj Hospital, Mahidol University, Bangkok, Thailand

*E-mail: kitipong.soo@mahidol.ac.th

Abstract

Allergic asthma, a chronic inflammatory airway disease influenced by genetic and environmental factors, poses a significant global health concern. Effective management of asthma relies on the use of corticosteroids, which are associated with complications and reduced quality of life. So, understanding the pathophysiology of asthma is crucial for the discovery of novel treatments. Ovalbumin (OVA)-induced allergic asthma mouse models could replicate key features of human asthma, aiding in studying acute and chronic allergic lung inflammation and providing insights for therapeutic advancements. Here, we compared two prominent mouse asthma models, the OVA-induced acute and chronic asthma mouse models. The mouse models of allergic asthma were induced by a series of sensitization and aerosol challenges with the chicken egg ovalbumin. Cells, and cytokines from bronchoalveolar lavage fluid (BALF) were examined. Lung tissues were collected for the histologic study of cell infiltration, goblet cell hyperplasia, and airway remodeling. Both acute and chronic asthma models showed airway inflammation by a significant increase in inflammatory cells and Th2 cytokines in BALF. The acute asthma model has a higher degree of airway eosinophilia and higher levels of IL-4, IL-5, and IL-13 as compared to the chronic asthma model. Hematoxylin and eosin (H&E) staining of lung tissues revealed a significant increase in inflammatory cell infiltration into the bronchi in the acute model, but no significant difference in the chronic model. Periodic acid-Schiff (PAS) staining showed that the airway goblet cells were significantly and similarly hyper-proliferated in both models. Trichrome staining showed an increase in collagen deposition around the bronchus of both models, but statistical significance was observed only in the chronic asthma model. In conclusion, the acute OVA asthma model showed a markedly severe eosinophilic immune response. However, airway remodeling was significant in the chronic model.

Keywords: Ovalbumin-induced asthma mouse model, lung inflammation, Th2 cytokines, goblet cell hyperplasia, airway remodeling

Introduction

Allergic asthma is a chronic inflammatory disease of the airways that leads to coughing, wheezing, shortness of breath, and chest tightness and is life-threatening in some cases. Genetic factors and environment play a critical role in its development.[1] The pathophysiology involves type 2 immune responses. Upon exposure to allergens, T-helper 2 (Th2) cells multiply

and release Th2 cytokines. Interleukin (IL)-4, crucial for Th2 differentiation, is essential for B cells to produce immunoglobulin E (IgE). IL-5 promotes eosinophilia, contributing to tissue damage in chronic asthma. Additionally, IL-13 triggers goblet cell hyperplasia and airway hyper-responsiveness.[2-5] The most effective strategy to control allergic asthma is to avoid allergens. Nonetheless, in most cases, medications remain necessary. While bronchodilators are recommended for short-term or occasional attacks, corticosteroids stand out as the sole drug capable of suppressing inflammation in the airways of individuals with asthma. However, it's essential to note that these drugs are immunosuppressive and carry numerous adverse side effects, such as high blood pressure, fluid retention, osteoporosis, metabolic imbalances, glaucoma, and an elevated risk of infections.[6,7]

Understanding asthma pathophysiology and exploring novel treatments are important. Albumin (OVA) is the most abundant glycoprotein found in chicken egg whites. It has a structure that is complex and large enough to induce a specific immune response and IgE-mediated airway hyperresponsiveness in mice.[8,9] Ovalbumin-induced asthma mouse models can replicate key features of allergic airway inflammation seen in human asthma, including bronchial eosinophilia, the production of Th2 cytokines (IL-4, IL-5, and IL-13), and airway remodeling. These models can represent both acute and chronic allergic lung inflammation.[10-12] Nevertheless, there are two types of these asthma models well recognized by researchers, the acute and chronic OVA-induced asthma models. In this study, we performed the OVA-induced acute and chronic asthma mouse models and compared their pathophysiology outcomes, including inflammatory cell profile, cytokine productions, and lung histology.

Methods

Animals

Male mice (C57BL/6), aged between 6 to 8 weeks old, were purchased from Nomura Siam International Co. Ltd. (Bangkok, Thailand). Mice were kept in a specific pathogen-free room on a 12-h to 12-h light-dark cycle with accessible food and water. All experiments and protocols were approved by the animal ethics committee of the Faculty of Medicine Siriraj Hospital (Mahidol University, Bangkok, Thailand): Siriraj Animal Care and Use Committee (SiACUC); COA no. 015/2562. All personnel working with animals were trained and are licensed by the Institute for Animals for Scientific Purpose Development (IAD) of the National Research Council of Thailand (NRCT), Bangkok, Thailand.

Reagents

Ovalbumin (OVA) from chicken egg white and aluminum hydroxide were purchased from Sigma-Aldrich (St Louis, Missouri, USA). Dip quick staining sets were brought from iMED Laboratories (Bangkok, Thailand). Hematoxylin and Eosin (H&E) staining kit (ab245880), Periodic Acid Schiff (PAS) staining kit (ab150680), and trichrome stain staining kit (ab150686) were purchased from Abcam (Cambridge, UK).

Acute asthma induction

The model was adapted from the protocol outlined by Kunikata T et al.[12] Mice were sensitized with an intraperitoneal (IP) injection of 300 µL phosphate buffer saline (PBS) containing 50 µg ovalbumin (OVA) and 25 µg alum on days 0 and 12. On days 22, 26, and 30, allergic groups were challenged with nebulization of 2% OVA (w/v) PBS for 30 min. Normal control mice were sensitized and challenged with PBS alone. 24 h after the last challenge, mice were terminated for bronchoalveolar lavage fluid (BALF) and lung tissue collection. **Figure 1a** shows the protocol and timeline of the acute asthma model.

Chronic asthma induction

The model was adapted from the protocol outlined by Schmidt M and Mattoli S.[13] Mice received sensitizations by intraperitoneal (IP) injection of 50 µg OVA with 25 µg aluminum hydroxide in 300 µL of PBS on days 0, 8, 15, and 22. In the challenge phase, from week 4 to week 10, mice were challenged with nebulization of 2% OVA (w/v) PBS for 30 min, three times a week (one day on and one day off) The normal control mice were sensitized and challenged with PBS in the same timeline. Mice were evaluated 24 h after the last challenge. **Figure 1b** shows the protocol and timeline of the chronic asthma model.

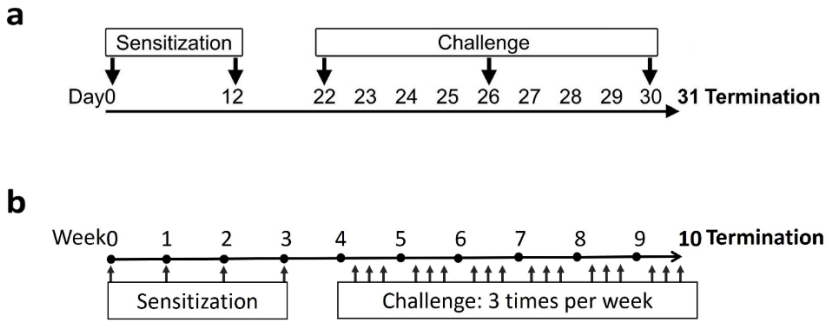

Figure 1. Acute (a) and Chronic (b) ovalbumin (OVA)-induced asthma mouse model. Male C57BL/6 mice were sensitized by intraperitoneal (IP) injection and challenged by nebulization with phosphate-buffered saline (PBS) or OVA as described in the material and method. 24 h after the final challenge, mice were sacrificed and processed for bronchoalveolar lavage fluid (BALF) and lung collection.

Analysis of bronchoalveolar lavage fluid (BALF)

Mice were euthanized 24 h after the last challenge. Three milliliters of BALF was collected by tracheal cannulation with 1 mL PBS containing 1% FBS, three repeats. The BALF cells were counted using a hemocytometer (BOE14V, BOECO, Germany) and an inverted microscope (Nikon Eclipse Ts2, Nikon Corporation, Tokyo, Japan). Cells in the BALF were transferred onto slides by cytocentrifugation of 0.5 mL BALF at 1,500 r.p.m. 10 min in Cytospin 4 machine (Thermo Fisher Scientific, Pittsburgh, PA, USA). The slide was airdried and stained with the Dip Quick staining kit (iMED Laboratories). A total number of 300 differentiated cells were evaluated under a light microscope (Nikon Eclipse Ti-U, Nikon Instruments, Tokyo, Japan) for identification of eosinophils, lymphocytes, and monocytes/ macrophages according to their morphological characteristics. The rest of the BALF was centrifuged and kept at -80°C until the measurement of IL-4, IL-5, and IL-13 by LEGENDplex™, bead-based immunoassay (BioLegend, San Diego, CA, USA).

Histological analysis

After the BALF collection, the big lope of the left lung was excised and kept in a 4% paraformaldehyde solution and maintained at 4 °C for fixation. The fixed lung was then embedded in a paraffin block. The block was cut at 4 µm thickness to make tissue slides by a microtome (CUT microtome, Thermo Scientific, USA). The tissue slides were transferred into glass slides, deparaffinized, and stained with H&E staining for the identification of immune cells; PAS staining for the identification of goblet cells; and trichrome staining for collagenous tissue. The stained slides were evaluated under the inverted light microscope (Nikon Eclipse Ti-U, Nikon Instruments, Tokyo, Japan). The quantification analysis was performed by image-J software (LOCI, University of Wisconsin-Madison, USA). The intensity of cell infiltration in

the lung was calculated by the black stained area (nucleus) normalized by the pink and black stained area (all cells and tissues without space).

The amounts of goblet cells and collagen were calculated referring to the positive stain area (red or blue stain areas, respectively) normalized by the length of the airway basement membrane. Similar anatomical sites were compared between each group.

Statistical analysis

Graphs and statistical indexes were processed using GraphPad Prism 8 software. (GraphPad Software, Inc., San Diego, CA, USA). The mean difference analysis between two sets of data was performed using a two-tailed Student's t-test. The mean analysis among the groups in the same or between models (acute and chronic) was done using a two-way analysis of variance (ANOVA) with Tukey's multiple comparison test. The data are expressed as the mean ± the standard error of the mean (SEM). A *p-value* < 0.05 was considered statistically significant.

Results

The ovalbumin (OVA)-induced acute asthma mouse model shows prominent immune responses and lung inflammation

The acute and chronic asthma mouse models were established by sensitizing and challenging the mice with OVA as described in the method. Acute asthmatic mice received two IP sensitizations and three nebulization challenges for one month. Chronic asthmatic mice received one sensitization per week for four weeks and then three challenges a week for an extended period of six weeks. BALF analysis showed significant increases in total cell count and eosinophils in both acute and chronic asthma models compared to their respective PBS controls. Interestingly, the chronic asthma model has a significant increase in monocyte and/or macrophage numbers compared to the control (**Figure 2a/b**). When comparing the two models, the acute asthmatic mice have significantly higher total cell count (*p-value* < 0.01) and eosinophils (*p-value* < 0.0001) than the chronic asthmatic mice; However, the chronic asthmatic mice have more monocytes and/or macrophages than the acute asthmatic mice (*p-value* < 0.01) (**Figure 2c**). When focusing on the percentage of differentiated cells, the PBS control from both acute and chronic asthma models showed a high percentage of monocytes (>80%) as the predominant cell population (**Figure 2d/e**). The acute asthma model showed a high predominant in eosinophil cells (92%), while the chronic asthma model has monocytes and/or macrophages (67%) as predominant cell populations (**Figure 2f**).

The levels of Th2 cytokines, IL-4, IL-5, and IL-13 were significantly increased in the BALF of asthmatic mice in both acute and chronic asthma models when compared to their respective PBS controls. Interleukine-4 is the predominant cytokine ranked at the highest level, and following by IL-5, and IL-13 respectively in both asthma models (**Figure 2g/h**). When comparing the cytokines levels between the two models (**Figure 2i**), all the Th2 cytokines in BALF of the acute asthma model were significantly much higher than in the chronic asthma model: 77.90 vs. 8.372 pg/mL IL-4 (*p-value* < 0.001), 50.93 vs. 5.503 pg/mL IL-5 (*p-value* < 0.01), and 24.09 vs. 2.023 pg/mL IL-13 (*p-value* < 0.01).

Taking together, inflammatory cell number and cytokine level in BALF indicate that the acute asthma mouse model showed a higher severity of airway eosinophilia and Th2 immune response than the chronic asthma model.

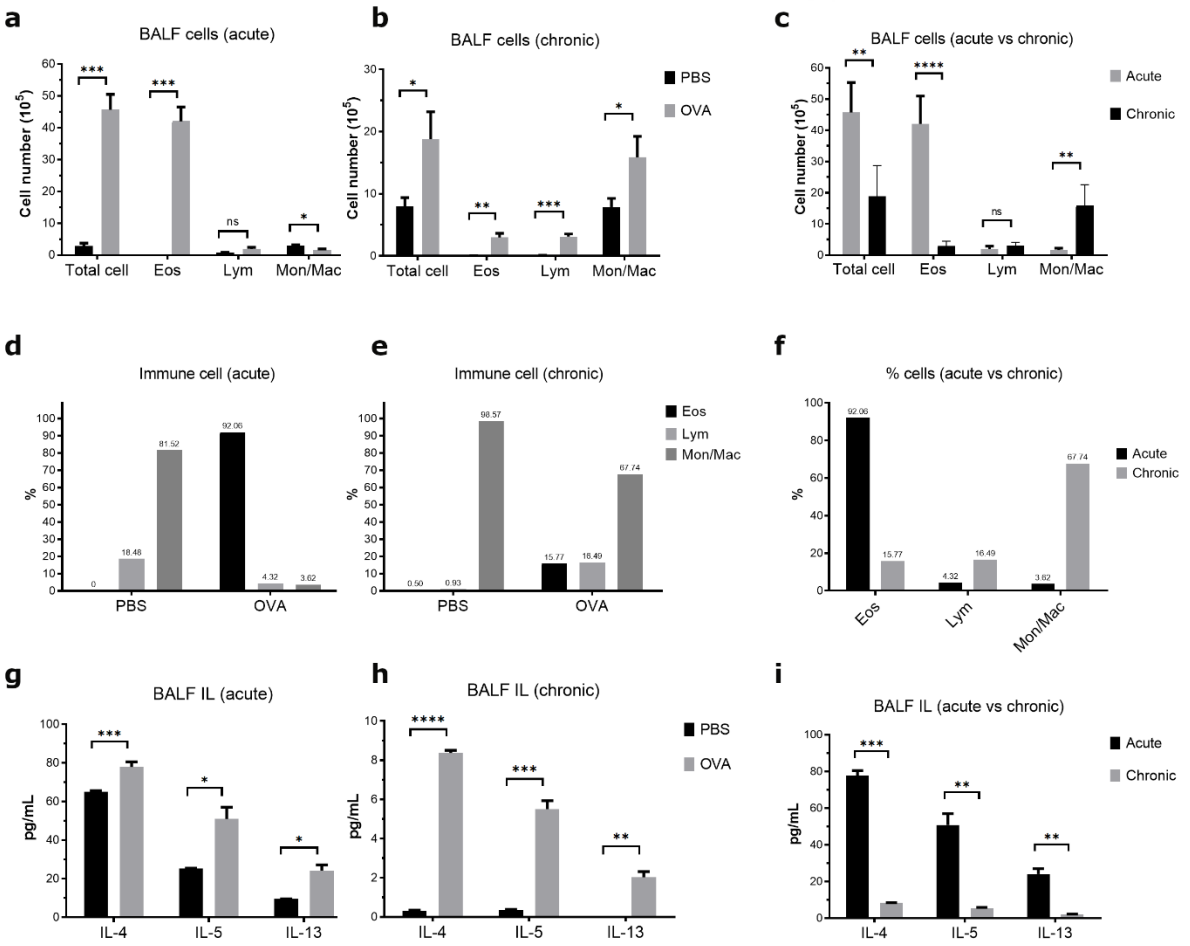

Figure 2. Broncho alveolar lavage fluid (BALF) cells and cytokines. Twenty-four hours after the final challenge, BALF was collected and analyzed for inflammatory cells and Th2 cytokines. The results were compared between the phosphate-buffered saline (PBS) control group and the ovalbumin (OVA) sensitized group in the same model, or between the acute and chronic asthma model. Total cells, eosinophils (Eos), lymphocytes (Lym), and monocytes/macrophages (Mon/Mac) were counted in acute (**a**) and chronic (**b**) asthma models. Comparison of cell number between both asthma models (**c**). Percentage of differentiated cells in acute (**d**) and chronic (**e**) models. Comparison of cell percentage between both models (**f**). Levels of Interleukin (IL)-4, IL-5, and IL-13 in acute (**g**) and chronic (**h**) asthma models. Comparison of cytokines levels between both models (**i**). The results are shown as mean ± standard error of the mean (SEM) (n=4-6). $^{*}p<0.05$, $^{**}p<0.01$, $^{***}p<0.001$, and $^{****}p<0.0001$ (two-tailed paired Student's t-test). (**Abbreviation:** ns, non-statistically significant).

The acute asthma mouse model showed evidence of inflammatory cell infiltration in the lung

The lung tissue of acute and chronic asthma mouse models was studied by H&E staining for cellular visualization. Consistent with the results of the BALF study, the immune cells were present in higher numbers around the airways of the acute asthmatic mice compared to the chronic asthmatic mice and the PBS-treated mice (**Figure 3a**).

The degree of cell infiltration was evaluated by the Image J software, indicating that there is a significant increase (*p-value* < 0.05) in cell accumulation in the lung tissue of the acute asthma model compared to its PBS control (**Figure 3b**). The chronic asthma model showed some amount of cell infiltration around the airway in lung tissue but was not significantly different from its control when calculated by the software (**Figure 3a/b**).

The percent increase in cell numbers was calculated. The acute asthma model has a 45% cell increase in the lung tissue compared to its PBS control and the chronic asthma model has only a 10% increase in cell number from the control (**Figure 3c**). Therefore, the OVA-induced acute asthma mouse model might be more suitable for clearer evidence of cell infiltration in lung histology.

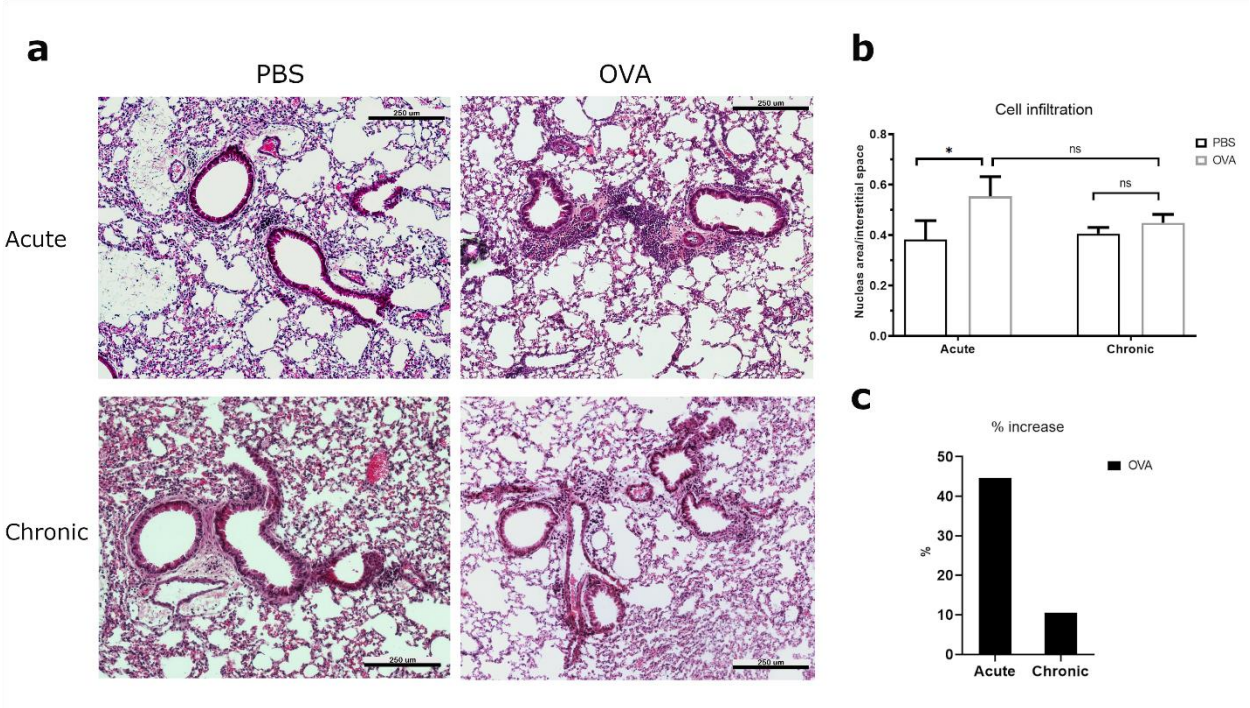

Figure 3. Airway inflammation and cell infiltration. Slides of lung tissue were deparaffinized and stained with Hematoxylin and eosin (H&E) staining. The cell nuclei were stained black, and the lung cells and connective tissues were in pink color. Lung histology was compared between the phosphate-buffered saline (PBS) control group and the ovalbumin (OVA) sensitized group in the same model and between the acute and chronic asthma models. (**a**) Representative image of lung infiltration. (**b**) Inflammatory cell accumulation around the airways was analyzed by ImageJ software. (**c**) The percentage of increase in cell infiltration of both asthma models compared to their respective control. Results are representative of two mice per group. The images are shown at 100x magnification, the scale bars denote 250 µm. The bar graphs are shown as mean ± standard error of the mean (SEM). $^{*}p<0.05$ (two-way analysis of variance [ANOVA]). (**Abbreviation:** ns, non-statistically significant).

The acute and chronic asthma mouse model showed obvious bronchial goblet cell hyperplasia

To evaluate the production of mucus inside the airway, the lung tissue of the mice was stained with PAS staining. The intracellular mucin was stained red inside the goblet cells, lining the airway basement membrane. The goblet cells were highly present in the airways of both acute and chronic asthmatic mice compared to the PBS-treated control mice (**Figure 4a**).

The amount of mucin-producing goblet cells was evaluated by the Image J software, indicating that there is a significant increase in goblet cell proliferation in the airways of both the acute and chronic asthma model compared to their respective PBS control (*p-value* < 0.0001) and there is no significant difference between the two models (**Figure 4b**).

The percent increase in goblet cell hyperproliferation was calculated based on the PBS control in each group. The acute and chronic asthma models showed a very high increased percentage of goblet cells in the lungs of asthmatic mice, about 700% and 900% respectively (**Figure 4c**). So, the OVA-induced acute and chronic asthma mouse model could reproduce a similar degree of goblet cell hyperplasia inside the lung.

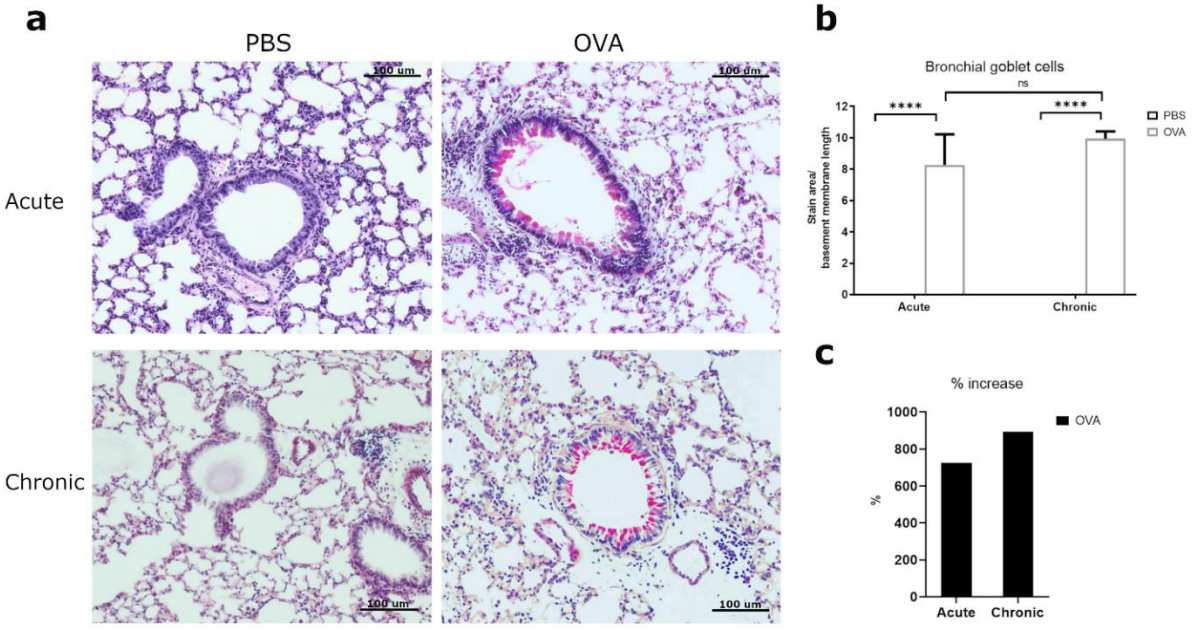

Figure 4. Mucus production and goblet cells hyperplasia in the lung. Lung tissues were stained with Periodic acid–Schiff (PAS) staining. Mucin granules are stained red inside the goblet cells lining the airway. Lung histology was compared between the phosphate-buffered saline (PBS) control group and the ovalbumin (OVA) sensitized group in the same model and between the acute and chronic asthma models. (**a**) Representative image of goblet cells hyperplasia. (**b**) Mucus production inside the airways was analyzed by ImageJ software. (**c**) The percentage of increase in mucus production of both asthma models compared to their respective control. Results are representative of two mice per group. The images are shown at 400x magnification, the scale bars denote 100 µm. The bar graphs are shown as mean ± standard error of the mean (SEM). $^{****}p<0.0001$ (two-way analysis of variance [ANOVA]). (**Abbreviation:** ns, non-statistically significant).

The chronic asthma mouse model showed a clearer sign of airway tissue remodeling

Trichrome staining of lung tissue revealed structural changes in collagen deposition (blue stain) airway epithelium and smooth muscle (red stain). The increase in size and length of ciliated cells and the thickness of smooth muscle cells is observed in the bronchus of OVA-induced asthmatic mice, especially in chronic asthma mice (**Figure 5a**). The amount of collagen tissue was also more evident in chronic asthmatic mice compared to the acute asthmatic mice and the PBS control mice.

When calculated by the software, collagen augmentation was observed in the lungs of both acute and chronic asthma models compared to their PBS controls, but the statistical significance was only present in the chronic asthma model (*p-value* < 0.05) (**Figure 5b**).

When comparing the percent increase in collagen density between both models, the chronic asthma model has a more than 300% increase in airway collagen density from its PBS control, and the acute model has about 200% increase from the control (**Figure 5c**). So, the OVA-induced chronic asthma mouse model is appropriate for the study of airway remodeling and lung fibrosis.

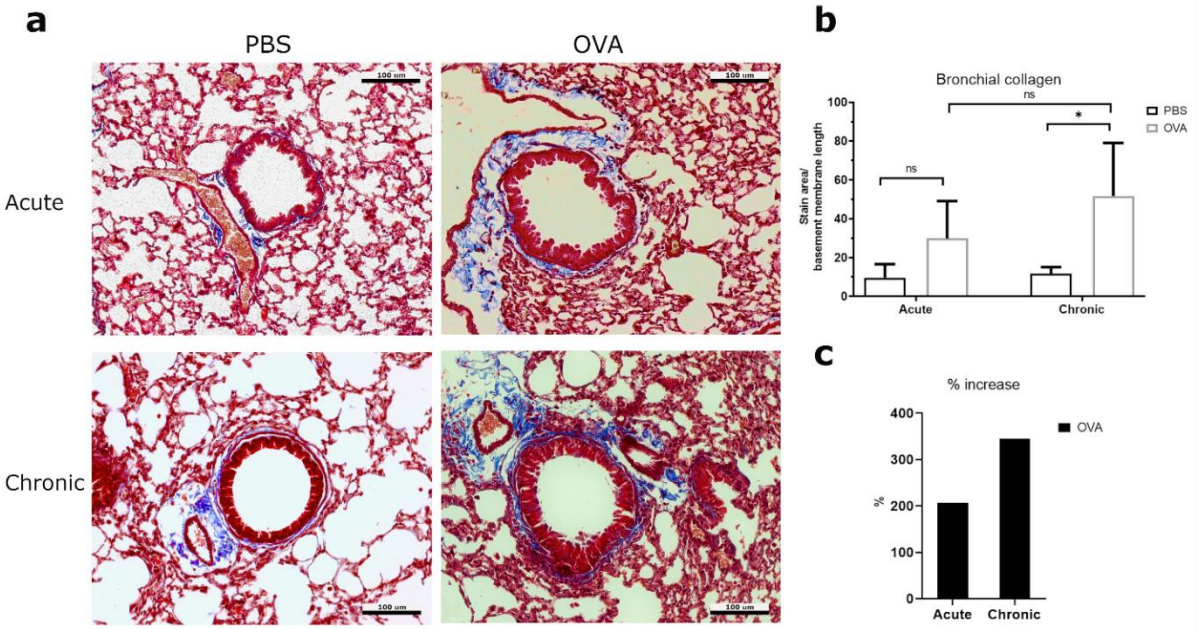

Figure 5. Airway remodeling and collagen deposition. Lung tissues were stained with trichrome stain. Collagen tissues are stained blue around the blood vessels and airway. Lung histology was compared between the phosphate-buffered saline (PBS) control group and the ovalbumin (OVA) sensitized group in the same model and between the acute and chronic asthma models. (**a**) Representative image of airway remodeling. (**b**) Collagen deposition around the airways was analyzed by ImageJ software. (**c**) The percentage of increase in bronchial collagen of both asthma models compared to their respective control. Results are representative of two mice per group. The images are shown at 400x magnification, the scale bars denote 100 µm. The bar graphs are shown as mean ± standard error of the mean (SEM). $^{*}p<0.05$ (two-way analysis of variance [ANOVA]). (**Abbreviation:** ns, non-statistically significant).

Discussion

Mice are the most studied species for animal models of asthma. In this study, we utilize the egg whites OVA to induce allergic lung inflammation in mice, the simplest and cheapest way to recreate asthma phenotypes in an *in vivo* model. Broncho alveolar lavage (BAL) could serve to diagnose many lung-related conditions, including asthma. In normal subjects, alveolar macrophages take about 80-90% of the cell population.[14] In our asthma mouse models, the PBS control mice showed >80% monocytes/macrophages in BALF. The acute asthma model has an increase in eosinophil number (>90%) and decreased the monocyte/macrophage cell population to less than 4%; while the chronic asthma model still has a high percentage of the macrophage cell population (68%) with an increase in number of another inflammatory cells. The increase in eosinophil is associated with acute inflammation caused by an allergic reaction and the increased macrophage is associated with efferocytosis in the resolution phase.[15]

The increase in inflammatory cells and Th2 cytokine levels in BALF of both the acute and chronic asthma models corresponds to commonality in immune responses associated with asthma in previous studies.[16,17] The higher degree of airway eosinophilia and elevated levels of IL-4, IL-5, and IL-13 in the acute model, compared to the chronic model, supports the notion that acute asthma is characterized by a more robust immune response.[18,19] The significant increase in inflammatory cell infiltration into the bronchi of the acute asthma model, as revealed by H&E staining, is consistent with the emphasis pronounced phase of the acute inflammatory nature.[19,20] In contrast, the absence of significant differences in inflammatory

cell infiltration in the chronic model suggests a sustained but perhaps less intense inflammatory response. The similar hyper-proliferation of airway goblet cells in both acute and chronic asthma models, as indicated by PAS staining, suggests a persistent airway remodeling process associated with chronic asthma, contributing to the characteristic symptoms and airway dysfunction.[20,21] The significant increase in collagen deposition around the bronchus in the chronic model underscores the long-term consequences of chronic asthma on airway structure and function, supporting the conclusion of airway remodeling in chronic asthma.[22]

Asthma in both humans and mice involves inflammatory responses, which are crucial to the pathogenesis of airway inflammation associated with airway hyperresponsiveness and remodeling. However, the mechanisms underlying allergen sensitization and responses may differ. Mouse models do not precisely replicate the lung inflammation observed in humans. While mice exhibit peribronchiolar collagen deposition, human asthma presents with limited subepithelial thickening.[23,24] In summary, the findings from our study provide comprehensive insights into the distinctive features of acute and chronic asthma. The robust immune response, associated with acute asthma, and the pronounced airway remodeling seen in chronic asthma highlight the complex and multifaceted nature of this disease. As asthma is no longer considered a single disease[25,26], the mouse model of allergic asthma might be useful to study any associated pathophysiologic conditions.

Conclusion

The establishment of acute and chronic allergic asthma models through OVA induction provided valuable insights into the pathophysiological aspects of these conditions, including allergic inflammation, Th2 immune response, eosinophilia, immune cell migration, and tissue remodeling. This would make good and simple models for studying pharmacological compounds and their responses in an *in vivo* system, which is not limited to only asthma disease but also other allergic inflammations and fibrosis conditions.

Acknowledgment

This research was supported by the Siriraj Foundation, Faculty of Medicine Siriraj Hospital, Mahidol University, Bangkok, Thailand (D-003658).

References

1. Lambrecht BN, Hammad H. The immunology of asthma. Nat Immunol. 2015 Jan;16(1):45-56.
2. Effros RM, Nagaraj H. Asthma: new developments concerning immune mechanisms, diagnosis and treatment. Curr Opin Pulm Med. 2007 Jan;13(1):37-43.
3. Holgate ST, Polosa R. The mechanisms, diagnosis, and management of severe asthma in adults. Lancet. 2006;368(9537):780-93.
4. Matsuoka T, Hirata M, Tanaka H, et al. Prostaglandin D2 as a mediator of allergic asthma. Science. 2000 Mar 17;287(5460):2013-7.
5. Hamid Q, Tulic M. Immunobiology of asthma. Annu Rev Physiol. 2009;71:489-507.
6. Bush A, Saglani S. Management of severe asthma in children. Lancet. 2010 Sep 4;376(9743):814-25.
7. O'Byrne PM, Parameswaran K. Pharmacological management of mild or moderate persistent asthma. Lancet. 2006 Aug 26;368(9537):794-803.
8. Brusselle G, Kips J, Joos G, Bluethmann H, Pauwels R. Allergen-induced airway inflammation and bronchial responsiveness in wild-type and interleukin-4-deficient mice. Am J Respir Cell Mol Biol. 1995 Mar;12(3): 254-9.

9. Cho YS, Kwon B, Lee TH, et al. 4-1 BB stimulation inhibits allergen-specific immunoglobulin E production and airway hyper-reactivity but partially suppresses bronchial eosinophilic inflammation in a mouse asthma model. Clin Exp Allergy. 2006 Mar;36(3):377-85.
10. Gueders MM, Paulissen G, Crahay C, et al. Mouse models of asthma: a comparison between C57BL/6 and BALB/c strains regarding bronchial responsiveness, inflammation, and cytokine production. Inflamm Res. 2009 Dec;58(12):845-54.
11. McMillan SJ, Xanthou G, Lloyd CM. Therapeutic administration of budesonide ameliorates allergen-induced airway remodelling. Clin Exp Allergy. 2005 Mar;35(3):388-96.
12. Kunikata T, Yamane H, Segi E, et al. Suppression of allergic inflammation by the prostaglandin E receptor subtype EP3. Nat Immunol. 2005 May;6(5):524-31.
13. Schmidt M, Mattoli S. A mouse model for evaluating the contribution of fibrocytes and myofibroblasts to airway remodeling in allergic asthma. Methods Mol Biol. 2013;1032:235-55.
14. Stanzel F. Bronchoalveolar lavage. In: Ernst A, Herth FJF, editors. Principles and practice of interventional pulmonology. New York: Springer; 2012. p. 165-76.
15. Robb CT, Regan KH, Dorward DA, Rossi AG. Key mechanisms governing resolution of lung inflammation. Semin Immunopathol. 2016 Jul;38(4):425-48.
16. Lambrecht BN, Hammad H, Fahy JV. The Cytokines of asthma. Immunity. 2019 Apr 16;50(4):975-91.
17. Bhakta NR, Woodruff PG. Human asthma phenotypes: from the clinic, to cytokines, and back again. Immunol Rev. 2011 Jul;242(1):220-32.
18. Daubeuf F, Frossard N. Eosinophils and the ovalbumin mouse model of asthma. Methods Mol Biol. 2014; 1178:283-93.
19. Tillie-Leblond I, Gosset P, Tonnel AB. Inflammatory events in severe acute asthma. Allergy. 2005 Jan;60(1): 23-9.
20. Nials AT, Uddin S. Mouse models of allergic asthma: acute and chronic allergen challenge. Dis Model Mech. 2008 Nov-Dec;1(4-5):213-20.
21. Casaro M, Souza VR, Oliveira FA, Ferreira CM. OVA-induced allergic airway inflammation mouse model. Methods Mol Biol. 2019;1916:297-301.
22. McMillan SJ, Lloyd CM. Prolonged allergen challenge in mice leads to persistent airway remodelling. Clin Exp Allergy. 2004 Mar;34(3):497-507.
23. Woodrow JS, Sheats MK, Cooper B, Bayless R. Asthma: The use of animal models and their translational utility. Cells. 2023 Apr 5;12(7):1091.
24. Kumar RK, Foster PS. Are mouse models of asthma appropriate for investigating the pathogenesis of airway hyper-responsiveness?. Front Physiol. 2012 Jul 31;3:312.
25. A plea to abandon asthma as a disease concept. Lancet. 2006 Aug 26;368(9537):705.
26. Gans MD, Gavrilova T. Understanding the immunology of asthma: Pathophysiology, biomarkers, and treatments for asthma endotypes. Paediatr Respir Rev. 2020 Nov;36:118-27.

F10

The Development, Physical Characterization, and Evaluation of Pharmaceutical and Biopharmaceutical Properties of the Intrapulmonary Drug Delivery System (DDS) of Nano-Andrographolide

Madumai Ketharam[1], Jiraporn Leanpolchareanchai[1], Suwabun Chirachanchai[2], Thitianan Kulsirirat[3], Korbtham Sathirakul[1*]

[1] *Faculty of Pharmacy, Mahidol University, Bangkok, Thailand*
[2] *The Petroleum and Petrochemical College, Chulalongkorn University, Bangkok, Thailand*
[3] *Department of Biopharmacy, Faculty of Pharmacy, Srinakharinwirot University, Nakhon Nayok, Thailand*

*E-mail: korbtham.sat@mahidol.ac.th

Abstract

Andrographolide is a traditional medicine widely used in Asian and Southeast Asian countries. Though it has been used for rheumatoid arthritis and upper respiratory tract infections for a long time, the conventional drugs have many drawbacks, such as poor solubility, rapid metabolization, and efflux by the efflux transporters. Developing a new drug delivery system for intra-pulmonary drug delivery is an advantage to overcome the drawbacks. In this study, we developed andrographolide-loaded poly (D, L-lactide-co-glycolide) (PLGA) polymeric nanoparticles using the single emulsion evaporation method to address the limitations of conventional andrographolide, such as poor solubility and rapid metabolism. The nanoparticles were characterized by size (hydrodynamic diameter), zeta potential, and encapsulation efficiency. The particle size of 163.46±1.05 nm, a zeta potential of -25.83±1.99, and a low polydispersity index of 0.077±0.011, indicating a narrow size distribution and formulation stability. The encapsulation efficiency was 48.99±1.33%, and the loading efficiency was 5.19±0.14%. The cytotoxicity studies in human small airway epithelial cells (HSAEC cells) showed that PLGA-loaded andrographolide (100 µg/mL) had low toxicity and was well-tolerated compared to conventional andrographolide. The permeability studies were performed using Transwell assays at concentrations of 12.5 and 25 µg/mL (more than 80% cell viability) in both andrographolide and nano-andrographolide. The permeability study indicated that conventional andrographolide exhibited higher permeability, while nano-andrographolide showed higher cellular uptake and more concentration intracellularly compared to conventional andrographolide. Consequently, nano-andrographolide emerged as a promising drug delivery system for intrapulmonary administration with low toxicity and enhanced cellular uptake in HSAEC cells.

Keywords: Andrographolide, nano-andrographolide, poly (D, L-lactide-co-glycolide), human small airway epithelial cells, permeability assay

Introduction

Andrographolide is a diterpenoid, a primary biologically active compound derived from *Andrographolide paniculate*. Andrographolide shows various pharmacological properties,

such as anti-inflammatory, anti-cancer, anti-thrombotic, hepatoprotective, etc. It is a popular folk medicine in China currently used for the treatment of rheumatoid arthritis, upper respiratory tract infections, asthma, laryngitis, and sore throat. This study aims to formulate andrographolide-loaded polymeric nanoparticles and investigate their toxicity and permeation in human small airway epithelial cells (HSAEC cells). There have been various studies conducted to assess the attributable efficacy of andrographolide on various pulmonary diseases, such as alleviated pneumonia, pulmonary fibrosis[1], alveolar hypercoagulation[2], and COVID-19.[3] Andrographolide is used in various formulations to exert therapeutic activity not only for local effects but also for systemic effects. The disadvantages of conventional andrographolide are low solubility, rapid metabolization, efflux by transporters, and poor bioavailability.

Drugs administered via the oral route have low bioavailability, leading to low concentrations in the blood. A short residence time in the blood may cause low pulmonary concentration and a high probability of drug distribution to uninjured organs.[4] This study aims to formulate poly (lactic-co-glycolic acid) (PLGA)-encapsulated andrographolide nanoparticles. PLGA is one of the most used polymers approved by the Food and Drug Administration (FDA) and the European Medicines Agency (EMA). Due to safety, biocompatibility, and biodegradation, it has been approved to be used in drug delivery systems.

Lung administration is an attractive route for pulmonary drug delivery as it offers more advantages than conventional routes and is an appropriate way of treating lung diseases. The lung is one of the portals transporting the drug into blood circulation. The main advantage of pulmonary drug delivery is the non-invasive technique that facilitates patient compliance. Nowadays, various drug delivery systems are being developed and extensively investigated to administer drugs through the pulmonary route.[5] Colloidal drug delivery systems have the most prominent advantages over other drug delivery systems. Solid lipid nanoparticles, polymeric nanoparticles, and liposomes have been extensively studied for many years for various lung diseases.[6] The anatomy and physiology of the lungs should be profoundly studied to develop the appropriate drug delivery system to overcome the challenges of the existing dosage forms. The enormous surface area is provided by the alveoli for gas exchange. Alveoli, blood arteries, lymphatic tissue, bronchi, and other smaller airways make up the interior part of the lungs. The bronchi are divided into primary and secondary bronchi, bronchioles, and alveoli. Moreover, the pulmonary capillaries that line each alveolus create a huge network with a surface area of nearly 70 m^2 that can serve as the blood-gas barrier.[5]

The nanoparticles are translocated through the alveolar epithelium via the endocytosis process. In some cases, the nanoparticles can be taken up to the cells via a non-endocytotic pathway called the paracellular pathway via tight junctions. Previous research shows polymeric nanoparticles penetrated through the cell membrane via transcellular pathways.[7] The PLGA nanoparticles are selected due to their biodegradability, biocompatibility, and size, which can be easily tuned when synthesizing nanoparticles. PLGA is also an FDA and EMA-approved polymer and widely used in the pharmaceutical industry as a polymeric organic compound with unique physical and chemical properties, making it one of the most efficient and popular polymers for drug delivery. PLGA has some unique advantages compared to other polymers, such as low toxicity (off-target toxicity), controlled release, direct action on the lesions through multiple routes of drug delivery, higher cellular internalization, and protection against enzymatic degradation. The safety of the PLGA polymer is greatly guaranteed, as the decomposition of the polymer leads to the monomers glycolic acid and lactic acid, which are easily metabolized and cleared by the body.[8] PLGA nanoparticles have promising characteristics, such as a smaller particles size and size lower than 200 nm that can easily escape from the phagocytotic process and can easily penetrate the pulmonary mucus membrane, even though they have a negative charge surface. According to the literature review, drug-loaded nano-

particles show low toxicity and good tolerability in normal cells, which increases the advantage of the PLGA nanoparticles as an appropriate drug delivery system for incorporating Andrographolide and applying to HSAEC cells.[9-10]

Methods

Formulating andrographolide-loaded PLGA nanoparticles

Andrographolide-loaded PLGA nanoparticles were prepared using the single-emulsion evaporation method and the modified single-emulsion evaporation method (diffusion). The PLGA polymer and andrographolide were dissolved separately in ethyl acetate and mixed together, followed by vortexed and sonicated for 15 min at room temperature. The prepared organic phase was added to a 1% w/v polyvinyl alcohol (PVA) solution while vortex mixing. The pre-emulsion was ultrasonicated for 2 min at 50% amplitude. Then the polymeric emulsion was evaporated at room temperature for 4 h and centrifuged at 12,000 rpm and 15°C followed by washing twice with deionized water. The resultant precipitate was vacuum desiccated and kept at 4 °C for further analysis.

Characterizing and determining the entrapment efficiency of the andrographolide-loaded PLGA nanoparticles

The particle characterization was done using the dynamic light scattering (DLS) method. The hydrodynamic particle size, polydispersity index (PDI), and zeta potential were measured using the Malvern Zetasizer. The encapsulation and loading efficiency were calculated using the validated HPLC method at a maximum wavelength of 225 nm.

Determining the cytotoxicity of the formulated drug

Airway Epithelial Cell Basal Media supplemented with Bronchial Epithelial Cell Growth Kit. After cells reached the confluent state, the cultured cells were subculture to be used for further cell studies. Cytotoxicity studies were done for conventional andrographolide and formulated PLGA-andrographolide nanoparticles. Cells (20,000 cells/well) were seeded on a 96-well plate and incubated at 37 °C, 5% CO_2 for 24 h. Then cells were treated with varying concentrations of nano-andrographolide and conventional andrographolide, incubated at pre-specified conditions for 24 h. The following day, 3-[4,5-dimethylthiazol-2-yl]-2,5 diphenyl tetrazolium bromide (MTT) working solution (0.5 mg/mL) was added to each well and incubated again for 3 h at 37 °C, 5% CO_2 for 24 h. After the incubation period, dimethyl sulfoxide (DMSO) was added to each well to dissolve the formazan crystals. The viability of the cells was recorded in terms of absorbance by using a microplate reader at a maximum wavelength of 570 nm.

Determining the permeability through transpermeability assay

The Transwell® assay was conducted to determine the permeability of the PLGA-drug-loaded nanoparticles. The Transwell® plate contains two chambers: a lower chamber and an upper chamber. After the subculturing process, 50,000 cells/well were seeded into the upper chamber of the Transwell® insert with the 400-microliter volume of the medium. The lower chamber was also filled with the 1200-microliter volume of the medium that supported cell growth and the movement of the drug molecules. After a 48-h incubation period (to make the cells adhere to the membrane surface and allow the drug molecules to interact with the cell line). After cells reached the confluent state, the medium in the upper chamber was removed and incubated for more than fourteen days to maintain the air-liquid interface (ALI). The medium in the lower chamber was changed once every three days throughout the period. The transepithelial-transendothelial electrical resistance (TEER) value

was measured before commencing the experiments. After getting the appropriate TEER values, the permeability assay was conducted in both apical to basolateral (A-B) and basolateral to apical (B-A) directions to determine the permeability and efflux ratio. The selected two concentrations corresponding to the highest viability of the cells were further used to analyze the permeability studies. The substance was added to the apical chamber (donor) to determine the apical to basolateral permeability, and the substance was added to the basolateral chamber (receiver) to determine the basolateral to apical permeability. The samples were collected at predetermined time intervals to determine the permeated amount of the drug. The following equations were used to calculate the apparent permeability and the efflux ratio:

Apparent permeability = P_{app} = $(dQ/dt) \times (1/C_0) \times (1/A)$

Efflux ratio = $P_{app\ [B \rightarrow A]} / P_{app\ [A \rightarrow B]}$

Statistical analysis

All data were presented as the mean ± standard deviation (SD) and co-efficient variation from three independently carried out experiments. Statistical analysis was carried out using Microsoft Excel 365, version 2312 and an independent t-test from SPSS Statistics version 18.

Results

Physicochemical characteristics and entrapment efficiency of the andrographolide nanoparticles

The hydrodynamic diameter and the zeta potential were measured using the DLS method, and the results were obtained as 163.46±1.05 nm and -25.83±1.99 mV with a PDI of 0.077±0.011. The encapsulation efficiency was 48.99±1.33%, and the loading efficiency was 5.19±0.14%. The mean value from each experiment was obtained from independently carried out triplicated experiments.

Cytotoxicity of the formulated drug

According to **Figure 1**, the results showed that andrographolide nanoparticles are well tolerated by HSAEC cells compared to conventional andrographolide at the same concentrations and showed low toxic potential. The highest concentration viability of conventional andrographolide was 37.13±1.76% and the lowest concentration viability of conventional andrographolide was 106.02±2.15%. Similarly, the highest concentration viability of nano-andrographolide was 80.93±1.88% and the lowest concentration viability of nano-andrographolide was 100.85±2.15%. Furthermore, there was no significant viability difference until 25 µg/mL between both compounds ($p > 0.05$).

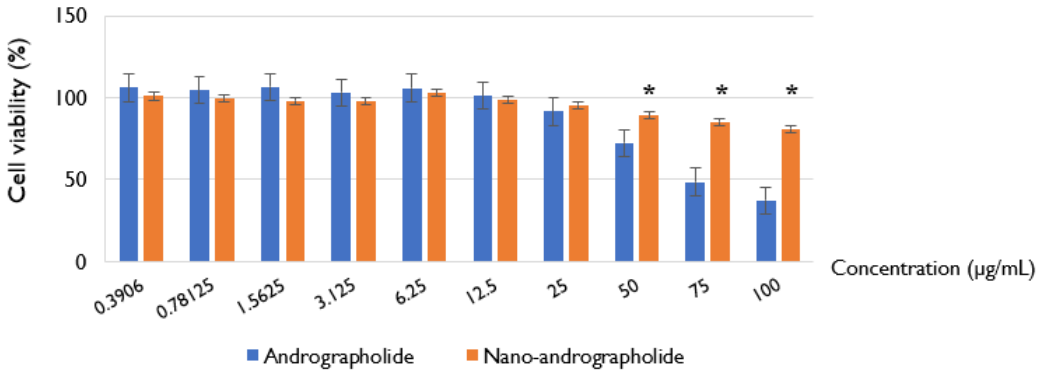

Figure 1. Cell viability percentage of andrographolide and nano-andrographolide. $^{*}p < 0.05$ represents the significant difference compared between andrographolide and nano-andrographolide.

Transpermeability assay

According to **Table 1**, in both concentrations, AG has the same P_{app} value for both influx permeability and efflux permeability. The resulting efflux ratio for andrographolide is one (ER = 1), which further indicates the mechanism of andrographolide as passive diffusion. The amount of andrographolide quantified on the receiver side at each time interval was significantly higher at 25 µg/mL compared to 12.5 µg/mL ($p < 0.05$). According to **Figure 2** Andrographolide and andrographolide-loaded PLGA nanoparticles have no significant difference ($p > 0.05$) in the amount detected on the receiver side in terms of apical to basolateral permeability in both concentrations However, the amount of andrographolide nanoparticles detected on the donor side (basolateral to apical) is significantly lower ($p < 0.05$) compared to the amount of andrographolide detected on the donor side (**Figure 3**). It clarifies that the efflux ratio of andrographolide is higher than that of andrographolide nanoparticles. As it is, the efflux ratio for andrographolide at 12.5 and 25 µg/mL is one in both concentrations. According to **Tables 2** and **Figure 4**, the efflux ratios for andrographolide-loaded nanoparticles (12.5 and 25 µg/mL) are 0.5 and 0.6, respectively. The intracellular concentration of andrographolide was calculated, and it was detected that the final quantity of andrographolide is lower than the amount of andrographolide nanoparticles inside the cells, which indicates that andrographolide nanoparticles have more uptake by the cells compared to conventional andrographolide.

Table 1. Influx and efflux apparent permeability of andrographolide.

Time (sec)	Amount andrographolide AB and BA (µg)			
	AG-AB (12.5)	AG-BA (12.5)	AG-AB (25)	AG-BA (25)
1800	0.559665971	1.092519468	1.202091659	2.34499387
3600	1.107927229	1.562668257	2.442199026	4.142071114
7200	1.833398946	2.045070086	4.241471319	5.103879113
10800	2.470909633	2.779844252	4.644262849	5.443780363
14400	2.241367929	2.983678961	4.773595785	6.060692584
18000	2.147052391	3.025530702	5.217369524	5.438552543
21600	2.152961527	2.918013056	4.997403326	5.457761872
		Efflux ratio		Efflux ratio
Influx (cm/s)	1.42857E-05	1	1.42857E-05	1
Efflux (cm/s)	1.42857E-05		1.42857E-05	

Table 2. Influx and efflux apparent permeability of nano-andrographolide.

Time (sec)	Amount nano-andrographolide (AGNP) AB and BA (µg)			
	AGNP-AB (12.5)	AGNP-BA (12.5)	AGNP-AB (25)	AGNP-BA (25)
1800	0.379878716	0.528815986	0.90336614	0.978366305
3600	0.701970375	0.789289857	1.859628194	1.669326971
7200	1.794953773	1.526354508	4.487459986	2.926952315
10800	2.143187196	1.674838453	4.735619843	3.641727143
14400	2.177345661	1.793283627	5.138164828	3.817977932
18000	2.148730491	1.789405176	5.125781887	3.761853067
21600	2.115295755	1.749448918	4.970100408	3.618079995
		Efflux ratio		Efflux ratio
Influx (cm/s)	1.42857E-05	0.5	1.78571E-05	0.6
Efflux (cm/s)	7.14286E-06		1.07143E-05	

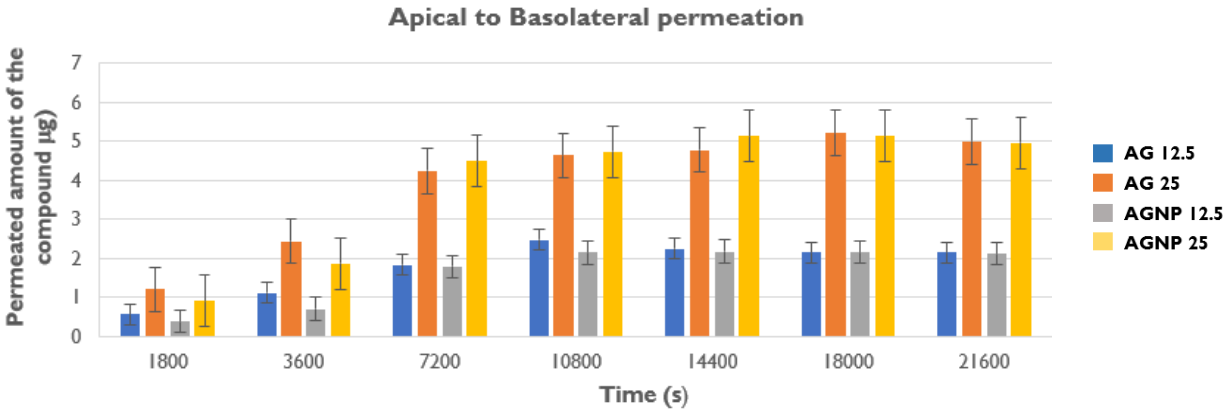

Figure 2. The cumulative amount of andrographolide and nano-andrographolide (12.5 and 25 µg/mL) permeated from apical to basolateral direction.

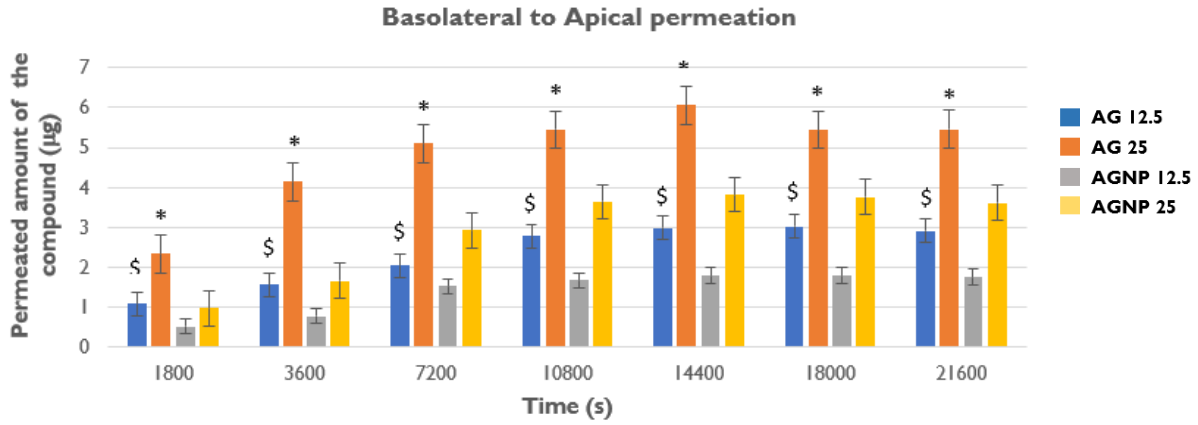

Figure 3. The cumulative amount of andrographolide and nano-andrographolide (12.5 and 25 µg/mL) permeated from basolateral to apical direction. $^{\$}p < 0.05$ represents the significant difference compared between andrographolide (12.5 µg/mL) and nano-andrographolide (12.5 µg/mL); $^{*}p < 0.05$ represents the significant difference compared between andrographolide (25 µg/mL) and nano-andrographolide (25 µg/mL).

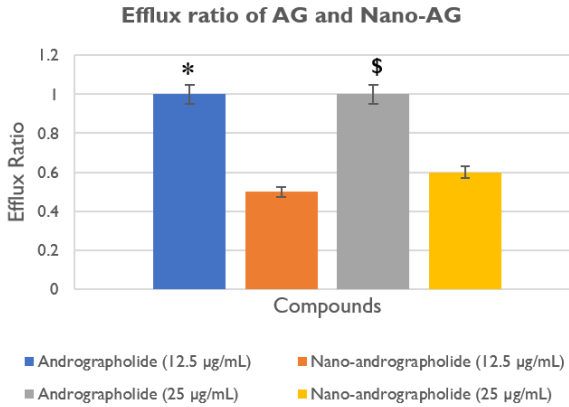

Figure 4. Comparison of efflux ratios of andrographolide and nano-andrographolide. $^{*}p < 0.05$ represents the significant difference compared between efflux ratio of 12.5 µg/mL andrographolide and 12.5 µg/mL nano-andrographolide; $^{\$}p < 0.05$ represents the significant difference compared between efflux ratio of 25 µg/mL andrographolide and 25 µg/mL nano-andrographolide.

Discussion

Andrographolide nanoparticles were formulated through a single emulsion evaporation method. Andrographolide is a lipophilic substance that can be incorporated into the PLGA polymers by the single emulsion evaporation method. Furthermore, the single-emulsion evaporation method was modified to the single emulsion diffusion method to reduce particle aggregation. Ethyl acetate was used as a solvent to dissolve the PLGA polymer and andrographolide compound. Ethyl acetate is a partially miscible solvent in the water phase. Therefore, the boiling point of this solvent is higher than the boiling point of the immiscible solvents in water such as dichloromethane and chloroform.

The single emulsion evaporation method was modified by adding water after preparing the pre-emulsion and before ultrasonicating to allow ethyl acetate to diffuse through the water phase which, further let the nanoparticles get precipitated and reduce the agglomeration of the particles. This modified diffusion method will increase the reproducibility of the nanoparticle formulation and promote the unimodal distribution of the particle size. Lower PDI and higher zeta potential values indicate the unimodally narrow distribution of the particle size and the stability of the formulation. The final concentration of DMSO in the stock solution was calculated and found to be 0.5% which is nontoxic to cells according to the literature review.[11] The results showed that andrographolide nanoparticles are well tolerated by HSAEC cells compared to conventional andrographolide at the same concentrations and show low toxic potential. The highest concentration viability of conventional andrographolide was 37.13±1.76%, and the lowest concentration viability of conventional andrographolide was 106.01±2.15%. According to our research, there was no significant difference in cell viability between andrographolide and nano-andrographolide until 25 µg/mL. Nano-andrographolide shows low toxicity at higher concentrations than conventional andrographolide. This might be due to the controlled release of the nanoparticles, in which the free drug might not be exposed to mitochondrial dehydrogenase until a certain time, which led to a cytoprotective effect.

The PLGA polymer had no cytotoxic effects; therefore, cell viability would not be reduced until the drug was released from the nanospheres.[12] As concentrations reduce, there is not much change in cell viability in nano-andrographolide, and sudden change was observed after 50 µg/mL. The viability of the cells treated with nano-andrographolide started at 100.85±2.15% and the final cell viability obtained at 100 µg/mL was 80.93±1.87%. There was a little reduction in cell viability compared to conventional andrographolide, whereas cell viability started at 106.01±2.15% and ended up at 37.13±2.15%, which indicates significant viability decreases when concentration increases ($p < 0.05$). Therefore, nano-andrographolide exerts a higher cytoprotective effect compared to conventional andrographolide. According to previous research studies, andrographolide showed less cytotoxic effects on normal cell lines compared to diseased cell lines due to the high level of protein expression and signal transducers.[13]

Andrographolide and andrographolide-loaded PLGA nanoparticles have no significant difference in the amount detected on the receiver side in terms of apical to basolateral permeability in both concentrations. However, the amount of andrographolide nanoparticles detected on the donor side (basolateral to apical) is significantly lower compared to the amount of andrographolide detected on the donor side. It clarifies that the efflux ratio of andrographolide is higher than that of andrographolide nanoparticles. As it is, the efflux ratio for andrographolide 12.5 and 25 µg/mL is one in both concentrations. The efflux ratios for andrographolide-loaded nanoparticles (12.5 and 25 µg/mL) are 0.5 and 0.6, respectively. The intracellular concentration of andrographolide was calculated, and it was detected that, the final quantity of andrographolide is lower than the amount of andrographolide nanoparticles

inside the cells, which indicates that andrographolide nanoparticles has more uptake by the cells compared to conventional andrographolide. Also, andrographolide inside the polymer might have been released in a controlled manner.[14]

Conclusion

The modified single emulsion evaporation method (diffusion method) was an applicable method to formulate hydrophobic polymeric nanoparticles. Nano-andrographolide was less toxic to cells compared to conventional andrographolide, which indicates the safety profile of nano-andrographolide. Nano-andrographolide showed a lower efflux ratio than conventional andrographolide, and the intracellular concentration of nano-andrographolide was higher than conventional andrographolide, in which controlled release was facilitated in nano compounds, which led to the development of a promising drug delivery system for a target delivery and locally treating pulmonary diseases.

Acknowledgement

The authors gratefully acknowledge Faculty of Pharmacy and Faculty of Graduate Studies, Mahidol University, Thailand for providing 2022 Mahidol Postgraduate scholarship and the Agriculture Research Development Agency (ARDA).

References

1. Karkale S, Khurana A, Saifi MA, Godugu C, Talla V. Andrographolide ameliorates silica induced pulmonary fibrosis. International Immunopharmacol. 2018 Sep;62:191-202.
2. Qian H, Yang H, Li X, Yang G, Zheng X, He T, et al. Andrographolide sulfonate attenuates alveolar hypercoagulation and fibrinolytic inhibition partly via NF-κB pathway in LPS-induced acute respiratory distress syndrome in mice. Biomedi Pharmacother. 2021 Nov;143:112209.
3. Ravichandran V. Identification of potential semisynthetic andrographolide derivatives to combat COVID-19 by targeting the SARS-COV-2 spike protein and human ACE2 receptor - An *in-silico* approach. Biointerface Res. Appl. Chem. 2023;13(2):155.
4. Byron PR, Patton JS. Drug delivery via the respiratory tract. J Aerosol Med. 1994;7(1):49-75.
5. Paranjpe M, Müller-Goymann CC. Nanoparticle-mediated pulmonary drug delivery: A review. Int J Mol Sci. 2014 Apr 8;15(4):5852-73.
6. Heidi M, Yun-Seok R, Xiao W. Nanomedicine in pulmonary delivery. Int J Nanomedicine. 2009:4:299-319.
7. Yacobi NR, Malmstadt N, Fazlollahi F, DeMaio L, Marchelletta R, Hamm-Alvarez SF, et al. Mechanisms of alveolar epithelial translocation of a defined population of nanoparticles. Am J Respir Cell Mol Biol. 2010 May;42(5):604-14.
8. Guo X, Zuo X, Zhou Z, Gu Y, Zheng H, Wang X, et al. PLGA-based micro/nanoparticles: An overview of their applications in respiratory diseases. Int J Mol Sci. 2023 Feb 22;24(5):4333.
9. Sánchez A, Mejía SP, Orozco J. Recent advances in polymeric nanoparticle-encapsulated drugs against intracellular infections. Molecules. 2020 Aug 18;25(16):3760.
10. Ungaro F, d'Angelo I, Miro A, La Rotonda MI, Quaglia F. Engineered PLGA nano and micro-carriers for pulmonary delivery: Challenges and promises. J Pharm Pharmacol. 2012 Sep;64(9):1217-35.
11. Ilieva Y, Dimitrova L, Zaharieva MM, Kaleva M, Alov P, Tsakovska I, et al. Cytotoxicity and microbicidal activity of commonly used organic solvents: A comparative study and application to a standardized extract from *Vaccinium macrocarpon*. Toxics. 2021 Apr 21;9(5):92.
12. Chiu HI, Samad NA, Fang L, Lim V. Cytotoxicity of targeted PLGA nanoparticles: A systematic review. RSC Advances. 2021 Mar 3;11(16):9433-49.
13. Liao H-Y, Huang C-C, Chao S-C, Chiang C-P, Tang B-H, Lee S-P, et al. Real-time monitoring the cytotoxic effect of andrographolide on human oral epidermoid carcinoma cells. Biosensors (Basel). 2022 May 6;12(5):304.
14. Nkabinde LA, Shoba-Zikhali LNN, Semete-Makokotlela B, Kalombo L, Swai HS, Hayeshi R, et al. Permeation of PLGA nanoparticles across different in vitro models. Curr Drug Deliv. 2012 Nov;9(6):617-27.

Developing Fluoride-Free Compressed Toothpaste Tablets from Guava Leaf Extracts

Varissara Nualdokrak[1], Waeowalee Choksawangkarn[1], Nuttinee Teerakulkittipong[2*]

[1] *Faculty of Science, Burapha University, Chonburi, Thailand*
[2] *Faculty of Pharmacy, Burapha University, Chonburi, Thailand*

*E-mail: nuttinee@go.buu.ac.th

Abstract

This research objectives are to compare the extraction conditions for guava (*Psidium guajava* L., Nong Khang Khok variety) leaves, to obtain an effective extraction method with high yields and to provide good biological activity in preventing tooth decay. This study aimed to develop fluoride-free toothpaste tablets using guava leaf extract. The research method was carried out according to the following procedures: optimization of guava leaves extraction methods by water extraction and ethanoic maceration, evaluation of total phenolic content, total flavonoid content, and antioxidant activity using DPPH radical scavenging assay. Three formulations of compressed toothpaste were developed using guava leaves water extract and 9 excipients. The wet flat tablet method was used to prepare the flat tablets. The tablets were compressed and evaluated after this. The results showed that water extraction and ethanolic maceration yielded no difference in phenolic and flavonoid compounds, but water extraction had higher antioxidant properties than maceration. All three formulations can be successfully pelletized. Their characteristics were spherical, light brown, with a weight of 250 mg per tablet, a hardness of 20–30, and a Newtonian brittleness of less than 1%, as per USP/NF39. The cleaning efficiency of formulation 3 is the highest due to its use of PVP-K30 as a filler and guava leaves as a flavoring agent. Therefore, aqueous extracts from guava leaves have the potential to be developed into fluoride-free toothpaste tablets. The formulation that was created had excellent physical properties, cleaning efficiency, and antibacterial activity.

Keywords: Guava leaves, compressed tablet toothpaste, bioactivity

Introduction

Tooth decay and periodontal disease are the most prevalent oral diseases in Thailand. According to epidemiological data on the oral health status of the population surveyed nationally every 5 years, these conditions have long-lasting negative impacts on the economy, society, and the physical, and mental health of individuals.[1] Consequently, the development of oral cleaning products is aimed at reducing plaque buildup, tooth decay, periodontal problems, and inhibiting bacteria in the oral cavity.[2] Traditional knowledge and the application of a specific mineral having these qualities fluoride have been combined to create this advancement. These days, toothpaste frequently contains fluoride.[3] Fluoride-containing toothpaste is one option for oral health care, as fluoride helps strengthen teeth and prevent tooth decay. However, excessive fluoride intake or for individuals allergic to fluoride can lead to abnormalities in the tooth enamel called dental fluorosis. Dental fluorosis presents mottled white spots or

cloudy white areas on the teeth. In severe cases, it can lead to small, chalky white areas of enamel breakdown that are prone to chipping.[4] Therefore, fluoride should be used in appropriate amounts. For those allergic to fluoride who still need to use toothpaste to kill oral bacteria and prevent oral and dental problems or reduce the growth of bacteria that cause oral health problems as a substitute for fluoride, there has been a study on key substances from Thai herbs to make fluoride-free toothpaste, such as guava, sea holly, and galangal.[5]

Guava (*Psidium guajava* L.) is an herbal plant that is widely recommended for use in public health due to its popularity as a common fruit. Guava has various medicinal properties, as evidence suggests. Studies have examined many guava plant parts, including the leaves, and found important compounds including quercetin and tannins that can inhibit oral micro-organisms. Studies have also revealed that guava leaves contain qualities that can take the role of fluoride.[6] Furthermore, guava is an easily accessible plant that is commonly grown using local varieties. In Chonburi province, there is a unique guava variety known as "Nong Khang Khok Guava," characterized by its round shape, light green skin, white flesh, crisp texture, and sweet taste, with a year-round harvest. To ensure continued production, farmers must remove some of the leaves during the growth phase of guava. This causes guava leaves to be wasted in great quantities in agriculture.[7] Additionally, other studies have investigated the use of guava leaf extracts to make toothpaste in various forms, such as thick pastes, solutions, and powders, but not in tablet form. Toothpaste products in tablet form are beneficial for controlling usage, preventing sharing with others, and reducing packaging waste. Reusable packaging can be used to store tablet products. Currently, there are toothpaste tablets available in other countries, with a growing trend expected.[8] Therefore, we are interested in studying the biological effects and antibacterial properties and developing fluoride-free toothpaste tablets from extracts of the Nong Khang Khok Guava leaves.

Methods

The extraction of guava leaves involves water and maceration

Guava leaves have been extracted by boiling in water for 15 min at a ratio of 10 g of guava leaves to 150 mL of distilled water. This method was described by Bangonsri et al.[6] Guava leaves are also extracted using 70% ethanol at room temperature for 4 days, with a ratio of 10 g of guava leaves to 150 mL of ethanol. This method was described by Seo et al.[9] The extract was then filtered using filter paper and evaporated using a rotary evaporator. The result of the extract was processed into a powder using a freeze-drying machine.

The testing for biological activity of extracts

Total phenolic content The gallic acid standard solutions were prepared at concentrations of 1.9532, 3.90, 7.813, 15.625, 31.25, 62.5, and 125 µg/mL. The guava leaf extracts obtained by boiling and maceration with 70% ethanol were prepared at concentrations of 62.5, 125, and 250 µg/mL. The preparation of a solution with a volume of 10 mL was done with 7% sodium carbonate (Na_2CO_3). The creation of 10 mL of 10% Folin-Ciocalteu reagent was done by diluting it with water in a 1:5 ratio. The creation of blank solutions was using the gallic acid standard solvent and guava leaf extracts solute that were boiled and macerated with 70% ethanol at a volume of 20 µL. The sodium carbonate solution, and Folin-Ciocalteu reagent have been mixed before measuring absorbance at 760 nm using a microplate reader.[10]

Total flavonoid content The standard solutions of quercetin were prepared at concentrations of 0.46875, 0.9375, 1.875, 3.75, 7.5, 15, and 30 µg/mL. The guava leaf extracts were obtained through boiling and maceration with 70% ethanol. They were prepared in concentrations of 62.5, 125, and 250 µg/mL. The aluminum chloride ($AlCl_3$) solution was

prepared at concentrations of 0.1 M with a volume of 25 mL. These extracts were then used to prepare blank solutions, each with a volume of 30 µL. The aluminum chloride solution, quercetin standard solutions, and extract were mixed and then incubated in the dark for 30 min before measuring the absorbance at 416 nm using a microplate reader.

Antioxidant activity using the DPPH radical scavenging assay The standard solutions of ascorbic acid were prepared at concentrations of 7.81, 15.62, 31.25, 62.50, and 125 mg/mL. The guava leaf extracts obtained by boiling and maceration with 70% ethanol, resulting in a concentration of 1 mg/mL. The DPPH solution was prepared at a concentration of 300 µM by dissolving 6 mg of DPPH in ethanol and adjusting the volume to 50 mL. The guava leaf extracts (both types) were mixed with the DPPH solution in a 1:1 proportion and incubated in the dark for 30 min. The absorbance at 517 nm was measured using a microplate reader.[9]

DPPH scavenging percentage = [A-(B-C) /A] x 100

Where: A is the absorbance of the control: solvent of the sample + DPPH.
B is the absorbance of DPPH + sample: test sample + DPPH.
C is the absorbance of the blank sample: test sample + ethanol.

The IC_{50} value (the concentration of the extract required to scavenge 50% of the DPPH radicals) was used to report the antioxidant activity.

The development of three compressed toothpaste tablets that contain guava leaf extracts and nine excipients

The wet granulation method was employed to process the guava leaf extract, which was then combined with binders, disintegrants, fillers, abrasives, sweeteners, and flavoring agents. The mixture was processed by granulating and drying it in a high-temperature air oven at 60 °C. The dried granules were then sieved and weighed to determine the weight of the remaining excipients (glidants, lubricants, and detergents). The excipients and dried granules were combined and compacted into tablets using a tablet compression machine.[8]

Evaluation of the tablet properties

1) *Physical properties* The weight variation was determined by randomly selecting 20 tablets, carefully weighing each one, calculating the average weight, and finding the deviation from the standard weight.[11]

2) *Hardness test of tablets* The hardness test tablets were carefully stored in a controlled environmental chamber. The hardness test process included using a 50 mm jaw to calibrate the machine and measuring the size of each tablet. If the tablet is round, it should be positioned parallel to the jaw and measure its hardness. The last part of the process is taking note of the hardness of each tablet and calculating the average.[11]

3) *Friability test of tablets* The test required tablets have been stored in an environmental chamber. If a tablet weighed 650 mg or less, multiple tablets were combined to reach a total weight of 6.5 g or more. A precision scale was to weigh the tablets. The friability test was conducted by setting the friability tester to rotate at 25 revolutions/min for 4 min. After the test, the tablets were weighted and calculated the weight difference, which should not be more than 1%.[11]

4) *Disintegration test of tablets* The test began by taking 6 tablets stored in an environmental chamber. The disintegration of each formulation of tablets was tested in water at 37 °C. If it took longer than 60 min for the tablet to disintegrate completely, the disintegration time would be recorded as more than 60 min.[11]

5) *Testing for moisture content of tablets* The tablet moisture meter was opened and warmed. A drying tray was placed inside the machine and then the tablet samples were tested by measuring 1-2 g of each tablet. Until the machine signal indicated completion then the %loss on drying value was recorded.[11]

Cleaning ability The test began by boiling 1 L of water and adding 2 tablespoons of lemon juice and a small amount of red food coloring. Eggs were prepared by boiling and cooling them in colored water at 25 °C for an hour. The eggs were patted dry and coated with each formulation of toothpaste tablets. The results were observed after scrubbing 5-10 times, whether after the test it was more or less clean.[12]

Antimicrobial activity

The well diffusion test was employed for testing antibacterial activity by using Mueller Hinton agar (MHA). The agar was prepared by weighing 38 g of MHA powder with 1 L of distilled water, then it was spread on a Petri dish, and incubated the culture. *Streptococcus mutans* with turbidity that adjusted to 0.5 McFarland were dropped on sterile paper plates. Test substances and control substances (e.g. antibiotics, ampicillin) were placed in the agar, and incubated at 37 °C for 18-24 h. *Streptococcus mutants* that are sensitive to antibiotics would not grow around the paper disc. Therefore, the size of the transparent area around a paper disc indicated the sensitivity of Streptococcus mutants to antibiotics.[13]

Results

The bioactivity of guava leaves has been tested to determine the total phenolic contents and total flavonoid content involves measuring the total phenolic contents of various guava leaf extracts obtained through two different extraction methods and comparing them with gallic acid standards. It was found that the boiling water extraction method yielded a total phenolic content of 4,831.11±1.23 mg of gallic acid equivalent (GAE) per g of extract, whereas the 70% ethanol extraction method yielded a total phenolic content of 4,564.45± 2.05 mg GAE/g of extract (**Table 1**).

Similarly, the total flavonoid content of guava leaf extracts was measured and obtained through different extraction methods. Comparing them with quercetin standards revealed that the boiling water extraction method yielded a total flavonoid content of 168.94±0.94 mg of quercetin equivalent (QE) per g of extract, while the 70% ethanol extraction method yielded a total flavonoid content of 246.40±0.89 mg QE/g of extract (**Table 1**).

The antioxidant action of guava leaf extracts was tested using the DPPH method and compared to ascorbic acid standards. The boiling water extraction method showed an IC_{50} value of 20.41±0.55 µg/mL, while the ethanolic extraction method showed an IC_{50} value of 22.92±0.58 µg/mL (**Table 1**). The total phenolic and flavonoid contents of guava leaf extracts obtained through boiling water and 70% ethanol extraction methods were not significantly different. However, the guava leaf extract obtained through boiling water extraction exhibited better antioxidant properties compared to the extract obtained through the 70% ethanol extraction method, as analyzed from the IC_{50} values, indicating a better inhibition of free radicals at a concentration of 50%.

Table 1. Results of the biological activity testing of guava leaf extracts using both methods.

Biological activity	Extraction of boiled guava leaves	Extraction of guava leaves with 70% ethanol
Total Phenolic Content (mg GAE/g extract)	4831.11±1.23^{A}	4564.45±2.05^{A}
Total Flavonoid Content (mg QE/g extract)	168.94±0.94^{A}	246.40±0.89^{A}
IC_{50} (µg/mL)	20.41±0.55^{B}	22.92±0.58^{A}

Data shown are the mean ± standard deviation of 3 replicate experiments. ^{A,B} Different letters indicate statistically significant differences (P<0.05).

The results of physical testing of toothpaste tablets made from guava leaves revealed that all three formulas could be successfully pressed into brown round tablets (**Figure 1** and **Table 2**). The three formulations exhibited a sweet, cool, refreshing taste, had less than 1% crispness, had moisture in the range of 4-6%, weighed 250 mg per tablet. and had hardness ranging from 20 to 30 newtons. In addition, it was found that the differences in weight and disintegration time among the three formulations were not statistically significant. The differentiating factor was that formulation 1 still had a lingering herbal aroma. In addition to the aroma of peppermint oil, and had a hardness of 30-45 newtons, which was too hard for chewable tablets. Therefore, it was developed into a second formulation by changing the aroma to potato juice to mask the herbal scent and adding lubricant to reduce hardness. However, this led to increased moisture content and tablet sticking, and made it difficult to squeeze. Formulation 3 has therefore been developed by increasing the amount of lubricant and adding glidant to help with the flow, to reduce moisture and help the tablets be pressed well, becoming toothpaste tablets with appropriate humidity, simple and right size (**Table 3**).

(A) (B) (C)

Figure 1. Toothpaste tablets. (A) Formulation 1; (B) Formulation 2; and (C) Formulation 3.

Table 2. Formulations of toothpaste tablets.

Ingredients in toothpaste tablets	Formulations		
	F1	F2	F3
Guava leaf	✓	✓	✓
Binder	✓	✓	✓
Disintegrant	✓	✓	✓
Diluent	✓	✓	✓
Abrasives	✓	✓	✓
Sweetener 1	✓	✓	✓
Sweetener 2	✓	✓	✓
Flavoring agent	✓	✓	✓
Lubricant	-	✓	✓
Detergent	✓	✓	✓
Glidant	-	-	✓

Table 3. Physical characteristics of all 3 formulations of compressed toothpaste tablets.

Physical characteristics	Formulations		
	F1	F2	F3
Color	brown	brown	brown
Odor	Herbal scent, peppermint oil	Guava oil	Guava oil
Flavor	sweet and cool	sweet and cool	sweet and cool
Appearance	round	round	round
Moisture	6.86%	7.14%	6.19%
Weight variation	0.2587±0.01 g	0.2563±0.00 g	0.2542±0.01 g
Disintegration	27.0±5.37 min	34.7±3.45 min	36.9±4.46 min
Friability test	0.31%	0.62%	0.00 %
Hardness	42.17±0.01 N	24.83±2.86 N	23.73±3.33 N

Data shown are the mean ± standard deviation of 3 replicate experiments.

The test results for the cleanliness of compressed toothpaste tablets revealed that residues from eggshells, food coloring, and orange juice mimicked plaque and lactic acid in the oral cavity. This was evidenced by the time required to brush between 5–10 times, reflecting the level of cleanliness achieved after testing (**Table 4**). Experimental results showed that compressed toothpaste tablet formulation 3 was more effective in cleaning compared to both formulations 1 and 2. This is because it required less time for cleaning and produced more foam during brushing (**Figure 2**).

Table 4. Cleaning efficiency of all 3 formulations of toothpaste tablets.

Formulations	Abrasiveness (rating)	Foaming ability	Cleaning ability
F1	2	+	++
F2	4	++	++
F3	6	+++	+++

(A) (B) (C)

Figure 2. Cleaning ability testing of toothpaste tablets using **e**ggshells.
(A) Formulation 1; (B) Formulation 2; and (C) Formulation 3.

From the results of the antibacterial testing activity against *S. mutans* using well diffusion test method, it was found that all 3 formulations had an Inhibition zone value in resisting the bacteria *S. mutans*. Especially formulation 3 was effective in resisting *S. mutans* bacteria better than the other two formulations. However, formulation 3 still had less ability to resist the growth of *S. mutans* bacteria than positive control (ampicillin) (**Figure 3** and **Table 5**).

Ampicillin (A)

(C) (B)

Figure 3. Well diffusion test of toothpaste tablets against *S. mutans*. (A) Formulation 1; (B) Formulation 2; and (C) Formulation 3.

Table 5. Efficacy of guava leaf extract toothpaste tablets in resisting *S. mutants* infection.

Formulations	Inhibition zone of guava leaf extract (mm)
F1	8.50±2.12
F2	8.67±1.53
F3	9.00±3.50
Ampicillin (positive control)	11.33±0.58

Data shown are the mean ± standard deviation of 3 replicate experiments.

Discussion

The results from the comparison of the extraction conditions from guava leaves using water and 70% ethanol extraction revealed that the total phenol and flavonoid content of the guava leaf extracts were not significantly different. However, the DPPH test for antioxidant activity showed that the aqueous extract of guava leaves has better antioxidant activity.[10] Water extraction contained 4,831.11±1.23 mg GAE/g of phenolic compounds and 168.94±0.94 mg QE/g of flavonoids, respectively.[6,14] These results are consistent with the findings of Morais-Braga et al.[15], which showed a higher quantity of phenolic compounds in water extracts compared to ethanolic extracts due to the solubility of compounds like phenolics and flavonoids in water-based solvents. Moreover, the DPPH assay for antioxidant activity demonstrated that the water-extracted guava leaf extract exhibited better anti-oxidant properties compared to the 70% ethanol maceration method, with an IC_{50} value of 20.41±0.55 μg/mL.[10] Therefore, the water extraction method yielded guava leaf extracts with higher phenolic content and better antioxidant properties when compared to 70% ethanol extraction.

All three formulations for fluoride-free compressed toothpaste tablet formulations from guava leaf water extracts of the Nong Khang Khok cultivar were developed using the wet granulation method.[8] The extracts were mixed with nine types of excipients to form a

dump mass, which was then dried and compressed into tablets following the method described by Somboon et al.[8] The quality assessment of the tablets revealed that all three formulations met the USP/NF39 standards,[11] with round shapes, brown color, cool minty taste and friability less than 1%, moisture content within 4-6%, weight of 250 mg per tablet, and hardness ranging from 20-30 newtons. The weight variation and disintegration time of all three formulations were similar. The distinguishing factor was that formulation 1 retained a lingering herbal scent besides the peppermint oil aroma and exhibited excessive hardness for chewable tablets. Hence, it evolved into formulation 2, which replaced the aroma with guava oil. However, this led to increased moisture content and tablet sticking, making tablet compression difficult. Therefore, formula 3 has been developed.

The cleanliness of the tablets was tested by simulating food coloring, orange juice residues resembling plaque, and lactic acid in the oral cavity. It was found that compressed tablet toothpaste formulation 3 was more effective in cleaning compared to formulations 1 and 2.[12] This is because it required less time for cleaning and produced more foam during brushing. Furthermore, testing for antibacterial activity against *S. mutans*, an oral bacterium, revealed that all three formulations exhibited inhibition zones, with formulation 3 showing better inhibition compared to the other two formulations. When compared to the antibiotic ampicillin, it was found that ampicillin had more effective inhibition against *S. mutans* than any of the three compressed tablet toothpaste formulations.[13]

Conclusion

This research proves that water-extracted guava leaf extract has the potential to create fluoride-free toothpaste tablets. The toothpaste formulations developed have good physical properties and are effective in cleaning the oral cavity.

Recommendation

Further studies should be conducted to investigate the long-term safety and efficacy of guava leaf extract toothpaste tablets.

Acknowledgment

The researcher would like to express gratitude to the Faculty of Pharmaceutical Sciences, Faculty of Science, and Green Natural Health Product Company for providing research funding, and the support of Long Thai Guava Garden for providing Nong Khang Khok guava leaves.

References

1. Hothiwong C. Factors associated with dental caries of children aged 3-5 years old in the Sweet Enough childcare center, Sop Prap District, Lampang province [Dissertation]. Chiang Mai: Chiang Mai University; 2015.
2. Chakrit A, Natthachon L, Abhisit D. Development of herbal toothtablet and evaluation of herbal tooth tablet satisfaction in volunteers [Thesis]. Chonburi: Burapha University; 2019.
3. CURAPROX. What is fluoride? Is it useful and necessary in toothpaste? [Internet]. 2023 [cited 2023 Dec 15]. Available from: https://www.curaprox.co.th/benefits-of-fluoride
4. Danpipat N. Fluoride in drinking water and dental fluorosis in Panomsarakham District, Chachoengsao Province; Problem solved by community participation. JHSR. 2007;1:19-27.

5. CURAPROX. Allergic to toothpaste. How can I get rid of it? With ways to prevent it. [Internet]. [date unknown] [cited 2023 Dec 15]. Available from: https://www.curaprox.co.th/benefits-of-fluoride.
6. Bangonsri P, Arom T, Watchareekun K, Urasha R. Development of mouthwash formulas from guava leaf extracts. Isan J Pharm Sci. 2006;2(1):35-42.
7. Agricultural Information Group, Chonburi Provincial Agriculture and Cooperatives Office. Product information of Chonburi Province, year 2021, product type "Guava Nong Khang Khok". [Internet]. 2021 [cited 2023 Dec 15]. Available from: https://www.opsmoac.go.th/chonburi-dwl-files-432991791226
8. Jetleela S. Herbal products part 1: Fun with producing herbal pills. [Internet]. 2013 [cited 2023 Dec 15]. Available from: https://www.pharmacy.mahidol.ac.th/th/knowledge/article/135
9. Seo J, Lee S, Elam ML, Johnson SA, Kang J, Arjmandi BH. Study to find the best extraction solvent for use with guava leaves (*Psidium guajava* L.) for high antioxidant efficacy. Food Sci Nutr. 2014 Mar;2(2):174-80.
10. Denchai R, Paiboon N, Pornsiri N, Rattana S. Antioxidant activities, total phenolics and total flavonoid contents of *Lepisanthes rubiginosa* crude extracts. Koch Cha Sarn J Sci. 2021;43(2):1-11.
11. Jetleela S. Herbal products part 1 : Enjoy producing herbal pills [Internet]. 2018 [cited 2 0 23 Dec 28]. Available from: https://www.pharmacy.mahidol.ac.th/th/knowledge/article/135
12. Shaheena S, Chintagunta AD, Dirisala VR, Sampath Kumar NS. Extraction of bioactive compounds from *Psidium guajava* and their application in dentistry. AMB Express. 2019 Dec 28;9(1):208.
13. Hudzicki, J. Kirby-Bauer disk diffusion susceptibility test protocol [Internet]. Washington DC: American society for microbiology; 2009 [cited 2023 Dec 15]. Available from https://asm.org/protocols/kirby-bauer-disk-diffusion-susceptibility-test-pro
14. Phan-ngam A, Rattana S, Sangthong B. Antioxidant effect of phenolic content. and flavonoids in guava takhop extract. J Sci Technol MSU. 2017;13:563-70.
15. Morais-Braga MF, Carneiro JN, Machado AJ, Sales DL, Dos Santos AT, Boligon AA, et al. Phenolic composition and medicinal usage of *Psidium guajava* Linn.: Antifungal activity or inhibition of virulence? Saudi J Biol Sci. 2017 Feb;24(2):302-313.

Developing Green Tea Compressed Toothpaste Tablets

Pichsinee Charlonewong[1], Waeowalee Choksawangkarn[1], Nuttinee Teerakulkittipong[2*]

[1] *Faculty of Science, Burapha University, Chonburi, Thailand*
[2] *Faculty of Pharmacy, Burapha University, Chonburi, Thailand*

*E-mail: nuttinee@go.buu.ac.th

Abstract

This research article aimed to investigate the antioxidants and antibacterial activities of green tea (*Camellia sinensis* var. assamica) in the form of green tea leaf extract and green tea powder and to develop a toothpaste tablet formulation containing fluoride. The dried green tea leaves were extracted using a boiling method with water as a solvent. The bio-activities of the green tea leaf extracts and green tea powder were studied, for example, the study of total phenolic content, total flavonoid content, and DPPH radical scavenging activity. The results showed that green tea leaf extract provides better phenolic compounds and DPPH antioxidants than instant green tea powder, but for flavonoid compounds, the instant green tea powder has a better effect. It can be concluded that green tea leaf extract is more effective in antioxidants than green tea powder. The reason is that the higher flavonoid content in green tea powder may not enhance the antioxidant effect as much as the phenolic content. Then, green tea leaf extract and green tea powder were developed into toothpaste tablets. The development formula consists of green tea ingredients that can be selected from green tea leaf extract, instant green tea powder, and auxiliary substances, mixed in proportion and made into granules using the wet granulation technique. The quality of the green tea tooth-paste tablets was evaluated by physical tests, cleanliness tests, and antibacterial tests. The results showed that the physical properties of the tablets were as follows: weight of 250 mg per tablet, hardness of 20-30 N, and friability of less than 1%. From the test of the cleanliness of green tea compressed toothpaste tablets, the results show that the tablets formulated with green tea leaf extract and green tea powder can cleanse with similar efficiency and it takes less time to scrub than when using only water. The antibacterial test against *S. mutans* showed that the toothpaste tablets made from green tea leaf extract have better antibacterial activity than the toothpaste tablets made from green tea powder, but both formulas can inhibit *S. mutans*. Therefore, it was found that green tea toothpaste tablets from both green tea leaf extract and green tea powder could be developed into a tablet form as they are reliable and effective in cleaning teeth and the oral cavity.

Keywords: Green tea, tablets, toothpaste, toothpaste tablets

Introduction

Today's tooth decay problem can be found in every age group and causes constant loss of teeth because of the increased consumption of starchy and sugary foods and the lack of consistent oral care in the correct way. Therefore, choosing appropriate oral hygiene products is important. When choosing an oral cleaning product, the effect of resisting tooth

decay should be taken into consideration. The toothpaste should contain fluoride which can treat and prevent tooth decay. The first discovery of fluoride's ability to resist tooth decay occurred in the United States, in the state of Colorado, and it later was developed for use in dental treatment. Today, fluoride toothpaste is the most widely used form of toothpaste due to its economical price and high efficiency in preventing tooth decay and gingivitis.[1] There are also herbs that contain many active ingredients that can be used to prevent tooth decay and help improve oral health, such as wheatgrass, nutmeg, and tea leaves. In green tea, there is epigallocatechin-3-gallate (EGCG), a substance in the catechin group that has the effect of resisting plaque that adheres to the surface of the teeth, and the study also found that there is a large amount of fluoride in green tea.

In the past, tea leaves were commonly used as herbal beverages. Tea was first drunk in China and has since spread to other countries around the world. It has been cultivated and propagated in various planting areas for international trade and export. With its unique taste and aroma, tea drinks quickly became popular. Additionally, tea leaves are a popular medicinal plant used to treat various diseases and it is known as a drink that can keep the body alert, refreshed, and not drowsy. Green tea leaves are tea leaves that go through a non-fermented production process or a process that does not allow fermentation to occur at all. They rely on high heat to cause the enzyme to become denatured, but they cannot change substances in the group polyphenol into other substances.[2] There is research on the important substances in green tea leaves. It was found that green tea leaves contain important substances in the catechin group such as fluoride and EGCG, which can be found in many green tea species such as Chinese species (*Camellia sinensis* var. sinensis) and Assamese species (*Camellia sinensis* var. assamica.) However, the amount of fluoride and EGCG vary depending on the geography and climate of the growing area. Tea components are effective in reducing tooth decay and the substances in the catechin group can help inhibit the growth of plaque on the tooth surface called *Streptococcus mutans*, depending on the concentration of the solution. They also help increase acid resistance on the tooth surface and will be more effective when mixed with fluoride.[3]

The amount of fluoride in the oral cavity will be reduced when the individuals gargle, eat, or drink immediately after brushing their teeth. Dry brushing or using a small amount of water to brush your teeth will help maintain the efficiency of fluoride in your mouth.[1] However, nowadays, toothpaste products are being developed in other formats, such as tablet form, because it is convenient to use and carry. Moreover, it uses only a little water to brush your teeth, is easy to control the amount of product used per time, and can reduce waste from toothpaste tube packaging.

Therefore, the researcher conducted a study to investigate the antioxidant and anti-bacterial activities of green tea (*Camellia sinensis* var. assamica) in the form of green tea leaf extract and instant green tea powder. The species was chosen because it is commonly grown among Thai farmers, resulting in easier access. Both forms of green tea were used to develop forms of toothpaste tablets that contain fluoride as an ingredient. The purpose was to develop a toothpaste form that can prevent tooth decay and provide good oral health, along with increasing the value of medicinal plants and raising the income of Thai farmers.

Methods

Preparation of green tea samples

Preparation of green tea leaves The dried green tea leaves of Assam species (*Camellia sinensis* var. assamica) used in this study were products from Choui Fong Tea Co. Ltd., Chiang Rai Province, Mae Chan District. They were taken to grind into fine powder and passed through a 16 mesh sieve. The extraction began by weighing 10 g of dried green tea leaves that

were ground into a fine powder in a 250 mL beaker. Next, the researcher brewed the tea by pouring 100 mL of distilled water at 75-80 °C into the beaker and stirring it well. Then, the beaker was put in a water bath at a temperature of 80-85 °C for 10 min[4] and left at room temperature. After it was cooled down, the resultant green tea leaf extract was filtered with Whatman no.1 filter paper. After that, it will be evaporated using a rotary evaporator at a temperature of 62-65 °C, and then freeze-dried[5] to get the extract in a form that is easy to test and press into tablets.

Preparation of green tea powder The green tea powder of Assam species (*Camellia sinensis* var. assamica) used in this study was the products by Chachuifong Co. Ltd., Chiang Rai, Mae Chan District.

Biological activity testing of the green tea

DPPH radical scavenging assay Ascorbic acid standard solutions were prepared at concentrations of 100, 50, 25, 12.5, 6.25, 3.125, and 1.562 µg/mL. Green tea leaf extract and green tea powder were dissolved in distilled water at a 1:1 ratio, percentage by mass per volume (%w/v) The green tea leaf extract was prepared at concentrations of 100, 50, 25, 12.5, 6.25, 3.125 and 1.562 µg/mL. Green tea powder was prepared at concentrations of 250, 125, 62.5, 31.25, 15.62, 7.81, and 3.90 µg/mL. Then, DPPH was prepared with a concentration of 300 µM by weighing 6 mg of the substance, dissolving it in ethanol, and adjusting the volume to 50 mL. Green tea leaf extract and green tea powder were pipetted at 100 µL each and added to the 96-well plate. DPPH was prepared at the concentration of 300 µM and volume of 100 µL and shaken gently to stimulate the reaction in the 96-well plate. The next step was to incubate them in the dark for 30 min at room temperature. Then, the light absorbance value at each concentration was measured with a microplate reader at a wavelength of 517 nm.[6]

$$\text{DPPH radical scavenging percentage} = [A-(B-C)/A] \times 100$$

A is the absorbance of the control : solvent of a substance 100 µL + DPPH 100 µL.
B is the absorbance of the DPPH + sample : test substance 100 µL + DPPH 100 µL.
C is the absorbance of the blank sample : test substance 100 µL + ethanol 100 µL.

This study used the IC_{50} value to report the results of inhibiting DPPH free radicals. IC_{50} is the concentration value of the extract that can absorb light from DPPH radical by 50%.

Determination of total phenolic content Gallic acid standards were prepared at concentrations of 1000, 500, 250, 125, 62.5, 31.25, and 15.625 µg/mL, and the prepared green tea (green tea leaf extract and green tea powder) were dissolved in distilled water at a 1:1 ratio, percentage by mass per volume (%w/v) Green tea leaf extracts and the green tea powder should have a final concentration of 250 µg/mL. The next step was to prepare a blank solution without green tea, consisting of 20 µL of distilled water, 100 µL of 10% Folin-Ciocalteu reagent, and 80 µL of 7% (w/v) sodium carbonate (Na_2CO_3). Green tea leaf extract or green tea powder (20 µL), 7% Na_2CO_3 (80 µL) and 10% Folin-Ciocalteu reagent (100 µL) were added to the 96-well plate and then shaken gently to stimulate the reaction. The reaction mixture was incubated in the dark for 30 min at room temperature. Then the light absorbance value at each concentration was measured with a microplate reader at a wavelength of 760 nm. The results were reported in mg of gallic acid equivalents (GAE) per g of extract.[7]

Determination of total flavonoid content Quercetin standards were prepared at concentrations of 25, 12.5, 6.25, 3.125, 1.562, 0.781, and 0.390 µg/mL. Green tea leaf extracts and green tea powder were dissolved in distilled water at a 1:1 ratio, percentage by mass per volume (%w/v) to get the final concentration of 1000 µg/mL. A solution without

green tea as a blank solution (30 µL of ethanol + 170 µL of 0.1% (w/v) $AlCl_3$) was prepared. The next part was to add green tea extract (green tea leaf extract and green tea powder) 30 µL each and 170 µL of 0.1% (w/v) $AlCl_3$ to a 96-well plate. They were shaken gently to stimulate the reaction and then incubated in the dark for 30 min at room temperature. The light absorbance value at each concentration was measured with a microplate reader at a wavelength of 416 nm and the results were reported in mg of quercetin equivalents (QE) per g of extract.[8]

Preparation of green tea toothpaste granules

Granulation process using wet granulation technique The first step was mixing green tea (from green tea leaf extract or green tea powder,) fluoride, and excipients in a mixer until it became homogeneous and then adding flavoring agents to the mixture. Next, an appropriate amount of water was added until the mixture became wet granules. Then the mixture was gilded through a 16 mesh sieve and baked in a hot air oven at 60 °C or maintained a moisture content of 4-6% to obtain dry granules.[9]

Compression process for green tea toothpaste granules The obtained dry granules were ground through a 16 mesh sieve, followed by adding auxiliary substances, including foaming agent, glidant, and lubricant, respectively. They were passed through a 60 mesh sieve orifice, mixed until becoming homogeneous with a mixer, and then hammered into tablets with a single punch tablet machine.

Physical Tests

Friability test A friability tester was utilized to evaluate tablet friability. The size of the pill compartment must be 283-291 mm in diameter and 36-40 mm in width, made with clear material. If 1 tablet weighs less than or equal to 650 mg, multiple tablets should be combined to have a final weight greater than or equal to 6.5 g for testing. If 1 tablet weighs more than 650 mg, bring 10 pills to test. The test required the machine to rotate at 25 revolutions/min for 4 min. The tablets passed the evaluation if they were not visibly cracked, broken, or chipped. When calculating the difference in pre- and post-experimental weight, both values must not exceed 1%. If the value exceeds 1%, the process will be repeated two more times, and then average the values. All three cycles must not exceed 1%.

$$\% \text{ Friability} = \frac{\text{Initial weight - Final weight}}{\text{Initial weight}} \times 100$$

Hardness test A hardness test was evaluated using a hardness meter. The tablets' hardness test was done by randomly selecting 10 tablets. As they were chewable tablets, the machine measured from the point of the tablet breaking force because it affected the tablets' ability to chew and disintegrate. Therefore, the researchers have set the hardness value at 20-30 N.

Weight variation test The test was done by randomly selecting 20 tablets, weighing each tablet precisely, and calculating the average weight of the pills and the standard deviation to calculate the percentage of relative standard deviation.

Disintegration test The test used an apparatus consisting of a temperature-controlled water bath, containers for the liquid medium, glass tubes with mesh bottoms, and a motor to pull the basket set to move up and down. In the test, liquid (usually water) was placed into a container and the temperature was controlled to 37±2 °C. When the specified temperature was reached, the tablet was placed into each tube and the disintegration time for each tablet was recorded. Lastly, the average disintegration time of toothpaste tablets and standard deviation were calculated.

Cleaning ability test

The test required 1 L of water mixed with 2 tablespoons of vinegar and a little food coloring, then boiled the water. After leaving the water to cool at 25 °C, the eggs were put in it for 1 h and then patted to dry. Next, green tea compressed toothpaste tablets were taken for testing by scrubbing it on the eggshells 5-10 times. The results of the cleanliness obtained can be seen after testing.

Antimicrobial activity test by well diffusion method

Mueller Hinton Agar (MHA) was prepared by weighing 38 g of MHA powder and dissolving it in 1 L of distilled water onto a petri dish. The infection *S. mutans* adjusted to 0.5 McFarland turbidity was dropped onto MHA culture medium and spread all over the plate. Then, a hole was made in the culture medium and green tea toothpaste tablets (green tea leaf extract and green tea powder) were placed into the prepared wells. The toothpaste tablets, along with the control well (ampicillin), were incubated at 37 °C for 18-24 h.[10] *S. mutans* sensitive to green tea toothpaste tablets and antibiotics will not grow around that hole. It will appear in the form of a clear circle around the hole, known as a zone of inhibition. Lastly, the size of the zone of inhibition (mm) were recorded and the average size and the standard deviation were calculated.

Statistical data analysis

Results are expressed as the mean ± standard deviation of three experiments, each experiment was repeated 3 times. Differences in the data sets were analyzed for variance (Analysis of Variance) using one way ANOVA and the average from data obtained from several sample groups which was a comparison of differences from 3 or more groups were analyzed by the Tukey method at the significance level ($P \leq 0.05$) using Minitab version 18.

Results

Comparison of extraction efficiency

The extraction of 10 g of dried green tea leaves (**Figure 1A**) began by boiling water for 10 min and then evaporating dried green tea leaves with a rotary evaporator at 62-65 °C. The next step was freeze-drying it to get the weight and %yield (**Table 1**) In this research, green tea powder (**Figure 1B**) was used in the testing, forming, and pressing of tablets in a form that did not involve extraction, so there was no %yield in this experiment.

Biological activity testing of the green tea leaf extract and green tea powder

From the test of the biological activity of green tea, it was found that green tea leaves that were water-extracted and green tea powder had differences in total phenolic content, total flavonoid content, and DPPH antioxidant activity. The green tea leaf extract was higher in phenolic content and DPPH antioxidant activity than green tea powder. As for the flavonoid test results, green tea powder had better results than green tea leaf extract (**Table 2**). The amount of total phenolic compounds was calculated from the straight-line equation of the standard graph of gallic acid solution (**Figure 2**) and the amount of total flavonoid compounds was calculated from the straight-line equation of the standard graph of quercetin solution (**Figure 3**).

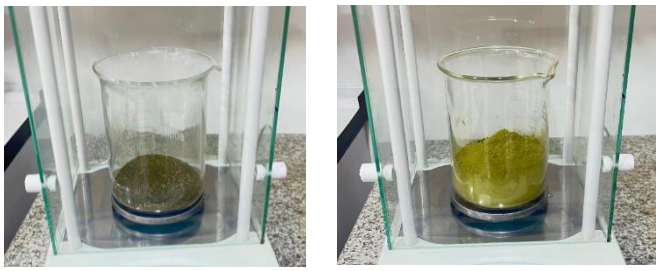

(A) (B)

Figure 1. Green tea. (A) Finely ground dried green tea leaves (B) Green tea powder.

Table 1. %Yield of green tea leaf extract and green tea powder.

Sample	Green tea	Dry weight of medicinal plants (g)	Weight of extract (g)	%Yield
1	Dried green tea leaves	10	2.64	26.4
2			2.66	26.2
3			1.37	13.7
1	Green tea powder	Not extracted	Not extracted	-

%Yield = (weight of extract / dry weight of medicinal plants) × 100

Table 2. Biological activity testing of green tea leaf extract and green tea powder.

Biological activity test	Dried green tea leaves	Green tea powder
Total phenolic content (mg GAE/g extract)	73.14 ± 5.96^{A}	48.14 ± 0.93^{B}
Total flavonoid content (mg QE/g extract)	6.98 ± 0.80^{B}	19.453 ± 4.06^{A}
DPPH scavenging activity (IC_{50}; mg/mL extract)	20.33 ± 1.33^{B}	44.53 ± 4.51^{A}

Data was expressed as mean±SD. Different letters indicate a statistically significant difference between green tea leaf extract and green tea powder ($P<0.05$).

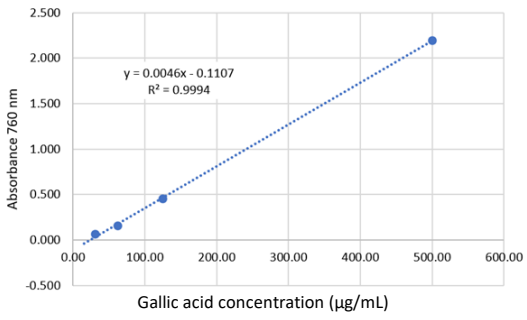

Figure 2. The standard graph of gallic acid solution to quantify total phenolic compounds of green tea extract and green tea powder.

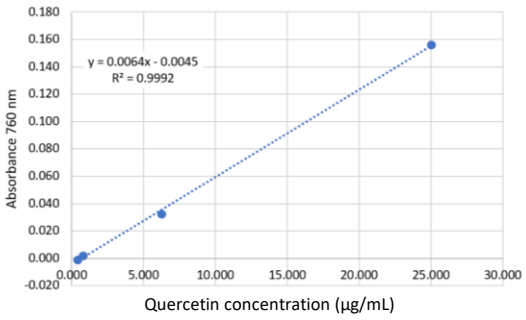

Figure 3. The standard graph of quercetin solution to quantify total flavonoid compounds of green tea extract and green tea powder.

Physical testing of toothpaste tablets

The physical testing of green tea compressed toothpaste tablets revealed that both green tea leaf extract formulation and green tea powder could be formed into pellets. These pellets had a round shape (**Figure 4**) and sweet taste, with a friability value of less than 1%, a moisture content ranging from 4% to 6%, and a weight of 250 mg per tablet. Additionally, they also exhibited a hardness value in the range of 20-30 N. The average tablet thickness and diameter are 4.01 mm and 9.57±0.01 mm, respectively. Green tea leaf tablets were brownish yellow and had a disintegration time of 23.75±3.14 min, while green tea powder tablets have a light green color and a disintegration time of 17.11±1.04 min (**Table 3**).

(A) (B)

Figure 4. Toothpaste tablets formulated with (A) green tea leaf extract and (B) green tea powder.

Table 3. Physical test results of green tea compressed toothpaste tablets.

Physical test	Green tea leaf extract	Green tea powder
Appearance	Round	Round
Odor	Green tea	Peppermint Oil
Color of pills	Yellow brown	Light green
Moisture (%)	5.31	5.89
Weight variation (g)	249.31±2.95	249.79±3.16
Hardness (N)	27±2.39	27±1.90
Thickness (mm)	4.01±0.05	4.01±0.03
Diameter (mm)	9.57±0.01	9.58±0.01
Friability (%)	0.278	0.551
Disintegration (min)	23.75±3.14	17.11±1.04

Testing cleanliness ability of toothpaste tablets

The results from the test of toothpaste tablet cleanliness ability by observing the scrubbing time and the cleanliness before and after the test demonstrated that both green tea leaf extract and green tea powder could cleanse the eggshells covering with food coloring and vinegar, which were similar to plaque and lactic acid in the mouth (**Figure 5**). Their cleansing abilities were not different, and it required less time to scrub the eggs clean than scrubbing with just water (**Figure 6** and **7**).

Figure 5. Shell eggs before doing the polishing test.

(A) (B)

Figure 6. Eggshells tested with (A) green tea leaf extract toothpaste tablets and (B) green tea powder toothpaste tablets.

Figure 7. Eggshells polished with water.

Antibacterial test against S. mutans

The test against *S. mutans* bacteria using the well diffusion test method revealed that toothpaste tablets formulated with green tea leaf extract tablets are more effective against *S. mutans* than green tea powder toothpaste tablets, but it still had less ability to resist the growth of *S. mutans* bacteria than ampicillin used as a positive control (**Table 4** and **Figure 8**).

Table 4. Antibacterial effect test of green tea compressed toothpaste tablet using well diffusion assay.

Test microbe	Zone of inhibition (mm)			
	Ampicillin (10 µl)*	Toothpaste tablets made from green tea leaf	Ampicillin (10 µl)*	Toothpaste tablets made from green tea powder
S. mutans	11	8.00±0	11	7.33±0.58

Data was expressed as mean±SD. * Positive control.

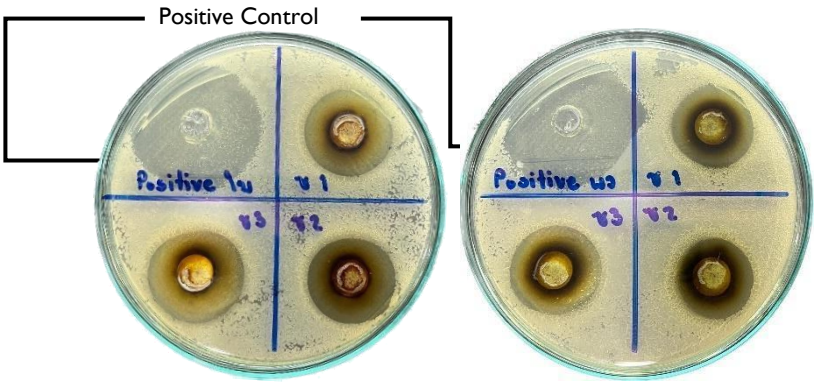

Figure 8. Well diffusion test against *S. mutans* by toothpaste tablets formulated with (A) green tea leaf extract and (B green tea powder.

Discussion

From the test of the biological activity of green tea, it was found that green tea leaves which were extracted with water and green tea powder had differences in total phenolic content, total flavonoid content, and DPPH antioxidant activity. The green tea leaf extract has phenolic content and DPPH antioxidant activity that was higher than green tea powder. As for the flavonoid test, green tea powder had higher results than green tea leaf extract. Consequently, green tea leaf extract was more effective in antioxidants than green tea powder. The reason is that the higher flavonoid content in green tea powder might not enhance the antioxidant effect as much as the phenolic content. This result is consistent with the research of Calderón-Oliver and Ponce-Alquicira.[11] The research pointed out that green tea leaves, which were extracted with hot water and tested for antioxidants using the DPPH assay, were effective in inhibiting DPPH and reducing free radicals. The antioxidant DPPH of green tea comes from both phenolics and flavonoids, but mostly found in the phenolic group. This is because green tea contains more phenolics than flavonoids and the phenolic structure is more suitable for inhibiting DPPH. Phenolics have a benzene ring with a hydroxyl group. They can allow hydrogen atoms to bond better with DPPH compared to flavonoids, which also have benzene rings but fewer hydroxyl groups. The extraction of green tea leaves in this research used hot water as a solvent. This solvent can extract phenolic compounds and flavonoids from the green tea leaves better compared to unextracted green tea powder.

However, in this experiment, the green tea powder had a higher flavonoid content. This is due to several factors. The first one is the size of the particles. In this experiment, green tea powder came in a very fine powder form, while the green tea leaves had to be frozen dry and ground into powder. Therefore, the particle size of green tea powder is smaller than the extracted green tea leaves, which helps flavonoids dissolve in water more easily. The next factor is that some flavonoids are heat tolerant and can dissolve in normal temperature water, so it can be explained that some flavonoids in green tea leaf extract and green tea powder may be more soluble in water with normal temperature than hot water. Hence, the green tea powder which was not extracted using hot water has a higher flavonoid content. In addition, the reason green tea powder has lower phenolic content and less effect against DPPH might be because it has not gone through the extraction process, so the phenolic antioxidants in green tea powder have not yet been extracted. As a result, the green tea leaf extract has a better effect against DPPH and higher phenolic content. The green tea leaf extract had a half maximal inhibitory concentration (IC_{50}) of 20.33±1.33 mg/mL and green tea powder had an IC_{50} value of 44.53±4.51 mg/mL. Compared to a standard substance, ascorbic acid has an IC_{50} value of 40.11±2.60 mg/mL. The green tea leaf extract with water has a better antioxidant effect against DPPH than green tea powder. Furthermore, studies have shown that antioxidant activity helps fight inflammation of the gums that can cause tooth decay.

From physical testing of green tea toothpaste tablets, it was found that both green tea leaf extract formulas and green tea powder can be formed into compressed toothpaste tablets, which have a round shape, a sweet taste, a friability value of less than 1%, a moisture content in the range of 4-6%, and a weight of 250 mg per tablet. Moreover, the hardness of the tablets is in the range of 20-30 N. The average tablet thickness and diameter are 4.01 mm and 9.57±0.01 mm, respectively. Green tea leaf tablets are brownish yellow and have a disintegration time of 23.75±3.14 min, while green tea powder tablets with a light green color have a disintegration time of 17.11±1.04 min. Therefore, the result indicated that both green tea leaf extract and the green tea powder used in this study can be developed into usable toothpaste tablets.

From the test of cleaning ability, both green tea leaf extract and green tea powder toothpaste tablets could clean eggshells covered in food coloring and vinegar, which simulated plaque and lactic acid in oral activity. By observing the results from the amount of scrubbing time (5-10) and the cleanliness before and after the test, the results of the experiment showed that toothpaste tablets formulated with green tea leaf extract and green tea powder can cleanse no differently and take less time to scrub clean than when using only water. In conclusion, toothpaste tablets formulated with both green tea leaf extract and green tea powder are efficient in cleaning the oral cavity.

From the results of antibacterial testing *S. mutans* by well diffusion test method, it was found that toothpaste tablets formulated with green tea leaf extract have antibacterial properties that work better against *S. mutans* than green tea powder toothpaste tablets, according to the zone of inhibition that occurred in the test. Toothpaste tablets formulated with green tea leaf extract had an effective zone of inhibition of 8.00±0 mm while toothpaste tablets formulated with green tea powder had an effective zone of inhibition of 7.33±0.58 mm. However, the toothpaste tablets formulated with green tea leaf extract still have less ability to resist the growth of *S. mutans* bacteria than ampicillin used as a positive control, which has a zone of inhibition of 11±0 mm. This is consistent with the research of Somboon and Bunyongsanchai[12] who studied the inhibition of germ (*S. mutans)* growth in tea leaves which were extracted with water at 90 °C at different times. The researchers found that the tea leaf extracts had antimicrobial properties against *S. mutans.* Additionally, the tea leaf

extracts that were obtained from the 15-min extraction process can inhibit the growth of *S. mutans* the most effectively.

Conclusion

This research aimed to examine the antioxidant activity and bacterial inhibition of Assam green tea (*Camellia sinensis* var. assamica) in the form of green tea leaf extract and instant green tea powder and to develop a toothpaste tablet formula that contains fluoride as an ingredient. The study found that green tea leaf extract and green tea powder are effective in cleaning the oral cavity. Both can be molded into toothpaste tablets efficiently and have the effect of inhibiting the bacteria *S. mutans.*

Acknowledgement

The researcher would like to express gratitude to the Faculty of Pharmaceutical Sciences, Faculty of Science, and Green natural health product company for providing research funding.

References

1. Krisdapong S. Spit don't rinse. JHS. 2017;26(2):348-59.
2. Samphanwetsopha S, Winayayong P, Panyamunwongsa P. The study of characteristics of Chiang Rai tea. [Internet]. Chiang Rai: Mae Fah Luang University; 2003 [cited 2023 Dec 14]. Available from: https://archives. mfu.ac.th/database/files/original/bc39 7f5d9365deae482d5fc5d8d2c13e.pdf
3. Kulrath P, Duangdee N, Supornpun N, Prateeptongkum E. Comparison of fluoride and catechin levels in green tea extract at various geographical locations in Thailand. J DMS. 2019;44(2):114-120.
4. Wongsa P, Rungruang N, Soiraya Y, Donlao N. Effect of drying method on tea extract from Assam green tea. [Internet]. Chiang Rai: Mae Fah Luang University; 2007 [cited 2023 Dec 14]. Available from: https://archives. mfu.ac.th/database /files/original/4f1a0962ba83eb9429a19b246f153bcc.pdf
5. Donlao N, Thepkorn T. Spray-drying optimization of pilot scale green tea extract. [Internet]. Chiang Rai: Mae Fah Luang University; 2011 [cited 2023 Dec 20]. Available from: https://archives.mfu.ac.th/database/ files/original/94cdb 6e5453d1f1673d7d504054b8986.pdf
6. Denchai R, Phaiboon N, Pornsiri N, Rattana S. Antioxidant activities, total phenolic and total flavonoid contents of *Lepisanthes rubiginosa* crude extract. Koch Cha Sarn. 2021;43(2):1-9.
7. Sanwiriyamongkol P, Srisuk P. Determination of phenolic compounds, proteins and antioxidant activity in rice water fraction extracted from Phayaleumkang glutinous rice. Isan J Pharm Sci. 2021;17(1):68-79.
8. Panngam A, Rattana S, Sangthong B. Antioxidant effect, phenolic content and flavonoids in guava takhop extract. J Sci Technol MSU. 2017;13:51-53.
9. Arpatangtakul C, Laohakulvivat N, Deedamrong A. Development of herbal toothtablet and evaluation of herbal toothtablet satisfaction in volunteers. [Undergraduate thesis]. Chonburi: Burapha University; 2019.
10. Hudzicki J. Kirby-Bauer disk diffusion susceptibility test protocol. ASM. 2009;15(1):1-23.
11. Calderón-Oliver M, Ponce-Alquicira E. Environmentally friendly techniques and their comparison in the extraction of natural antioxidants from green tea, rosemary, clove, and oregano. Molecules. 2021 Mar 26; 26(7):1869.
12. Somboonsin P, Boonyongsunchai P. Development of tea extract oral film for the inhibition of *Streptococcus mutans* causing the unpleasant mouth odor. [[Undergraduate thesis on the internet]. Bangkok: Mahidol University; 2011 [cited 2023 Dec 14]. Available from: https://pharmacy.mahidol.ac.th/TH/service-research-special-abstract.php?num=10&year =2554

คำสั่งสมาคมเภสัชวิทยาแห่งประเทศไทย

เรื่อง แต่งตั้งคณะกรรมการจัดการประชุมวิชาการประจำปีสมาคมเภสัชวิทยาแห่งประเทศ

ครั้งที่ 45 ปี พ.ศ. 2567

สมาคมเภสัชวิทยาแห่งประเทศไทยร่วมกับภาควิชาเภสัชวิทยา คณะแพทยศาสตร์ศิริราชพยาบาล มหาวิทยาลัยมหิดล เป็นเจ้าภาพในการจัดประชุมวิชาการประจำปีสมาคมเภสัชวิทยาแห่งประเทศไทย ครั้งที่ 45 ในหัวข้อ Bridging the Gap: Innovations and Translations in Pharmacology ระหว่างวันที่ 15-17 พฤษภาคม 2567 ณ โรงแรมแมนดาริน กรุงเทพ เพื่อให้การดำเนินงานการจัดประชุมดำเนินการไปด้วยดี จึงขอแต่งตั้งผู้มีรายนามดังต่อไปนี้เป็นคณะกรรมการจัดประชุมวิชาการประจำปีสมาคมเภสัชวิทยาแห่งประเทศไทย ครั้งที่ 45 ปี พ.ศ. 2567

คณะกรรมการที่ปรึกษา

1. ศ.เกียรติคุณ นพ.บุญเจือ ธรณินทร์
2. ดร.อุดม จันทรารักษ์ศรี
3. รศ.ดร.ภญ.จุฑามาศ สัตยวิวัฒน์
4. รศ.ดร.ภญ.อรพรรณ มาตังคสมบัติ
5. รศ.ดร.ภก.ชัยชาญ แสงดี
6. รศ.ดร.พรเพ็ญ เปรมโยธิน
7. รศ.พญ.สุมนา ชมพูทวีป
8. พล.ต.รศ.ดร.บพิตร กลางกัลยา
9. รศ.ดร.ภญ.ศรีจันทร์ พรจิราศิลป์
10. รศ.ดร.ภญ.จินตนา สัตยาศัย
11. รศ.ดร.ภญ.มยุรี ตันติสิระ
12. รศ.ดร.ภญ.สุพัตรา ศรีไชยรัตน์
13. ศ.ดร.เกศรา ณ บางช้าง
14. รศ.นพ.สุพรชัย กองพัฒนากูล
15. รศ.จันทนี อิทธิพานิชพงศ์

<u>หน้าที่</u>

ให้คำปรึกษาและสนับสนุนการดำเนินงานของคณะกรรมการดำเนินงานฝ่ายต่าง ๆ ให้สามารถจัดการประชุมวิชาการประจำปีสมาคมเภสัชวิทยาแห่งประเทศไทย ครั้งที่ 45 ปี พ.ศ. 2567 เป็นไปด้วยความเรียบร้อย

คณะกรรมการฝ่ายอำนวยการจัดการประชุม

1. ศ.ดร.พญ.อุไรวรรณ	พานิช	ประธาน
2. รศ.ดร.ภญ.รัตติมา	จีนาพงษา	กรรมการ
3. รศ.ดร.ภก.ศิวนนท์	จิรวัฒโนทัย	กรรมการ

4. รศ.พญ.สมฤดี	ฉัตรสิริเจริญกุล	กรรมการ
5. ผศ.ดร.สมพลนาท	สัมปัตตะวนิช	กรรมการ
6. ผศ.ดร.พญ.สุวิมล	นิยมในธรรม	กรรมการและเลขานุการ
7. อ.ดร.พญ.วีรวรรณ	ตั้งบุญจิตร	ผู้ช่วยเลขานุการ

หน้าที่

1. ดำเนินการจัดประชุมวิชาการประจำปีสมาคมเภสัชวิทยาแห่งประเทศไทย ครั้งที่ 45 ปี พ.ศ. 2567 ให้เป็นไปด้วยความเรียบร้อยและบรรลุวัตถุประสงค์
2. ดูแลเรื่องเอกสารการดำเนินงานโครงการ อาทิ หนังสือขออนุมัติไม่เป็นวันลาและเบิกค่าลงทะเบียนการขอหน่วยกิตศึกษาต่อเนื่อง
3. ประสานงานการดำเนินการด้านต่าง ๆ ให้เป็นไปด้วยความเรียบร้อย
4. สรุปโครงการหลังเสร็จสิ้นการจัดงาน

คณะกรรมการฝ่ายวิชาการ

1. รศ.ดร.ภก.ศิวนนท์	จิรวัฒโนทัย	ประธาน
2. ศ.ดร.พญ.อุไรวรรณ	พานิช	กรรมการ
3. รศ.ดร.นพ.อดิศักดิ์	วงศ์ขจรศิลป์	กรรมการ
4. รศ.ดร.นพ.ประวิทย์	อัครเสรีนนท์	กรรมการ
5. รศ.พญ.สมฤดี	ฉัตรสิริเจริญกุล	กรรมการ
6. ผศ.ดร.นพ.กิติพงศ์	สุนทราภา	กรรมการ
7. ผศ.ดร.พญ.พินภัทร	ไตรภัทร	กรรมการ
8. ผศ.ดร.สมพลนาท	สัมปัตตะวนิช	กรรมการ
9. ผศ.นพ.วีระเทพ	ฉัตรธนโชติกุล	กรรมการ
10. ผศ.พญ.พิณพิไล	จูทะสมพากร	กรรมการ
11. ผศ.ดร.พญ.สุวิมล	นิยมในธรรม	กรรมการ
12. อ.ดร.พญ.วีรวรรณ	ตั้งบุญจิตร	กรรมการและเลขานุการ
13. นายเอกลักษณ์	ไม้หอม	ผู้ช่วยเลขานุการ

หน้าที่

1. วางแผน จัดทำกำหนดการและหัวข้อการประชุม
2. ประสานงานเชิญวิทยากร
3. รวบรวมประวัติวิทยากรและเอกสารประกอบการบรรยาย

คณะกรรมการฝ่ายลงทะเบียน

1. ผศ.พญ.พิณพิไล	จูทะสมพากร	ประธาน
2. ผศ.ภญ.อรรัตน์	โลหิตนาวี	กรรมการ
3. ผศ.ดร.ภญ.สกลวรรณ	ประพฤติบัติ	กรรมการ
4. นางสาวณัฐนันท์	เขมามุตตานาค	กรรมการ
5. นางเสนอ	สุขเอี่ยม	กรรมการ
6. อ.ดร.พญ.วีรวรรณ	ตั้งบุญจิตร	กรรมการและเลขานุการ
7. นางสาวบุญยานุช	อ่อนวิมล	ผู้ช่วยเลขานุการ

หน้าที่

1. จัดทำระบบสำหรับการลงทะเบียน และชำระค่าลงทะเบียน

2. เปิดบัญชีออมทรัพย์เพื่อรับเงินค่าลงทะเบียนเข้าร่วมวิชาการ
3. จัดทำและดูแลการลงทะเบียนงานประชุม
4. จัดทำรายชื่อสำหรับผู้ลงทะเบียนเข้าร่วมประชุม
5. จัดเตรียมใบเสร็จรับเงิน เอกสารเกี่ยวกับการเบิกจ่ายตามระเบียบให้ผู้ลงทะเบียน

คณะกรรมการฝ่ายประชาสัมพันธ์ และเทคโนโลยีสารสนเทศ (ไอที)

1.	ผศ.ดร.สมพลนาท	สัมปัตตะวนิช	ประธาน
2.	อ.นพ.เมธา	ใหญ่กว่าวงศ์	กรรมการ
3.	นายต้นปี	ศิริพันธ์บุญ	กรรมการ
4.	ผศ.ดร.พญ.สุวิมล	นิยมในธรรม	กรรมการและเลขานุการ
5.	นางสาวพิศาลศรี	กระต่ายทอง	ผู้ช่วยเลขานุการ

<u>หน้าที่</u>

1. จัดทำเอกสาร สื่อ สิ่งพิมพ์ วีดีทัศน์ เพื่อประชาสัมพันธ์โครงการประชุมฯ และดูแลการเผยแพร่ประชาสัมพันธ์ผ่านสื่อออนไลน์ และหน่วยงานต่าง ๆ
2. ดำเนินการด้านบันทึกภาพนิ่ง ภาพเคลื่อนไหว ในกิจกรรมต่าง ๆ ของการจัดประชุม

คณะกรรมการจัดทำวีดีทัศน์ชีวประวัติ ศาสตราจารย์ นายแพทย์อวย เกตุสิงห์ และ รศ.ดร. จิรวัฒก์ สดาวงศ์วิวัฒน์

1.	ศ.ดร.พญ.อุไรวรรณ	พานิช	ประธาน
2.	รศ.ดร.พญ.กาญจนา	เกษสอาด	กรรมการ
3.	รศ.ดร.ภญ.รัตติมา	จีนาพงษา	กรรมการ
4.	นศพ.ปราบ	ศิริวัฒนอักษร	กรรมการ
5.	สถานเทคโนโลยีการศึกษาแพทยศาสตร์		กรรมการ
6.	นพ.วรากร	เวชเจริญยิ่ง	กรรมการ
7.	นายต้นปี	ศิริพันธ์บุญ	กรรมการ
8.	นางเสนอ	สุขเอี่ยม	กรรมการและเลขานุการ
9.	นางสาวธารารัตน์	เหลือธนานนท์	ผู้ช่วยเลขานุการ

<u>หน้าที่</u>

1. ดำเนินการด้านบันทึกภาพนิ่ง ภาพเคลื่อนไหว ชีวประวัติของ ศาสตราจารย์ นายแพทย์อวย เกตุสิงห์ และ รศ.ดร.จิรวัฒก์ สดาวงศ์วิวัฒน์
2. ดำเนินการบันทึกเสียงวีดีทัศน์ ชีวประวัติของ ศาสตราจารย์ นายแพทย์อวย เกตุสิงห์ และ รศ.ดร.จิรวัฒก์ สดาวงศ์วิวัฒน์

คณะกรรมการฝ่ายต้อนรับ พิธีการ สันทนาการ และกิจกรรม

1.	ผศ.พญ.วีรวดี	จันทรนิภาพงศ์	ประธาน
2.	ผศ.ดร.พญ.สุวิมล	นิยมในธรรม	กรรมการ
3.	นางเสนอ	สุขเอี่ยม	กรรมการ
4.	นางสาวดวงพร	กฤตพิชญ์นันท์	กรรมการและเลขานุการ
5.	นางสาวฐิตาภา	บริพันธ์	ผู้ช่วยเลขานุการ

<u>หน้าที่</u>

1. จัดเตรียมคำกล่าวต้อนรับ คำกล่าวเปิดและปิดงาน คำกล่าวแนะนำวิทยากร
2. จัดเตรียมพิธีกร และผู้ดำเนินรายการในกิจกรรมต่าง ๆ ของการประชุม
3. ดำเนินการต้อนรับและอำนวยความสะดวกแก่วิทยากร
4. ดำเนินการด้านพิธีการต่าง ๆ อาทิ พิธีเปิดและปิดโครงการ การมอบรางวัล รวมถึงกิจกรรมระหว่างการประชุม
5. กำกับดูให้การดำเนินการด้านพิธีการและกิจกรรมการประชุมเป็นไปตามกำหนดการ

คณะกรรมการฝ่ายการเงินและจัดหารายได้

1. รศ.พญ.สมฤดี	ฉัตรสิริเจริญกุล	ประธาน
2. ศ.ดร.พญ.อุไรวรรณ	พานิช	กรรมการ
3. รศ.ดร.ภก.ศิวนนท์	จิรวัฒโนทัย	กรรมการ
4. ผศ.ดร.พญ.สุวิมล	นิยมในธรรม	กรรมการ
5. ผศ.ดร.นพ.กิติพงศ์	สุนทราภา	กรรมการ
6. ผศ.พญ.พิณพิไล	จูทะสมพากร	กรรมการ
7. ผศ.ดร.สมพลนาท	สัมปัตตะวนิช	กรรมการและเลขานุการ
8. นางสาวพิศาลศรี	กระต่ายทอง	ผู้ช่วยเลขานุการ

<u>หน้าที่</u>

1. กำหนดรูปแบบและเงื่อนไขในการสนับสนุนการประชุม
2. ประสานงานและติดตามการจัดหารายได้และเงินสนับสนุนการประชุม การจัดทำใบเสร็จและบัญชีงบประมาณสนับสนุนที่ได้รับ
3. ประสานงานฝ่ายต่าง ๆ ในการดูแลกิจกรรมของผู้สนับสนุนการประชุมให้เป็นไปด้วยความเรียบร้อย
4. ดูแลเรื่องการยืมเงิน การเบิก-จ่าย เก็บรวบรวม ตรวจสอบและจัดทำเอกสารประกอบการเบิกจ่ายของโครงการ
5. จัดหาของที่ระลึกสำหรับวิทยากร
6. ทำรายงานสรุปค่าใช้จ่ายโครงการ

คณะกรรมการฝ่ายสถานที่ และโสตทัศนูปกรณ์

1. ผศ.ดร.พญ.สุวิมล	นิยมในธรรม	ประธาน
2. ศ.ดร.พญ.อุไรวรรณ	พานิช	กรรมการ
3. ผศ.ดร.สมพลนาท	สัมปัตตะวนิช	กรรมการ
4. นายสนอง	แพใหญ่	กรรมการ
5. นางสมา	วงศ์แก้วนาวา	กรรมการ
6. นางสาวม่านนภา	สิมมา	กรรมการ
7. นางสาวพิศาลศรี	กระต่ายทอง	กรรมการและเลขานุการ
8. นายปิยะชาติ	ทองสวัสดิ์	ผู้ช่วยเลขานุการ

<u>หน้าที่</u>

1. ดำเนินการด้านการจองโรงแรม อาหารและของว่าง สถานที่จัดประชุม ที่พักวิทยากร และส่วนลดห้องพักผู้เข้าร่วมประชุม
2. ดำเนินการเรื่องสถานที่ เวที สำหรับวิทยากร พื้นที่และบอร์ดการนำเสนอผลงานรูปแบบโปสเตอร์ ตลอดจนพื้นที่ของผู้สนับสนุนการประชุมสำหรับแสดงสินค้าผลิตภัณฑ์

3. ดำเนินการเรื่องการจัดการทำป้ายชื่อและฉากหลังการประชุม ป้ายชื่อวิทยากรบนเวทีการประชุม
4. กำกับดูแลด้านฝ่ายโสตฯ จัดเตรียมอุปกรณ์คอมพิวเตอร์ เครื่องพิมพ์ อุปกรณ์เครื่องเสียง และการเชื่อมต่อระบบออนไลน์ในการประชุม

คณะกรรมการฝ่ายเอกสารสิ่งพิมพ์ ประเมินผลและรางวัล

1. รศ.ดร.ภก.ศิวนนท์	จิรวัฒโนทัย	ประธาน
2. ศ.ดร.พญ.อุไรวรรณ	พานิช	กรรมการ
3. รศ.ดร.ภญ.รัตติมา	จีนาพงษา	กรรมการ
4. ผศ.ดร.พญ.สุวิมล	นิยมในธรรม	กรรมการ
5. อ.ดร.พญ.วีรวรรณ	ตั้งบุญจิตร	กรรมการ
6. รศ.ดร.ภญ.นันทีทิพ	ลิ้มเพียรชอบ	กรรมการ
7. ผศ.ดร.ภญ.สกลวรรณ	ประพฤติบัติ	กรรมการ
8. ผศ.ดร.ภญ.จันทิมา	เมทนีธร	กรรมการ
9. ผศ.ภญ.อรรัตน์	โลหิตนาวี	กรรมการ

<u>หน้าที่</u>

1. รวบรวมบทคัดย่อ และบทความของผู้เข้าร่วมงาน และจัดทำรูปแบบ E-Book และทำ QR code สำหรับรูปเล่ม
2. ดำเนินการจัดทำรูปเล่ม Proceeding
3. ประสานงานกับฝ่ายวิชาการในการขอสไลด์จากวิทยากรจัดทำ QR code สำหรับเอกสารประกอบการประชุม
4. กำหนดรูปแบบการประกวดผลงานเพื่อรับรางวัล กำหนดเกณฑ์การตัดสินผลการนำเสนอผลงานและดำเนินการด้านการตัดสินผลงาน
5. ติดต่อผู้ทรงคุณวุฒิในการประเมินบทความ บทคัดย่อ ตลอดจนการประกวดผลงานนำเสนอในการประชุมเพื่อรับรางวัล
6. ออกแบบและจัดทำใบประเมินบทความ บทคัดย่อ ตลอดจนการประกวดผลงานนำเสนอในการประชุมเพื่อรับรางวัล
7. รวบรวมผลการตัดสินและประสานกับฝ่ายต่าง ๆ ในการจัดทำเกียรติบัตรและรางวัล

ทั้งนี้ ตั้งแต่บัดนี้เป็นต้นไป จนถึง วันที่ 30 มิถุนายน 2567

สั่ง ณ วันที่ 28 ธันวาคม พ.ศ. 2566

ศาสตราจารย์ ดร.เกศรา ณ บางช้าง
นายกสมาคมเภสัชวิทยาแห่งประเทศไทย

คำสั่งสมาคมเภสัชวิทยาแห่งประเทศไทย

เรื่อง แต่งตั้งคณะกรรมการจัดการประชุมวิชาการประจำปีสมาคมเภสัชวิทยาแห่งประเทศไทย ครั้งที่ 45

พ.ศ. 2567 (เพิ่มเติม)

ด้วยสมาคมเภสัชวิทยาแห่งประเทศไทยร่วมกับภาควิชาเภสัชวิทยา คณะแพทยศาสตร์ศิริราชพยาบาล มหาวิทยาลัยมหิดล เป็นเจ้าภาพในการจัดประชุมวิชาการประจำปีสมาคมเภสัชวิทยาแห่งประเทศไทย ครั้งที่ 45 ในหัวข้อ “Bridging the Gap: Innovations and Translations in Pharmacology” ระหว่างวันที่ 15-17 พฤษภาคม 2567 ณ โรงแรมแมนดาริน กรุงเทพ เพื่อให้การดำเนินงานการจัดประชุมดำเนินการไปด้วยดี จึงขอแต่งตั้งผู้มีรายนามดังต่อไปนี้เป็นคณะกรรมการจัดประชุมวิชาการประจำปีสมาคมเภสัชวิทยาแห่งประเทศไทย ครั้งที่ 45 ปี พ.ศ. 2567

คณะกรรมการผู้ทรงคุณวุฒิพิจารณาผลงานวิชาการ

1. ศ. ดร. ภญ.จินตนา สัตยาศัย คณะแพทยศาสตร์ มหาวิทยาลัยขอนแก่น
2. ศ. ดร. ภญ.วิจิตรา ทัศนียกุล คณะแพทยศาสตร์ มหาวิทยาลัยขอนแก่น
3. ศ. ดร. ภก.วีรพล คู่คงวิริยพันธุ์ คณะแพทยศาสตร์ มหาวิทยาลัยขอนแก่น
4. รศ. ดร. ภญ.ลัดดาวัลย์ เส็งกันไพร คณะแพทยศาสตร์ มหาวิทยาลัยขอนแก่น
5. ผศ. ดร. ภญ.นนทญา นาคคำ คณะแพทยศาสตร์ มหาวิทยาลัยขอนแก่น
6. ผศ. ดร. พญ.ปาจรีย์ ลิลิตการตกุล คณะแพทยศาสตร์ จุฬาลงกรณ์มหาวิทยาลัย
7. ผศ. ดร.วัชรี ลิมปนสิทธิกุล คณะแพทยศาสตร์ จุฬาลงกรณ์มหาวิทยาลัย
8. รศ. ดร.ปิยนุช วงศ์อนันต์ คณะแพทยศาสตร์ จุฬาลงกรณ์มหาวิทยาลัย
9. รศ. ดร. พญ.วรรณรัศมี เกตุชาติ คณะแพทยศาสตร์ จุฬาลงกรณ์มหาวิทยาลัย
10. รศ. ดร. สพญ.สุพัตรา ศรีไชยรัตน์ คณะแพทยศาสตร์ จุฬาลงกรณ์มหาวิทยาลัย
11. ดร.ปฏิภาค เขื่อนจินดา คณะแพทยศาสตร์ จุฬาลงกรณ์มหาวิทยาลัย
12. ศ. ดร. ภก.ปิติ จันทร์วรโชติ คณะเภสัชศาสตร์ จุฬาลงกรณ์มหาวิทยาลัย

13. รศ. ดร.วรรณา ชัยเจริญกุล	วิทยาลัยแพทยศาสตร์นานาชาติจุฬาภรณ์ มหาวิทยาธรรมศาสตร์
14. ผศ. ดร.นายแพทย์ สุกิจ รุ่งอภินันท์	คณะแพทยศาสตร์ มหาวิทยาลัยเชียงใหม่
15. รศ. ดร.วุฒิไกร นิ่มละมูล	คณะแพทยศาสตร์ มหาวิทยาลัยเชียงใหม่
16. รศ. ดร.ณัฏฐกานต์ จิรัณธนัฐ	คณะแพทยศาสตร์ มหาวิทยาลัยเชียงใหม่
17. รศ. ดร. ภญ.รัตติมา จีนาพงษา	คณะเภสัชศาสตร์ มหาวิทยาลัยนเรศวร
18. รศ. ดร. ภก.มนุพัศ โลหิตนาวี	คณะเภสัชศาสตร์ มหาวิทยาลัยนเรศวร
19. รศ. ดร. ภญ.นันทีทิพ ลิ้มเพียรชอบ	คณะเภสัชศาสตร์ มหาวิทยาลัยนเรศวร
20. ผศ. ดร. ภก.ณัถวุฒิ แซ่ลิ้ม	คณะเภสัชศาสตร์ มหาวิทยาลัยนเรศวร
21. ผศ. ดร. ภก.ศราวุฒิ อู่พุฒินันท์	คณะเภสัชศาสตร์ มหาวิทยาลัยนเรศวร
22. ผศ. ดร. ภญ.ภัควดี เสริมสรรพสุข	คณะเภสัชศาสตร์ มหาวิทยาลัยนเรศวร
23. ผศ. ภญ.อรรัตน์ โลหิตนาวี	คณะเภสัชศาสตร์ มหาวิทยาลัยนเรศวร
24. ผศ. ดร. ภญ.สกลวรรณ ประพฤติบัติ	คณะเภสัชศาสตร์ มหาวิทยาลัยนเรศวร
25. ศ. เกียรติคุณบุญเจือ ธรณินทร์	คณะแพทยศาสตร์ศิริราชพยาบาล มหาวิทยาลัยมหิดล
26. รศ. ดร. นพ.อดิศักดิ์ วงศ์ขจรศิลป์	คณะแพทยศาสตร์ศิริราชพยาบาล มหาวิทยาลัยมหิดล
27. ศ. ดร. พญ.อุไรวรรณ พานิช	คณะแพทยศาสตร์ศิริราชพยาบาล มหาวิทยาลัยมหิดล
28. รศ. ดร. ภก.ศิวนนท์ จิรวัฒโนทัย	คณะแพทยศาสตร์ศิริราชพยาบาล มหาวิทยาลัยมหิดล
29. ผศ. พญ.วีรวดี จันทรนิภาพงศ์	คณะแพทยศาสตร์ศิริราชพยาบาล มหาวิทยาลัยมหิดล
30. ผศ. ดร. พญ.พินภัทร ไตรภัทร	คณะแพทยศาสตร์ศิริราชพยาบาล มหาวิทยาลัยมหิดล
31. ผศ. นพ.วีระเทพ ฉัตรธนโชติกุล	คณะแพทยศาสตร์ศิริราชพยาบาล มหาวิทยาลัยมหิดล
32. อ. ดร. พญ.วีรวรรณ ตั้งบุญจิตร	คณะแพทยศาสตร์ศิริราชพยาบาล มหาวิทยาลัยมหิดล
33. อ. นพ.เมธา ใหญ่กว่าวงศ์	คณะแพทยศาสตร์ศิริราชพยาบาล มหาวิทยาลัยมหิดล
34. ผศ. ดร. พญ.สุวิมล นิยมในธรรม	คณะแพทยศาสตร์ศิริราชพยาบาล มหาวิทยาลัยมหิดล
35. ผศ. ดร.สมพลนาท สัมปัตตะวนิช	คณะแพทยศาสตร์ศิริราชพยาบาล มหาวิทยาลัยมหิดล
36. ผศ. ดร.สุพัตรา ลิ่มสุวรรณโชติ	คณะวิทยาศาสตร์ มหาวิทยาลัยสงขลานครินทร์

หน้าที่

เป็นคณะกรรมการพิจารณาผลงานวิชาการ นำเสนอผลงาน ในการประชุมวิชาการประจำปีสมาคมเภสัชวิทยาแห่งประเทศไทย ครั้งที่ 45 พ.ศ. 2567

คณะกรรมการตัดสินการนำเสนอผลงาน

1. ผศ. ดร. ภญ.นนทญา นาคคำ	คณะแพทยศาสตร์ มหาวิทยาลัยขอนแก่น
2. รศ. ดร. พญ.วรรณรัศมี เกตุชาติ	คณะแพทยศาสตร์ จุฬาลงกรณ์มหาวิทยาลัย
3. รศ. ดร.ปิยนุช วงศ์อนันต์	คณะแพทยศาสตร์ จุฬาลงกรณ์มหาวิทยาลัย
4. รศ. ดร. ภญ.มยุรี ตันติสิระ	คณะเภสัชศาสตร์ จุฬาลงกรณ์มหาวิทยาลัย
5. รศ. ดร. ภญ.สุรีย์ เจียรณ์มงคล	คณะเภสัชศาสตร์ จุฬาลงกรณ์มหาวิทยาลัย
6. ศ. ดร. ภก.ปิติ จันทร์วรโชติ	คณะเภสัชศาสตร์ จุฬาลงกรณ์มหาวิทยาลัย
7. ศ. ดร.เกศรา ณ บางช้าง	วิทยาลัยแพทยศาสตร์นานาชาติจุฬาภรณ์ มหาวิทยาธรรมศาสตร์
8. รศ. ดร.วรรณา ชัยเจริญกุล	วิทยาลัยแพทยศาสตร์นานาชาติจุฬาภรณ์ มหาวิทยาธรรมศาสตร์
9. ผศ. ดร.มยุรี ธาราสุข	วิทยาลัยแพทยศาสตร์นานาชาติจุฬาภรณ์ มหาวิทยาธรรมศาสตร์
10. ผศ. ดร.ตุลยากร เปล่งสุริยการ	วิทยาลัยแพทยศาสตร์นานาชาติจุฬาภรณ์ มหาวิทยาธรรมศาสตร์
11. รศ. ดร. นพ.อดิศักดิ์ วงศ์ขจรศิลป์	คณะแพทยศาสตร์ศิริราชพยาบาล มหาวิทยาลัยมหิดล
12. ผศ. ดร. นพ.กิติพงศ์ สุนทราภา	คณะแพทยศาสตร์ศิริราชพยาบาล มหาวิทยาลัยมหิดล
13. ผศ. พญ.พิณพิไล จูทะสมพากรศ	คณะแพทยศาสตร์ศิริราชพยาบาล มหาวิทยาลัยมหิดล
14. อ. ดร. พญ.วีรวรรณ ตั้งบุญจิตร	คณะแพทยศาสตร์ศิริราชพยาบาล มหาวิทยาลัยมหิดล
15. ผศ. ดร.สมพลนาท สัมปัตตะวนิช	คณะแพทยศาสตร์ศิริราชพยาบาล มหาวิทยาลัยมหิดล
16. รศ. ดร.ภญ.พรพรรณ วิวิธนาภรณ์	คณะแพทยศาสตร์โรงพยาบาลรามาธิบดี มหาวิทยาลัยมหิดล
17. ผศ. ดร. ภญ.สกลวรรณ ประพฤติบัติ	คณะเภสัชศาสตร์ มหาวิทยาลัยนเรศวร

18. ผศ. ดร.วันดี อุดมอักษร คณะวิทยาศาสตร์ มหาวิทยาลัยสงขลานครินทร์

หน้าที่

เป็นคณะกรรมการพิจารณาการตัดสินรางวัลการนำเสนอผลงาน ในการประชุมวิชาการประจำปีสมาคมเภสัชวิทยาแห่งประเทศไทย ครั้งที่ 45 พ.ศ. 2567

ทั้งนี้ ตั้งแต่บัดนี้เป็นต้นไป จนถึง วันที่ 30 มิถุนายน 2567

สั่ง ณ วันที่ 10 พฤษภาคม พ.ศ.2567

ศาสตราจารย์ ดร.เกศรา ณ บางช้าง

นายกสมาคมเภสัชวิทยาแห่งประเทศไทย

รายชื่อผู้สนับสนุนงานประชุม

- RI Technologies Ltd.
- Eppendorf (Thailand) Co., Ltd.
- Gibthai Co., Ltd.
- BioDesign Co., Ltd.
- Bio-Active Co., Ltd.
- Theera Trading Co., Ltd.
- K Agro-Innovate Institute under Kasikornthai Foundation
- Roche Thailand Ltd.
- Prima Scientific Co., Ltd.

Agilent

everlife
RI Technologies

Cell Analysis Division

Microplate Automation & Detection

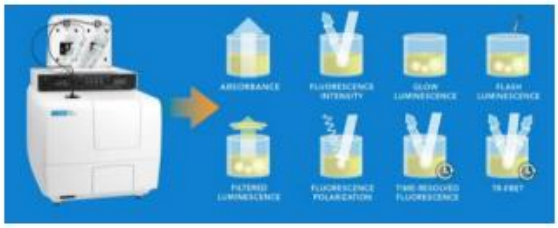

Efficiently handle a wide range of applications

- Microplate readers deliver flexibility and ease of use over a range of applications.
- The monochromator-based instruments provide UV-Vis detection while the filter-based readers deliver offer performance and value.

Cell Imaging & Microplate Detection

Agilent BioTek automated cell imagers and microscopes bring your science to life, capturing spectacular images, z-stacks, montages and time lapse sequence.

NovoCyte Flow Cytometry

The adaption of flow cytometry for environmental studies, extracellular vesicle analysis, and the ability to use upwards of 30+ different parameters for more comprehensive analysis

Real-Time Cell Metabolic Analysis

- Cell Mito Stress
- Glycolysis
- Real-time ATP rate
- Palmitate Oxidation Stress
- Mito Fuel Flex
- Cell energy phenotype

Analyzer measures and reports the oxygen consumption rate (OCR), proton efflux rate (PER) or extracellular acidification rate (ECAR), as well as ATP production rates of live cells

Cardio and CardioECR Systems

- High frequency measurement of cell-induced electrical impedance
- Simultaneously assess cardiomyocyte contractility, viability & electrophysiology

xCELLigence RTC CardioECR

- Continuously measures cell invasion and migration (CIM)
- Monitors cell health, behavior, and function using label-free cellular impedance.

xCELLigence RTCA DP

RI Technologies Ltd.
Lot No. 1244, Pattanakarn Road, Suanluang,
Bangkok 10250, Thailand
Tel: +66 2 853 3584-7
Email: info@ri.co.th | www.ri.co.th

Platinum Sponsor

Gold Sponsor

We are your helping hands

illumina AUTHORIZED CHANNEL PARTNER

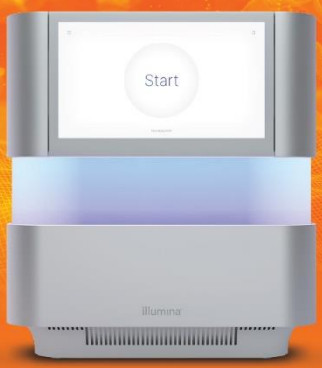

The NextSeq™ 2000

The NextSeq™ 2000 assists both new and experienced users in achieving fast turnaround times and reducing operating costs.

10X GENOMICS

Visium HD Spatial Gene Expression

Perform whole transcriptome gene expression analysis at single cell scale with continuous tissue coverage.

Enhance your H&E and IF imaged samples with high-resolution spatial transcriptomics from the same tissue section.

PROCEEDINGS

The 45th International Meeting of the Pharmacological and Therapeutic Society of Thailand

THE PHARMACOLOGICAL AND THERAPEUTIC SOCIETY OF THAILAND

มหาวิทยาลัยมหิดล
Mahidol University